Quantum Gravity, Generalized Theory of Gravitation, and Superstring Theory-Based Unification

Edited by
Behram N. Kursunoglu
Stephan L. Mintz
and
Arnold Perlmutter

Quantum Gravity, Generalized Theory of Gravitation, and Superstring Theory-Based Unification

This page intentionally left blank.

Quantum Gravity, Generalized Theory of Gravitation, and Superstring Theory-Based Unification

Edited by

Behram N. Kursunoglu
Global Foundation Inc
Coral Gables, Florida

Stephan L. Mintz
Florirda International University
Miami, Florida

and

Arnold Perlmutter
University of Miami
Coral Gables. Florida

Kluwer Academic Publishers
New York, Boston, Dordrecht, London, Moscow

eBook ISBN: 0-306-47104-3
Print ISBN: 0-306-46485-3

©2002 Kluwer Academic Publishers
New York, Boston, Dordrecht, London, Moscow

All rights reserved

No part of this eBook may be reproduced or transmitted in any form or by any means, electronic, mechanical, recording, or otherwise, without written consent from the Publisher

Created in the United States of America

Visit Kluwer Online at: http://www.kluweronline.com
and Kluwer's eBookstore at: http://www.ebooks.kluweronline.com

PREFACE

"Orbis Scientiae 1999" constitutes the 28th conference on High Energy Physics and Cosmology that were begun in 1964. It has now become an institution by itself under the aegis of which the physicists convene annually in South Florida. It created a *Belle Époque* in Coral Gables. The series of Orbis Scientiae started with the participants of highest distinction in physics of the 20th Century. After its first two decades the conferences have been placed in the hands of younger and promising physicists.

The 1999 meeting was the last conference of the millennium. The topics that were covered did not give the impression of laying the foundations of great advancements in theoretical physics. Work on such concepts as strings or super strings, is being actively pursued. It is of course true that revolutions in physics are not frequent. Finding the neutrino massiveness was quite exciting but did not provide enough basis for further progress in the field of neutrino physics.

Recent efforts with regard to extensive studies, gamma ray bursts do manifest themselves as exceptionally important events. There are many papers in the literature studying theoretical implications of the energy dependence of the gamma rays. In this field one of us (Kursunoglu) had published a paper in the Physical Review in 1975. Our first conference in 2000 or rather its Orbis Scientiae will certainly contain some topics on this matter.

It is quite conceivable that in the Big Bang creation of the Universe, very high-energy dependent gamma rays must have played an important role especially causing very fast initial expansion of the early Universe. This may well have been the mechanism for the existence of the so-called inflationary behavior of the process of creation. We are looking forward to the Orbis Scientiae 2000 to include in its program this subject matter.

The Chairman and Trustees of the Global Foundation, Inc. wish to gratefully acknowledge the generous support of this conference by Lady Blanka Rosenstiel, Founder and President of the American Institute of Polish Culture, Chopin Foundation and Honorary Consul of the Republic of Poland in Miami, and to Dr. and Mrs. Edward Bacinich of Palm Beach, Florida

Behram N. Kursunoglu
Stephan L. Mintz
Arnold Perlmutter
Coral Gables, Florida

About the Global Foundation, Inc.

The Global Foundation, Inc., which was established in 1977, utilizes the world's most important resource... people. The Foundation consists of distinguished men and women of science and learning, and of outstanding achievers and entrepreneurs from industry, governments, and international organizations, along with promising and enthusiastic young people. These people convene to form a unique and distinguished interdisciplinary entity to address global issues requiring global solutions and to work on the frontier problems of science.

Global Foundation Board of Trustees

Behram N. Kursunoglu, Global Foundation, Inc., Chairman of the Board, Coral Gables.

M. Jean Couture, Former Secretary of Energy of France, Paris

Manfred Eigen*, Max-Planck-Institut, Göttingen

Willis E. Lamb*, Jr., University of Arizona

Louis Néel*, Université de Gronoble, France

Richard Wilson, Harvard University

Henry King Stanford, President Emeritus, Universities of Miami and Georgia

Former Trustees

Robert Herman, University of Texas

Robert Hofstadter*, Stanford University

Walter C. Marshall, Lord Marshall of Goring

Frederick Reines*, Irvine, California

Abdus Salam*, Trieste, Italy

Glenn T. Seaborg*, Berkeley, California

Eugene P. Wigner*, Princeton University

Lord Solly Zuckerman, London

*Nobel Laureate

GLOBAL FOUNDATION'S RECENT CONFERENCE PROCEEDINGS

Making the Market Right for the Efficient Use of Energy
Edited by: Behram N. Kursunoglu
Nova Science Publishers, Inc., New York, 1992

Unified Symmetry in the Small and in the Large
Edited by: Behram N. Kursunoglu, and Arnold Perlmutter
Nova Science Publishers, Inc., New York, 1993

Unified Symmetry in the Small and in the Large - 1
Edited by: Behram N. Kursunoglu, Stephen Mintz, and Arnold Perlmutter
Plenum Press, 1994

Unified Symmetry in the Small and in the Large - 2
Edited by: Behram N. Kursunoglu, Stephen Mintz, and Arnold Perlmutter
Plenum Press, 1995

Global Energy Demand in Transition: The New Role of Electricity
Edited by: Behram N. Kursunoglu, Stephen Mintz, and Arnold Perlmutter
Plenum Press, 1996

Economics and Politics of Energy
Edited by: Behram N. Kursunoglu, Stephen Mintz, and Arnold Perlmutter
Plenum Press, 1996

Neutrino Mass, Dark Matter, Gravitational Waves, Condensation of Atoms and Monopoles, Light Cone Quantization
Edited by: Behram N. Kursunoglu, Stephen Mintz, and Arnold Perlmutter
Plenum Press, 1996

Technology for the Global Economic, Environmental Survival and Prosperity
Edited by: Behram N. Kursunoglu, Stephen Mintz, and Arnold Perlmutter
Plenum Press, 1997

25th Coral Gables Conference on High Energy Physics and Cosmology

Edited by: Behram N. Kursunoglu, Stephen Mintz, and Arnold Perlmutter
Plenum Press, 1997

Environment and Nuclear Energy
Edited by: Behram N. Kursunoglu, Stephan Mintz, and Arnold Perlmutter
Plenum Press, 1998

Physics of Mass
Edited by: Behram N. Kursunoglu, Stephan Mintz, and Arnold Perlmutter
Plenum Press, 1999

Preparing the Ground for Renewal of Nuclear Power
Edited by: Behram N. Kursunoglu, Stephan Mintz, and Arnold Perlmutter
Plenum Press, 1999

Confluence of Cosmology, Massive Neutrinos, Elementary Particles & Gravitation
Edited by: Behram N. Kursunoglu, Stephan Mintz, and Arnold Perlmutter
Plenum Press, 1999

International Energy Forum 1999
Edited by: Behram N. Kursunoglu, Stephan Mintz and Arnold Perlmutter
Plenum Press, 2000

International Conference on Orbis Scientiae 1999
Quantum Gravity, Generalized Theory of Gravitation and Superstring Theory-based Unification
Edited by: Behram N. Kursunoglu, Stephan Mintz, and Arnold Perlmutter
Plenum Press, 2000

Global Foundation, Inc.

A Nonprofit Organization for Global Issues Requiring Global Solutions, and for problems on the Frontiers of Science

Center for Theoretical Studies

MILLENNIUM'S LAST

INTERNATIONAL CONFERENCE
ON
ORBIS SCIENTIAE 1999

QUANTUM GRAVITY, GENERALIZED THEORY OF GRAVITATION AND SUPERSTRING THEORY-BASED UNIFICATION

(28th Conference on High Energy Physics and Cosmology Since 1964)

December 16 - 19, 1999
Lago Mar Resort
Fort Lauderdale, Florida

This conference is supported in part by
National Science Foundation
Alpha Omega Research Foundation
Lady Blanka Rosenstiel

Sponsored by:
Global Foundation Inc.

P. O. Box 249055
Coral Gables, Florida 33124-9055
Phone: (305) 669-9411
Fax: (305) 669-9464
E mail: kursungf@gate.net
Web:http://www.gate.net/~kursungf

Conference Hotel:
Lago Mar Resort

1700 South Ocean Lane
Fort Lauderdale. Florida 33316
Reservations: 1-800-255-5246
(954) 523-65 11
Fax: (954) 524 6627
The special group rate: $120/night
One-bedroom suite w/ Ocean view

DEDICATION

The trustees of the Global Foundation and members of the 28th Orbis Scientiae 1999, dedicate this conference to Dr. Joseph Lannutti of Florida State University. The late Professor Lannutti was a loyal and active member of this series of conferences on the frontiers of physics since 1964. He also served as a member of Global Foundation's Advisory Board. Professor Lannutti was instrumental in bringing experimental research in high energy physics to Florida. We shall all miss Joseph. We extend our deepest condolences to his wife Peggy Lannutti and all the other members of his family.

--NOTES--

1. Each presentation is allotted a maximum of 25 minutes and an additional 5 minutes for questions.
2. Moderators are requested not to exceed the time allotted for their sessions.

Moderator: Presides over a session. Delivers a paper in own session, if desired, or makes general opening remarks.

Dissertator: Presents a paper and submits it for publication in the conference proceedings at the conclusion of the conference.

Annotator: Comments on the dissertator's presentation or asks questions about same upon invitation by the moderator.

CONFERENCE PROCEEDINGS

1. The conference portfolio given to you at registration contains instructions to the authors from the publisher for preparing typescripts for the conference proceedings.

2. Papers must be received at the Global Foundation by February 15, 2000.

3. An edited Conference Proceedings will be submitted to the Publisher by March 14, 2000.

BOARD OF TRUSTEES

Dr. Behram N. Kursunoglu
Chairman
Global Foundation, Inc.

Mr. Jean Couture
Pans, France

Dr. Manfred Eigen*
Gõttingen, Germany

Dr. Willis E. Lamb*
Tucson, Arizona

Dr. Louis Neel*
Meudon, France

Dr. Henry King Stanford
President Emeritus
Universities of Miami and Georgia

Dr. Richard Wilson
Harvard University

Dr. Arnold Perlmutter
Secretary of the Global Foundation
University of Miami

Mrs. Sevda A. Kursunoglu
Vice-president, Global Foundation
Global Foundation, Inc.

FORMER TRUSTEES

Robert Herman
University of Texas

*Robert Hofstadter**
Stanford University

Walter C. Marshall
Lord Marshall of Goring

*Frederick Reines**
Irvine, California

*Abdus Salam **
Trieste, Italy

*Glenn T. Seaborg**
Berkeley California

*Eugene P. Wigner**
Princeton University

Lord Solly Zuckerman
London, UK

*Nobel Laureate

INTERNATIONAL ADVISORY COMMITTEE

Ralph A. Alhper
Union College

Nicola Cabibbo
Instituto Nazionale de Fisica Nucleare, Rome

Louise Dolan
University of North Carolina

Harald Fritzsch
Sektion Physik der Universität Munich

Morton Hamermesh
University of Minnesota

Alan Krisch
University of Michigan

V. Alan Kostelecky
Indiana University

William Louis
LANL

Sydney Meshkov
CALTECH

Yoichiro Nambu
University of Chicago

Pierre Ramond
University of Florida

Arnold Perlmutter
University of Miami

Paul Frampton
University of North Carolina

Vigdor L. Teplitz
Southern Methodist University

Thursday, December 16,1999
LAKEVIEW ROOM

8:00 AM Registration

1:30 PM SESSION I: **Cosmological Parameters Unifying Elementary Particle Physics and Cosmology I**

Moderator: **Behram N. Kursunoglu,** Global Foundation, Inc.
"The Ascent of Gravity"

Annotators: **Gerald Eigen,** University of Bergen, Norway

Session Organizer: **Behram N. Kursunoglu**

3:00 PM Coffee Break

3:15 PM SESSION II: **Cosmological Parameters Unifying Elementary Particle Physics and Cosmology II**

Moderator: **Paul H. Frampton,** University of North Carolina

Dissertators: **Alexander Vilenkin,** Tufts University
"Eternal Inflation and the Present Universe"

Thomas W. Kephart, Vanderbilt University
"Cosmic Rays, Cosmic Magnetic Fields and Monopoles"

Paul Frampton,
"Conformality, Particle Phenomenology and the Cosmological Constant"

Annotator: **Sarada Rajeev,** Rochester University

Session Organizer: **Paul Frampton**

4:45 PM SESSION III: **Superstring Theory Based Unification**

Moderator: **Louise Dolan,** University of North Carolina

Dissertators: **Louise Dolan,**
"Superstrings on Anti-de Sitter Space"

Ergin Sezgin, Texas A&M University
"Branes, Singletons and Higher Spin Gauge Theories"

Stephan L. Mintz, Florida International University

"Weak Production of Λ and Σ° by Electron Scattering from Protons and the Weak Strangeness-changing current"

Anotator: **Richard Arnowitt,** Texas A&M University
Session Organizer: **Louise Dolan**

6:15 PM **Orbis Scientiae adjourns for the day**

Friday, December 17, 1999

8:30 AM SESSION IV: **Neutrinos: Theory and Experiment**

Moderator: **Pierre Ramond,** University of Florida

Dissertators: **Steve Barr,** University of Delaware
"Neutrino Oscillations, Some Theoretical ideas"

Wojciech Gajewski, University of California, Irvine
"SuperKamiokande Results"

Jon Urheim, University of Minnesota
"Long Baseline Neutrino Experiments"

Annotator: **Stephan L. Mintz,** Florida International University
Session Organizer: **Pierre Ramond**

10:00 AM Coffee Break

10:15 AM SESSION V: **Recent Progress on Old and New Ideas I**

Moderator: **Arnold Perlmutter,** University of Miami

Dissertators: **A.J. Meyer II,** Optonline, New York
"The Unification of G and e " (15 minutes)

Osher Doctorow, Culver City, CA
"Quantum Gravity" (15 minutes)

Freydoon Mansouri, University of Cincinnati
"AdS Black Holes, their Microstructure, and Their Entropy"

Richard P. Woodard, University of Florida
"An Invariant Operator Which Measures the Local Expansion of Space-time"

Annotator : **Doris Rosenblum** Southern Methodist University

Session Organizer: **Arnold Perlmutter**

12:00 PM Lunch Break

1:30 PM SESSION VI: **Recent Progress on Old and New Ideas II**

Moderator: **Don Lichtenberg,** Indiana University

Dissertators: **Thomas Ferbel,** University of Rochester
"An Update on the Top Quark"

Thomas Curtright, University of Miami
"Phase-Space Quantization of Field Theory"

Pran Nath, Northeastern University
"CP Violation Effects on the Supersymmetric Muon Anomaly"

Annotator: **Alan Krisch,** University of Michigan

Session Organizer: **Don Lichtenberg**

3:00PM Coffee Break

3:15 PM SESSION VII: **CPT and Lorentz Symmetry**

Moderator: **Robert Bluhm,** Colby College

Dissertators : **Alan Kostelecky,** Indiana University
" Theory and Tests of Lorentz and CPT Violation"

Blayne Heckel, University of Washington
"Torsion-balance Test of Lorentz Invariance"

Ron Walsworth, Harvard-Smithsonian Center
" New Clock-Comparison Tests Of Lorentz Violation"

Annotator: **Pran Nath**

Session Organizer: **Alan Kostelecky**

4:45PM SESSION VIII: **Recent Progress on Old and New Ideas III**

Moderator: **Vigdor L. Tepiitz,** Southern Methodist University

Dissertators: **Vigdor L. Tepiitz**
"Detecting Strongly Interacting Massive Particles"

Don Lichtenberg
"Whither Hadron Supersymmetry"

Richard Arnowitt, Texas A&M University
'CP Violating Phases In D-brane and Other Models''

Annotator: **Frederick Zechariasen,** CALTECH

Session Organizer: **Vigdor L. Teplitz**

6:00 PM **Orbis Scientiae adjourns for the day**

6:30PM WELCOMING COCKTAILS. FOUNTAINVIEW LOBBY

Courtesy of Lago Mar Resort

7:30PM CONFERENCE BANQUET, PALM GARDEN ROOM

Courtesy of Maria and Edward Bacinich

Murray Gell-Mann (Invited) , Santa Fe Institute

"After Dinner Address to Orbis Scientiae 1999"

Saturday, December 18, 1999

8:30AM SESSION IX: **New Ideas**

Moderator: **Pierre Ramond,** University of Florida

Dissertators: **Kevin McFarland,** University of Rochester
"Muon Storage Rings"

Konstantin Matchev, Fermi Laboratory
"What is new with New Dimensions"

Igor R. Klebanov. Princeton University
"Breaking Supersymmetry in the AdS/CFT Correspondence"

Anotator: **S.M. Trochin,** IHEP- Protvino

Session Organizer: **Pierre Ramond**

10:30AM Coffee Break

10:45 AM SESSION X: **Spin of the Proton**

Moderator: **Alan Krisch,** University of Michigan

Dissertators: **L.D. Soloviev,** IHEP-Protvino
"Meson Masses and Spin Structure in the string Quark Model"

W. T.Lorenzon, University of Michigan
" the Spin Content of the Proton"

S.M. Troshin, IHEP-Protvino
"Unitarity Bounds on Helicity-Flip Amplitudes In Elastic p-p Scattering"

Annotator: **Behram N. Kursunoglu**

Session Organizer: **Alan Krisch**

12:15PM **Orbis Scientiae adjourns for the day**

Sunday, December 19, 1999

9:00AM SESSION XI: **Recent Progress on Old and New Ideas IV**

Moderator: **Sydney Meshkov,** CALTECH

Dissertators: **Sarada Rajeev,** University of Rochester
'Tarton Model and Structure Functions from QCD"

Robert Bluhm , Colby College
"Searching for Spontaneous Lorentz Symmetry Breaking in the Ground State of Hydrogen"

Glampiero Mancinelll, Stanford University
"Performances and First Results from BaBar"

Annotator: **Alan Kostelecky**

10:15 AM Coffee Break

10:30 AM SESSION XII: **The Latest Developments In High Energy Physics and Cosmology**

Moderator: **Sydney Meshkov,** CALTECH

Dissertators: **Gerald Eigen** , University of Bergen, Norway
"CP violation, A Key for Understanding Our Universe"

Francis Halzen, Wisconsin Madison

Sydney Meshkov
"Current Status of LIGO"

Annotator: **Pierre Ramond**

Session Organizer: **Sydney Meshkov**

12:30 PM **Orbis Scientiae 1999 Adjourns**

CONTENTS

SECTION I
Cosmological Parameters
Unifying Elementary Particle Physics
and Cosmology

Variable Speed of Light Cosmology 3
Behram N. Kursunoglu

Energy Dependence of the Speed of Light Emerging from Cosmic Regions 9
Arnold Perlmutter

Conformality, Particle Phenomenology and the Cosmological Constant 13
Paul H. Frampton

Eternal Inflation and the Present Universe 25
Alexander Vilenkin

Cosmic Rays, Cosmic Magnetic Fields, and Magnetic Monopoles 33
Thomas W. Kephart, Thomas J. Weiler, and Stuart D. Wick

SECTION II
Super Strings and Black Holes

Vertex Operators for Strings on Anti – De Sitter Space 43
L. Dolan

The Structure of a Source Modified WZW Theory 53
Sharmanthie Fernando and Freydoon Mansouri

SECTION III
Recent Progress on New and Old Ideas I

The Unification of the Gravitational Constant G, with the Electric Charge, e, Via an Extended Non-Stationary, Axi-Symmetric, Space-Time and Corresponding Thermodynamics – The Super Spin Model 63
A.J. Meyer II

Magnetic Monopoles, Massive Neutrinos and Gravitation Via Logical – Experimental Unification Theory (LEUT) and Kursunoglu's Theory 89
Osher Doctorow

SECTION IV
Recent Progress in New and Old Ideas II

An Update on the Properties of the Top Quark 101
T. Ferbel

The Supersymmetric Muon Anomaly 111
Pran Nath

Schrödinger's Cataplex 121
Thomas Cutright

The Weak Production of Neutral Hyperons in Electron Proton Scattering 133
S.L. Mintz

SECTION V
CPT, Lorentz Symmetry, and Neutrino Oscillation

Torsion Balance Test of Spin Coupled Forces 153
Blayne R. Heckel, Eric G. Adelberger, Jens H. Gandlach, Michael G. Harris, and H. Erick Swanson

Recent Results in Lorentz and CPT Tests 161
V. Alan Kostelecky

Searching for Lorentz Violation in the Ground State of Hydrogen 173
Robert Bluhm, V. Alan Kostelecky, and Neil Russell

Neutrino Oscillations: Some Theoretical Ideas 181
Stephen M. Barr

SECTION VI
Recent Progress on New and Old Ideas III

SIMP (Strongly Interacting Massive Particle) Search 197
Vigdor L. Teplitz, Rabindra N. Mohapatra, Fred Olness, and
Ryszard Stroynowski

Wither Hadron Supersymmetry 203
D.B. Lichtenberg

The Mystery of Nucleon Spin 209
W. Lorenzon

Performance and First Results from BABAR 217
Giampiero Macinelli

Index 227

This page intentionally left blank.

Quantum Gravity, Generalized Theory of Gravitation, and Superstring Theory-Based Unification

This page intentionally left blank.

Section I

Cosmological Parameters Unifying Elementary Particle Physics and Cosmology

This page intentionally left blank.

VARIABLE SPEED OF LIGHT COSMOLOGY

Behram N. Kursunoglu

Global Foundation Inc.
Coral Gables, Florida
kursun@globalfoundationinc.org

In the past two or three years there have been many papers in the field of the Energy dependence of the speed of light emitted from regions of cosmic distances where phenomenon of gamma ray bursts are taking place. These very interesting cosmic events have inspired many theorists to research on the implications of gamma ray speed dependence on energy or variable speed of light. The work depends to a large extent on making guesses with regard to the behavior of such gamma rays, which provide some information on the source of the gamma rays especially the mechanism for the explosive expansion of the early universe. The cosmic regions like, for example, the cores of some galaxies containing super massive black holes provide powerful sources of gravitational acceleration of particles to very high energies to produce X-rays and even gamma rays. These are like experimental demonstration of gravity acting as a source of the electromagnetism and more precisely, these cosmic phenomena provide, beyond any shadow of doubt, dramatic demonstration for the *"Unified theory of electromagnetism and gravitation"*. In the general relativistic theory of gravitation electromagnetic energy and momentum do act as a source of gravity but in the unified theory gravity itself can act as a source of electromagnetism. In fact the unified theory does more: it brings in the short-range weak and strong forces.

Observations demonstrate that the explosive behavior of the cosmic regions is greatly affected by the energy dependence of the emitted gamma rays. Here what we have is comparable to an inflationary behavior for which energy is provided by the emission of gamma rays. In 1975, I calculated the speed of electromagnetic waves from the unified field theory of electromagnetism and gravitation'. For the propagation of light in the presence of a gravitational field we use the equation:

[1] Behram N. Kursunoglu, Physical Review D Volume 14, Number 6, 15 September 1976.

Quantum Gravity. Generalized Theory of Gravitation, and Superstring Theory-Based Unification
Edited by Kursunoglu *et al.*. Kluwer Academic / Plenum Publishers, New York. 2000

$$g_{\mu\nu}dx^{\mu}dx^{\nu}=0, \tag{1}$$

where $g_{\mu\nu}$ is the metric of space-time representing gravitational potentials with μ and ν ranging from 1 to 4. However in space-time geometry pertaining to a unified theory of electromagnetism and gravitation the metric is defined by the symmetric tensor $b_{\mu\nu}$ as described below:

$$b_{\mu\nu}\, dx^{\mu}\, dx^{\nu} = 0, \tag{2}$$

where

$$b_{\mu\nu} = \frac{(1+\frac{1}{2}\Omega)g_{\mu\nu}-T_{\mu\nu}}{(1+\Omega-A^2)^{1/2}} \tag{3}$$

and where

$$\Omega=\frac{1}{2}\Phi_{\mu\nu}\Phi^{\mu\nu},\quad \Lambda=\frac{1}{4}\Phi_{\mu\nu}\, f_{\mu\nu}, f_{\mu\nu}=\frac{1}{2}\varepsilon^{\mu\nu\rho\sigma}\Phi_{\rho\sigma} \tag{4}$$

The energy dependence of the speed of light is computed here, by using the equation (2), in a straightforward way. In fact Erwin Schrödinger had obtained the same result a long time ago[2] by using Born-Infeld non-linear electrodynamics. The reason for the complicated procedure adopted by Schrödinger was due to the fact that his version of the non-symmetric generalization of the general theory of relativity did not include the metric $b_{\mu\nu}$. The calculation of a variable speed of light has been performed[1] for which a special case, irrespective of polarization and frequency, is given by

$$V^2= \frac{1+\Omega-\Lambda^2}{(1+\frac{1}{2}\Omega+I)^2}\sin^2\theta + \cos^2\theta, \tag{5}$$

where θ represents one of the angles to determine direction of the wave normal. The speed in the direction of coordinates are obtained by setting $\theta = 0$ for the "1" direction, $\theta = 1/2\pi$ and $\Phi = 0$ for the "2" direction, and $\theta = 1/2\pi$, $\Phi = 1/2\pi$ for the "3" direction thus the variable speed of light in the "3" direction is given by

$$V^2 = \frac{1+\Omega-\Lambda^2}{(1+\frac{1}{2}\Omega+I)}, \quad I^2=\frac{1}{4}\Omega^2+\Lambda^2 \tag{6}$$

We can now determine the energy dependence of the speed of light to be an invariant result. The numerator can be written as

$$1+q^{-2}\Omega-q^{-4}\Lambda^2=(1+\frac{1}{2}q^{-2}\Omega)^2 - q^{-4}c^2p_{\mu}p^{\mu}, \tag{7}$$

---

[2] E. Schrödinger, Proc. R. Irish Acad. 47A.77(1942). To this author's knowledge, the report by E. Schrödinger mentioned in the text does not seem to have been published.

where

$$c^2 p_\mu p^\mu = \frac{1}{4}\,\Omega^2 + \Lambda^2 = I^2, \tag{8}$$

By using the identities

$$T^\nu{}_\rho T^\rho{}_\mu = \delta^\nu_1\,(\frac{1}{4}\Omega^2 + \Lambda^2) \tag{9}$$

we can write

$$cp_\mu = T_{\mu\rho} v^\rho, \tag{10}$$

where v^ρ is a unit vector ie: $v^\rho v^\rho = 1$.

The metric tensor $b_{\mu\nu}$ and the parameter q were introduced or rather discovered in 1950 while as a graduate student in Cambridge University I was working on a new formulation of Einstein's and Schrodinger's non-symmetric unified field theories. The use of the metric tensor $b_{\mu\nu}$ led to the existence of a fundamental length parameter r_0, which is related to the parameter q by an equation of state[3].

$$r_0^2 q^2 = \frac{c4}{2G}, \tag{11}$$

where q^2 has the dimensions of energy density

From (6) it is clear that v^2 is less than 1 and the region from where light is emerging depending on its total energy content could partition this energy among the massive particles and as it may have happened in the creation of the universe leading to a very fast expansion in its early fractional seconds of birth. We can thus imagine that the energy dependence of the speed of light bursting out from a cosmic region must have been the early part of the Big Bang creation of the universe. Hence we are able to consider the Big Bang taking place in several stages whose effect on the early Universe were actually the foundation of the creation process. An explicit display of energy dependence can be obtained by observing that the numerator in equation (6) can be expressed in the form of equation (10), which represents a momentum density four vector.

By splitting the general anti-symmetric field into the sum of a background field and a radiation field we can see that the momentum density vector $p\mu$ is expressible as

$$p_\mu = (T^\nu{}_{o\mu} + T^\nu{}_{1\mu} + T^\nu{}_{1\mu})\, v_\nu. \tag{12}$$

representing the sum of momentum densities of photon, massive particle, and interaction of photon with the massive particle. Thus we see that the gamma ray bursts provide a source of energy for massive particles in a cosmic region to acquire large energies to lead to fast expansion of matter contained in the region.

It is quite interesting to observe that variable speed of light does not present any difficulties with regard to some cosmological behavior of the universe like for example the

[3] Behram N. Kursunoglu, Phys. Rev.**88,** 1369 (1952)

problem of flatness or copious production of monopoles since the process of monopole condensation does not leave any room for the existence of free monopoles. The flatness of the Universe in the unified field theory is a consequence of, as a result of the expansion of the universe, increasing size of r_0. In this theory there exists no free monopoles all of them as a result of *monopole condensation* have been confined to create elementary particles. *Monopole condensarion* contrary to Bose-Einstein condensation, takes place at very high temperatures. In fact in this theory all the participating field equations are fully compatible with one another. At microcosmic distances the theory yields masses that result from using length scales much shorter than so-called Planck length of 10^{-33} cm. The most general form for the mass is obtained as

$$m = \frac{c^2}{2G} r_0 \tag{13}$$

Where $r_0 \approx 10^{-53}$ cm for proton and for the Universe $r_0 \approx 10^{27}$ cm. How many protons can I put side by side to make the Universe?

It is rather remarkable to see that various papers on the subject have been based on a proper analysis without having the benefit of a metric of space-time. All of these considerations are of course compatible with Einstein's theory of gravity. Where c the speed of light, relates time to space. In order to pursue further the significance of varying of the speed of light and its role in the important quantities like Planck Scale length and Planck Scale mass could be affected. Should we then imagine two different metrics one describing the propagation of photons and the other describing gravity itself, which is space-time metric, and the associated particles of gravitons? This would complicate simple things. The best way to describe propagation of photons and gravitons is the use of a unified field theory where gravity and electromagnetism are unified like we have introduced in this paper where the most general metric is expressible as

$$b_{\mu\nu} = Ag_{\mu\nu} + BT_{\mu\nu}, \tag{14}$$

where the functions A and B, as follows from the definition (3) above, are given by

$$A = \frac{(1+\frac{1}{2}\Omega)}{(1+\Omega-\Lambda^2)^{1/2}}, \tag{15}$$

$$B = \frac{1}{(1+\Omega-\Lambda^2)^{1/2}} \tag{16}$$

It must be understood that the invariant functions Ω and Λ contain besides free electromagnetic field also the background fields and the interaction between the two fields. At this point I would like to quote from my Paper 1 referred here earlier: "A possible direct experimental test of the result (5) could be based on the emission of radiation from a pulsar where the interplay between the field on the surface of the neutron star and electromagnetic wave may be described as a nonlinear effect of the kind predicted in this paper. Thus the

directional effect of emission of radiation implied by equation (5) might be due to dispersion intrinsic to a pulsar itself arising from the high densities and field strengths. The net effect could manifest itself by time delay in the arrival of some radiation. In this case, one should observe an asymmetric broadening of the radiation independent of bandwidths.

NASA's $326 million project to launch The Gamma Ray Large Area Space Telescope into Earth orbit in 2005 will open new windows to study gamma ray bursts coming from distant cosmic regions, which should reveal the presence of violent cosmic phenomena. These gamma rays are, most likely, the result of the acceleration of particles by the powerful gravitational forces. Thus gravitation is acting as a source of the electromagnetism and, therefore, these cosmic phenomena do vindicate unification of gravity with electromagnetic forces. It is thus cosmic acceleration of particles that reveal information about the gamma rays bursting regions of the universe.

This page intentionally left blank.

ENERGY DEPENDENCE OF THE SPEED OF LIGHT EMERGING FROM COSMIC REGIONS

Arnold Perlmutter

Department of Physics
University of Miami
Coral Gables, FL 33124

Observations of very high energy γ-rays from cosmological sources have increased in frequency and refinement. Among the numerous examples of the emissions by Gamma Ray Bursters (GRB), several have led to estimates of the variation of the speed of the photons as function of their energy. Several authors have proposed that quantum-gavitational fluctuations in the space time background may endow the conventional particle vacuum with nontrivial optical properties, such as a frequency-dependent refractive index, birefringence, and a diffusive spread in the apparent velocity of light.[1],[2],[3]

A particular example, the active galaxy Markarian 421,[4] has lent itself to interesting analysis[5] of the time delay of the signal of multi-TeV γ-rays. They use the result that various approaches to quantum gravity lead to a description of first order effects of a time dispersion[5], given by

$$\Delta t = \xi \frac{E}{E_{QG}} \frac{L}{c} \qquad (1)$$

where Δt is the time delay relative to the standard energy-independent speed of light, c; ξ is a model-dependent factor of order 1; E is the energy of the observed radiation; E_{QG} is the assumed energy scale for quantum gravitational effects which can couple to the electromagnetic radiation, and L is the distance over which the radiation has propagated. While they state that E_{QG} is generally assumed to be of the order of E_p, Planck energy ($\cong 10^{19}$GeV), some string theory work suggests that it would be as low as 10_{16}GeV[6].

Using the value of the redshift of Markarian 421 to be 0.031, which translates to a distance of 1.1 x 10^{16} light-seconds for an assumed Hubble constant of 85km/s/Mpc, they obtain a lower bound on E_{QG}/ξ of 4 x 10^{16}GeV[5]. If ξ = 3/2, as indicated from recent calculations of D-brane theory[7], then E_{QG} > 6 x 1016GeV. Calculations in the context of loop gravity[3] lead to a value of ξ as large as 4, suggesting an energy scale larger than 1.6 x 10^{17}GeV.

In the Unified Gravitational theory of Kursunoglu[8], there is an exact formula for the dependence of the light speed on the field variables of the electromagnetic radiation. For

Quantum Gravity, Generalized Theory of Gravitation and Superstring Theory-Based Unification
Edited by Kursunoglu *etal*. Kluwer Academic / Plenum Publishers. New York, 2000

the purposes of this paper, this speed can be written as

$$v = c\left(\frac{1 + \frac{1}{2}\Omega + I}{1 + \frac{1}{2}\Omega + W}\right)^{\frac{1}{2}}, \tag{2}$$

where $W = \frac{E^2+B^2}{}$ is the energy density, $\Omega = B^2 - E^2$ and A = B. E are invariants of the field, and $I^2 = \frac{1}{4}\Omega^2 + \wedge^2$. Note that W,Ω and ∧ are actually multiples of q^2, given by

$$q^2 r_0^2 = \frac{c^4}{2G}, \tag{3}$$

where r_0 is a fundamental length, c is the speed of light and G is the gravitational constant. The q^2 is therefore an energy density associated with a vacuum and is presumed to be much larger than W,Ω, and Λ. Again, for the purposes of this discussion, we will assume that W >> Ω, Λ, although in the future it is hoped that one can find ways of estimating Ω and A. Hence, we may write eq. (2) as

$$v \cong c\left(\frac{1}{1 + \frac{W}{q^2}}\right)^{\frac{1}{2}}, \tag{4}$$

and for W << 1,

$$v \cong c\left(1 - \frac{1}{2}\frac{W}{q^2}\right). \tag{5}$$

The time delay is then given by

$$\Delta t = \frac{1}{2}\frac{W}{q^2} \cdot \frac{L}{c}, \tag{6}$$

giving a value of the ratio $\frac{W}{q^2} = 4.2 \times 10^{-14}$, if we use the input of Biller et al.(5)

Since it is clear that we must have $\frac{W}{q2} = \frac{E,}{EQG}$, then the factor ξ in eq. (1) must be $\frac{1}{2}$ This gives a value $E_{QG} > 4.8 \times 10^{16}$GeV.

We can now calculate limits on q^2 and r_0 from E_{QG} and eq. (3). We have

$$E_{QG} > 4.8 \times 10^{16}\text{GeV} = q^2 r_0^3 = \frac{c^4}{2G} r_0. \tag{7}$$

This gives $r_0 = 1.25 \times 10^{-35} cm$, which is about three orders of magnitude smaller than Planck length, just as E_{QG} is about three orders of magnitude less than Planck energy. Finally the energy density from eq. (7), is given by

$$q^2 = 3.9 \times 10^{118} erg/cm^3.$$

References

1. G. Amelino et al, *Nature* (London) **393,** 763 (1998)
2. R. Gambini and J. Pullin, *Phy. Rev. D* **59,** 124021 (1999)
3. L.J. Garay, *Phys. Rev. Letters* 80, 2508 (1998)
4. J. Gaidos et al, *Nature* (London) **383**, 319 (1996)
5. S.D. Biller et al, *Phys. Rev. Letters* **83**, 2108 (1999)
6. E. Witten, *Nucl. Phys.*B471, 135 (1996)
7. J. Ellis et al, *Oxford Report No. OUTP-99-05P* (to be published)
8. B. Kursunoglu, *Phys. Rev.* D **14**, 1518 (1976)

This page intentionally left blank.

CONFORMALITY, PARTICLE PHENOMENOLOGY AND THE COSMOLOGICAL CONSTANT

Paul H. Frampton

Department of Physics and Astronomy,
University of North Carolina,
Chapel Hill, NC 27599-3255.

Abstract

Conformality is the idea that at TeV scales enrichment of the standard model particle spectrum leads to conformal invariance at a fixed point of the renormalization group. Some aspects of conformality in particle phenomenology and cosmology are discussed.

Alternative to "Grand" Unification

In GUT theories there is an unexplained hierarchy between the GUT scale and the weak scale which is about 14 orders of magnitude. There is the question of why these very different scales exist and how are the scales stabilized under quantum corrections?

Supersymmetry solves the second of these problems but not the first. Supersymmetry has some *successes:* (i) the cancellation of some UV divergences; (ii) the technical naturalness of the hierarchy; (iii) the unification of the gauge couplings; and (iv) its natural appearance in string theory.

On the other side, supersymmetry definitely presents several *puzzles:* (i) the "mu" problem - why is the Higgs at the weak scale not at the GUT scale?; (ii) breaking supersymmetry leads to too large a cosmological constant; and (iii) is supersymmetry really fundamental for string theory since there are solutions of string theory without supersymmetry.

These general considerations led naturally to the suggestion [1, 2, 3, 4, 5, 6] that supersymmetry and grand unification should be replaced by conformality at the TeV scale. Here it will be shown that this idea is possible, including explicit examples containing the standard model states. Further it will be shown that conformality is a much more rigid constraint than supersymmetry. Conformality predicts additional states at the TeV scale and a rich inter-family structure of Yukawa couplings.

Quantum Gravity Generalized Theory of Gravitation. and Supersrting Theory-Based Unification
Edited by Kursunoglu *et al.*. Kluwer Academic / Plenum Publishers. New York. 2000

Conformality as a Hierarchy Solution

First we note that quark and lepton masses, the QCD scale and weak scale are small compared to a (multi-) TeV scale. At the higher scale they may be put to zero, suggesting the addition of further degrees of freedom to yield a quantum field theory with conformal invariance. This has the virtue of possessing naturalness in the sense of 't Hooft [7] since zero masses and scales increases the symmetry.

The theory is assumed to be given by the action:

$$S = S_0 + \int d^4x \alpha_i O_i \tag{1}$$

where S_0 is the action for the conformal theory and the O_i are operators with dimension below four which break conformal invariance softly.

The mass parameters α_i have mass dimension $4 - \Delta_i$ where Δ_i is the dimension of O_i at the conformal point.

Let M be the scale set by the parameters ai, and hence the scale at which conformal invariance is broken. The for $E \gg M$ the couplings will not run while they start running for $E < M$. To solve the hierarchy problem we assume M is near to the TeV scale.

d = 4 CFTs

In enumerating the CFTs in 4 spacetime dimensions, we must choose the N of SU(N). To leading order in $1/N$, the RG β-functions always vanish as they coincide with the $N = 4$ case [8, 9]. For finite N the situation is still under active investigation. To prove the β– functions vanish when $N = 0$ is rendered more difficult by the fact that without supersymmetry the associated nonrenormalization theorems are absent.

We extract the candidates from compactification[10] of the Type IIB superstring on AdS_5 x S^5/W.

Let W C $SU(4)$ denote a discrete subgroup of $SU(4)$. Consider irreducible representations of WWW Suppose there are k irreducible representations R_i, with dimensions d_i with $i = 1, ..., k$. The gauge theory in question has gauge symmetry

$$SU(Nd_1) \text{ x } SU(Nd_2) \text{ x } ... SU(Nd_k) \tag{2}$$

The fermions in the theory are given as follows. Consider the 4 dimensional representation of Γ induced from its embedding in $SU(4)$. It may or may not be an irreducible representation of Γ. We consider the tensor product of 4 with the representations R_i:

$$4 \otimes Ri = \oplus_j n_i^j R_j \tag{3}$$

The chiral fermions are in bifundamental representations

$$(1, 1, .., Nd_i, 1, ..., \overline{Nd_j}, 1, ..) \tag{4}$$

with multiplicity n_i^j defined above. For $i = j$ the above is understood in the sense that we obtain n_i^i adjoint fields plus n_i^i singlet fields of $SU(Nd_i)$.

Note that we can equivalently view n_i^j as the number of trivial representations in the tensor product

$$(4 \otimes R_i \otimes Rj^*)_{trivial} = n_i^j \tag{5}$$

The asymmetry between i and j is manifest in the above formula. Thus in general we have $n_i^j \neq n_j^i$ and so the theory in question is in general a chiral theory. However if Γ? is a real subgroup of *SU(4),* i.e. if 4 = 4* as far as Γ representations are concerned, then we have by taking the complex conjugate:

$$n_i^j = (4 \otimes R_i \otimes R_j) = (4 \otimes Ri \otimes Ej^*)^*_{trivial} = (4^* \otimes R_i \otimes R_j)_{trivial} = (4 \otimes R_i^* \otimes R_j)_{trivial} = n_j^i . \tag{6}$$

So the theory is chiral only if 4 is a complex representation of Γ, i.e. only if $4 \neq 4^*$ as a representation of Γ. If Γ? were a real subgroup of *SU*(4) then $n_i^j = n_j^i$.

If Γ is a complex subgroup, the theory is chiral, but it is free of gauge anomalies. To see this note that the number of chiral fermions in the fundamental representation of each group $SU(Nd_i)$ plus Nd_i times the number of chiral fermions in the adoint representation is given by

$$\sum_j n_i^j \; Nd_j = 4Nd_i \tag{7}$$

(where the number of adjoints is given by n_i^i). Similarly the number of anti-fundamentals plus Nd_i times the number of adjoints is given by

$$\sum_j n_j^i \, Nd_j = \sum Nd_j (4 \otimes R_j \otimes R_i^*)_{trivial} = \sum Nd_j \, (4^* \otimes R_j^* \otimes R_i)_{trivial} = 4Nd_i \tag{8}$$

Thus, comparing with Eq.(7) we see that the difference of the number of chiral fermions in the fundamental and the antifundamental representation is zero (note that the adjoint representation is real and does not contribute to anomaly). Thus each gauge group is anomaly free. The requirement of anomaly cancellation is, of course, a familiar one in string theory [12, 13] as well as in model building beyond the standard model [14, 15, 16, 17].

In addition to fermions, we have bosons, also in the bifundamental represenations. The number of bosons M_i^j in the bifundamental representation of $SU(Nd_i) \otimes SU(Nd_j)$ is given by the number of R_j representations in the tensor product of the representation **6** of *SU*(4) restricted to Γ with the R_i representation. Note that since **6** is a real representation we have

$$M_i^j = (6 \otimes R_i \otimes R_j^*)_{trivial} = (6 \otimes R_i^* \otimes R_j)_{trivial} = M_j^i$$

In other words for each M_i^j we have a *complex*scalar field in the corresponding bifundamental representation, where complex conjugation will take us from the fields labeled by M_i^j to M_j^i.

The fields in the theory are naturally summarized by a graph, called the quiver diagram [11], where for each gauge group *SU(Ndi)* there corresponds a node in the graph, for each chiral fermion in the representation (Nd_i, Nd_j), n_j^i in total, corresponds a directed arrow from the *i*-th node to the j-th node, and for each complex scalar in the bifundamental of $SU(Nd_i) \times SU(Nd_j)$, M_i^j in total, corresponds an *undirected* line between the *i*-th node and the *j*-th node

Interactions. Gauge fields interact according to gauge coupling which, combined with corresponding theta angle for i th group, is writable as

$$\tau_i = \Theta_i + \frac{i}{4\pi g_i^2} = \frac{\tau d_i}{|\Gamma|}$$

where τ is complex parameter (independent i) and $|\Gamma|$ = order Γ.

Yukawa interactions. Triangles in quiver. Two directed fermion sides and an undirected scalar side.

$$S_{Yukawa} = \frac{1}{4\pi g^2} \sum d^{abc} Tr \Psi^a_{ij} \Phi^b_{jk} \Psi^c_{ki}$$

in which d^{abc} is ascertainable as Clebsch-Gordan coefficient from product of trivial representaionsoccurringrespectivelyin$(4 \otimes R_i \ddot{A} R_j^*)$,$(6 \otimes R_j \otimes R_k^*)and(4 \otimes R_k, \otimes R_i^*)$.

Quartic scalar interactions. Quadrilaterals in quiver. Four undirected sides. The coupling computable analagously to above.

Conformality. To leading order in 1/N all such theories are confromal[8, 9].

Are they conformal for higher orders?

YES, for $N = 2$. All such $N = 2$ theories are obtainable.

YES, for $N = 1$: non-renormalization theorems ensure flat direction(s).

UNKNOWN for $N = 0$.

Conformality for $N = 0$. We can offer a plausibility argument for a conformal S fixed point. If only one independent coupling occurs then the S-duality of the progenitor Type IIB superstring implies $g \rightarrow 1/g$ symmetry. If the next to leading order in 1/N is asymptotically free then IR flow increases g. Therefore for large g IR flow decreases g. Hence $\beta_g = 0$ for some intermediate g.

Applications of Conformality to Particle Phenomenology.

It is assumed that the Lagrangian is *nearly* conformal. That is, it is the soft-breaking of a conformal theory.

The soft breaking terms would involve quadratic and cubic scalar terms, and fermion mass terms. In the quiver diagram, these correspond respectively to 2-gons and triangles with undirected edges, and 2-gons with compatibly directed edges.

$$S = S_0 + \int \alpha_{ab} Tr\ \Psi^a_{lj} * \Psi^b_{ji} * + \alpha^2_{cd} Tr \Phi^c_{1j} * \Phi^d_{ji} *$$

$$+\alpha_{efg} Tr \Phi^{c}_{ij*} \Phi^{f}_{jk*} \Phi^{g}_{ki*} + c.c.$$

Depending on the sign of the scalar mass term the conformal breaking could ind gauge symmetry breaking.

Consider a gauge subgroup $SU(Ndi)$ x $SU(Ndj)$ and suppose that $< \Phi_{ij*} > \neq 0$ Assume for simplicity that $d_i = d_j = d$. Then the VEV can be represented by a Squ matrix with diagonal entries. The symmetry breaking depends on the eigenvalues. there are two equal eigenvalues and the rest zero we get:

$$SU(Nd) \text{ x } SU(Nd) +$$

$$\text{SU(2)}_{diagonal} \text{ x U(1) x } SU(\text{Nd} - 2) \text{ x } SU(\text{Nd} - 2)$$

With more such VEVs and various alignments thereof a rich pattern of gauge symme breakings can emerge.

GENERAL PREDICTIONS.

Consider embedding the standard model gauge group according to:

$$SU(3) \times SU(2) \times U(1) \subset \bigotimes_i SU(Nd_i)$$

Each gauge group of the SM can lie entirely in a SU(Nd_i) or in a diagonal subgroup of a number thereof.

Only bifundamentals (including adjoints) are possible. This implies no (8,2), etc. A conformality restriction which is new and satisfied in Nature!

No $U(1)$ factor can be conformal and so hypercharge is quantized through its incorporation in a non-abelian gauge group. This is the "conformality" equivalent to the GUT charge quantization condition in e.g. $SU(5)$!

Beyond these general consistencies, there are predictions of new particles necessary to render the theory conformal.

The minimal extra particle content comes from putting each SM gauge group in one $SU(\text{Ndi})$. Diagonal subgroup embedding *increases* number of additional *states*.

Number of fundamentals plus Nd_i times the adjoints is $4Nd_i$. Number N_3 of color triplets and N_8 of color octets satisfies:

$$N_3 + 3N_8 \geq 4 \times 3 = 12$$

Since the SM has $N_3 = 6$ we predict:

$$\Delta N_3 + 3N_8 \geq 6$$

The additional states are at TeV if conformality solves hierarchy. Similarly for color scalars:

$$M_3 + 3M_8 \geq 6 \times 3 = 18$$

The same exercise for $SU(2)$ gives $\Delta N_2 + 4N_3 > 4$ and $\Delta M_2 + 2M_3 \geq 11$ respectively.

FURTHER PREDICTIONS

Yukawa and Quartic interactions are untouched by soft-breaking terms. These are therefore completely determined by the IR fixed point parameters. So a rich structure for flavor is dictated by conformal invariance. This is to be compared with the MSSM (or SM) where the Yukawa couplings are free parameters.

GAUGE COUPLING UNIFICATION

Above the TeV scale couplings will not run. The couplings are nevertheless related, and not necessarily equal at the conformal scale.

For example, with equal $SU(Nd)$ couplings embed $SU(3)$, $SU(2)$, and $U(1)$ diagonally into 1, 3, 6 such groups respectively to obtain proximity to the correct ratios of the low-energy SM gauge couplings.

Some illustrative examples of model building using conformality:

We need to specify an embedding $\Gamma \subset SU(4)$.

Consider Z_2. It embeds as $(-1, -1, -1, -1)$ which is real and so leads to a non-chiral model.

Z_3. One choice is $4 = (\alpha, \alpha, \alpha, 1)$ which maintains N=1 supersymmetry. Otherwise we may choose $4=(\alpha, \alpha, \alpha^2, \alpha^2)$ but this is real.

Z_4. The only N = 0 complex embedding is $4=(i, i, i, i)$. The quiver is as shown on the next transparency with the $SU(N)^4$ gauge groups at the corners, the fermions on the edges and the scalars on the diagonals. The scalar content is too tight to break to the SM.

Naming the nodes 0, 1, 2, 3, 4 we identify 0 with color and the diagonal subgroups (1,3) and (2,4) with weak and hypercolor respectively. There are then three families in

$$(3, \bar{3}, 1) + (1, 3, \bar{3}) + (\bar{3}, 1, 3)$$

and one anti-family.

We suppose that the soft conformal breaking excludes a mass term marrying the third family to its mirror.

There are sufficient scalars to break to the SM with three families.

This is an existence proof.

Simplest three family model has $N = 1$ supersymmetry.

$$Z_3. \quad 4 = (\alpha, \alpha, \alpha, 1)$$

Fermions and scalars are:

$$\sum_{i=1}^{3}(3_i, \bar{3}_{i+1}) + \sum_{i=1}^{3}(8+1)_i$$

$$\beta_g^{(1)} = -\frac{g^3}{16\pi^2}\left[\frac{11}{3}C_2(G) - \frac{2}{3}T(R_W) - \frac{1}{6}T(R_R)\right]$$

Find:

$$\beta_g^{(1)} \sim 9 - 9 = 0$$

for all three $SU(3)$ factors in supersymmetric trinification.

NON-ABELIAN ORBIFOLDS

We consider all non-abelian discrete groups up to order g < 32. There are exactly 45 such groups. Because the gauge group arrived at is $\otimes_i \mathrm{SU}(Nd_i)$ we can arrive at $SU(4) \times \mathrm{SU}(2) \times SU(2)$ by choosing $N = 2$.

To obtain chiral fermions one must have $\mathbf{4} \neq \mathbf{4}^*$ This is not quite sufficient because for $N = 2$, if **4** is complex but pseudoreal, the fermions are still non-chiral [6].

This last requirement eliminates many of the 45 candidate groups. For example $Q_{2n} \subset SU(2)$ has irreps of appropriate dimensions but cannot sustain chiral fermions. because these irreps are , like $SU(2)$, pseudoreal.

This leaves 19 possible non-abelian R with g ≤ 31, the lowest order being $g = 16$. This gives only two families.

The smallest group which allows three chiral familes has order $g = 24$ so we now describe this model.

Using only D_N, Q_{2N}, S_N and T

(T = tetrahedral S_4/Z_2) one already finds 32 of the 45 non-abelian discrete groups with $g \leq 31$:

g	
6	$D_3 \equiv S_3$
8	D_4, $Q = Q_4$
10	D_5
12	D_6, Q_6, T
14	D_7
16	D_8, Q_8, $Z_2 \times D_4$, $Z_2 \times Q$
18	D_9, $Z_3 \times D_3$
20	D_{10}, Q_{10}
22	D_{11}
24	D_{12}, Q_{12}, $Z_2 \times D_6$, $Z_2 \times Q_6$, $Z_2 \times T$ $Z_3 \times D_4$, $Z_3 \times Q$, $Z_4 \times D_3$, S_4
26	D_{13}
28	D_{14}, Q_{14}
30	D_{15}, $D_5 \times Z_3$, $D_3 \times Z_5$

The remaining 13 of the 45 non-abelian discrete groups with $g \leq 31$ are twisted products:

g	
16	$Z_2 \tilde{\times} Z_8$(two, excluding D_8), $Z_4 \tilde{\times} Z_4$ $Z_2 \tilde{\times} (Z_2 \times Z_4)$(two)
18	$Z_2 \tilde{\times} (Z_3 \times Z_3)$
20	$Z_4 \tilde{\times} Z_5$
21	$Z_3 \tilde{\times} Z_7$
24	$Z_3 \tilde{\times} Q$, $Z_3 \tilde{\times} Z_8$, $Z_3 \tilde{\times} D_4$
27	$Z_9 \tilde{\times} Z_3$, $Z_3 \tilde{\times} (Z_3 \times Z_3)$

Successful $g = 24$ model is based on the group $\Gamma = Z_3, \times Q$.

The fifteen irreps of Γ are

1, 1′, 1″, 1‴ 2,

1α, 1′α, 1″α, 1‴α, 2α,

1α–1, 1′α^{-1}, 1″α^{-1}, 1‴α^{-1}, 2α^{-1}

The same model occurs for $\Gamma = Z_3 \times D_4$. The multiplication table is shown below.

	1	$1'$	$1''$	$1'''$	2
1	1	$1'$	$1''$	$1'''$	2
$1'$	$1'$	1	$1'''$	$1''$	2
$1''$	$1''$	$1'''$	1	$1'$	2
$1'''$	$1'''$	$1''$	$1'$	1	2
2	2	2	2	2	$1+1'$ $1''+1'''$
1α	1α	$1'\alpha$	$1''\alpha$	$1'''\alpha$	2α
$1'\alpha$	$1'\alpha$	1α	$1'''\alpha$	$1''\alpha$	2α
$1''\alpha$	$1''\alpha$	$1'''\alpha$	1α	$1'\alpha$	2α
$1'''\alpha$	$1'''\alpha$	$1''\alpha$	$1'\alpha$	1α	2α
2α	2α	2α	2α	2α	$1\alpha+1'\alpha$ $1''\alpha+1'''\alpha$

etc.

The general embedding of the required type can be written:

$\mathbf{4} = (1\alpha^{a1},\ 1'\alpha^{a2}\ \ 2\alpha^{a3})$

The requirement that the **6** is real dictates that

$a_1 + a_2 = -2a_3$

It is therefore sufficient to consider for $N = 0$ no surviving supersymmetry only the choice:

$\mathbf{4} = (\ 1\alpha,\ 1',\ 2\alpha)$

It remains to derive the chiral fermions and the complex scalars using the procedures already discussed (quiver diagrams).

$D_4 \times Z_3$ MODEL.

VEVs for these scalars allow to break to the following diagonal subgroups as the only surviving gauge symmetries:

$SU(2)_{1,2,3} \rightarrow SU(2)$

$SU(2)_{5,6,7} \rightarrow SU(2)$

$SU(4)_{1,2} \rightarrow SU(4)$

This spontaneous symmetry breaking leaves the Pati-Salam type model:

$SU(4) \times SU(2) \times SU(2)$

with three chiral fermion generations

$3\ [(\ 4,\ 2,\ 2) + (\ 4\ 2,\ 2)]$

INCLUSION OF GRAVITY.

The CFT arrived at is in a flat spacetime background which does not contain gravity.

One way to introduce the four-dimensional graviton introduces an extra spacetime dimension and truncates the range of the fifth dimension. The four-dimensional graviton then appears by compactification of the higher-dimensional graviton, as is certainly the path suggested by the superstring.

Although conformality solves the hierarchy between the weak scale and the GUT scale, the hierarchy existing in non-string theory without gravity, it is clear that classical gravity violates conformal invariance because of its dimensional Newton coupling constant. The inclusion of gravity in the conformality scheme most likely involves a change in the spacetime at the Planck scale; one possibility being explored is noncommutative spacetime coordinates [18]. Another even more radical idea is the one already mentioned to invoke [19] at TeV scales an extra spacetime coordinate.

SUMMARY.

Conformality is seen to be a rigid organizing principle. Many embeddings remain to be studied. Soft breaking of conformal symmetry deserves further study, as does the even more appealing case of spontaneous breaking of conformal symmetry.

The latter could entail flat directions even in the absence of supersymmetry and if this is really possible one would need to invoke a symmetry different from supersymmetry to generate the flat direction.

This would lead naturally to an explanation of the vanishing cosmological constant different from any where a fifth spacetime dimension is invoked [20, 21].

New particles await discovery at the TeV scale if the conformality idea is valid.

Acknowledgement.

This work was supported in part by the US Department of Energy under Grant No. DE-FG02-97ER41036.

REFERENCES

1. P.H. Frampton Phys Rev D60 041901 (1999).
2. P.H. Frampton and W.F. Shively, Phys Lett **B454** 49 (1999).
3. P.H. Frampton and C. Vafa. hep-th/9903226.
4. P.H. Rampton, Phys. Rev. **D60,** 085004 (1999).
5. P.H. Frampton, Phys. Rev. **D60,** 121901 (1999).
6. P.H. Frampton and T.W. Kephart. hep-th/9912028.
7. G. 't Hooft. Cargese Summer School. (1979). page 135.
8. M. Bershadsky, Z. Kakushadsky and C. Vafa, Nucl. Phys. **523,** 59 (1998).
9. M. Bershadsky and A. Johansen, Nucl Phys **B536** 141 (1998).
10. J. Maldacena, Adv Theor Math Phys 2 231 (1998).
11. M. Douglas and G. Moore. hep-th/9603167.
12. P.H. Frampton and T.W. Kephart, Phys. Rev. Lett. **50,** 1343 (1983).
13. P.H. Frampton and T.W. Kephart, Phys. Rev. Lett. **50,** 1347 (1983).
14. P.H. Frampton and S.L. Glashow, Phys. Lett. **B190,** 157 (1987);
15. P.H. Frampton and S.L.Glashow, Phys. Rev. Lett. **58,** 2168 (1987).
16. P.H. Frampton, Phys. Rev. Lett. **69,** 2889 (1992).
17. P.H. Frampton and D. Ng, Phys. Rev. **D45,** 4240 (1992)
18. S. Minwalla, M. Van Raamsdonk and N. Seiberg. hep-th/9912072.
19. I. Antoniadis, Phys. Lett. **B246,** 377 (1990).
20. S. Kachru, M. Schulz and E. Silverstein. hep-th/0001206
21. N. Arkani-Hamed, S. Dimopoulos, N. Kaloper and R. Sundrum. hep-th/0001197

This page intentionally left blank.

ETERNAL INFLATION AND THE PRESENT UNIVERSE

Alexander Vilenkin

Department of Physics and Astronomy,
Tufts University, Medford, MA 02155

INTRODUCTION

I am going to discuss the structure of the universe on super-large scales, so large that we are never going to observe them. I shall argue, however, that this analysis may help us understand some features of the universe within the observable range. This is based on the work done with my student Vitaly Vanchurin at Tufts arid with Serge Winitzki at Cambridge University.

Let me begin with a brief introduction to eternal inflation. As we know, inflation is a nearly exponential expansion of the universe,

$$a(t) \approx eHt, \tag{1}$$

which is driven by the potential energy of a scalar field W, called the inflaton. a(t) in Eq.(1) is the scale factor and the expansion rate H is determined by the inflaton potential V(φ). Inflation ends when ϕ starts oscillating about the minimum of the potential. Its energy is then dumped into relativistic particles and is quickly thermalized.

A remarkable feature of inflation is that generically it never ends completely. At any time, there are parts of the universe that are still inflating[1,2]. The reason is that the evolution of φis influenced by quantum fluctuations. This applies in particular to the range of φnear the maximum of V(φ), where the potential is very flat. As a result, thermalization does not occur everywhere at the same time. We can introduce a decay constant Γ such that t = 1/Γ is the characteristic time it takes φ to get from the maximum to the minimum of the potential. Then the total inflating volume in the universe is proportional to

$$V_{inf} \propto e^{-\Gamma t}\ e^{3Ht}. \tag{2}$$

The first factor on the right-hand side describes the exponential decay of the inflating volume due to thermalization, while the second factor describes the exponential expansion of the regions which still continue to inflate. For flat potentials required for successful inflation, we typically have $\Gamma \ll 3H$, so that Vinf grows exponentially with time. The thermalized volume grows at the rate $dV_{therm}/dt = \Gamma dV_{inf}/dt$ and thus V_{therm} also grows exponentially.

Different thermalized regions in such eternally inflating universe may have very different properties. Here are some examples.

Quantum Gravity. Generalized Theory of Gravitation. and Superstring Theon-Bused Unification
Edited by Kursunoglu *et al.*. Kluwer Academic / Plenum Publishers. New York. 2000

The potential $V(\varphi)$ may have several minima corresponding to vacua with different physical properties. For example, the values of some constants of Nature (e.g., the electron mass or the cosmological constant) or cosmological parameters (such as the amplitude of density fluctuations, the baryon to entropy ratio, etc.) could be different in the corresponding thermalized regions. A more interesting possibility is that the "constants" are related to some slowly-varying fields and take values in a continuous range. For example, the inflaton could be a complex field, $\varphi = |\varphi| \exp(i\chi)$, with a potential having the shape of a "deformed Mexican hat" (that is, with some χ-dependence). Then different paths that φ can take from the top of the potential to the bottom will result in different magnitudes of density fluctuations $\delta p/p$. The amplitude of the fluctuations will therefore be different in different parts of the universe. Another example is a field χ (unrelated to the inflaton) with a self-interaction potential $V(\chi)$. If $U(\chi)$ is a very slowly varying function of χ, then it can act as an effective cosmological constant. Quantum fluctuations will randomize χ during inflation, and observers in different parts of the universe will measure different values of $U(\chi)$.

Perhaps the most important example is the spectrum of cosmological density fluctuations. The density fluctuation $\delta\rho/\rho(l)$ is determined by the quantum fluctuation $\delta\varphi(l)$ of the inflaton field φ at the time when the corresponding comoving scale l crossed the horizon. Different realizations of quantum fluctuations $\delta\varphi(l)$ result in different density fluctuations spectra in widely separated parts of the universe. This uncertainty is present in *all* models of inflation.

In all these examples, we have parameters χ which we cannot possibly predict with certainty. All we can hope to do is to determine the probability distribution $P(\chi)$.

An eternally inflating universe is inhabited by a huge number of civilizations that will measure different values of x. We can define the probability $P(\chi)d\chi$ as being proportional[3] to the number of observers who will measure x in the interval $d\chi$. Now, observers are where galaxies are, and thus $P(\chi)d\chi$ is proportional to the number of galaxies in regions where χ takes values in the interval dx. We can then write

$$P(\chi) \propto F(\chi) v(\chi), \tag{3}$$

where $F(\chi)d\chi$ is the fraction of volume in thermalized regions with χ in the interval dx, and $V(\chi)$ is the number of galaxies per unit volume (as a function of x). It is convenient to consider comoving regions and to measure their volumes at the time of thermalization. The calculation of $v(\chi)$ is a standard astrophysical problem, and here I shall focus on the volume factor $F(x)$.

In this discussion I am trying to avoid the word "anthropic", because it makes some people very upset, but what I want to emphasize is that the approach I have just outlined is as quantitative and predictive as it can possibly be. Once $P(\chi)$ is calculated, we can predict, for example, that χ should have a value in a certain range with 95% confidence.

The first attempts to implement this approach encountered an unexpected difficulty. It can be traced down to the fact that eternal inflation never ends, and the number of galaxies in an eternally inflating universe is infinite at $t \to 8$. In order to calculate the volume fraction $F(\chi)$, one therefore has to compare infinities, which is an inherently ambiguous procedure. One can introduce a time cutoff and include only galaxies that formed prior to some time t_c, with the limit $t_c \to 8$ at the end. One finds, however, that the resulting probability distributions are extremely sensitive to the choice of the time coordinate t[4, 5]. Linde, Linde and Mezhlumian[6] attempted to determine the most probable spectrum of density fluctuations using the proper time along the worldlines of comoving observers, which they regarded as the most natural

choice of the time coordinate. They found a probability distribution suggesting that a typical observer could find herself at a deep minimum of the density field. On the other hand, if one uses the expansion factor along the worldlines as the time coordinate, one recovers the standard result[7]. Coordinates in general relativity are arbitrary labels, and such gauge-dependence of the results is, of course, an embarrassment.

The rest of the paper is organized as follows. After reviewing the physics of eternal inflation, I shall discuss the origin of the gauge-dependence problem and its proposed resolution. Then, as a specific application, I shall analyze the spectrum of density fluctuations measured by a typical observer. Finally, I shall briefly summarize the conclusions.

ETERNAL INFLATION

The metric of an inflating universe has a locally Robertson-Walker form,

$$ds^2 = dt^2 - a^2(t)dx^2, \tag{4}$$

with the expansion rate given by

$$a/a \approx H(W) = [8\pi V(\varphi)/3]^{1/2} \tag{5}$$

The potential $V(\varphi)$ is assumed to be a slowly varying function of W. As a result, H is a slowly varying function of the coordinates, and we have an approximately de Sitter space with a horizon distance H^{-1}. The classical slow-roll evolution equation for W is

$$W_{cl} \approx -H'(W)/4\pi \tag{6}$$

Quantum fluctuations of W can be represented as a random walk with random steps taken independently in separate horizon-size regions, with one step per Hubble time H^{-1}. The rms magnitude of the steps is

$$\delta\varphi_{rms} = (H/2\pi). \tag{7}$$

We do not have a completely satisfactory derivation of this stochastic picture in the general case. Its main justification is that it reproduces the results of quantum field theory in de Sitter space for a free scalar field of mass $m \ll H$ (that is, the two-point function obtained by averaging a classical stochastic field coincides with the quantum two point function). For flat inflaton potentials, the dynamics of φ should be close to that of a free field, so one expects the stochastic picture to apply with a good accuracy.

Let us define the distribution $F(\varphi, t)d\varphi$ as the volume occupied by φ in the interval $d\varphi$ at time t. It satisfies the Fokker-Planck equation[1, 8, 9, 10, 11, 4]

$$\partial_t F + \partial_\varphi J = 3H^\alpha F, \tag{8}$$

where

$$J = -\frac{1}{8\pi^2}\partial_\varphi (H^{\alpha+2}F) - \frac{1}{4\pi}H^{\alpha-1}H'F. \tag{9}$$

The first term of the flux J describes quantum "diffusion" of the field φ, while the second term corresponds to the classical "drift" described by Eq.(6). The parameter Q in Eqs.(8),(9) represents the freedom of time parametrization, with the time variable t related to the proper time τ according to $dt = H^{1-\alpha}d\tau$. Hence, $\alpha = 1$ corresponds to the proper time, $t = \tau$, and $\alpha = 0$ to the scale factor time, $t = \ln a$.

A great deal of research has been done on the properties of the Fokker-Planck equation (8) and on its solutions. To summarize the conclusions, there are some good news and some bad news. The good news is that the asymptotic form of the solutions of (8) is

$$F(\phi, t) \longrightarrow F(\phi) e^{\gamma t} \qquad (t \to \infty). \tag{10}$$

The overall factor $e^{\gamma t}$ drops out in the normalized distribution, and thus one gets a stationary asymptotic distribution for φ. The bad news is that $F(\varphi)$ has a strong dependence on a, so that the results are very sensitive to the choice of the time coordinate[4]. This very disturbing result lead some authors to doubt that a meaningful definition of probabilities in an eternally inflating universe is even in principle possible [4, 6]. We shall see, however, that these pessimistic conclusions may have been premature.

THE PROPOSAL

The gauge dependence of the probability distributions obtained using a constant-time cutoff can be understood as follows. The factor $F(\mathcal{X})$ in Eq.(3) is the probability distribution of the fields $\mathcal{X}$ on the thermalization hypersurface Σ_* which separates inflating and thermalized spacetime regions. It is an infinite spacelike surface which plays the role of the big bang for the thermalized region that lies to its future. Due to the stochastic nature of inflation, this surface is rather irregular and is in general multiply connected. The time variable t is usually defined in terms of some geometric or scalar field variables, and since these variables are subject to significant fluctuations, the cutoff surface $\Sigma_c : t = const$ is also expected to be rather irregular. The intersection with Σ_c cuts an infinite number of predominantly small pieces off the surface Σ_*, and the distribution $F(\mathcal{X})$ is to be calculated on this population of pieces. A change of the time variable t results in a deformation of the cutoff surface, accompanied by a substantial change in the population of the regions of $\Sigma*$ that are being included. The resulting probability distribution is also substantially modified.

The resolution of the gauge dependence problem that I proposed in Ref.16 is to calculate the probability distribution for $\mathcal{X}$ within a single, connected domain on the thermalization surface Σ_*. If the field $\mathcal{X}$ varies in a finite range, it will run through all of its values many times in a sufficiently large volume. We expect, therefore, that the distribution $F(\mathcal{X})$ will converge rapidly as the volume is increased. It does not matter which thermalized domain we choose to calculate probabilities: all domains are statistically equivalent, due to the stochastic nature of quantum fluctuations in eternal inflation. This is a very simple prescription, and I am a bit embarrassed that I did not, think of it earlier, having thought about this problem for a number of years.

With this prescription, the volume distribution $F(\mathcal{X})$ can be calculated directly from numerical simulations, and we have done that in Ref.13. In some cases an analytic calculation is also possible. Suppose, for example, that the potential $V(\varphi x)$ is essentially independent of $\mathcal{X}$ for $|\varphi| < \varphi_0$, where W0 is in the deterministic slow-roll range, where quantum fluctuations of f and x can be neglected compared to the classical drift. Then, the evolution of φ at $\varphi > j_0$ is monotonic, and a natural choice of the time variable in this range is $t = \varphi$ The probability distribution for X on the constant-"time" surface $\varphi = \varphi_0$ is

$$F_{0,}(\mathcal{X}) = F(\varphi_0, \mathcal{X}) = const. \tag{11}$$

since all values of $\mathcal{X}$ are equally probable at $\varphi < \varphi_0$. We are interested in the probability distribution on the thermalization surface, $F(\mathcal{X}) = F(\varphi_*, \mathcal{X})$, where $\varphi*$ is the value of

φ at thermalization. This is given by[16]

$$F(\chi) \propto F_0(\chi_0) \exp[3N(\chi_0)] det \left| \frac{\partial \chi_0}{\partial \chi} \right|. \quad (12)$$

Here, $\mathcal{X}_o$ is the value of $\mathcal{X}$ at φ = φ_0 that classically evolves into $\mathcal{X}$ at φ ∗, *N(x0)* is the number of e-foldings along this classical path, exp(3*N*) is the corresponding enhancement of the volume, and the last factor is the Jacobian transforming from *Xo* to x. In many interesting cases, $\mathcal{X}$ does not change much during the slow roll. Then,

$$F(\mathcal{X}) \propto \exp[3N(\mathcal{X})]. \quad (13)$$

In a more general case, when the diffusion of $\mathcal{X}$ is not negligible at φ> φ_0, the distribution $F(\mathcal{X})$ can be found by solving the Fokker-Planck equation with t = W in the range $\varphi_0 < \varphi < \varphi^*$ and with the initial condition (11). The corresponding form of the equation was derived in Ref. 13,

$$\frac{\partial F}{\partial \varphi} = -\partial_\chi^2 \left(\frac{H^3 F}{2\pi H'_\varphi} \right) - \partial_\chi \left(\frac{H'_\chi}{H'_\varphi} F \right) - \frac{12\pi H}{H'_\varphi} F. \quad (14)$$

We have solved this equation with the same parameters that we used in numerical simulations and compared the resulting probability distribution F($\mathcal{X}$) with the distribution obtained directly from the simulations. We found very good agreement between the two (see Ref.13 for details).

DENSITY FLUCTUATIONS

As a specific application of the proposed approach, let us consider the spectrum of density perturbations in the standard model of inflation with a single field W. The perturbations are determined by quantum fluctuations δφ; they are introduced on each comoving scale at the time when that scale crosses the horizon and have a gauge-invariant amplitude[7]

$$\delta \rho/\rho = 8 \pi H \delta \varphi / H', \quad (15)$$

where $H_I = dH/d\varphi$. With an rms fluctuation (δ φ)$_{rms}$ = $H/2\pi$, this gives

$$(\delta\rho/\rho)_{rms} = 4H^2 / |H'|. \quad (16)$$

Fluctuations of φon different length scales are statistically independent and can be treated separately. We can therefore concentrate on a single scale corresponding to some value φ = φ_0, disregarding all of the rest.

On the equal-"time" surface φ = φ_0, the fluctuations δ φ can be regarded as random Gaussian variables with adistribution

$$F_0(\delta\varphi \propto \exp\left[-\frac{2\pi^2}{H_0^2} (\delta\varphi)^2 \right], \quad (17)$$

where $H_0 = H$ (W0). We are interested in th distribution F(dj)on the terminalization surface φ = φ*. This will be different from F 0 if there is some correlation between δφ and the amount of inflationary expansion in the period between φ_0 and φ*. In fact, there is such a correlation. If φ fluctuates in the direction opposite to the classical roll, then inflation is prolonged and the expansion factor is increased. Otherwise, it is decreased, and we can write

$$F(\delta\varphi) \propto F_0(\delta\varphi) \exp(3H_0 \delta t), \quad (18)$$

where

$$\delta t = -(4\pi/H'_0)\delta\varphi \tag{19}$$

is the time delay of the slow roll due to the fluctuation $\delta\varphi$.

Combining Eqs.(17)-(19), we obtain[16]

$$F(\delta\varphi) \propto \exp\left[-\frac{2\pi^2}{H_0^2}(\delta\varphi - \bar{\delta\varphi})^2\right], \tag{20}$$

which describes Gaussian fluctuations with a nonzero mean value,

$$\delta\varphi = 3H_0^3/\pi H'0. \tag{21}$$

This is different from the standard approach[7] which disregards the volume enhancement factor and uses the distribution (17). The effect, however, is hopelessly small. Indeed,

$$\frac{\bar{\delta\varphi}}{(\delta\varphi)_{rms}} = \frac{6H_0^2}{H'_0} \sim \left(\frac{\delta\rho}{\rho}\right)_{rms} \sim 10^{-5}. \tag{22}$$

We thus see that the standard results remain essentially unchanged.

CONCLUSIONS

Eternally inflating universes can contain thermalized regions with different values of the cosmological parameters, which we have denoted generically by $\mathcal{X}$. We cannot then predict $\mathcal{X}$ with certainty and can only find the probability distribution P($\mathcal{X}$). Until recently] it was thought that calculation of P inevitably involves comparing infinite volumes, and therefore leads to ambiguities. My proposal is to calculate P in a single thermalized domain. The choice of the domain is unimportant, since all thermalized domains are statistically equivalent. This apprach gives unambiguous results. When applied to the spectrum of density fluctuations, it recovers the standard results with a small correction $O(10^{-5})$.

It should be noted that this approach cannot be applied to models where $\mathcal{X}$ is a discrete variable which takes different values in different thermalized regions, but is homogeneous within each region. One can take this as indicating that no probability distribution for a discrete variable can be meaningfully defined in an eternally inflating universe. Alternatively] one could try to introduce some other cutoff prescription to be applied specifically in the case of a discrete variable. Some possibilities have been discussed in Refs.17, 18. This issue requires further investigation.

ACKNOWLEGEMENTS

It is a pleasure to thank Berham Kursunoglu for organizing this stimulating and enjoyable meeting. This work was supported in part by the National Science Foundation.

REFERENCES

1. A. Vilenkin, Phys. Rev. **D27,** 2848 (1983).
2. A. D. Linde, Phys. Lett. **B175,** 395 (1986).
3. A. Vilenkin, Phys. Rev. Lett. **74,** 846 (1995).

4. A. D. Linde, D. A. Linde, and A. Mezhlumian, Phys. Rev. **D49,** 1783 (1994).
5. S. Winitzki and A. Vilenkin, Phys. Rev. **D53,** 4298 (1996).
6. A. D. Linde, D. A. Linde, and A. Mezhlumian, Phys. Lett. **B345,** 203 (1995); Phys. Rev. **D54,** 2504 (1996).
7. For a review of density fluctuations in inflationary scenarios, see, e. g., V. F. Mukhanov, H. A. Feldman, and R. H. Brandenberger, Phys. Rep. **215,** 203 (1992).
8. A. A. Starobinsky, in Lecture Notes in Physics Vol. 246 (Springer, Heidelberg, 1986).
9. A.S. Goncharov, A.D. Linde and V.F. Mukhanov, Int. J. Mod. Phys. **A2**, 561 (1987).
10. Y. Nambu and M. Sasaki, Phys. Lett. **B219,** 240 (1989); K. Nakao, Y. Nambu and M. Sasaki, Prog. theor. phys. **80,** 1041 (1988).
11. D. S. Salopek and J. R. Bond, Phys. **Rev.D43,** 1005 (1991).
12. A. Vilenkin, Phys. Rev. Lett. **81,** 5501 (1998).
13. V. Vanchurin, A. Vilenkin and S. Winitzki, gr-qc/9905097.
14. A. Vilenkin, Phys. Rev. **D52,** 3365 (1995).
15. A. Vilenkin and S. Winitzki, Phys. Rev. **D55,** 548 (1997).

This page intentionally left blank.

COSMIC RAYS, COSMIC MAGNETIC FIELDS, AND MAGNETIC MONOPOLES

Thomas W. Kephart, Thomas J. Weiler, and Stuart D. Wick

Department of Physics and Astronomy,
Vanderbilt University,
Nashville, TN 37235.

Abstract

Observations and models of galactic and extragalactic magnetic fields lead to the conclusion that monopoles of mass $\lesssim 10^{15}$ GeV are accelerated in these fields to relativistic velocities. We explore the possible signatures of a cosmic flux of relativistic monopoles impinging on the earth.

INTRODUCTION

We discuss the possibility that light magnetic monopoles are cosmic ray primaries. The inferred strength and coherence size of existing extragalactic magnetic fields suggest that any monopole with a mass near or less than 10^{15} GeV would have been accelerated in magnetic fields to relativisitic velocities. On striking matter, such as the Earth's atmosphere, these relativistic monopoles will generate a particle cascade. Here we investigate the shower signatures of relativistic magnetic monopoles.

The monopole flux is limited only by Parker's upper bound Fp $\sim 10^{-15}/\text{cm}^2/\text{s}/\text{sr}$ [1], which results from requiring that monopoles not short–circuit our Galactic magnetic fields faster than their dynamo can regenerate them. Since the Parker bound is several orders of magnitude above the observed highest–energy cosmic ray flux, existing cosmic ray detectors can meaningfully search for a monopole flux.

Because of their mass and integrity, a single monopole primary will continuously induce air–showers, in contrast to nucleon and photon primaries which transfer nearly all of their energy at shower initiation. Thus we expect the monopole shower to be readily distinguished from non–monopole initiated showers. However, we also investigate the possibility that the hadronic interaction of the monopole is sufficiently strong to produce air–showers with dE/dx comparable to that from nuclear primaries, in which case existing data would already imply a meaningful limit on the monopole flux. One may even speculate that monopoles with a large dE/dx have been observed, as the primaries producing the enigmatic showers above the GZK cutoff at $\sim 5 \times 10^{19}$ eV [2, 3].

Quantum Grav ity Generalized Theory of Gra vitation and Superstring Theory -Based Unification
Edited by Kursunoglu *et al* Kluwer Academic / Plenum Publishers New York 2000

MONOPOLES IN MAGNETIC FIELDS

The number density and therefore the flux of monopoles emerging from a phase transition are determined by the Kibble mechanism [4], where at the time of the phase transition, roughly one monopole or antimonopole is produced per correlated volume. The resulting monopole number density today is

$$nM \sim 10^{-19} \ (T_c/10^{11}\text{GeV})^3 (l_H/\xi c)^3 \ \text{cm}^{-3} \tag{1}$$

where ξc is the phase transition correlation length, bounded from above by the horizon size l_H at the time when the system relaxes to the true broken-symmetry vacuum. The correlation length may be comparable to the horizon size (second order or weakly first order phase transition) or considerably smaller than the horizon size (strongly first order transition).

To avoid overclosing the universe, the monopole mass density today, relative to the closure value, is

$$\Omega M \sim 0.1 \, (M/10^{13}\text{GeV})^4 (l_H/\xi_c)3. \tag{2}$$

Hence, monopoles less massive than $\sim 10^{13}(\xi_c/l_H)^{3/4}$ GeV are allowed. Requiring that the Kibble flux be less than the Parker limit $F = FP < 10^{-15}/\text{cm}_2/\text{sec/sr}$, one derives a combined mass bound [3]

$$M \lesssim 10^{11}(\xi_c/\text{lH}) \, \text{GeV} \tag{3}$$

which is stronger than the curvature constraint by about two orders of magnitude.

The general expression for the relativistic monopole flux may be written [3]

$$F_M = c \, n_M/4\pi \sim 2 \times 10^{-4} \left(\frac{M}{10^{15}\text{GeV}}\right)^3 \left(\frac{l_H}{\xi_c}\right)^3 \ \text{cm}^{-2} \ \text{sec}^{-1} \ \text{sr}^{-1} . \tag{4}$$

The energy–density constraint for relativistic monopoles is stronger than that for non–relativistic monopoles,

$$\Omega \text{RM} \sim \left(\frac{\langle \text{EM} \rangle}{\text{mpl}}\right) \left(\frac{F_M}{\text{Fp}}\right) \ , \tag{5}$$

where mP1 is the Plank mass. This shows that a Kibble monopole flux respecting the Parker limit cannot overcurve the universe, regardless of the nature of the monopole–creating phase transition (parameterized by ξ_c/lH), as long as $(\text{EM}) \lesssim m\text{Pl}$.

Although minimal $SU(5)$ breaking gives monopoles of mass ~ 1017 GeV, there are ample theoretical possibilities for producing monopoles with mass $\lesssim 10^{15}$ GeV and the possibility of strong interaction cross–sections that avoid proton decay [5,6,7,8]. Based on the Kibble mechanism for monopole production, bounds on the universe's curvature constrain the monopole mass to less than 10^{13} GeV, while a comparison of the Kibble flux to the Parker limit constrains the monopole mass to less than 10^{11} GeV. However, we note that in higher dimensional cosmologies, the Kibble flux given in eq. (4) may be altered. If the Kibble flux estimate is changed, then the straightforward Parker upper limit $\text{Fp} \leq 10^{-15}/\text{cm}^2/\text{sec/sr}$ becomes the only reliable bound on the monopole flux. Thus, in the spirit of generality, we will let M be a free parameter and use the Kibble mechanism as a rough guide to F_M. We will, of course, require that F_M obey the Parker limit. We also will assume that proton decay is avoided in a way that does not restrict the parameter M.

Monopole Structure

Monopoles are topological defects with a non-trivial internal structure; the core of the monopole is a region of restored unified symmetry. Monopoles are classified [4] by their topological winding, but for the case of GUT monopoles this classification is too coarse. In an $SU(5)$ GUT the fundamental minimally-charged monopole is six-fold degenerate. For an appropriate Higgs potential there are four other types of stable bound states formed from the fundamental monopoles [9, 10]. In this work we need to distinguish between those monopoles with color–magnetic charge and those with only ordinary ($U_{EM}(1)$) magnetic charge. Thus, we adopt the nomenclature *"q–*monopoles" for those monopoles with color–magnetic charge and "*l–*monopoles" for those with only the ordinary magnetic charge. The possible confinement of magnetic monopoles has recently been considered [11] via the formation of Z_3 color–magnetic "strings." If such a mechanism was realized one result could be the formation of color–singlet "baryonic–monopoles." The fusion of three differently colored strings produces a baryon–like composite of fundamental GUT monopoles. The internal structure of a baryonic–monopole would approximate that of an ordinary baryon in the QCD string model, but with q–monopoles in the place of quarks. Thus, the baryonic–monopole structure is quite different from a single *l–*monopole and, as such, we expect it to have a very different cross–sectionand cosmic ray shower profile.

Monopole Acceleration

The kinetic energy imparted to a magnetic monopole on traversing a magnetic field is [3]

$$E_K = gB\ 1c\vec{\xi}\,.\,\hat{dv}\,, \tag{6}$$

where

$$g = e/2\alpha = 3.3 \times 10^{-8} \text{ esu} \quad (\text{or } 3.3 \times 10^{-8} \text{dynes/G}) \tag{7}$$

is the Dirac magnetic charge, B is the magnetic field strength, $\vec{\xi}$ specifies the field's coherence length and direction, C is the curve describing the monopole path, and $\hat{dv}$ is the direction of the monopole velocity at a given point along the path. Galactic magnetic fields and magnetic fields in extragalactic sheets and galactic clusters range from about 0.1 to 100μG, while their coherence lengths range from 10^{-4} to about 30Mpc [12, 13]. These fields can accelerate a monopole from rest to the energy range 2×10^{20} to 5×10^{23} eV. Monopoles that random walk N steps through a set of domains are expected to pick up an additional factor of $\sqrt{N}$ in their energy. For extragalactic sheets, which we expect to dominate the spectrum, this number can be roughly estimated to be of order $N \sim H_0^{-1}/50\text{Mpc} \sim 100$, and so $E_{max} \sim 10^{25}$ eV. Hence, monopoles with mass below $\sim 10^{15}$ GeV are relativistic. The rest of this talk is devoted to the novel phenomenology of relativistic monopoles. As a prelude to calculating monopole signatures in various detectors, we turn to a discussion of the interactions of monopoles with matter.

RELATIVISTIC MONOPOLE ENERGY LOSS IN MATTER

Regardless of the interaction, the fact that the monopole is conserved in each interaction, due to its topological stability, argues for kinematics rather different from those applying to nucleon or photon primaries. The differing kinematics in turn argues for differing signatures. However, our explorations of possible strong interactions will

include a model where q-monopoles are excited and their hadronic cross–section grows after impact, so that the energy transfer is large enough to stop the monopole very quickly. In this model, the monopole's hadronic signature may be similar to that from a nucleon.

The strong interaction of a monopole is difficult to assess. Color confinement ensures that all monopoles are color singlet objects, and so have no classical long–range color–magnetic field. However, we expect l-monopoles and q-monopoles to have very different hadronic interactions. Although l-monopoles lack a color–magnetic charge, the unbroken symmetry in their core ensures that gluon and light quark fields will leak out from the center to the confinement distance $\Lambda_{QCD}^{-1} \sim$ fm.

We will resume the discussion of the monopole's hadronic interaction with matter after first discussing in some detail their better–understood electromagnetic interactions. The electromagnetic interaction of the monopole may dominate the hadronic interaction because the electromagnetic coupling of the monopole is large, $\alpha_M = g^2 = \frac{1}{4\alpha} \simeq 34$ and mediated by a long–range field. At large distances and high velocities, the magnetic monopole mimics the electromagnetic interaction of a heavy ion of charge $Z \sim \frac{1}{2}\alpha \simeq 68$. We will view the monopole as a classical source of radiation, while treating the matter–radiation interaction quantum mechanically. In this way, the large electromagnetic coupling of the monopole is isolated in the classical field, and the matter–radiation interaction can be calculated perturbatively.

Electromagnetic Interactions

We consider here the energy losses of the monopole due to the three electromagnetic processes: collisions (ionization of atoms), e^+e^- pair production, and bremsstrahlung. It will turn out that Bethe–Heitler pair production will be the dominant mechanism for the growth of the total shower electron number N_e, which in turn is the source generating the Cherenkov and radio wave signatures. On the other hand, the bremsstrahlung process will be the major energy loss mechanism and so is the main contributor to the nitrogen fluorescence signature.

The monopole-matter electromagnetic interaction for $\gamma < 100$ is well reported in the literature [14, 151. Previous works include atomic excitations and ionization losses with electrons in the absorber. The density suppression effect is also included. These effects are collectively referred to as "collisional" energy losses.

For $\gamma > 100$ the expression for collisional energy losses needs to be modified [16, 17], and *QED* effects like primary particle bremsstrahlung and electron-positron pair production can become operative. As we are interested in the energy loss of ultrarelativistic monopoles in matter, we will need to consider these processes. Here we only have space to collect the results. See [15] and [17] for more details.

$$\frac{dE}{dx} = \frac{dE_{\text{coll}}}{dx} + \frac{dE_{\text{pair}}}{dx} + \frac{dE_{\text{brem}}}{dx} + \frac{dE_{\text{had}}}{dx} \tag{8}$$

where

$$\frac{dE_{\text{coll}}}{dx} = -\frac{\pi N_e}{m_e}\left[\ln\left(\frac{m_e\beta^2\gamma^2}{I}\right) - \frac{\delta}{2}\right]. \tag{9}$$

N_e is the electron number density of the absorber, I is the mean ionization energy of the medium, and δ is the density effect;

$$\frac{dE_{\text{pair}}}{dx} \simeq -\frac{16}{3\times 10^3}\frac{g^2e^2Z\alpha N_e}{m_e}\gamma\ln(\gamma) \simeq -\frac{Z\alpha N_e}{10^3 m_e}\gamma\ln(\gamma), \tag{10}$$

where Z is the atomic number of the atoms comprising the absorber;

$$\frac{dE_{\rm rad}}{dx} \simeq -\frac{16}{3}\frac{ZN_e\,\alpha\,\alpha_M^2}{M}\gamma\ln\gamma \simeq -\frac{137}{3}\frac{ZN_e}{M}\gamma\ln(\gamma), \tag{11}$$

and the energy loss for baryonic-monopoles can be approximated as

$$\frac{dE_{\rm had}}{dx}(x) \simeq -\frac{\gamma\,\Lambda_{QCD}}{\lambda(x)} \simeq -\gamma\,\Lambda_{QCD}\,N_n\,l(x)\,\sigma_{\rm had}, \tag{12}$$

where $l(x) = 1$ for l-monopoles, but for q-monopoles the strong cross-section $\sigma(x) = l(x)$ shad is explicitly a function of column depth x.

Monopole Electromagnetic Signatures

Signature events for l-monopoles are discussed with a specific emphasis on 1) the general shower development, 2) Cherenkov signatures, and 3) earth tomography with relativistic l-monopoles. The general shower characteristics are developed first, as the other signatures are derivable from that model. The I-monopoles will be highly penetrating primaries, interacting mostly via the electromagnetic force and all the while maintaining their structural integrity. On average, there will be a quasi-steady cloud of secondary particles traveling along with the l-monopole. Thus, we will call this type of shower "monopole–induced."

Given a fast monopole passing through matter, the various electromagnetic processes can inject energetic photons, electrons, and positrons into the absorbing medium. If the energy of these injected secondary particles is sufficient, they may initiate a particle cascade. In [17] we review a simple model to describe such a cascade. An electromagnetic cascade can be initiated by an electron, positron or photon. In the simple model we consider, the photon pair production length is equal to the electron (or positron) radiation length. In this model, originally developed by Heitler [18], photon and electron showers will develop identically. After reaching the shower maximum at $X_{\rm max}$ the shower size decreases exponentially with column depth. The attenuation length for the shower decay after $X_{\rm max}$ is approximately 200 $\frac{\rm g}{\rm cm2}$.

A monopole is highly penetrating and, as such, can initiate many cascades before stopping, but the energy injected into the absorber in any single interaction must be greater than Ec for a subshower to develop. This restricts the inelasticity to h $\gtrsim \frac{E_c}{E_0} \simeq 10^{-12}\left(\frac{E_0}{10^{20}\rm eV}\right)^{-1}$, for monopole–matter interactions which can develop subshowers and contribute to the quasi–steady cloud of secondary particles traveling with the monopole. Lower inelasticity events will contribute directly to ionization without intermediate particle production. For shower development the main process is pair production. For a monopole of boost factor $10^5 < \gamma < 10^7$ the shower size will be $\sim 10^{5\pm1}$ particles.

It is surprising, and may seem counter–intuitive, that the shower profile changes very little while the monopole passes through a medium boundary. For example, in traveling from the earth's mantle into air the shower size is reduced by $\sim$ 30% while the density decreases by $\sim 10^{-4}$. In a more dense medium there are more interactions per unit path–length but the subshowers range out more quickly. Thus, the monopole-induced quasi-steady shower is mostly fixed by the properties of the monopole and only weakly determined by the absorber medium.

The lateral profile is approximately uniform out to a lateral cutoff given by the Molière radius

$$R_M = 7.4 \frac{g}{cm^2} \left(\frac{\xi_e}{35 g/cm^2}\right)\left(\frac{100 MeV}{E_c}\right). \quad (13)$$

As defined, the Molière radius is independent of the incident monopole energy, being determined only by the spread of low energy particles resulting from multiple Coulomb scattering. Within a distance R_M of the monopole path will be $\sim$ 90% of the shower particles [19].

Monopole Cherenkov Signatures

When a charge travels through a medium with index of refraction n, at a velocity $\beta > \frac{1}{n}$, Cherenkov radiation is emitted. The total power emitted in Cherenkov radiation per unit frequency ν and per unit length l by a charge Ze is given by the Frank-Tamm formula

$$\frac{d^2W}{d\nu\, dl} = \pi\alpha Z^2 \nu \left[1 - \frac{1}{\beta^2 n^2}\right]. \quad (14)$$

The maximal emission of the Cherenkov light occurs at an angle $\theta \max = \arccos(\frac{1}{n\beta})$ where θ is measured from the radiating particle's direction. Magnetic monopoles radiate Cherenkov light directly [20] for $\beta_M > \frac{1}{n}$, where Z^2 is replaced with $\left(\frac{1}{2\alpha}\right)^2 \simeq$ 4700 for minimally charged monopoles. Cherenkov light from an electric charge source is linearly polarized in the plane containing the path of the source and the direction of observation. However, the polarization of Cherenkov light from a magnetic charge will be rotated 90 degrees from that of an electric charge. This rotated polarization in principle offers a unique Cherenkov signature for monopoles [21].

The monopole-induced shower also contributes to the Cherenkov signal. In particular, an electric charge excess (of roughly 20% the shower size) will emit coherent Cherenkov for wavelengths $\lambda >> R_M$. For coherent Cherenkov the Z^2 factor will be large: $10^8 \lesssim Z^2 \lesssim 10^{10}$. The proposed RICE array may be sensitive to such a monopole signature.

Earth Tomography with Relativistic Monopoles

Direct knowledge about the composition and density of the Earth's interior is lacking. Analysis of the seismic data is currently the best source of information about the Earth's internal properties [22,23]. However, another potential probe would be the study of highly penetrating particles which could pass through the Earth's interior and interact differently depending upon the composition and density of material traversed. Thus, it may be possible to directly measure the density profile of the Earth's interior [24]. Over a significant range of masses and initial energies, monopoles can pass through a large portion of the Earth's interior and emerge with relativistic velocities.

Upgoing Monopole-Induced Shower

An upgoing monopole-induced shower will be created along the path followed by an upgoing monopole. When a monopole passes through a medium boundary the shower size will change to reflect the shower regeneration rate of the new medium. The nitrogen fluorescence signal for upgoing monopoles is too weak to be measured, but Cherenkov light may be an observable signal. The future OWL/Airwatch experiment may be able to see such an event. Radio–Cherenkov emission from the moon may also be observable. An attempt to infer the high energy neutrino flux incident on the moon

by detecting the associated radio emission from showers in the lunar regolith has been undertaken recently [25]. Monopoles should penetrate the moon and emit sufficient power in radio–Cherenkov to be observable by the same means.

Baryonic–Monopole Air Showers

The natural acceleration of monopoles to energies above the GZK cutoff at $E_{GZK} \sim 5 \times 10^{19}$ eV, and the allowed abundance of a monopole flux at the observed super–GZK event rate motivates us to ask whether monopoles may contribute to the super–GZK events. As a proof of principle, we have studied a simple model of a baryonic–monopole interaction in air which produces a shower similar to that arising from a proton primary. To mimic a proton–induced shower the monopole must transfer nearly all of its energy to the shower in a very small distance. The large inertia of a massive monopole makes this impossible if the cross–section is typically strong, ~ 100 mb [26]. The cross–section we seek needs to be much larger.

We model our arguments on those of [11] where three q–monopoles are confined by Z_3 strings of color–magnetic flux to form a color–singlet baryonic monopole. We further assume that 1) the cross–section for the interaction of the baryonic–monopole with a nucleus is geometric; in it's unstretched state (before hitting the atmosphere) the monopole's cross–section is roughly hadronic, $\sigma_0 \sim \Lambda^{-2}$ (where $\Lambda = \Lambda_{QCD}$); 2) each interaction between the monopole and an air nucleus transfers an $O(1)$ fraction of the exchanged energy into stretching the chromomagnetic strings of the monopole; 3) the chromomagnetic strings can only be broken with the formation of a monopole–antimonopole pair, a process which is highly suppressed and therefore ignored; other possible relaxation processes of the stretched string are assumed to be negligible [27]; 4) the energy transfer per interaction is soft, $\frac{\Delta E}{E} \equiv \eta \sim \frac{\Lambda}{M}$. The color-magnetic strings have a string tension $\mu \simeq \Lambda 2$. Therefore, when $O(1)$ of the energy transfer $(\gamma\Lambda)$ stretches the color–magnetic strings (assumption 2), the length $L \sim \Lambda^{-1}$ increases by $\delta L = dE/\mu$, so that the fractional increase in length is $\delta L/L = \gamma$. Consequently, the geometrical cross–section grows $\propto \gamma$ after each interaction.

Already after the first interaction, the cross–section is sufficiently large to shrink the subsequent interaction length to a small fraction of the depth of the first interaction. Thus, $O(1)$ of the monopole energy is transferred to the air nuclei over a short distance, just as in a hadron–initiated shower. A quantitative analysis yields the total distance traveled between the first interaction and the (η^{-1})th interaction is

$$\Delta X \sim (\frac{\pi^2}{3})(\frac{\Lambda^2}{\gamma N}). \tag{15}$$

Thus, the stretchable chromomagnetic strings of the baryonic monopole provide an example of a very massive monopole which nevertheless transfers $O(1)$ of its relativistic energy to an air shower over a very short distance. This baryonic monopole is therefore similar to the air–shower signature of a primary nucleon or nucleus in this respect.

Acknowledgement.

This work was supported in part by the U.S. Department of Energy grant no. DE-FG05-85ER40226, the Vanderbilt University Research Council, and NASA/Tennessee Space Grant Consortium.

REFERENCES

1. E. N. Parker, Astrophys. J. **160,** 383 (1970).
2. N.A. Porter, Nuovo Cim. **16,** 958 (1960); E. Goto, Prog. Theo. Phys. **30,** 700 (1963).
3. T.W. Kephart and T.J. Weiler, Astropart. Phys. 4 271 (1996); Nucl. Phys. (Proc. Suppl.) **51B,** 218 (1996).
4. T. W. Kibble, Phys. Rept. **67,** 183 (1980), and references therein.
5. S. F. King and Q. Shafi, Phys. Lett. **B422,** 135 (1998)[hep-ph/9711288].
6. D.K. Hong, J. Kim, J.E. Kim,and K.S. Soh, Phys. Rev. **D27,** 1651 (1983).
7. N. G. Deshpande, B. Dutta and E. Keith, Nucl. Phys. Proc. Suppl. **52A,** 172 (1997)[hep-ph/9607307]; Phys. Lett. **B388,** 605 (1996)[hep-ph/9605386]; Phys. Lett. **B384,** 116 (1996)[hep-ph/9604236].
8. P. H. Frampton and B. Lee, Phys. Rev. Lett. **64,**619 (1990); P. H. Frampton and T. W. Kephart, Phys. Rev. **D42,** 3892 (1990).
9. C.L. Gardner and J.A. Harvey, Phys. Rev. Lett. **52,** 879 (1984).
10. T. Vachaspati, Phys. Rev. Lett. **76,** 188 (1996)[hep-ph/9509271]; H. Liu and T. Vachaspati, Phys. Rev. **D56,** 1300 (1997)[hep-th/9604138].
11. A. S. Goldhaber, Phys. Rept. 315, 83 (1999)[hep-th/9905208].
12. For a review see P. P. Kronberg, Rept. Prog. Phys. **57,** 325 (1994).
13. D. Ryu, H. Kang, and P.L. Biermann, Astron. & Astrophys. **335,** 19 (1998)[astro-ph/9803275].
14. G. Giacomelli, in: ***Theory and Detection of Magnetic Monopoles in Gauge Theories,*** ed. N. Craigie p.407 (Singapore: World Scientific Publishing Co., 1986).
15. S.P. Ahlen, Rev. Mod. Phys. **52,** 121 (1980).
16. S.D. Wick, Ph. D. Thesis, Vanderbilt University, 1999.
17. S. D. Wick, T.W. Kephart, T.J. Weiler, and P.L. Biermann, [astro-ph/0001233].
18. W. Heitler, ***The Quantum Theory of Radiation,*** (Oxford: Clarendon Press, 1954).
19. Particle Data Group, Phys. Rev. D **50,** 1173 (1994).Prentice-Hall, 1952).485 (1940).
20. D.R. Tompkins, Phys. Rev. 138,B248 (1965).
21. R. Hagstrom, Phys. Rev. Lett. **35,** 1677 (1975).
22. T. Lay and T.C. Wallace, ***Modern Global Seismology*** (New York: Academic Press, 1995).
23. Properties of the Solid Earth, in Rev.Geophys. **33,** (1995); also at the URL: http://earth.agu.org/revgeophys.
24. This idea has been exploited in neutrino physics as neutrinos are sufficiently weakly interacting to pass through We earth largely unimpeded for neutrino energies $\lesssim 10^{15}$ eV.
25. P. W. Gorham, K. M. Liewer, and C. J. Naudet,[astro-ph/9906504] and Proc. 26th International Cosmic Ray Conf. (ICRC99),Salt Lake City, UT, Aug. 17-25, 1999.
26. R.N. Mohapatra and S. Nussinov,Phys. Rev. **D57,** 1940 (1998); in I.F.M. Albuquerque, G. Farrar, and E.W. Kolb, Phys. Rev. **D59,** 015021 (1999) it is noted that a baryon mass above 10 GeV produces a noticeably different shower profile, and a baryon mass above 50 GeV is so different as to be ruled out.
27. In the other extreme, it has been proposed [28] that the origin of the super–GZK events is the gauge bosons radiated by cosmic monopole–string networks when the stretched strings relax.
28. V. Berezinsky, X. Martin, and A. Vilenkin, Phys. Rev. **D56,** 2024 (1997); V. Berezinsky and A. Vilenkin, Phys. Rev. Lett. **79,** 5202 (1997); V. Berezinsky, P. Blasi, and A. Vilenkin, astro-ph/9803271 and Phys. Rev. **D,** to appear.

Section II
Super Strings and Black Holes

This page intentionally left blank.

VERTEX OPERATORS FOR STRINGS ON ANTI-DE SITTER SPACE

L. Dolan

Department of Physics, University of North Carolina
Chapel Hill, North Carolina 27599-3255, USA

INTRODUCTION

M-theory and Type IIB string theory on anti-de Sitter (AdS) space is conjectured to be dual to a conformal field theory on the boundary of the AdS space. Recent formulations[1,2] of the IIB string on $AdS5$ x S^5 may be useful in giving precise data about the large 't Hooft coupling limit of the four-dimensional $N = 4$ super Yang-Mills, which is conformal and lives on the boundary of AdS_5. Earlier[3], a quantizable worldsheet action was given for the IIB string on AdS_3 x S^3 x M with background Ramond-Ramond flux, where M is T^4 or $K3$. The vertex operators for this model can be explicitly computed in the bulk[4]. Correlation functions constructed from these vertex operators, restricted to the boundary of AdS_3 will be those of a two-dimensional space-time conformal field theory. M-theory on either AdS_4 x S^7 or AdS_7 x S^4 is dual to either three or six-dimensional conformal field theories, but these constructions, outside of the supergravity limit, remain elusive.

In this talk, we describe the difficulties in formulating strings on AdS, and new worldsheet variables which the AdS_3 vertex operators are expressed in terms of. In flat space, constraint equations on these vertex operators follow from the physical state conditions coming from an $N = 4$ superconformal algebra. We generalize[4] the constraint equations to AdS for the vertex operators for the massless states that are independent of the compactification M, and show they are given in terms of the $D = 6$, $N = (2,0)$ supergravity and tensor field multiplets linearized around

Quantum Gravity, Generalized Theory of Gravitation and Superstring Theory-Based Unification
Edited by Kursunoglu *et al.*, Kluwer Academic I Plenum Publishers New York, 2000

AdS_3 x S^3. We work to leading order in α', but because of the high degree of symmetry of the model, we expect our result for the vertex operators to be exact. Tree level n-point correlation functions for $n \geq 4$ presumably have α' corrections.

COVARIANT WORLD SHEET FIELDS

P-brane solutions with an anti-de Sitter metric include non-zero flux of Ramond-Ramond (RR) boson fields. In the Ramond-Neveu-Schwarz (RNS) formalism, these RR target space fields couple to 2d spin fields in the worldsheet action for strings on AdS space. This violates superconformal worldsheet symmetry , since worldsheet supercurrents are not local with respect to the spin fields, and makes the worldsheet conformal field theory difficult to understand.

This problem has been overcome in some special cases. The Berkovits-Vafa formalism for manifest Lorentz covariant and supersymmetric quantization on R^6 x M uses the following worldsheet fields. The bosonic fields $x^p(z, z)$ contain both left- and right-moving modes. In addition there are left-moving fermi fields $\theta^a_L(z), p^a_L(z)$ of spins 0 and 1, together with ghosts $\sigma_L(z)$, $_{PL}(z)$, and right-moving counterparts of all these left-moving fields. These variables allow Ramond-Ramond background fields to be incorporated without adding spin fields to the worldsheet action as follows: in the AdS_3 x S^3 case, i.e. after adding RR background fields to the worldsheet action, one can integrate out the p's, so that the model has ordinary conformal fields x^p, θ^a, θ^a (all now with both left- and right-moving components) as well as the ghosts[3].

$N = 4$ SUPERVIRASORO GENERATORS

The $N = 4$ superconformal generators with $c = 6$ are given in flat space by[3]

$$
\begin{aligned}
T &= -\frac{1}{2}\partial x^m \partial x_m - p_a \partial\theta^a - \frac{1}{2}\partial\rho\partial\rho - \frac{1}{2}\partial\sigma\partial\sigma + \partial^2(\rho + i\sigma) + T_C \\
G^+ &= -e^{-2\rho - i\sigma}(p)^4 + \tfrac{i}{2}e^{-\rho}p_a p_b \partial x^{ab} \\
&\quad + e^{i\sigma}(-\frac{1}{2}\partial x^m \partial x_m - p_a\partial\theta^a - \frac{1}{2}\partial(\rho + i\sigma)\partial(\rho + i\sigma) + \frac{1}{2}\partial^2(\rho + i\sigma)) + G_C^+ \\
G^- &= e^{-i\sigma} + G_C^- \\
J &= \partial(\rho + i\sigma) + J_C \\
\tilde{G}^+ &= e^{iH_C}(-e^{-3\rho - 21\sigma}(p)^4 + \tfrac{i}{2}e^{-2\rho - i\sigma}p_a p_b \partial x^{ab} \\
&\quad + e^{-\rho}(-\frac{1}{2}\partial x^m \partial x_m - p_a\partial\theta^a - \frac{1}{2}\partial(\rho + i\sigma)\partial(\rho + i\sigma) + \frac{1}{2}\partial^2(\rho + i\sigma)) + e^{-\rho - i\sigma}\tilde{G}_C^- \\
J^+ &= e^{\rho + i\sigma}J_C^+ \\
J^- &= e^{-\rho - i\sigma}J_C^- .
\end{aligned}
$$

CONSTRAINT EQUATIONS FOR VERTEX OPERATORS

The expansion of the massless vertex operator in terms of the worldsheet fields is

$$V = \sum_{m,n=-\infty}^{\infty} e^{m(i\sigma+\rho)+n(i\bar{\sigma}+\bar{\rho})}\, V_{m,n}(x,\theta,\bar{\theta})\,.$$

In flat space, the constraints from the left and right-moving worldsheet super Virasoro algebras are:

$$\begin{aligned}
(\nabla)^4 V_{1,n} &= \nabla_a \nabla_b \partial^{ab} V_{1,n} = 0 \\
\tfrac{1}{6}\epsilon^{abcd}\nabla_b \nabla_c \nabla_d V_{1,n} &= -i\nabla_b \partial^{ab} V_{0,n} \\
\nabla_a \nabla_b V_{0,n} - \tfrac{i}{2}\epsilon_{abcd}\partial^{cd} V_{-1,n} = 0\,, &\qquad \nabla_a V_{-1,n} = 0\,;
\end{aligned}$$

$$\begin{aligned}
\bar{\nabla}^4 V_{n,1} &= \bar{\nabla}_{\bar{a}}\bar{\nabla}_{\bar{b}}\bar{\partial}^{\bar{a}\bar{b}} V_{n,1} = 0 \\
\tfrac{1}{6}\epsilon^{\bar{a}\bar{b}\bar{c}\bar{d}}\bar{\nabla}_{\bar{b}}\bar{\nabla}_{\bar{c}}\bar{\nabla}_{\bar{d}} V_{n,1} &= -i\bar{\nabla}_{\bar{b}}\bar{\partial}^{\bar{a}\bar{b}} V_{n,0} \\
\bar{\nabla}_{\bar{a}}\bar{\nabla}_{\bar{b}} V_{n,0} - \tfrac{i}{2}\bar{\epsilon}_{\bar{a}\bar{b}\bar{c}\bar{d}}\bar{\partial}^{\bar{c}\bar{d}} V_{n,-1} = 0\,, &\qquad \bar{\nabla}_{\bar{a}} V_{n,-1} = 0 \\
\partial^p \partial_p V_{m,n} &= 0
\end{aligned}$$

for $-1 \le$ m,n ≤ 1, with the notation $\nabla a = d/d\theta^a$, $\nabla_a = d/d\theta^a$, $a^{ab} = -\sigma^{pab}\partial p$. In flat space, these equations were derived by requiring the vertex operators to satisfy the physical state conditions

$$\begin{aligned}
G_0^- V = \tilde{G}_0^- V = \bar{G}_0^- V = \bar{\tilde{G}}_0^- V = T_0 V = \bar{T}_0 V = 0, \\
J_0 V = \bar{J}_0 V = 0\,, \quad G_0^+ \tilde{G}_0^+ V = \bar{G}_0^+ \bar{\tilde{G}}_0^+ V = 0
\end{aligned}$$

where T_n, $G_n^{\pm}$, $G_n^{\pm}$, J_n, $J_n^{\pm}$ and corresponding barred generators are the left and right N = 4 worldsheet superconformal generators. These conditions further imply $V_{m,n} = 0$ for $m > 1$ or $n > 1$ or $m < 1$ or n < 1, leaving nine non-zero components.

In curved space, we modify these equations as follows:

$$\begin{aligned}
F^4 V_{1,n} &= F_a F_b K^{ab} V_{1,n} = 0 \\
\tfrac{1}{6}\epsilon^{abcd} F_b F_c F_d V_{1,n} &= -iF_b K^{ab} V_{0,n} + 2iF^a V_{0,n} - E^a V_{-1,n} \\
F_a F_b V_{0,n} - \tfrac{i}{2}\epsilon_{abcd} K^{cd} V_{-1,n} = 0\,, &\qquad F_a V_{-1,n} = 0\,;
\end{aligned}$$

$$\begin{aligned}
\bar{F}^4 V_{n,1} &= \bar{F}_{\bar{a}}\bar{F}_{\bar{b}}\bar{K}^{\bar{a}\bar{b}} V_{n,1} = 0 \\
\tfrac{1}{6}\epsilon^{\bar{a}\bar{b}\bar{c}\bar{d}}\bar{F}_{\bar{b}}\bar{F}_{\bar{c}}\bar{F}_{\bar{d}} V_{n,1} &= -i\bar{F}_{\bar{b}}\bar{K}^{\bar{a}\bar{b}} V_{n,0} + 2i\bar{F}^{\bar{a}} V_{n,0} - \bar{E}^{\bar{a}} V_{n,-1} \\
\bar{F}_{\bar{a}}\bar{F}_{\bar{b}} V_{n,0} - \tfrac{i}{2}\bar{\epsilon}_{\bar{a}\bar{b}\bar{c}\bar{d}}\bar{K}^{\bar{c}\bar{d}} V_{n,-1} = 0\,, &\qquad \bar{F}_{\bar{a}} V_{n,-1} = 0.
\end{aligned}$$

There is also a spin zero condition constructed from the Laplacian:

$$(F_a E_a + \tfrac{1}{8}\epsilon_{abcd} K^{ab} K^{cd}) V_{n,m} = (\bar{F}_{\bar{a}} \bar{E}_{\bar{a}} + \tfrac{1}{8}\bar{\epsilon}_{\bar{a}\bar{b}\bar{c}\bar{d}} \bar{K}^{\bar{a}\bar{b}} K^{\bar{c}\bar{d}}) V_{n,m} = 0\,.$$

We derived[4] the curved space equations by deforming the corresponding equations for the flat case, which were presented above, by requiring invariance under the $PSU(2/2)$ transformations that replace the $d = 6$ super Poincare transformations of flat space. The Lie algebra of the supergroup $PSU(2/2)$ contains six even generators K_{ab}, $\in SO(4)$ and eight odd generators E_a, F_a. They generate the following infinitesmal symmetry transformations of the constraint equations:

$$\Delta_a^- V_{m,n} = F_a V_{m,n}\,, \quad \Delta_{ab} V_{m,n} = K_{ab} V_{m,n}$$

$$\Delta_a^+ V_{1,n} = E_a V_{1,n}\,, \quad \Delta_a^+ V_{0,n} = E_a V_{0,n} + iF_a V_{1,n}\,, \quad \Delta_a^+ V_{-1,n} = E_a V_{-1,n} - iF_a V_{0,n}\,.$$

LINEARIZED ADS SUPERGRAVITY EQUATIONS

The AdS supersymmetric constraints imply

$$F_a F_b K^{ab} V_{1,1} = 0\,, \qquad \bar{F}_{\bar{a}} \bar{F}_{\bar{b}} \bar{K}^{\bar{a}\bar{b}} V_{1,1} = 0$$

$$(F_a E_a + \tfrac{1}{8}\epsilon_{abcd} K^{ab} K^{cd}) V_{1,1} = (\bar{F}_{\bar{a}} \bar{E}_{\bar{a}} + \tfrac{1}{8}\bar{\epsilon}_{\bar{a}\bar{b}\bar{c}\bar{d}} \bar{K}^{\bar{a}\bar{b}} K^{\bar{c}\bar{d}}) V_{1,1} = 0\,.$$

We can gauge fix to zero the vertex operators $V_{-1,1}$ $V_{1,-1}$ $V_{0,-1}$, $V_{-1,0}$, $V_{-1,-1}$, and therefore they do not correspond to propagating degrees of freedom. Furthermore this gauge symmetry can be used both to set to zero the components of $V_{1,1}$ with no θ's or no θ's, and to gauge fix all components of $V_{0,1}$, $V_{1,0}$, $V_{0,0}$ that are independent of those of $V_{1,1}$. The physical degrees of freedom are thus described by a superfield

$$\begin{aligned} V_{1,1} &= \theta^a \bar{\theta}^{\bar{a}} V^{--}_{a\bar{a}} + \theta^a \theta^b \bar{\theta}^{\bar{a}} \sigma^m_{ab} \bar{\xi}^-_{m\,\bar{a}} + \theta^a \bar{\theta}^{\bar{a}} \bar{\theta}^{\bar{b}} \sigma^m_{\bar{a}\bar{b}} \xi^-_{m\,a} \\ &+ \theta^a \theta^b \bar{\theta}^{\bar{a}} \bar{\theta}^{\bar{b}} \sigma^m_{ab} \sigma^n_{\bar{a}\bar{b}} (g_{mn} + b_{mn} + \bar{g}_{mn}\phi) + \theta^a (\bar{\theta}^3)_{\bar{a}} A^{-+\,\bar{a}}_a + (\theta^3)_a \bar{\theta}^{\bar{a}} A^{+-\,a}_{\bar{a}} \\ &+ \theta^a \theta^b (\bar{\theta}^3)_{\bar{a}} \sigma^m_{ab} \bar{\chi}^{+\,\bar{a}}_m + (\theta^3)^a \bar{\theta}^{\bar{a}} \bar{\theta}^{\bar{b}} \sigma^m_{\bar{a}\bar{b}} \chi^{+\,a}_m + (\theta^3)_a (\bar{\theta}^3)_{\bar{a}} F^{++\,a\bar{a}}\,. \end{aligned}$$

This has the field content of $D = 6$, $N = (2,0)$ supergravity with one supergravity and one tensor multiplet. In flat space, the surviving constraint equations imply that the component fields Φ are all on shell massless fields, that is $\sum_{m=1}^{6} \partial^m \partial^m \Phi = 0$ and in addition

$$\partial^m g_{mn} = -\partial_n \phi\,, \quad \partial^m b_{mn} = 0\,, \quad \partial^m \chi^{\pm b}_m = \partial^m \bar{\chi}^{\pm\bar{b}}_m = 0$$

$$\partial_{ab} \chi^{\pm b}_m = \partial_{\bar{a}\bar{b}} \chi^{\pm\bar{b}}_m = 0\,, \quad \partial_{cb} F^{\pm\pm b\bar{a}} = \partial_{\bar{c}\bar{b}} F^{\pm\pm\bar{b}a} = 0\,,$$

where

$$F^{+-a\bar{a}} = \partial^{\bar{a}\bar{b}} A^{+-a}_{\bar{b}}\,, \quad F^{-+a\bar{a}} = \partial^{ab} A^{-+\bar{a}}_b\,, \quad F^{--a\bar{a}} = \partial^{ab}\partial^{\bar{a}\bar{b}} V^{--}_{b\bar{b}}$$

$$\chi^{-a}_m = \partial^{ab} \xi^-_{mb}\,, \quad \bar{\chi}^{-\bar{a}}_m = \partial^{\bar{a}\bar{b}} \bar{\xi}^-_{m\bar{b}}\,.$$

The equations of motion for the flat space vertex operator component fields describe $D = 6$, $N = (2,0)$ supergravity expanded around the six-dimensional Minkowski metric.

In $AdS_3 \times S^3$ space there are corresponding gauge transformations which reduce the number of degrees of freedom similarly, but the Laplacian must be replaced by the Ads Laplacian, and the constraints are likewise deformed. We focus on the vertex operator V_{11} that carries the physical degrees of freedom. We show the string constraint equations are equivalent to the $D = 6$, $N = (2,0)$ linearized supergravity equations expanded around the $AdS_3 \times S^3$ metric.

For the bosonic field components of the vertex operators the *AdS* constraint equations result in

$$\Box h^g_{\bar{a}} V^{--}_{ag} = -4\,\sigma^m_{ab}\,\sigma^n_{gh}\,\delta^{bh}\,h^g_{\bar{a}}\,G_{mn}$$

$$\Box h^g_{\bar{a}}\,h^h_{\bar{b}}\,\sigma^m_{ab}\,\sigma^n_{gh}\,G_{mn} = \tfrac{1}{4}\epsilon_{abce}\epsilon_{fghk}\,\delta^{ch}\,h^f_{\bar{a}}\,h^g_{\bar{b}}\,F^{++ek}$$

$$\Box h_g^{\bar{a}}\,F^{++ag} = 0\,, \quad \Box h_g^{\bar{a}}\,A_a^{-+g} = 0\,, \quad \Box h^g_{\bar{a}}\,A_g^{+-a} = 0$$

$$\epsilon_{eacd}\,t_L^{cd}\,h^b_{\bar{a}}\,A_b^{+-a} = 0\,, \qquad \epsilon_{\bar{e}\bar{b}\bar{c}\bar{d}}\,t_R^{\bar{c}\bar{d}}\,h_a^{\bar{a}}\,A_{\bar{a}}^{-+\bar{b}} = 0$$

$$\epsilon_{eacd}\,t_L^{cd}\,h_b^{\bar{a}}\,F^{++ab} = 0\,, \qquad \epsilon_{\bar{e}\bar{b}\bar{c}\bar{d}}\,t_R^{\bar{c}\bar{d}}\,h^a_{\bar{a}}\,F^{++\bar{a}\bar{b}} = 0$$

$$t_L^{ab}\,h^g_{\bar{a}}\,h^h_{\bar{b}}\,\sigma^m_{ab}\,\sigma^n_{gh}\,G_{mn} = 0\,, \quad t_R^{\bar{a}\bar{b}}\,h_a^{\bar{g}}\,h_b^{\bar{h}}\,\sigma^m_{\bar{g}\bar{h}}\,\sigma^n_{\bar{a}\bar{b}}\,G_{mn} = 0\,.$$

We have expanded $Gmn = 9_{mn} + bmn + gmnf$. The $SO(4)$ Laplacian is $= \frac{1}{8}\ \varepsilon_{abcd}\ t_L^{ab}\ t_L^{cd} = \frac{1}{8}\varepsilon_{\bar{a}\bar{b}\bar{c}\bar{d}}\ t_R^{\bar{a}\bar{b}}\ t_R^{\bar{c}\bar{d}}$. In order to compare this with supergravity, we need to reexpress the above formulas containing the right- and left-invariant vielbeins $t_L^{ab}, t_R^{\bar{a}\bar{b}}$ in terms of covariant derivatives D_p on the group manifold. So we write

$$\mathcal{T}_L^{cd} \equiv -\sigma^{p\,cd}\,D_p\,, \qquad \mathcal{T}_R^{\bar{c}\bar{d}} \equiv \sigma^{p\,\bar{c}\bar{d}}\,D_p\ .$$

Acting on a scalar, $T_L = tL$ and $T_R = t_R$, since both just act geometrically. But they differ in acting on fields that carry spinor or vector indices. For example, on spinor indices,

$$t_L^{ab} V_e = \mathcal{T}_L^{ab}\,V_e + \tfrac{1}{2}\delta^a_e\,\delta^{bc} V_c - \tfrac{1}{2}\delta^b_e\,\delta^{ac} V_c\,.$$

For $AdS_3 \times S^3$ we can write the Riemann tensor and the metric tensor as

$$\bar{R}_{mnp\tau} = \tfrac{1}{4}\,(\,\bar{g}_{m\tau}\bar{R}_{np} + \bar{g}_{np}\bar{R}_{m\tau} - \bar{g}_{n\tau}\bar{R}_{mp} - \bar{g}_{mp}\bar{R}_{n\tau}\,)$$

$$\bar{g}_{mn} = \tfrac{1}{2}\,\sigma^{ab}_m\,\sigma_{n\,ab}\,.$$

The sigma matrices σ^{mab} satisfy the algebra

$$\sigma^{mab}\sigma^{n}_{ac} + \sigma^{nab}\sigma^{m}_{ac} = \eta^{mn}\delta^{b}_{c}$$

in flat space, where η^{mn} is the six-dimensional Minkowski metric, and $1 \leq a \leq 4$. Sigma matrices with lowered indices are defined by $\sigma^{m}_{ab} = \frac{1}{2}\varepsilon_{abcd}\sigma^{mcd}$, although for other quantities indices are raised and lowered with δ^{ab}, so we distinguish σ^{m}_{ab} from $\delta_{ac}\delta_{bd}\sigma^{mcd}$. In curved space, η_{mn} is replaced by the $AdS_3 \times S^3$ metric $\bar{g}_{mn}$.

We then find from the string constraints that the six-dimensional metric field g_{rs}, the dilaton ϕ, and the two-form b_{rs} satisfy

$$\begin{aligned}\tfrac{1}{2}D^{p}D_{p}b_{rs} = &-\tfrac{1}{2}(\sigma_{r}\sigma^{p}\sigma^{q})_{ab}\delta^{ab}D_{p}[g_{qs}+\bar{g}_{qs}\phi] + \tfrac{1}{2}(\sigma_{s}\sigma^{p}\sigma^{q})_{ab}\delta^{ab}D_{p}[g_{qr}+\bar{g}_{qr}\phi]\\ &-\bar{R}_{\tau rs\lambda}b^{\tau\lambda} - \tfrac{1}{2}\bar{R}_{r}^{\ \tau}b_{\tau s} - \tfrac{1}{2}\bar{R}_{s}^{\ \tau}b_{r\tau}\\ &+\tfrac{1}{4}F^{++gh}_{\text{asy}}\sigma^{ab}_{r}\sigma^{ef}_{s}\delta_{ah}\delta_{be}\delta_{gf}\end{aligned}$$

$$\begin{aligned}\tfrac{1}{2}D^{p}D_{p}(g_{rs}+\bar{g}_{rs}\phi) = &-\tfrac{1}{2}(\sigma_{r}\sigma^{p}\sigma^{q})_{ab}\delta^{ab}D_{p}b_{qs} + \tfrac{1}{2}(\sigma_{s}\sigma^{p}\sigma^{q})_{ab}\delta^{ab}D_{p}b_{rq}\\ &-\bar{R}_{\tau rs\lambda}(g^{\tau\lambda}+\bar{g}^{\tau\lambda}\phi) - \tfrac{1}{2}\bar{R}_{r}^{\ \tau}(g_{\tau s}+\bar{g}_{\tau s}\phi) - \tfrac{1}{2}\bar{R}_{s}^{\ \tau}(g_{r\tau}+\bar{g}_{r\tau}\phi)\\ &+\tfrac{1}{4}F^{++gh}_{\text{sym}}\sigma_{rga}\sigma_{shb}\delta^{ab}.\end{aligned}$$

This is the curved space version of the flat space zero Laplacian condition $\delta^{\Pi}f_{\text{pbrs}} = \partial^{p}\partial_{p}g_{rs} = \partial p\partial p\phi = 0$.

Four self-dual tensor and scalar pairs come from the string bispinor fields F^{++ab}, V^{--}_{ab}, , $A^{+\ -a}_{b}$, $A^{-\ +b}_{a}$. From the string constraint equations they satisfy

$$\sigma^{p}_{da}D_{p}F^{++ab}_{\text{asy}} = 0$$

$$\tfrac{1}{4}[\delta^{Ba}\sigma^{r}_{ga}D_{r}F^{++gH}_{\text{sym}} - \delta^{Ha}\sigma^{r}_{ga}D_{r}F^{++gB}_{\text{sym}}] = -\tfrac{1}{4}\epsilon^{BH}{}_{cd}F^{++cd}_{\text{asy}}$$

We also find

$$\begin{aligned}&\tfrac{1}{2}D^{p}D_{p}V^{--}_{cd} - \tfrac{1}{2}\delta^{gh}\sigma^{p}_{ch}D_{p}V^{--}_{gd} + \tfrac{1}{2}\delta^{gh}\sigma^{p}_{dh}D_{p}V^{--}_{cg} + \tfrac{1}{4}\epsilon_{cd}{}^{gh}V^{-}_{gh}\\ &= -4\sigma^{m}_{ce}\sigma^{n}_{df}\delta^{ef}G_{mn}.\end{aligned}$$

The last constraints can be written as

$$\epsilon_{eacd}t^{cd}_{L}h_{b}^{\ \bar{a}}F^{+-ab} = 0 \qquad \epsilon_{\bar{e}\bar{b}\bar{c}\bar{d}}t^{\bar{c}\bar{d}}_{R}h^{a}_{\ \bar{a}}F^{+-\bar{a}\bar{b}} = 0$$
$$\epsilon_{eacd}t^{cd}_{L}h_{b}^{\ \bar{a}}F^{-+ab} = 0, \qquad \epsilon_{\bar{e}\bar{b}\bar{c}\bar{d}}t^{\bar{c}\bar{d}}_{R}h^{a}_{\ \bar{a}}F^{-+\bar{a}\bar{b}} = 0$$

where

$$F^{+-a\bar{a}} \equiv \delta^{\bar{a}\bar{b}}A^{+-a}_{\bar{b}} + t^{\bar{a}\bar{b}}_{R}A^{+-a}_{\bar{b}}$$
$$F^{-+a\bar{a}} \equiv \delta^{ab}A^{-+\bar{a}}_{b} + t^{ab}_{L}A^{-+\bar{a}}_{b},$$

where

$$F^{+-a\bar{a}} \equiv \delta^{\bar{a}\bar{b}} A_{\bar{b}}^{+-a} + t_R^{\bar{a}\bar{b}} A_{\bar{b}}^{+-a}$$
$$F^{-+a\bar{a}} \equiv \delta^{ab} A_b^{-+\bar{a}} + t_L^{ab} A_b^{-+\bar{a}},$$

so F^{+-ab} and F^{-+ab} satisfy equations similar to those for F^{++ab}.

Independent conditions on the fermion fields are

$$\Box h_a^{\bar{g}} \sigma_{\bar{a}\bar{b}}^m \xi_{m\bar{g}}^- = -\sigma_{\bar{g}\bar{h}}^m \epsilon_{\bar{e}\bar{d}\bar{a}\bar{b}} h_a^{\bar{h}} \delta^{\bar{g}\bar{d}} \bar{\chi}_m^{+\bar{e}}$$
$$\Box h^g{}_{\bar{a}} \sigma_{ab}^m \bar{\xi}_{mg}^- = -\sigma_{gh}^m \epsilon_{edab} h^h{}_{\bar{a}} \delta^{gd} \chi_m^{+e}$$
$$t_L^{ab} h^g{}_{\bar{a}} \sigma_{ab}^m \bar{\xi}_{mg}^- = 0, \qquad t_R^{\bar{a}\bar{b}} h_a^{\bar{g}} \sigma_{\bar{a}\bar{b}}^m \xi_{m\bar{g}}^- = 0$$
$$t_L^{ab} \sigma_{ab}^m h_g^{\bar{a}} \bar{\chi}_m^{+g} = 0, \qquad t_R^{\bar{a}\bar{b}} \sigma_{\bar{a}\bar{b}}^m h_{\bar{g}}^a \chi_m^{+\bar{g}} = 0$$
$$\epsilon_{deab} t_L^{ab} h^g{}_{\bar{a}} h^h{}_{\bar{b}} \sigma_{gh}^m \chi_m^{+e} = 0, \qquad \epsilon_{\bar{d}\bar{e}\bar{a}\bar{b}} t_R^{\bar{a}\bar{b}} h_a^{\bar{g}} h_b^{\bar{h}} \sigma_{\bar{g}\bar{h}}^m \bar{\chi}_m^{+\bar{e}} = 0.$$

We now show that the AdS_3 x S^3 supersymmetric vertex operator constraint equations are equivalent to the linearized supergravity equations for the supergravity multiplet and one tensor multiplet of $D = 6$, $N = (2,0)$ supergravity expanded around the AdS_3 x S^3 metric and a self-dual three-form. We give the identification of the string vertex operator components in terms of the supergravity fields.

We will see that the two-form b_{mn} is a linear combination of *all* the oscillations corresponding to the five self-dual tensor fields and the anti-self-dual tensor field, *including the oscillation with non-vanishing background.* In flat space, b_{mn} corresponds to a state in the Neveu-Schwarz sector. In our curved space case, the string model describes vertex operators for AdS_3 background with Ramond-Ramond flux. When matching the vertex operator component fields with the supergravity oscillations, we find that not only the bispinor V_{ab}^{--} (which is a Ramond-Ramond field in the flat space case), but also the tensor b_{mn} include supergravity oscillations with non-vanishing self-dual background.

The linearized supergravity equations are given by

$$D^p D_p \phi^i = \tfrac{2}{3} \bar{H}^i_{prs} g^{6prs}$$

$$\tfrac{1}{2} D^p D_p h_{rs} - \bar{R}_{\tau rs\lambda} h^{\tau\lambda} + \tfrac{1}{2} \bar{R}^\tau_r h_{\tau s} + \tfrac{1}{2} \bar{R}^\tau_s h_{\tau r} - \tfrac{1}{2} D_s D^p h_{pr} - \tfrac{1}{2} D_s D^p h_{pr} + \tfrac{1}{2} D_r D_s h^p_p$$
$$= -\bar{H}^{i\ pq}_r g^i_{spq} - \bar{H}^{i\ pq}_s g^i_{rpq} + 2 h^{pt} \bar{H}^{i\ q}_{rp} \bar{H}^i_{stq}$$

$$D^p H_{prs} = -2 \bar{H}^i_{prs} D^p \phi^i$$
$$+ B^i [-\bar{H}^{i\ pq}_r D_p h_{qs} + \bar{H}^{i\ pq}_s D_p h_{qr} + \bar{H}^{i\ q}_{rs} D^p h_{pq} - \tfrac{1}{2} \bar{H}^{i\ q}_{rs} D_q h^p{}_p]$$

where we have defined $H_{prs} \equiv g^6_{prs} + B^i g^i_{prs}$ as a combination of the supergravity exact forms $g^6 \equiv db^6, g^i \equiv db^i$, since we will equate this with the string field

strength $H = db$. We will choose $B^I = 2$. In zeroeth order, the equations are $R_{rs} = -H^i_{rpq} H^{i\,pq}_s$.

We define the vertex operator components in terms of the supergravity fields g^i_{prs}, g^6_{prs}, h_{rs}, ϕ^i, $1 \le i \le 5$, (and $2 \le I \le 5$) as

$$H_{prs} \equiv g^6_{prs} + 2\, g^1_{prs} + B^I\, g^I_{prs}$$

$$g_{rs} \equiv h_{rs} - \tfrac{1}{6} \bar{g}_{rs}\, h^\lambda_\lambda$$

$$\phi = -\tfrac{1}{3}\, h^\lambda_\lambda$$

$$F^{++\,ab}_{sym} = \tfrac{2}{3}(\sigma_p \sigma_r \sigma_s)^{ab}\, B^I\, g^I_{prs} + \delta^{ab}\, \phi^{++}$$

$$F^{++\,ab}_{asy} = \sigma^{p\,ab}\, D_p\, \phi^{++}$$

$$\phi^{++} = 4 C^I\, \phi^I$$

which follows from choosing the graviton trace h^λ_λ to satisfy $\phi^1 - h^\lambda_\lambda = -2 C^I \phi^I$, and we have used $H_{prs} = \partial_p b_{rs} + \partial_r b_{sp} + \partial_s b_{pr}$.

The combinations $C^I \phi^I$ and $B^I g^I_{prs}$ reflect the SO(4)R symmetry of the $D = 6, N = (2,0)$ theory on $AdS_3 \times S^3$. We relabel $C^I = C^I_{++}$, $B^I = B^I_{++}$. To define the remaining string components in terms of supergravity fields, we consider linearly independent quantities $C^I_e\, \phi^I\, B^I_e\, g^I_{prs}$, $l = ++, +-, -+, --$

$$F^{+-\,ab}_{sym} = \tfrac{2}{3}(\sigma_p \sigma_r \sigma_s)^{ab}\, B^I_{+-}\, g^I_{prs} + \delta^{ab}\, \phi^{+-}$$

$$F^{+-\,ab}_{asy} = \sigma^{p\,ab}\, D_p\, \phi^{+-}$$

$$\phi^{+-} = 4 C^I_{+-}\, \phi^I$$

$$F^{-+\,ab}_{sym} = \tfrac{2}{3}(\sigma_p \sigma_r \sigma_s)^{ab}\, B^I_{-+}\, g^I_{prs} + \delta^{ab}\, \phi^{-+}$$

$$F^{-+\,ab}_{asy} = \sigma^{p\,ab}\, D_p\, \phi^{-+}$$

$$\phi^{-+} = 4 C^I_{-+}\, \phi^I$$

V^{--}_{ab} is given in terms of the fourth tensor/scalar pair $C^I_{--}\, \phi^I$, $B^I_{--}\, g^I{}_{mnp}$ through

$$D^p D_p V^{--}_{cd} - \delta^{gh} \sigma^p_{ch} D_p V^{--}_{gd} + \delta^{gh} \sigma^p_{dh} D_p V^{--}_{cg} + \tfrac{1}{2} \epsilon_{cd}{}^{gh} V^{--}_{gh} = -8\, \sigma^m_{ce}\, \sigma^n_{df}\, \delta^{ef}\, G_{mn}\,.$$

With these field definitions, the string constraint equations for the AdS_3 vertex operators reduce to the linearized supergravity equations for the vertex operator field components.

The fermion constraints imply the linearized AdS supergravity equations for the gravitinos and spinors, due to the above correspondence for the bosons and the supersymmetry of the two theories.

REFERENCES

1. N. Berkovits, *Super-Poincare Covariant Quantization of the Superstring,* hep-th/0001035.

2. N. Drukker, D. Gross, and A. Tseytlin, *Green-Schwarz String in AdS3 x S^5: Semiclassical Partition Function,* hep-th/0001204.

3. N. Berkovits, C. Vafa, and E. Witten, *Conformal Field Theory of AdS Background With Ramond-Ramond Flux,* **JHEP 9903: 018, 1999,** hep-th/9902098.

4. L. Dolan and E. Witten, *Vertex Operators for AdS3 Background With Ramond-Ramond Flux,* **JHEP 11:003:1999,** hep-th/9910205.

5. L. Romans, *Self-Duality for Interacting Fields,* Nucl. Phys. B276 (1986) 71.

This page intentionally left blank.

The Structure of a Source Modified WZW Theory

Sharmanthie Fernando[a]*, Freydoon Mansouri[b]+
[a]Physics Department, Northern Kentucky University, Highland Heights, KY 41099.
[b]Physics Department, University of Cincinnati. Cincinnati, OH 45221.

Abstract

In 2+1 dimensions, the Chern-Simons Gauge theory of a simple group G on a manifold with boundary is known to lead to a WZW theory. When a source characterized by the Cartan subalgebra H of G is coupled to the Chern-Simons theory, the corresponding WZW theory is modified. We study the consequences of this modification on the corresponding Kac-Moody and the Virasoro algebras. The relevance of this development to the microscopic structure of the AdS3 black hole is pointed out.

1 Introduction

It has been known for sometime [l] that, for a simple gauge group G, the Chern-Simons theory in 2+1 dimensions on a manifold with boundary leads to a WZW theory. It is also known [l, 21 that when a source characterized by the Cartan subalgebra H of G is coupled to the Chern-Simons theory, the corresponding WZW theory is modified. The main purpose of this work is to study the structure of Kac-Moody and Virasoro algebras of the modified theory and compare and contrast them with the corresponding algebras in the absence of a source.

Our initial motivation for studying such algebras was to understand the microscopic structure of the AdS3 black hole [3], which is a solution of free Einstein's equations with a negative cosmological constant. It is well known that the free Einstein theory in 2$1 dimensions with or without a cosmological constant can be formulated as a free Chern Simons theory [4, 51 which has at most a small number of degrees freedom. To account for the degrees of freedom which are responsible for the black hole entropy, a number of interesting suggestions have been made. In one way or another, these suggestions make use of a conformal field theory on some boundary. In one of these [6], use is made of the asymptotic behavior of the black hole solution [7] to obtain a conformal field theory at infinite boundary. In this case, one does not directly count the states but makes use of a formula due to Cardy [8] for the asymptotic density of states. In another

*email address: fernando@physung.phy.uc.edu
email address: Mansouri@uc.edu

Quantum Gravity, Generalized Theory of Gravitation. and Superstring Theory-Based Unification
Edited by Kursunoglu *et al.*. Kluwer Academic / Plenum Publishers. New York. 2000

approach [9, 10], Chern-Simons theory is studied on a manifold with boundary, where the boundary is identified with an apparent horizon. One advantage of this approach is that one can directly count the states. But the central charge of the corresponding conformal field theory is different from the previous case, and the role and the location of the apparent horizon boundary is not well understood.

A third possibility is to consider a Chern-Simons theory coupled to source on a manifold with boundary. The motivation for adding a source is the requirement that all the information concerning the black hole, e.g., its discrete identification group, be encoded in the Chern-Simons theory. It is easy to demonstrate that the free Chern-Simons theory is not sufficient for this purpose [12, 13, 11], so that the inclusion of the source is essential. This brings us back to the primary motivation underlying the present work. In section 2, we review some known results on free Chern-Simons theory on a manifold with boundary and the corresponding WZW theory. In section 3, we study how this WZW theory is modified in the presence of a source. In particular, we point out that the resulting conformal field theory has a twisted Kac-Moody algebra. Finally, the implications of this result for the entropy of the AdS_3 black hole are discussed in section 4.

2 Chern-Simons Action and Boundary Effects

For a simple or a semi-simple group, the Chern Simons action has the form

$$I_{cs} = \frac{1}{4\pi} \mathrm{Tr} \int_M A \wedge \left(dA + \frac{2}{3} A \wedge A \right) \tag{1}$$

where Tr stands for trace and

$$A = A_\mu dx^\mu \tag{2}$$

We require the 2+1 dimensional manifold M to have the topology R x Σ, with Σ a two-manifold and R representing the time-like coordinate x0. Moreover, in accord with Mach's principle, we take the topology of Σ to be trivial in the absence of sources, with the possible exception of a boundary. Then, subject to the constraints

$$F^b[A] = \frac{1}{2}\epsilon^{ij}(\partial_i A^b_j - \partial_j A^b_i + \epsilon^b{}_{cd} A^c_i A^d_j) = 0 \tag{3}$$

the Chern-Simons action for a simple group G will take the form

$$I_{cs} = \frac{k}{2\pi} \int_R dx^0 \int_\Sigma d^2x \left(-\epsilon^{ij} \eta_{ab} A^a_i \partial_0 A^b_j + A^a_0 F_a \right) \tag{4}$$

where $i, j = 1,2$.

Up to this point, our analysis is independent of whether the manifold M does or does not have a boundary. Let us now assume that the two dimensional surface Σ has the topology of a disc. The main advantage of this approach is that it is not necessary to identify this boundary with a specific physical boundary such as a horizon. The manifold M is still a topological manifold without a metric, and the topological features of the Chern-Simons theory is maintained. Moreover, since there is no notion of a distance in M, any physics which can be extracted from the Chern-Simons theory on such a manifold, must be independent of the *size* of the disc and hence of the location of the boundary relative to some internal features such as a source.

From our point of view, a Chern-Simons theory on a manifold with boundary must have the correct information encoded in it so that it can describe a physical system of

interest. So, the topology of the manifold M must be chosen with the specific physics in mind. As pointed out in the introduction, one of the applications we have in mind is the entropy of the AdS3 black hole. In that case. to be compatible with Mach's principle, there can be no non-trivial features within M in the absence of matter. This means that in the absence of sources, a Wilson loop in M is contractible to a point and that to have non-trivial observables, we must couple the Chern-Simons theory to sources. Therefore, what we wish to explore here is a Chern-Simons theory coupled to a source on a manifold with boundary. For comparison and contrast with other works, let us first consider the theory in the absence of a source.

The main features of a Chern-Simons theory on a manifold with boundary has been known for sometime [l, 2]. Here, with $M = R$ x Σ we identify the two dimensional manifold Σ with a disc D. Then, the boundary of M will have the topology $R \times S^{l}$. We parametrize R with τ and S^{l} with ϕ. In this parametrization, the Chern-Simons action on a manifold with boundary can be written as

$$S_{cs} = \frac{k}{4\pi}\int_M Tr(AdA + \frac{2}{3}A^3) + \frac{k}{4\pi}\int_{\partial M} A_\phi A_\tau. \tag{5}$$

The surface term can be justified by, e.g., requiring the cancellation of the surface terms which arise in the variation of the first term. It vanishes in the gauge in which At = 0 at the boundary. In this action, let $A = \tilde{A} + A\tau$ and $d = dt\frac{\partial}{\partial\tau} + d$. Then, the resulting constraint equations for the field strength take the form

$$\tilde{F} = 0. \tag{6}$$

They can be solved exactly by the ansatz [l, 2]

$$\tilde{A} = -\tilde{d}UU^{-1}, \tag{7}$$

where $U = U(\phi,\tau)$ is an element of the gauge group G. Using this solution, the Chern-Simons action given by Eq. (5) can be rewritten as

$$S_{WZW} = \frac{k}{12\pi}\int_M Tr(U^{-1}dU)^3 + \frac{k}{4\pi}\int_{\partial M} Tr(U^{-1}\partial_\phi U)(U^{-1}\partial_\tau U). \tag{8}$$

We thus arrive at a WZW action and can take over many result already available in the literature for this model. As in any WZW theory, the change in the integrand of this action under an infinitesimal variation δU of U is a derivative. We interpret this to mean that U = U(ϕ, τ), i.e., it is independent of the third (radial) coordinate of the bulk. In other words, the information encoded in the disc depends only on its topology and is invariant under any scaling of the size of the disc.

The above Lagrangian is invariant under the following transformations of the U field [2]:

$$U(\phi,\tau) \to \Omega-(\phi)U\,\Omega(\tau) \tag{9}$$

where $\bar{\Omega}$ (ϕ) and $\Omega(\tau)$ are any two elements of G. To obtain the conserved currents, let U $\to$ U + dU. The corresponding variation of the action leads to SWZW $\to$ SWZW + δSWZW, where

$$\delta S_{WZW} = \frac{k}{2\pi}\int_{\partial M}(\partial_\tau(U^{-1}\partial_\phi U)\delta U. \tag{10}$$

We thus obtain an infinite number of conserved currents:

$$J_\phi = -\frac{k}{2}U^{-1}\partial_\phi U = J^a T_a. \tag{11}$$

Here, T_a are the generators of the algebra of the group G, and $J\phi$ is a function of ϕ only because $\partial\tau.J\phi = 0$.

If we expand $J\phi$ in a Laurent Series, we obtain

$$J_\phi = \Sigma J_n z^{-n}, \tag{12}$$

where $z = \exp(i\phi)$. As usual, J_n satisfy the Kac-Moody algebra

$$[J_n, J_m] = f_c^{ab} J_{m+n} + \frac{1}{2} kng^{ab}\delta_{m+n,0} \tag{13}$$

The corresponding energy momentum tensor for the action *SWZW* can be computed using the Sugawara construction :

$$T_{\phi\phi} = \frac{1}{2kz^2} J_\phi J_\phi = \frac{1}{2k}\Sigma J^a_{n-m} J^a_m z^{-n-2} = \Sigma L_n z^{-n-2}, \tag{14}$$

where

$$L_n = \frac{1}{2k}\Sigma J^a_{(n-m)} J^a_m. \tag{15}$$

The L_n operators satisfy the following Virasoro algebra:

$$[L_n, L_m] = (n-m)L_{n+m} + \frac{c}{12} n(n^2-1)\delta_{n+m,0}, \tag{16}$$

with c the central charge.

3 The Coupling of a source

Next, we couple a source to the Chern-Simons action on the manifold M which, as in the previous section, has the boundary R × S^1. In general, we take the source to be a representation of the group G [12, 13]. To be specific, let us consider a source action given by [1, 2]

$$S_{source} = \int d\tau Tr[\lambda\omega(\tau)^{-1}(\partial_\tau + A_\tau)\omega(\tau)]. \tag{17}$$

Here $\lambda = \lambda^a H_a$ where H_a are elements of the Cartan subalgebra H of G. The quantity $w(t)$ is an arbitrary element of G. The above action is invariant under the transformation $w(t) \to w(\tau)h(\tau)$, where $h(\tau)$ commutes with λ.

Now the total action on M is,

$$S_{total} = \frac{k}{4\pi}\int Tr(AdA + \frac{2}{3}A^3) + \frac{k}{4\pi}\int A_\tau A_\phi + \int d\tau Tr(\lambda\omega(\tau)^{-1}(\partial_\tau + A_\tau)\omega(t) \tag{18}$$

The new constraint equation takes the form,

$$\frac{k}{2\pi}\tilde{F}(x) + \omega(\tau)\lambda\omega^{-1}(\tau)\delta^2(x - x_p) = 0, \tag{19}$$

where x_p specifies the location of the source, heretofore taken to be the origin. The solution to the above equation is given by

$$\tilde{A} = -\tilde{d}\tilde{U}\tilde{U}^{-1}, \tag{20}$$

where[2]

$$\tilde{U} = Uexp(\frac{1}{k}\omega(\tau)\lambda\omega^{-1}(\tau)\phi) \tag{21}$$

The new effective action on the boundary ∂M is then

$$S_{total} = S_{WZW} + \frac{1}{2\pi}\int_{\partial M} Tr(\lambda U^{-1}\partial_\tau U). \tag{22}$$

This Lagrangian is also invariant under the following transformation:

$$U(\phi,\tau) \to \overline{\Omega}(\phi)U\Omega(\tau) \tag{23}$$

where $\Omega(\tau)$ commute with λ. Varying the action under the above symmetry transformation, we get

$$\delta S_{total} = \delta S_{WZW} + \delta S_{source}, \tag{24}$$

where [11]

$$\delta S_{source} = \frac{1}{2\pi}\int Tr\left(-U^{-1}\delta U[U^{-1}\partial_\tau U, \lambda]\right). \tag{25}$$

Hence, the requirement that $\delta S_{total} = 0$ will give rise to the conservation equation

$$\partial_\tau\left(-\frac{k}{2}U^{-1}\partial_\phi U + \frac{1}{2}[lnU, \lambda]\right) = 0. \tag{26}$$

Thus, the new total current is given by [11]

$$\hat{J}_\phi = -\frac{k}{2}U^{-1}\partial_\phi U + \frac{1}{2}[lnU, \lambda]. \tag{27}$$

A solution of $\hat{J}\phi$ can be written in terms of the current in the absence of the source:

$$\hat{J}_\phi = e^{\frac{\lambda\tau}{k}} J_\phi e^{-\frac{\lambda\tau}{k}} \tag{28}$$

Then, it is easy to check that

$$\partial_\tau \hat{J}_\phi = 0. \tag{29}$$

We can also rewrite $\hat{J}_\phi$ in the form [11]

$$\hat{J}_\phi = \hat{U}^{-1}\partial_\phi \hat{U}, \tag{30}$$

where

$$\hat{U} = e^{\frac{\lambda\tau}{k}} U e^{-\frac{\lambda\tau}{k}}. \tag{31}$$

With the new currents at our disposal, the next step is to see how this modification affects the properties of the corresponding conformal field theory. In this respect, we note from Eq. (28) that our new currents $\hat{J}\phi$ are related to the currents J ϕ in the absence of the source by conjugation with respect to the elements of the Cartan subalgebra H of the group G. This kind of conjugation *has been noted in the study of Kac-Moody algebras [14]. So, to understand how the coupling to a source affects structure of the source-free conformal field theory, we follow the analysis of reference [14] and express the algebra of the group G of rank r in the Cartan-Weyl basis. Let H^i be the elements of the Cartan subalgebra and denote the remaining generators by E^α. Then,

$$[H^i, H^j] = 0$$

$$[H^i, E^\alpha] = \alpha^i E^\alpha$$

$$[E^\alpha, E^\alpha] = \left\{ \begin{array}{c} \epsilon(\alpha,\beta)E^{\alpha+\beta} \quad \text{if } \alpha+\beta \text{ is a root} \\ 2\alpha^{-2}(\alpha.H) \quad \text{if } \alpha = -\beta \\ 0 \quad \text{otherwise} \end{array} \right\} \tag{32}$$

In this expression, $1 \leq i,j \leq r$, and α, β are roots. Now we can rewrite the affine Kac-Moody algebra g of the sourceless theory of the last section in this basis as follows:

$$[H^i_m, H^j_n] = km\delta^{ij}\delta_{m,-n}$$

$$[H^i_m, E^\alpha_n] = \alpha^i E^\alpha_{m+n}$$

$$[E^\alpha_m, E^\alpha_n] = \left\{ \begin{array}{c} \epsilon(\alpha,\beta)E^{\alpha+\beta}_{m+n} \quad \text{if } \alpha+\beta \text{ is a root} \\ 2\alpha^{-2}(\alpha.H_{m+n} + km\delta_{m,-n}) \quad \text{if } \alpha = -\beta \\ 0 \qquad \text{otherwise} \end{array} \right\} \tag{33}$$

We also note from the last section that in the absence of the source the element Lo of the Virasoro algebra and the currents J^a_n have the following commutation relations:

$$[L_0, J^a_n] = nJ^a_n. \tag{34}$$

With these preliminaries, it follows from Eq. (31) that the symmetry algebra of our solution $\hat{U}(\phi, t)$ can be realized as an inner automorphism of the algebra g in the form $g(J_n) = \gamma J_n \gamma^{-1}$, where, suppressing the coupling k,

$$\gamma = e^{i\lambda.H} \tag{35}$$

The map g has the property $g_N = 1$. This implies that $N\lambda.\alpha$ is an integer multiple of 2π, for all roots $\alpha \in g$. The algebra g in the modified Cartan-Weyl basis is given by

$$\hat{g}(H^i) = H^i$$

$$\hat{g}(E^\alpha) = e^{i\lambda.\alpha}E^\alpha \tag{36}$$

Thus, the basis of $\hat{g}$ consists of the elements H^i_m and E^α_n where $m \in Z$ and $n \in (Z + \frac{\lambda.\alpha}{2\pi})$. These operators satisfy a Kac-Moody algebra which is formally the same as those of g but with rearranged (fractional) values of the suffices. Hence the algebra $\hat{g}$ can be viewed as the "twisted" version of the algebra g.

Given their formal similarity in structure, it remains to see to what extent the algebra g and its twisted version $\hat{g}$ are physically equivalent. To get some insight, let us see to what extent we can undo the twisting. To this end, we introduce a new basis for $\hat{g}$

$$F^\alpha_n = E^\alpha_{n+\lambda.\alpha/2\pi}, \qquad I^i_\alpha = H^i_n + k\lambda^i\delta_{n,0}/2\pi, \tag{37}$$

The new operators, F^α_n and I^i_n satisfy the untwisted algebra of g. So, in this basis the presence of the source does not affect the Kac-Moody algebra. However, in this basis the Virasoro algebra is modified. For example, instead of the operator L_0 we get

$$L'_0 = L_0 - \lambda.H/2\pi. \tag{38}$$

This change has important physical implications. For one thing, it implies that the symmetry of the ground state has been reduced from G to H. In other words, in the absence of the source, the ground state is a linear representation of G whereas in the presence of the source, the ground state is a non-linear representation of G which is linear with respect to the subgroup H. Similarly, the loop group symmetry LG is broken down to LG/H. This turns out to have important consequences for the black hole entropy, as we shall see in the next section.

4 The Entropy of the AdS_3 Black Hole

Consider first a derivation by Strominger [6], in which use is made of an earlier work by Brown and Henneaux [7]. Starting with standard (metrical) Einstein theory with a negative cosmological constant, these authors demonstrated that under suitable boundary conditions the asymptotic symmetry group of AdS3 gravity is generated by two copies of Virasoro algebra with central charges

$$c_L = c_R = \frac{3l}{2G}. \tag{39}$$

where l is the radius of curvature of the AdS_3 space, and G is Newton's constant. The presence of such a symmetry indicates that there is a conformal field theory at the asymptotic boundary. It was shown by Strominger that the BTZ solution satisfies the Brown-Henneaux boundary conditions and possessed an asymptotic symmetry of this type. So, he identified the degrees of freedom of the black hole in the bulk with those of the conformal field theory at the infinite boundary. Then, using Cardy's formula [8] for the asymptotic density of states, he showed that the entropy of this conformal field theory is given by

$$S = \frac{2\pi r_+}{4G}, \tag{40}$$

in agreement with Bekenstein-Hawking formula.

The strength as well as the weakness of this derivation rests on its independence from the details of the black hole's microscopic structure. It relies only on the diffeomorphism invariance of Einstein's metrical theory and the asymptotic symmetry of the black hole solution. These features are, however, not limited to the BTZ solution [11] and apply to other regular horizonless solutions also. This is clear from the work of Brown and Henneaux [7], which preceded the discovery of BTZ black hole. In particular, to any of the horizonless solutions which have asymptotic Virasoro symmetries, we can associate a conformal field theory with non-trivial degrees of freedom. We would then be led to assign the corresponding entropy to the horizonless solutions also.

To obtain the entropy given by Eq. (40) from a more intrinsic microscopic structure, attempts have been made to derive this expression from Chern-Simons theory on a manifold with boundary. Most of these attempts [9, 10, 15, 16] are based on pure Chern-Simons theory for which the manifold M is identified with space-time. An alternative possibility [12. 13, 11] is to consider a Chern-Simons theory coupled to a source on a manifold M with boundary, which is not identified with space-time. What all the approaches using the Chern-Simons theory have in common is that in one way or another they lead to a conformal field theory in which one can count the states directly. Among the features in which they differ are the values of the central charge c and the lowest eigenvalue Δ_0 of the operator L_0. Both of these quantities figure prominently in the computation of the asymptotic density of states. When Δ_0 vanishes, Cardy's formula [8] states that

$$\rho(\Delta) \approx exp\{2\pi\sqrt{\frac{c\Delta}{6}}\} \tag{41}$$

In this expression, $\rho(\Delta)$ is the number of states for which the eigenvalue of L_0 is Δ, and it holds for large Δ.

When the lowest eigenvalue Δ_0 does not vanish, the analysis is somewhat more subtle, and the asymptotic density of states for large Δ is given by [15]

$$\rho(\Delta) \approx exp\{2\pi\sqrt{\frac{(c-24\Delta_0)\Delta}{6}}\}\rho(\Delta_0) = exp\{2\pi\sqrt{\frac{c_{eff}\Delta}{6}}\}\rho(\Delta_0). \tag{42}$$

From the analysis of the last section, it follows that in the presence of a source the eigenvalue Δ_0 is in general non- vanishing. We therefore expect that the expression for the entropy of the AdS_3 black hole obtained in our approach will be different from those obtained by other (sourceless) approaches based on Chern-Simons Theory. The details will be given elsewhere.

This work was supported, in part by the Department of Energy under the contract number DOE-FG02-84ER40153.

References

[1] E. Witten, Comm. Math. Phys. **121** (1989) 351.

[2] S. Elitzur, G. Moore, A. Schwimmer and N. Seiberg, Nucl. Phys **B326** (1989) 108.

[3] M. Bañados, C. Teitelboim and J. Zanelli, Phys. Rev. Lett. **69** (1992) 1849; M. Bañados, M. Henneaux, C. Teitelboim and J. Zanelli, Phys. Rev. D **48** (1993) 1506.

[4] A. Achucarro, P. Townsend, Phys. Lett.B **180** (1986) 35.

[5] E. Witten, Nucl. Phys. **B311** (1988) 46; **B323** (1989) 113.

[6] A.Strominger, hep-th/9712252, J. High Energy Physics **02** (1998) 009.

[7] J. D. Brown and M. Henneaux, Comm. Math. Phys. **104** (1986) 207.

[8] J. A. Cardy, Nucl. Phys. **B270** (1986) 186.

[9] S. Carlip, Phys. Rev. **D51** (1995) 632; **D55** (1997) 878.

[10] A.P. Balachandran, L. Chandar, A. Momen, Nuc. Phys. **B461** (1996) 581; eprint archive gr-qc/9506006

[11] F. Ardalan, S. Fernando, F. Mansouri, Cincinnati preprint UCTP102.00, to appear in the Proceedings of the Sixth International Wigner Symposium, Istanbul, Turkey, August, 1999.

[12] S. Fernando, F. Mansouri, Int. Jour. Mod. Phys. **A 14** (1999) 505; hep-th/9804147.

[13] S. Fernando, F. Mansouri, Proceedings of XXII Johns Hopkins Workshop on *Novelties in String Theory,* ed. L. Brink and R. Marnelius, Goteborg, Sweden, August 20-22, 1998; hep-th/9901163.

[14] P. Goddard and D. Olive, Int. Jour. Mod. Phys. **A1** (1986) 303.

[15] S. Carlip, hep-th/9806026; also references cited therein.

[16] M. Bañados, Phys. Rev **D52** (1995) 5815; also hep-th/9901148.

Section III

Recent Progress on New and Old Ideas I

This page intentionally left blank.

THE UNIFICATION OF THE GRAVITATIONAL CONSTANT 'G' WITH THE ELECTRIC CHARGE 'e' VIA AN EXTENDED NON-STATIONARY AXI-SYMMETRIC SPACE-TIME AND CORRESPONDING THERMODYNAMICS: THE SUPER SPIN MODEL

A.J. Meyer, II

International Scientific Projects, Inc.
PO Box 3477
Westport Connecticut, 06880 USA
Email: ajmeyer@optonline.net

INTRODUCTION

The Total Mass of the Super Spin Model Universe is a Function of only Four Fundamental Parameters.

This is a brief review of the Super Spin Model (SSM), wherein the relationship,

$$M=4\pi^2(hc/G)^{1/2}exp(hc/e^2),$$

was established for a non-stationary axi-symmetric space-time, where Mc^2 is the space-time's total conserved energy.

Also established were three additional independent equations for the mass 'M' of such non-stationary axi-symmetric space-times, which led to a set of formal linkages among:

The Universal Gravitational Constant 'G',
The Fundamental Quantum of Electric Charge 'e',
The Fundamental Quantum of Action, Planck's Constant' 'h',
The Speed of Light 'c' in Vacuo and
The Electron and Proton Masses, me and mp.

This set of connections, in turn, led to linkages among the four fundamental forces – the Gravitational, Electromagnetic, Strong, and Weak. These linkages are discussed in Meyer (1995). The present paper primarily consists of a brief synopsis of the unification of 'G' and 'e' along with a short overview of the Super Spin Model.

[1] $h = h/2\pi$

Quantum Gravity. Generalized Theory of Gra vitation, and Superstring Theory -Based Unification
Edited by Kursunoglu *et al,* Kluwer Academic / Plenum Publishers. New York 2000

The Super Spin Model yields a mathematical relationship between the universal gravitational constant 'G' and the fundamental electric charge quantum 'e' in terms of only Planck's constant 'h', the speed of light 'c' and the proton and electron masses 'm_p' and 'm_e'.

From this relationshp, it is now possible to compute the value of G with much greater accuracy than the current experimentally measured value of 6.673×10^{-8} $cm^3/gm/sec^2$, which has a relative standard uncertainty of 1.5×10^{-3}.

The new theoretical value of G as calculated in terms of the better-measured values of the above fundamental parameters is: 6.672941×10^{-8} $cm^3/gm/sec^2$. This new value has a relative standard uncertainty of only 1.092×10^{-6}. Providing this model is correct, the new value of G is over a thousand times more accurate than the current[2] experimentally measured value.

A Sample of Additional Predictions Calculated Directly from the Super Spin Model

The Mass 'M' of the universe is predicted to be:

$$M = 4\pi^2\sqrt{(hc/G)}\exp(hc/e^2) = 2.8062060 \times 10^{56}\ gm;$$ which implies:

The gravitational radius of the universe is: 2.0835498×10^{28} cm.

The present decay time for an isolated neutron in vacuo is predicted to be:

$$t_n = (\pi^2/ce^2)^{3/2}\ Gm_n\ (m_p/m_e)^{1/2} exp(\ hc/e^2) = 15.317381 \text{ minutes.}$$

The present Cosmic Background Radiation Temperature[3] is predicted to be between: 2.7193 K and 2.736 K.

The present value of the Hubble "constant" is predicted to be:

2.159167×10^{-18}/ sec = 66.593 km/secMpc.

The present age of the universe is predicted to be: 15.253369 billion years.

The present density of the universe is predicted to be: 3.303909×10^{-31} gm/cm^3.

The Cosmic Temperature at Creation is predicted to have been: 5.277739×10^{31} K.

The total Number of protons 'N_P,' in the universe is predicted to be: 2^{266}

The total Number of electrons 'N_e', in the universe is predicted to be: 2^{266}.

The relative abundance of Helium in the universe is predicted to be: <~ 25.79%.

The present Number of "flywheel" neutrinos 'N_ν' is predicted to be: 3.05×1091.

The present average energy 'ε_ν' of the "flywheel" neutrinos is predicted to be: 0.0015lev.

There is a more complete list in the earlier published SSM paper, Meyer (1995). However, the calculated values for G etc. in that paper are based upon the 1986 publication from N.I.S.T. while those in this paper are based upon the 1998 findings.[4]

---

[2] December, 1999.

[3] The SSM gives the average Cosmic Background Radiation (CBR) photon energy as a function of F as: $\varepsilon_\gamma = \{(hc^5/G)^{1/2}/[2\pi\ exp(hc/2e^2)]\}\ \{43\pi[2 - [2(1+sin\Phi)]^{1/2}]/[8sin\Phi(5\Phi - 3sin\Phi\ cos\ \Phi)]\}^{1/4}$. Where Φ is an expansion parameter, which at present is predicted by the SSM to be: 1.52413073, The average photon energy as a function of temperature may be approximated as $\varepsilon_\gamma = \pi[8/15]^{1/4}$ kT, or as $\varepsilon_\gamma = 3[\xi(4)/\xi(3)]$kT. The latter form (with the Riemann zeta functions) is based upon integration over an infinite range of frequencies and gives the present CBR temperature as: T = 2.7360 K. The equation, $\varepsilon_\gamma = \pi[8/15]^{1/4}$ kT, which is based upon a calculation of the average photon's volume, assumes that photons completely filled the space of the early universe before matter condensation took place, gives the present CBR temperature as: T=2.7193K. The actual CBR temperature may reside in the range between 2.7193 K and 2.7360 K, with the mean temperature being 2.7277 K. See.Meyer(1995)

4 CODATA Recommended Values of the Fundamental Physical Constants: 1998, Peter J. Mohr and Barry N. Taylor, National Institute of standards and Technology, Gaithersburg, MD 20899-8401, USA

OVERVIEW

In this paper, a few highlights of a cosmological model, dubbed the Super Spin Model (SSM), are presented. The Model comprises a set of equations linking the universal gravitational constant 'G' to the electron charge 'e' and to other fundamental parameters.

These interconnections are then interlinked with equations describing the strong and weak forces in terms of the same fundamental parameters.

This model is based upon the Kerr family [Kerr (1963)] of stationary solutions for the empty space - axi-symmetric - Einstein-Maxwell - source free - equations. An expanded Kerr topology and thermodynamics is used which incorporates both the inner and outer event horizon areas as a measure of entropy, thereby achieving Third Law consistency.

These results are then extended to include non-stationary axi-symmetric space-times, which possess non-stationary "evolving" event horizons.

Due to their parametric simplicity, the Kerr family of solutions for the empty space axi-symmetric Einstein-Maxwell source free equations (i.e., uncharged Kerr black holes) provide a rich laboratory in which to perform "gedanken versuchen." This uncharged family is determined by just two parameters: E and $\mathcal{J}$, where $E=Mc^2$ is the total energy of the space-time and '$\mathcal{J}$' is its total angular momentum. This family is represented by the following metric:

KERR MERIC

$$g_{ij}\,dx^i dx^j = \begin{pmatrix} \frac{2R_g r - \sigma^2}{\sigma^2}du^2 & \frac{-aR_z^2 \sin^2\theta}{\sigma^2}du d\phi & dudr & 0 \\ \frac{-aR_z^2 \sin^2\theta}{\sigma^2}d\phi du & \frac{R_\phi^4 \sin^2\theta}{\sigma^2}d\phi^2 & -a\sin^2\theta d\phi dr & 0 \\ drdu & -a\sin^2\theta dr d\phi & 0 & 0 \\ 0 & 0 & 0 & \sigma^2 d\theta^2 \end{pmatrix}$$

Where:

$R_g = GM/c^2$ = Gravitational radius of space-time,

a = Space-time's specific angular momentum radius = J/Mc,

$\sigma^2 = r^2 + a^2\cos^2\theta$ = Space-time's rotation radial coordinate offset,

$R_z^2 \equiv 2R_g r$

$\gamma^2 \equiv R_z^2 - r^2 - a^2$,

$R_\phi^4 \equiv (r^2 + a^2)^2 + \gamma^2 a^2 \sin^2\theta$,

Mc^2 = Conserved total energy of space-time,

$J = I\mathcal{J}$ $I = aMc$ = Scalar value of space-time's angular momentum.

Such that:

$-8, \leq r \leq +8$,

$-8 \leq u \leq +8$,

$0 \leq \phi \leq 2\pi$,

$0 \leq \theta \leq \pi$.

Note, there exist two non-negative event horizon radii, r_+ and r_-, which are the conjugate solutions of the equation: $\gamma^2(r) = 0$, which are:

$$r_\pm = R_g \pm [R_g^2 - a^2]^{1/2}.$$

They can be re-written as:

$$r_{\pm} = R_g\,[1 + sin(\pm \Phi)] \Rightarrow$$

$$a^2 = r_+ r_- = R_g^2 cos^2(\Phi) \text{ and } r_+ + r_- = 2R_g.$$

Hence, the space-time's specific angular momentum radius is parameterized in terms of M and $\pm\Phi$:

$$a = a(\pm\Phi) = R_g\, cos(\Phi) = GMcos(\Phi)/c^2.$$

The angle 'Φ' is therefore a measure of the magnitude of the space-time's angular momentum (and/or expansion state). That is:

$$J(M, \pm \Phi) = a(\pm\Phi)Mc = R_g Mc cos(\Phi) = GM^2 cos(\Phi)/c \equiv |\mathcal{J}(M, \pm \Phi)|.$$

As is easily seen, $\Phi = \pm 0$, implies a maximally rotating Kerr space-time and $\Phi = \pm \pi/2$ implies a static Schwarzschild space-time.

WHY DOES THE UNIVERSE EXPAND?

In the beginning when the universe was in a super-dense energy state, how could it possibly expand and overcome the intense gravitational fields that should have reduced it to a state of permanent and complete gravitational collapse?

According to the Super Spin Model, the reason the universe expands is due to its initial structure - its topology. If energy were distributed in the form of maximally rotating Planck density string, then it would naturally begin to expand in three dimensions in spite of its huge density. Such a string is already "pre-inflated" in one dimension, while "compressed" in the other three.

One may visualize this beginning state as a circle of light—a geonic[5] pseudo ring singularity — a closed string of maximum energy density light consisting of Planck mass photons–*"primatons."* See Wheeler (1955) and Meyer (1980).

THE DESCRIPTION OF THE SSM UNIVERSE (U) AS A ROTATING NON-STATIONARY AM-SYMMETRIC SPACE-TIME

One way to produce a model of a non-stationary axi-symmetric space-time, is to characterize the entire family of stationary uncharged Kerr solutions for the empty space axi-symmetric Einstein-Maxwell source free equations as the set of ordered pairs:

$$\{< M, J >\} = \{< M, J(\pm \Phi) > \ni [-\pi/2 \le \Phi \le \pi/2]\}.$$

Such a parameterization gives the entire family of Kerr solutions in terms of only two parameters 'M' and 'Φ' and only two universal constants 'G' and 'c'. That is any member of the Kerr Metric Family can be represented as the ordered pair:

$$< M, J(\Phi) > = < M, GM^2 cos(\Phi)/c >$$

From (A), by treating $\pm\Phi$, as a dual-time dependent variable, it is possible to transform the Kerr metric for the *stationary family* of *complete* event horizons into a *single dual-*

[5] Geons are gravitational electromagnetic entities They are objects wherein light has sufficient energy to be gravitationally confined. That is, light, itself. forms a sort of black hole Wheeler developed this concept in 1954.

valued time-varying metric which governs the evolution of incomplete event horizons growing in both directions in both $r_{\pm}$ and $\theta\pm = \pi/2 \pm \Phi$, starting from $\Phi = \pm 0$, where:

$$r_{\pm}(0) = R_g \text{ and } \theta_{\pm}(0) = \pi/2.$$

For the stationary metric **(A),** when $\gamma^2(r) = 0 \Rightarrow r_{\pm} = R_g \pm [R_g^2 - a^2]^{1/2}$, then $ds_{\pm} = 0$. However, this is not generally true when the metric coefficients of (A) are written as a function of the parameter Φ. That is, for the metric **(A):**

$ds_{\pm}/d\Phi$ is generally $\neq 0$, for $\gamma^2(r_{\pm}) = 0$, when $\pm\Phi$ is a dual-time dependent variable.

Rewriting **(A)** in terms of its past directed and future directed non-stationary event horizons, we get:

$$ds_{\pm}^2 = \sigma_{\pm}^2 d\theta^2 - 2a\sin^2\theta dr_{\pm} d\phi + 2dr_{\pm} du_{\pm} + \frac{R_{z\pm}^4 \sin^2\theta d\phi^2}{\sigma_{\pm}^2} - \frac{2aR_{z\pm}^2 \sin^2\theta d\phi du_{\pm}}{\sigma_{\pm}^2} + \frac{a^2 \sin^2\theta du_{\pm}^2}{\sigma_{\pm}^2}.$$

Where the boundry conditions of 'U' are:

$0 \le r_{-} \le R_g \le r_{+} \le 2R_g$,

$0 \le \theta_{-} \equiv \pi/2 - \Phi \le \theta \le \pi/2 + \Phi \equiv \theta_{+}$,

$0 \le \phi \le 2\pi$,

$-\infty \le u \le +\infty$.

And: $r_{\pm} = R_g[1 + \sin(\pm\Phi)]$ = *event horizon radii,*

$\sigma_{\pm}^2 = r_{\pm}^2 + a^2\cos^2\theta$ = *"rotation offset" radii,*

$R_{z\pm}(\Phi) = [2R_g r_{\pm}]^{1/2} = [r_{\pm}^2 + a^2]^{1/2} = R_g[2(1 \pm \sin\Phi)]^{1/2}$:= *the radii of gyration of event horizons and*

$\Omega\pm(\Phi) = c\, d\phi/du_{\pm} = -g_{u\phi}(\Phi)c/g_{\phi\phi}(\Phi) = ac/(R_{z\pm})^2 = c\cos\Phi/[2R_g(1 \pm \sin\Phi)]$ *are the dual event horizon rotation rates.*

For a constant M, one can see that the *moments of inertia* are $I_{\pm} = M(R_{z\pm})^2$, since:

$I_{\pm}\Omega_{\pm} = J(\pm\Phi) = a(\pm\Phi)Mc = R_g Mc\cos(\Phi) = GM^2\cos(\Phi)/c = \hbar\ (\pm = \Phi)$

The above formulations are valid for the subset, U, of the axi-symmetric space-time manifold,[6] *M,* such that *U* is isomorphic to the intrinsically non-stationary region which is partially bounded by or swept out by the two "incomplete" event horizons with radii: $r_{\pm} = r(\Phi(t_{\pm}))$, provided that the initial configuration (fluctuation) of the space-time is isomorphic to a Planck density closed string, spinning at the speed of light, (i.e. a geonic pseudo ring singularity). Note that at $\Phi = \pm\pi/2$ the U becomes identical to a Schwarzschild black hole with complete and stationary event horizons. It is also critical to notice, that for constant Φ (the stationary case), the $r\pm$ are the loci of null hyper-surfaces, but for variable Φ (the non-stationary case) the $r\pm$ loci are null only where:

$$\cos^2\theta = \sin^2\Phi \Rightarrow \theta = \theta_{\pm} \equiv \pi/2 \pm \Phi$$

---

[6] There might also exist an independent **anti** $M \equiv -M$ simultaneously created with equal energy and angular momentum, but with opposite parity

ABOUT THE BOUNDARY CONDITIONS:

The Heisenberg uncertainty principle dictates that the initial conditions are calculated when: [7] $\sin\Phi = \sin\Phi_\chi \approx \Phi_\chi \equiv \pm\sqrt{\pi}/N_w$,

where: $N_w = M/m_w \equiv R_g/R_w \equiv$ either the *dimensionless mass* or the *dimensionless gravitational radius* of U,

where: $m_w \equiv (hc/G)^{1/2} \equiv$ *Planck mass*

and $R_w \equiv (Gh/c^3)^{1/2} \equiv$ *Planck radius*.

In this model, only the initial boundary conditions are posited a-priori. The final boundary conditions are "teleological," based upon positing that F is a function of some temporal variable 't'. That is, $\Phi = \Phi(t)$ is a time varying function, with $sgn(\Phi) = sgn(t)$ and with $\Phi \sim \pm 0$ corresponding to $t \sim \pm 0$

The initial state is a maximally rotating gravitationally closed Planck density string of mass M. This initial state is also isomorphic, at least in terms of its mass and angular momentum, to an extreme Kerr black hole, and is topologically quasi-isomorphic to its ring singularity.

The final state, at $\Phi = \pm\pi/2$ is a Schwarzschild black hole of mass M, which is the fully expanded non-rotating Kerr solution with:

$a(\pm\pi/2) = 0$,

$r(-\pi/2) = 0$ and

$r(+\pi/2) = 2R_g \equiv$ Rs, the Schwarzschild radius.

Note: The excess angular momentum energy, given by $\Delta E_j = Mc_2[1-1/\sqrt{2}]$, not taken up by the expansion, see Christodoulu (1970), is hypothesized to be taken up by the generation of flywheels surmised to be a species of neutrinos. Some of the excess may also be stored in the rotational energy of galaxies, stars and other spinning and rotating objects.

---

[7] This is due to the fad that the creation process has to be complete and its minimum space-time granularity increased to the Planck limit before the universe is as old as its Compton time $\sim 10^{-104}$ second. Otherwise it would return to the vacuum. See the further section **"TEMPORAL MEASURE"** and Meyer (1995).

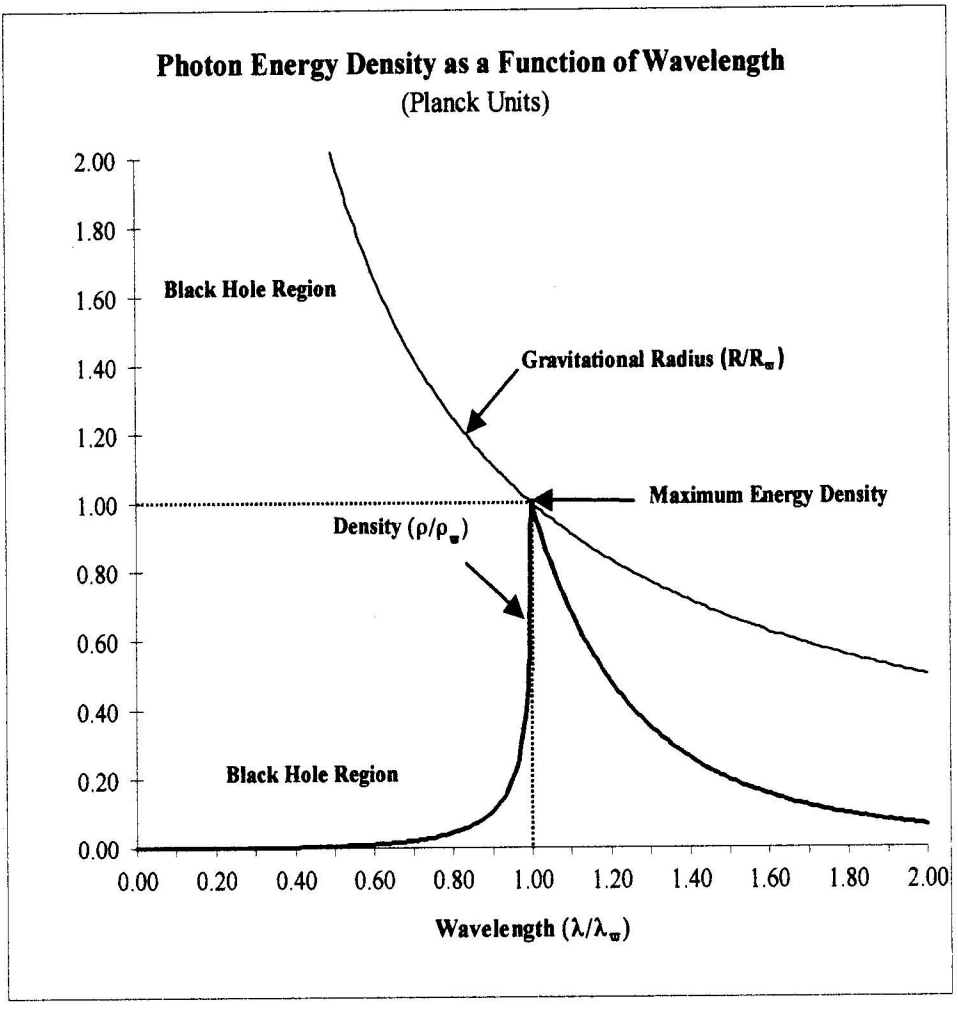


Figure 1. This illustrates how energy density is inversely propoxtional to the square of the energy, while wavelength is inversely proportional to the energy. In general, any infinite mass object has zero density if its volume is proportional to its gravitational radius raised to any power greater than unity.

That is: $\lambda \rightarrow 0 \quad \Rightarrow \rho \rightarrow 0,$

$\lambda \rightarrow \lambda_\omega \Rightarrow \rho \rightarrow \rho_\omega,$

$\lambda \rightarrow \infty \quad \Rightarrow \rho \rightarrow 0.$

Where: $\lambda_\omega = 2\pi R_\omega = 2\pi(G\hbar/c^3)^{1/2},$

$\rho_\omega c^2 = c^7/8\pi^2 G^2\hbar.$

THE INITIAL CONDITIONS:

When: $r_{\pm}(\Phi) = R_g \pm \delta_r \cong R_g$,

$\theta_{\pm}(\Phi) = \pi/2 \pm \delta_\theta \cong \pi/2$ and

$|\Phi| \leq |\Phi_\chi| = \sqrt{\pi}/N_w \cong 0$,

there exists an extreme gravitationally closed Planck density string of length,[8] $C_{\gamma\pm}$, where:

$$C_{\gamma\pm} = \int_0^{2\pi} [g_{\phi\phi(\gamma=0)}]^{1/2}\, d\phi = 4\pi R_g,$$

which $\Rightarrow$

$\exists$ Maximum Possible Electromagnetic Energy Density[9] $= \rho_w c^2 = c^7/8\pi^2 G^2 h$.

$\exists$ Maximum Possible Action for the Gravitationally Closed Space $= |\mathcal{J}(0)| = GM^2/c$.

$\exists$ Maximum Possible String Tension $= T_w = Mc^2/C_{\gamma\pm} = c4/4\pi G$.

$\exists$ Maximum Possible Vacuum Polarization Energy $= \varepsilon_{evacw} = e^2(c^3/hG)^{1/2}$.

$\exists$ Maximum Possible Photon Energy $= \varepsilon_{\gamma w} = (hc^5/G)^{1/2}$. (See **Figures 1,2,3 & 4**)

In other words, our main postulate is that the initial fluctuation is a non-singular coherent toroidal electromagnetic disturbance of Planck density, ρ_w. This fluctuation is formally identical to a toroidal geon, or a closed circular string composed of N_w primaton photons, with total initial angular momentum magnitude:

$$J(0) = [\mathcal{J}(0) \bullet \mathcal{J}(0)]^{1/2} =$$

$$\hbar[N_w^4 + 2N_w^2 + 3]^{1/2} \approx$$

$$\hbar(N_w)^2 = R_g Mc.$$

The inner and outer event horizon areas are calculated by:

$$A(\pm\Phi) = \int_{(\pi/2-\Phi)}^{(\pi/2+\Phi)} \int_0^{2\pi} \sqrt{(g_{\phi\phi}\, g_{\theta\theta})}\, d\phi d\theta = 4\pi R_{z\pm}^2 \sin(\pm\Phi) = 8\pi R_g^2 \sin(\pm\Phi)[1 + \sin(\pm\Phi)].$$

Therefore, the *total net* horizon area for the SSM Universe is reckoned by:

$$A_U^{(2)}(\Phi) = A(+\Phi) + A(-\Phi) = 16\pi(R_g \sin\Phi)^2.$$

Moreover, the spatial volume or hyper-surface area of the SSM U is calculated as:[10]

$$A_U^{(3)}(\Phi) = 4\pi R_g^3 \sin\Phi(5\Phi - 3\sin\Phi\cos\Phi).$$

We also find that the total space-time volume or 4-volume (ignoring the $\sqrt{-1}$ coefficient) as a function the expansion parameter Φ is:

$$A_U^{(4)}(\Phi) = (8\pi c/3)\, t_s(\Phi) R_g^3 \sin^2\Phi\,(3 + 2\sin^2\Phi - \sin^4\Phi).$$

Of course, the length $C_{\gamma\pm}$, is the one dimensional "area:"

$$A_U^{(1)}(\Phi) = 4\pi R_g.$$

---

[8] $\forall\, \Phi\, \varepsilon\, \gamma\, (r_\pm(\Phi)) = 0$, $C_{\gamma\pm} = \int_0^{2\pi} [g_{\phi\phi(\gamma=0)}]^{1/2} d\phi = 4\pi R_g$ = circumference of both inner and outer event horizons at the "equator" (the space orthogonal to the axis of symmetry $\mathcal{J}(0)$, i.e. $\theta - \pi/2$.) Note, *the circumference is constant for all* Φ and hence, *is independent* of the event horizon radii.

[9] See **Figure 1.** and the discussion about maximum energy density electromagnetic quanta in Meyer (1980).

[10] This spatial volume calculation is worked out in Meyer (1995).

TEMPORAL MEASURE

Please note, there always exists a net time interval, $\Delta t_s(\Phi)$, (which is the difference between the current future directed and past-directed time displacements, i.e.:

$$\Delta t_s(\Phi) \equiv t_+(\Phi) - \frac{1}{c}\left(\underset{\text{future directed}}{u_+(\Phi)} - \underset{\text{past directed}}{u_-(\Phi)}\right) = \frac{R_g}{c}\left[-ln(1-sin\Phi) - ln(1+sin\Phi)\right] = -\frac{R_g}{c}ln(1-sin^2\Phi).$$

In general: $ct_s(\pm\Phi) = -R_g\, ln(cos^2\Phi).$

Therefore, for the small angle at creation $\Phi=\Phi_\chi \equiv \pm(\sqrt{\pi})/N_w$, one gets:

$$ct_s(\pm\Phi_\chi) = -R_g\, ln(1-sin^2\Phi_\chi) \approx R_g\Phi_\chi^2 = \pi R_g/N_w^2 = \pi\hbar/Mc,$$

which is *one half*[11] the Compton wavelength of the SSM universe. And at maximum expansion, when, $\Phi=\pm\pi/2$:

$$ct_s(\pm\pi/2) = -R_g\, ln[1-sin^2(\pm\pi/2)] = +\infty.$$

The past-directed time[12] is:

$$t_-(\Phi) \equiv u_-(\Phi)/c = R_g\, ln(1+sin\Phi)/c$$

Note, when $\Phi=\Phi_*$, then $t_-(\Phi_*)$ = 15.25 billion years.[13]

Again, please see **Figures 2,3** and **4,** which provide schematics showing how the SSM universe evolves.

The expansion parameter, F, grows in both directions away from an origin $\Phi \sim \pm 0$. That is, the space-time expands, "both ways" in time. In the beginning, the space-time or "creation ring is a closed cosmic string with an "inflated" circumference of 276.75 billion light-years. Since $\boldsymbol{J}$, the angular momentum vector, is a cosine function of Φ, then by increasing $|\Phi|$ the angular momentum magnitude is decreased and the space expands.

As Φ approaches $\pm\pi/2$, the outer event horizon approaches the Schwarzchild radius and the inner event horizon radius approaches zero.

The state of the original SSM string universe is balanced on a "razor's edge," where the "centrifugal" acceleration is precisely balanced with the gravitational. However, due to the tiny areas of the primaton event horizons, the string will rapidly "evaporate" via Hawking radiation into its *ergosphere*[14] within 2.60 x 10^{-39} seconds.

Reiterating, we transform the entire family of metrics into one dual $\Phi=\Phi(t_\pm)$, time varying metric, so that Φ grows in both directions away from the origin $\sim \pm 0$ That is, the space-time expands as Φ grows in both positive and negative temporal directions from *when* or *where*: $\Phi = \Phi_\chi \equiv \pm\sqrt{\pi}/N_w \sim \pm\, 0$.

At this epoch the space-time is a closed cosmic string with "inflated" circumference — a pseudo ring singularity — which is a circle of Planck density primaton light — a Planck density toroidal geon.

---

[11] This might mean there were two universes created. That is, there might be another U created with opposite parity, so that the net angular momentum would be zero. In this paper we shall just be concerned with one of them.

[12] One can see that the maximum past time is always finite and the maximum future time is always infinite.

[13] In the SSM, the 'present' is defined as the time when $\Phi = \Phi_* \equiv sin^{-1}[(m_p - m_e)/(m_p + m_e)]$. See the further section: **"ON THE DETERMINATION OF m_p & m_e"**

[14] The SSM ergosphere is defined as the region:

$\{<\mathbf{r}, \theta, \phi, \Phi>\} \ni (-\pi/2 \le \Phi \le \pi/2) \wedge (0 \le \phi \le 2\pi) \wedge [\,0 \le (\pi/2 - \Phi) \le \theta \le (\pi/2 + \Phi) \le \pi\,] \wedge$
$(r_{ergo-} \le r \le r_{ergo+}) \ni \{\, 0 \le r_{ergo-} \equiv R_g[\,1 - (1 - cos^2\Phi cos^2\theta)^{1/2}\,] \le r_- \equiv R_g(1 - sin\Phi) \le R_g \le r_+ \equiv R_g(1 + sin\Phi)$
$\le r_{ergo+} \equiv R_g[\,1 + (1 - cos^2\Phi cos^2\theta)^{1/2}\,] \le 2R_g \equiv R_S\,\}$

Since, $|\mathcal{J}|=R_g M\, c\cos\Phi$, then by increasing the absolute magnitudes of, $|t_+|$ and $|t_-|$ i.e. $|\pm\Phi|$ the angular momentum is decreased and the space expands.

The major hypothesis is that the universe starts as a "stringy" toroidal geon with an initial (post creation) angular momentum magnitude of $|\mathcal{J}(0)|= R_g Mc = hN_w^2$, and with total post creation constant energy $E=Mc^2 > 0$. That is, after creation $dE/d\Phi=0$.

The energy E, just after the creation event, is hypothesized to equal the total electromagnetic (EM) energy of the manifold, *M*. Moreover, this EM energy E is localized within U(±0), a string-like sub-region of *M*, at $t_\pm=\pm 0$. That is, it is postulated that all energy was created originally as light, coherent light in the form of a maximum density toroidal geon, U(±0). Where U is a set including and bounded by the two incompletely propagated event horizons.

The region U (See **Figures 2-4**) is defined as:

$$\mathbf{U = \{ < r, \theta, \phi, t_\pm(\Phi_\pm) > \ni [(r_- \le r \le r_+), (\pi/2 - |\Phi| \le \theta \le |\Phi| + \pi/2), (0 \le \phi \le 2\pi), (-\pi/2 \le \Phi \le \pi/2), (0 \le |t_\pm| \le \infty)] \} \subseteq \mathcal{M}.}$$

One aspect of the *Super-spin* hypothesis is that the expanding space-time U(Φ) stores its excess angular momentum in rotating matter and neutrinos and upon full expansion settles down to the Schwarzschild metric along a future directed time coordinate.

Another aspect is: if the standard FRW model is assumed, then the U will appear to not have enough mass for gravitational closure. Nevertheless, it is closed in the SSM metric.

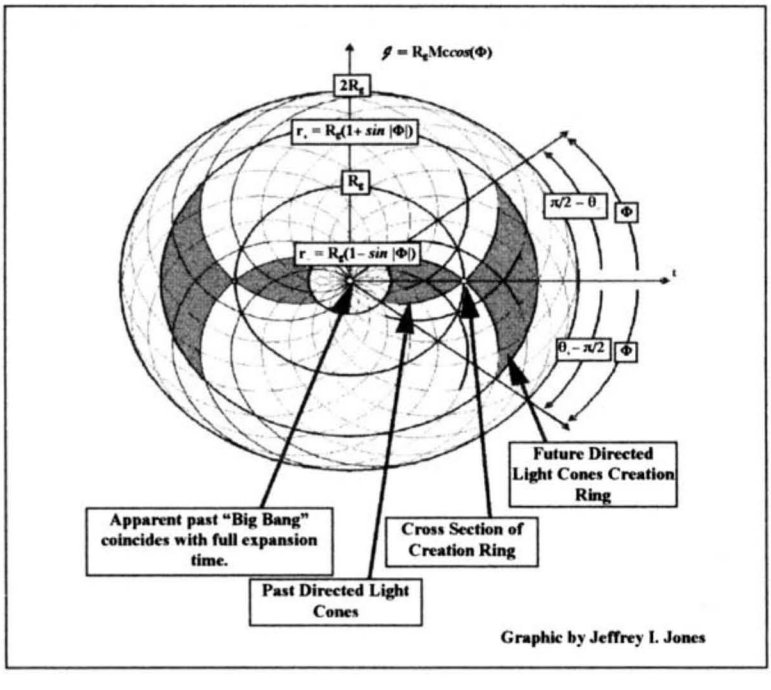


Figure 2. Profile of future directed and past directed light cones starting at creation ring as projected onto the following space: $\{< \pm t, \theta, \phi > \ni (\pi/2 - \Phi \le \theta \le \pi/2 + \Phi) \wedge (\phi - \textbf{constant})\}$

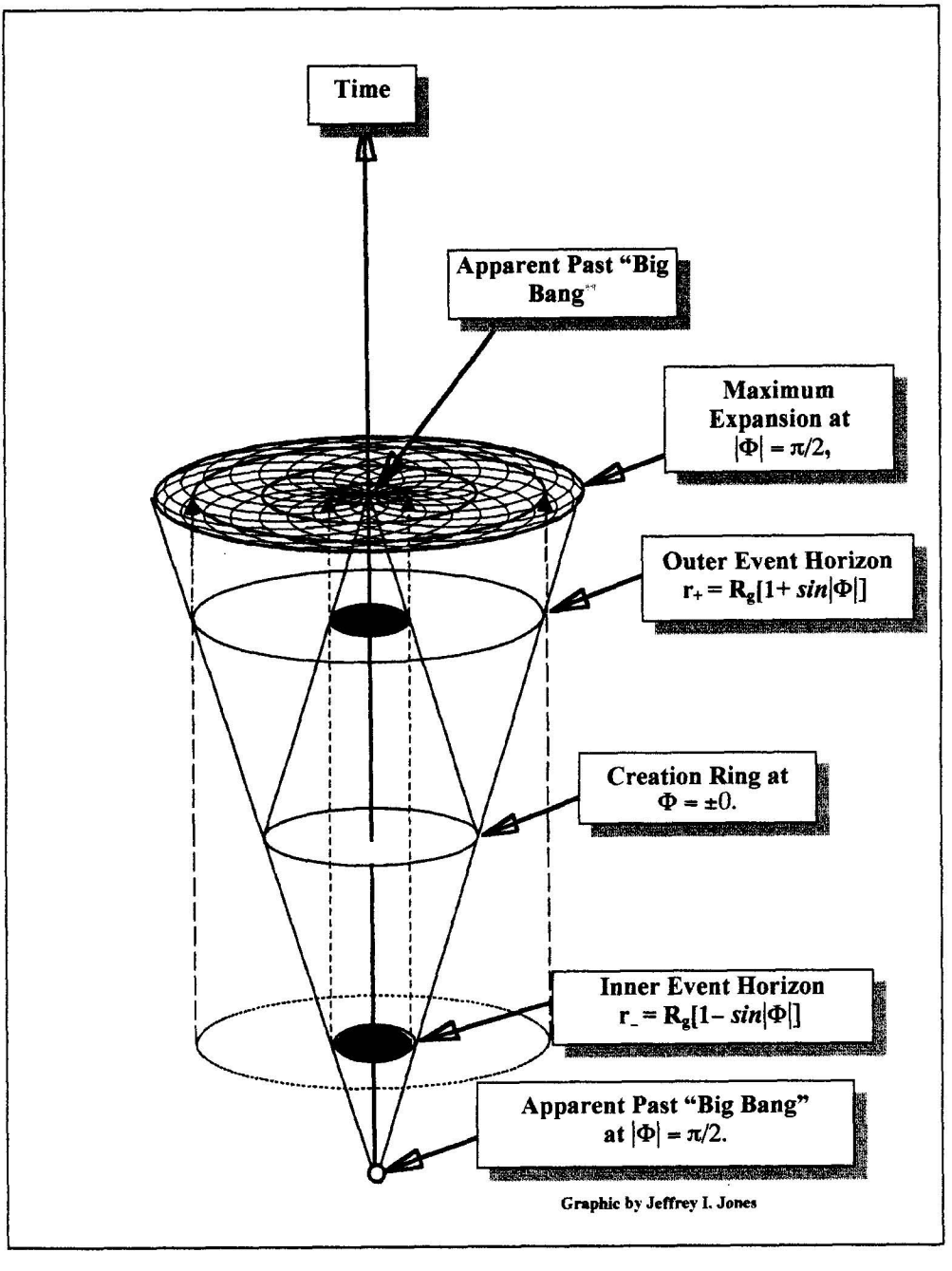


Figure 3. Portrait of evolution of SSM universe

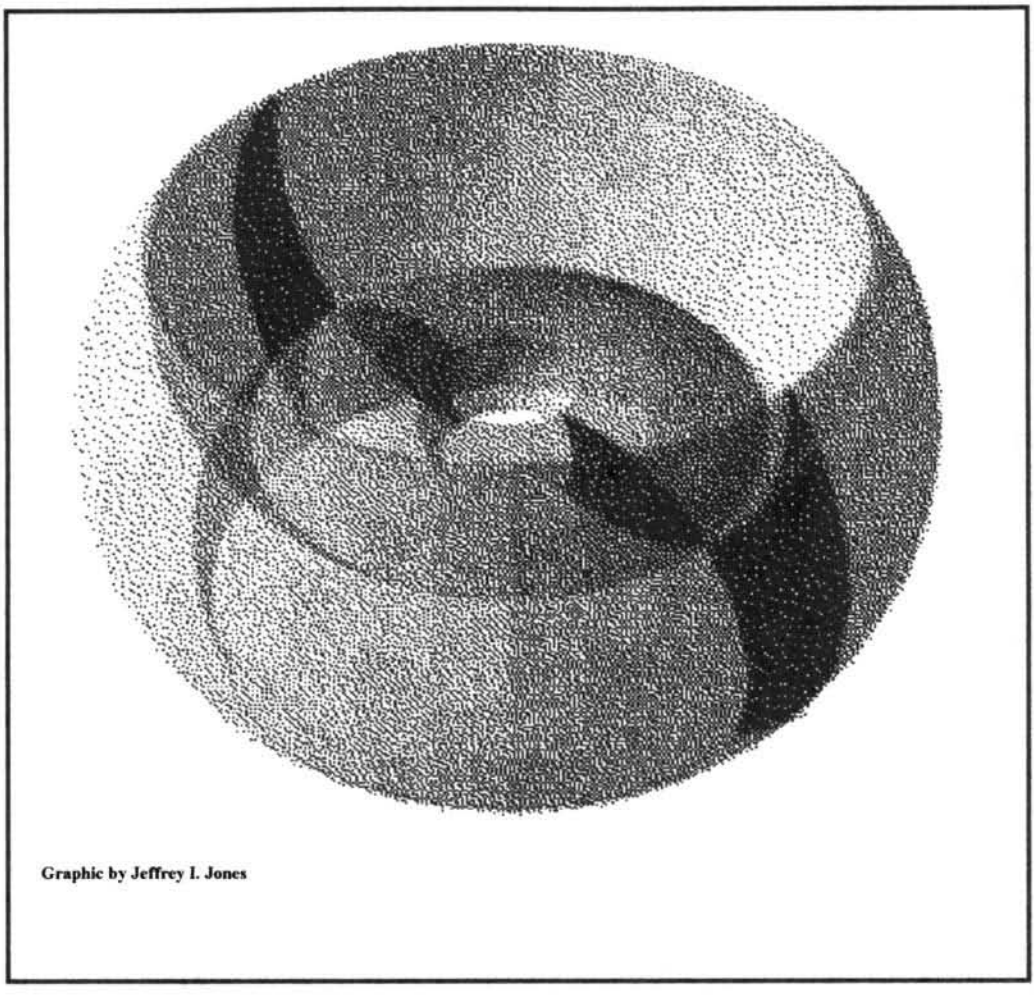


Figure 4 (Solid View of Figure's 2 & 3)

This illustrates the loci of future and past-directed light cones, starting at creation ring as projected in the following space:

$$\{<\pm t,\theta,\phi\ > \ni \quad (\pi/2\ -\ \Phi \leq\ \theta \leq \pi/2+\Phi) \wedge (0 \leq \phi \leq\ 2\pi)\}$$

The darkest region is a two-dimensional $\{< \pm t,\ \theta >\}$ profile of light cones as shown in Figure 2. Only two-dimensional projections of three- space are shown in the above solid.

OUTLINE OF THE SOLUTION FOR THE MASS OF THE SSM UNIVERSE

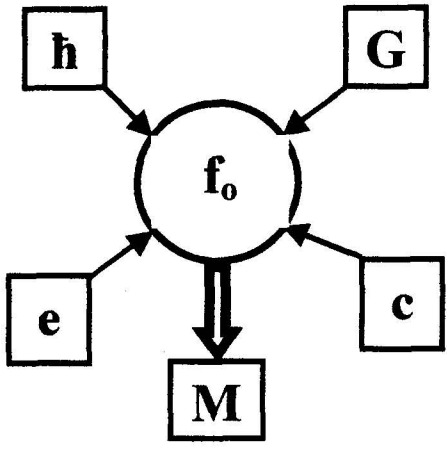


Figure 5. Schematic for the Solution for the Mass of the SSM Universe

The solution for the mass **M** of the SSM Universe was obtained by noting that Unn (1976) found the vacuum could exhibit a measurable temperature induced by acceleration And since, an initial condition for the SSM Universe was the existence of a maximal spinning string – there was acceleration. The String Mass puzzle was solved by Meyer (1995) in the form of equation (1), by utilizing:

The Unruh temperature,
Bose-Einstein statistics,
Momenta phase space conservation,
The axi-symmetric metric and the
Initial boundary conditions,

along with the identities:

$$\varepsilon_{e\,vac} = e^2 R_w = Gm_{eg}^2/R_w, = kT_{evac} = \alpha G m_w^2/R_w = \alpha\varepsilon_w.$$

Where: $\alpha \equiv e^2/hc$.

Note: $\varepsilon_{eg} = m_{eg}c^2 = [\alpha hc^5/G]^{1/2} = d\alpha\ \varepsilon_w = ec^2/dG \equiv$ Gravitational Electromagnetic Unification Energy.

In summary, the above conditions, principles, and equations led to the determination o the expectation function:

$$< f_\varpi > = 8\pi^2/N_\varpi = 2/[\exp(\varepsilon_\varpi/kT_{evac}) - 1] \Rightarrow$$

$$N_\varpi = 4\pi^2\,[\exp(1/\alpha) - 1] \cong 4\pi^2 \exp(1/\alpha) \Rightarrow$$

$$\mathbf{M = f_0(c,e,G,\hbar) = 4\pi^2 m_\varpi \exp(1/\alpha) = 4\pi^2[\hbar c/G]^{1/2}\exp(\hbar c/e^2).} \qquad (1)$$

THE REST MASS OF U

The irreducible energy 'E_q' of any Kerr black hole or axi-symmetric rotating space-time with finite event horizons is the energy that can't be radiated away by slowing down the rate of rotation. This energy is equal to the energy of the space-time system 'U' at rest with respect to the rest of the manifold '*M* at infinity. That is:

$$E_q = \text{Total Energy - Kinetic Energy} = \text{Rest Energy} = \text{Irreducible Energy}.$$

This irreducible energy for any Kerr black hole starting at some initial '$\Phi \equiv \Phi_0$' was shown by Christodoulu (1970) to be determined by:

$$E_q = Mc^2 [(1 + sin|\Phi_0|)/2]^{1/2}.$$

It is quite apparent, though here stated without formal proof, that Christodoulu's formula also holds for the class of toroidal geons such that when we start with $\Phi = \Phi_0 = \pm 0$ and $|J(0)| = R_g Mc$, and we increase $|\Phi|$ without radiating away any significant amount of energy through the actual final event horizons; we will find that upon reaching $|\Phi| = \pi/2$ (the Schwarzschild or final "rest" state) that, $E[1-1/\sqrt{2}]$, or around 29% of the total energy is unaccounted for. This implies the rest mass of the SSM universe is:

$$M_0 = M/\sqrt{2}$$

Reiterating, the entire family of stationary Kerr metrics is transformed into a single, $\Phi = \Phi(t_\pm) = \pm\Phi$, dual time varying metric, $(-\pi/2 \leq \Phi \leq \pi/2)$, so that Φ grows in both directions away from the origin $F \sim 0$. That is, the space-time expands, "both ways" from when or where:

$$\Phi_\chi = \pm\pi^{1/2}/N_w = \pm 1/4\pi^{3/2}\, exp(e^2/\hbar c) = \pm 1.374791 \times 10^{-61} \approx 0.$$

At this epoch the space-time is a closed cosmic string with "inflated" and ever-constant circumference:

$$C_{t_\pm} = 4\pi GM/c^2 = 2.618212253 \times 10^{29} \text{ cm} = 276.75 \text{ billion light-years}.$$

Since $|J| = GM^2 cos(\Phi)/c$, then by increasing the absolute magnitudes of $t_\pm$, the angular momentum is decreased and the space expands.

TWO DERIVATIONS WHICH CLOSELY DETERMINE THE MEAN CHARGED FERMION MASS '$m_0 \equiv (m_p + m_e)/2$'

The mass **M** of this model universe has been determined from theory. But, how are other masses, such as the masses of the electron and proton, going to be determined?

Fortunately, it turned out, the mean stable charged fermion mass '$\mathbf{m_0}$' could be closely determined from theory in at least two ways.

First Derivation of the Approximate Mean Stable Charged Fermion Mass 'm_0'

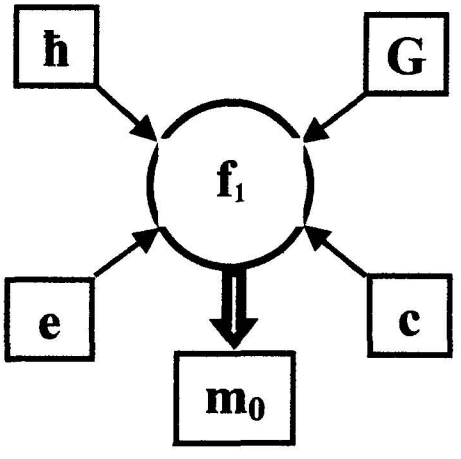


Figure 6.
Schematic for first derivation of the approximate mean stable charged fermion mass 'm_0'

In this derivation the mass, m_0, was determined by the use of:

Phase space conservation,
Both initial and end-state boundary conditions and
The exterior red-shifted Hartle-Hawking event horizon temperature[15] at infinity. See Hartle and Hawking (1976)

After some calculation, see Meyer (1995), we then get:

$$m_0 \equiv (m_p + m_e)/2 = f_1(c, e, G, \hbar) \approx$$

$$4(\pi/50)^{1/3}[\hbar c/G]^{1/2} exp(-\hbar c/3e^2) / x_{rf} = 8.369992 \times 10^{-25} gm. \quad (2)$$

[15] Where, $x_{rf} = 3/5 + [\pi e^2/hc]^2 + \ldots \approx 3/5$ is the Fermi coefficient at the exterior red-shifted Hartle-Hawking temperature. This is the Fermi coefficient for a Fermi-Dirac gas at the vacuum temperature of the outer event horizon of a Schwarzschild black hole red shifted to infinity. It is calculated by using a series obtained by Sommerfeld. Note that at a temperature of absolute zero in a flat Minkowski vacuum, the Fermi coefficient will be exactly equal to 3/5.

Second Approximate Determination of Mean Stable Charged Fermion Mass 'm_0'

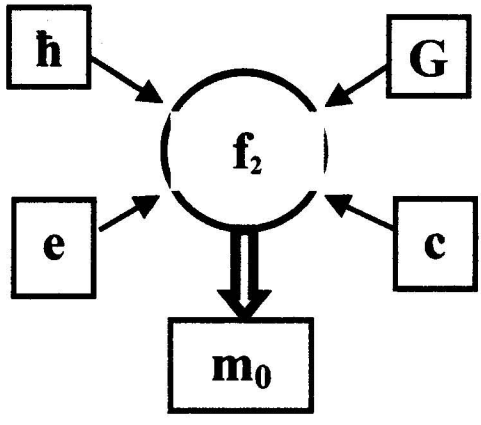


Figure 7
Schematic for second derivation of the approximate mean stable charged fermion mass 'm_0'

This alternate approximate solution for m_0 is obtained by using:

The end-state conditions,
The Fermi-Dirac statistics,
The Debye distribution approximation,
And by blue-shifting the external temperature of the Hartle-Hawking vacuum at infinity, to a temperature[16] associated with the charged particle zitterbewegung. This temperature is determined at a time uncertain within an internally red-shifted wave-period from the outer event horizon's 2-surfaceboundary.

After some calculation, see Meyer (1995), we then get:

$$m_0 \equiv (m_p + m_e)/2 = f_2(c, e, G, \hbar) \approx$$

$$\{3x_{bf}/[10(\pi e^2/\hbar c)^2]\}^{1/6}(\hbar c/G)^{1/2} exp(-\hbar c/3e^2) = 8.361938 \times 10^{-25} gm. \quad (3)$$

[16] Where, $x_{bf} = 3/5 + \Sigma gi(\alpha)\ldots \approx 3/5$, is the Fermi coefficient at the interior blue shifted Hartle-Hawking temperature,

ON AN INDEPENDENT THEORETICAL DETERMINATION OF THE SOMMERFELD FINE STRUCTURE CONSTANT '$\alpha = e^2/hc$'

By equating the two close solutions for $\mathbf{m_0}$, an approximate solution for 'α' appears. This rough methodology shows promise that the Sommerfeld fine structure constant 'α' may, in principle, be theoretically determined with greater accuracy than accomplished by current experimental means.

Equating **(2)** with **(3)** yields:

$$4(\pi/50)^{1/3}/x_{rf}(\alpha) = [(3x_{bf}(\alpha)/10(\pi\,\alpha)^2]^{1/6}.$$

Since,

$$x_{rf}(\alpha) \approx x_{bf}(\alpha) \approx 3/5,$$

Then:

$$1/\alpha \approx (5\pi)^2(4)^3/[(2)^{1/2}(3)^4]$$

This rough method produces an error ratio of 0.00597.

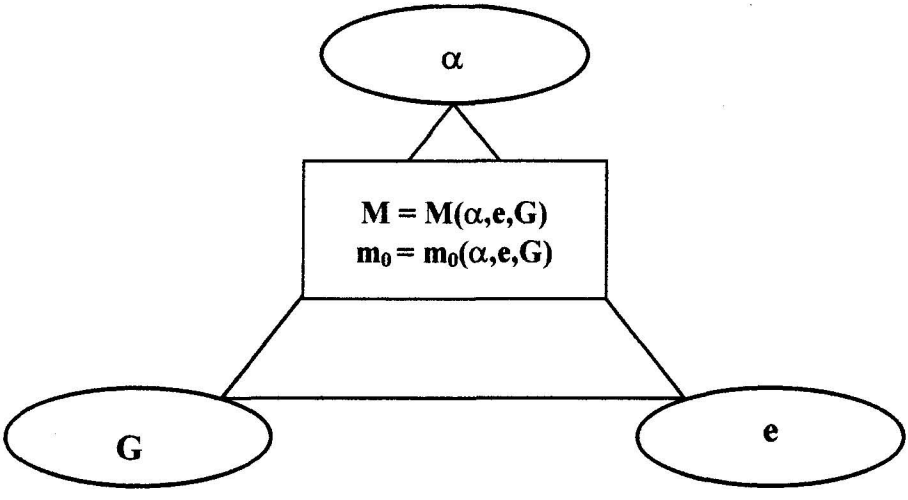


Figure 8. It is easy to see that both **M** & $\mathbf{m_0}$ can be expressed in terms ofjust 3 fundamental constants: α, **e** and **G.**

THE DETERMINATION OF G = G(h,c,e,m_0)

From the new non-stationary metric $g_{ij}(\Phi)$, the rescaled Hamiltonian is formed:

$$\mathcal{H} = -\mu^2/2 = g_{ij}dx^i dx^j/d\lambda^2 = g^{ij}p_i p_j \Rightarrow$$
$$m^2 + mm_0 + (Jm_0c/GM^2)^2 = 0 \Rightarrow$$
$$\exists\, N_q = 2^n, \ni N_q = M/(m_0\sqrt{2}) \;\&\; n \in \{\text{integers} > 0\}. \qquad (4)$$

Due to the above results, the solution for n and hence N_q can be accurately determined by direct calculation. This is because **M** has been determined via **(1)** and m_0 has also been closely determined by **(1)** *and* [**(2)** or **(3)**]. Also, a has been roughly determined by **(2)** *and* **(3).**

Therefore, a "reincarnation" of Sir Arthur Eddington's famous "Cosmical Number", Eddington (1939), reappears as:

$$N_q = 2^{267}.$$

Therefore, a connection between **G** & **e** is established.

$$G = 8\pi^4\hbar c\, exp(2\hbar c/e^2)/[N_q m_0]^2 = 6.67294103 \times 10^{-8}\ cm^3/gm\cdot sec^2. \qquad (5)$$

ON THE DETERMINATION OF m_p & m_e

From the quadratic in **(4)** above, it also follows that:

$$m_+ = m_0(1+sin\Phi)$$
$$m_- = m_0(1-sin\Phi)$$

where Φ is chosen as the positive branch.

Now we know:

$$m_e + m_p = 2m_0$$

These equations suggest the hypothesis:
The proton and the electron mass are mass-time conjugates, i.e. the prot electron exhibit mass, charge, time andparity conjugation.

This implies that the proton and electron are *"time vintaged" anti-particles.* Therefore, we posit that:

$$m_p \equiv m_+ = m_0(1+sin\Phi)$$
$$m_e \equiv m_- = m_0(1-sin\Phi)$$

If this hypothesis is true, then at the present, when:

$$\Phi \equiv \Phi_* = sin^{-1}[(m_e + m_p)/(m_p - m_e)] \doteq 1{,}52413073 \text{ radians},$$

the SSM should be able to predict the current values of certain other phenomena, which also depend upon Φ

That is, if our universe is a SSM type universe, then at present, when $\Phi \equiv \Phi_*$, the model should be able to predict current values of other phenomena, which also depend upon Φ, such as the CBR temperature and the density ofour universe.

In the SSM universe the CBR temperature 'T_γ', as a function of Φ is derived as:

$$T_\gamma(\Phi) =$$
$$\zeta(3)(\hbar c^5/G)^{1/2}\{(43\pi\{2-[2(1+sin\Phi)]^{1/2}\})/[8sin\Phi(5\Phi-3sin\Phi cos\Phi)]\}^{1/4}/(6\pi k\zeta(4)exp(\hbar c/2e^2)).$$

Therefore, the present CBR temperature," $T\gamma(\Phi)$, at $\Phi = \Phi_*$, should be: 2.7360 K

---

[17] Please see footnote 3.

The average mass density 'ρ_U', of the SSM universe as a function of Φ, is determined as:

$$\rho_U(\Phi) = (c/2\pi)^5/[2\hbar sin\Phi(5\Phi - 3sin\Phi cos\Phi)[Gexp(\hbar c/e^2)]^2].$$

Therefore, the present average mass density, $\rho_U(\Phi)$, should be: $3.3039085 \times 10^{-31}$ gm/cm^3.

PREDICTED INCONSISTENCIES BETWEEN THE SSM AND THE STANDARD MODEL

The major difference between most conformal mass scaling models and the Super Spin Model is that; in the SSM, the direction and magnitude of the mass scaling is also charge and parity conjugated with time. Moreover, in the SSM, the total rest mass is constant and time invariant, even though individual particle rest masses are rescaled "covariantly" and "contravariantly," according to their temporal senses, charges and parities. This is possible, because the SSM metric is non-stationary, dual time asymmetric and non-symmetric under spatial inversion.

Why hasn't proton decay been observed? At creation, after pair production, where did all the antimatter go? According to the SSM, m, and m- are "time vintaged" anti-particles whose rest masses, by being geared to a dual valued time dependent metric, will vary relative to the amount of Φ displacement, or equivalently to the amount of time elapsed since their mutual creation via pair production. Therefore, the original anti-matter did not mysteriously leave the universe! It is still with us and a part of us!

Moreover, if m_+ and m. are indeed m_p and m_e respectively, then there is no apparent reason to expect the proton to decay, unless the electron also is capable of decaying. This is because the proton's structure should mirror the structure of its time-vintaged anti-particle, the electron, unless basic particle topologies are also time and parity dependent. This does not seem to be the case, since each proton-antiproton and electron-positron pair appear to retain topological equivalence under spatial inversion and time reversal.

It then follows that the SS Model contradicts aspects of the Standard quark-lepton Model. Since in the Standard Model the proton and other hadrons are composed of quarks; but the electrons and other leptons are regarded as fundamental point-like particles. Nevertheless, over the past three decades there has been considerable evidence that the proton has structure, e.g. Krisch (1976).

This evidence, taken along with the SSM inferred isomorphism of the electron and proton topologies is in accord with some particle string theories and is also consistent with certain elements of the elementary particle theory put forth by Behram Kursunoglu (1974), (1976).

In the Kursunoglu "Orbiton Model," both the proton and the electron are structurally isomorphic; both formed as singularity-free, "onion-like,'' alternating magnetic field structures - "orbitons."

In summary, if the inferences derived from SSM are correct, it follows that, proton decay should not only be "difficult," but impossible to observe, and the universe should appear to consist predominantly of matter, with the appearance of very little, if any, naturally occurring anti-matter. This is because ancient anti-matter is implicit, and has been rescaled as electrons (or protons).

Shortly after the Big Spin creation, when: $t_{0\pm} \approx \pm 1.824 \times 10^{-5}$ seconds, the metric was still almost unitary, i.e.

$$ds^2(t_{0+}) \approx ds^2(t_{0-}).$$

At this point the U's energy density, $\rho u(\Phi_{0\pm}) = 5.7059 \times 10^{14}$ gm-c^2/cm^3, and the temperature, $T(\Phi_{0\pm}) = 2.8518 \times 10^{12}$ K, were such that it became possible, within an instant,

for matter-antimatter pairs (*with unresolvable rest mass difference*) to start condensing. Technically, virtual pairs at $\Phi = 0$, have identical matter - anti-matter masses.

As $|\Phi|$ continued to increase, the U got cooler and less dense, globally producing only neutrinos, which incrementally stored the decrements in the U's angular energy and momentum. Moreover, after the requisite time had passed since $t_{0\pm}$, because of the time varying metric's asymmetric duality, observers would notice two sets containing equal numbers of oppositely, but equally charged particles with unequal rest masses:

$$m_{\pm} = m_0(1 \pm sin\Phi).$$

One can surmise that there would be considerable theoretical difficulties for residents of the SSM universe, if they assumed that these two energy levels were constant; i.e. if they assumed that the electron and proton rest masses were constant

Moreover, if they regarded this assumption as true, a-priori, it would be then be incumbent upon them to create laws requiring the conservation of "lepton" and "baryon" number. Furthermore, addtional laws stipulating the conservation of other attributes that appeared to be associated with "leptonness" and "baryonness" would also have to be created.

Of course, similar rescaling processes will occur for pair production of other types of particles produced at other energy levels. At the creation epoch, the proton and electron had equal rest masses of mass m_0. That is, they were anti-particles of each other then, but not at later times.

In the SSM U, local pair production at various energy levels can take place in what appears to the observer to be a flat space-time which nevertheless registers intrinsically different energy 'gauges', but which in 'reality' are a spectrum of hyper-surfaces with different curvatures, locally appearing to be flat; i.e. locally Minkowskian and Lorentz invariant. Hence, the flat space Dirac equation correctly yields pairs of oppositely charged particles with *equal* rest masses.

Nevertheless, within the rules of the "standard model" a nagging question remains unanswered. "Why are there only two (apparently) stable rest masses, associated with the same charge quantum magnitude 'e', that appear from among the spectrum of "possible rest energy levels?" This charge magnitude equality, but rest mass difference, would lead an observer to postulate the existence of a "law" for "heavy charge" or "baryon" conservation and consequently classify the long-lived charged baryons and leptons as "different as apples and oranges" instead of just "fruit" - or the vintaged anti-particles they actually are in this type of space-time.

OTHER TOPICS

Was "Let There Be Light" of Genesis a Bubble or a String?

There is no apparent reason that a non-rotating bubble membrane fluctuation would be stable. It should rapidly absorb the high pressure vacuum (EM) energy and "flash back" into the flat vacuum from whence it sprang within the Compton time of the universe which is about 10^{-104} sec.

However, in the SSM, the angular momentum of the maximally spinning string induces a coarser granularity by a factor of N_w upon both the spatial and temporal quanta of the fluctuation's active region. That is, the previously indivisible quanta become Planck sized.

Thus, the creative process produces a real space-time with new indivisible spatial and temporal quanta (R_w and t_w), each respectively greater by a factor of N_w than the universe's

Compton length and time; thereby "closing all the hatches" and stopping the massive virtual fluctuation from "sinking" back into the vacuum.

In other words the Creator "writes a check " to the vacuum for 2.8×10^{56} grams of energy and then "changes the *banking rules* before it can clear."

This process creates an actual massive rotating space-time U, initially consisting of the combined coherent directed energy of $N_w=1.289\times10^{61}$ primaton photons forming a closed Planck density string or "circle of light."

Again in other words, the angular momentum components of the fluctuation produce a topological transformation inducing a nonreversible Planckian space-time-energy "granularity," which acts as a one-way valve, thereby preventing the return of the ~1056 gm of energy back to the vacuum within ~ 10^{-104} seconds.

Rotation Neutrinos

Another aspect of the SUPER SPIN hypothesis is that the expanding space-time stores its excess angular momentum in rotating matter and neutrinos and upon approaching full expansion settles down to the Schwarzschild metric along a future directed time coordinate.

Entropy

Furthermore, it has also been found that the thermodynamics of black holes and non-stationary geons became consistent with classical thermodynamics by introducing an augmented definition of the "Bekenstein-Hawking" entropy formula, extended to include the inner event horizon area as a measure of "negentropy" thereby producing third law consistency. By extending this augmentation to the SSM, the gravitational entropy as a function of Φ is determined as:

$$S(\pm\Phi) = 4\pi k\,[N_w \sin\Phi]^2 \geq 0,\ \forall\Phi.$$

It is easy to see that entropy will increase along both positive and negative temporal directions as both temporal displacements increase away from the origin in both positive and negative time.

This extension, applied to maximally rotating, maximum density geons, results in a low initial gravitational entropy value upon the creation of the Planck density string at $\Phi=\Phi_\chi$. This value is:

$$S(\Phi_\chi) = 4\pi^2 k, \text{ where } \Phi_\chi = \pm\sqrt{\pi} / N_w \text{ and 'k' is Boltzman's constant.}$$

Notice that both directions and senses of the temporal dimension, i.e. time and anti-time began (were created) at $\Phi = 0$, along with the other spatial dimensions.

It is simple, but interesting, to observe that anti-time trajectories cannot reach the "terra incognita" beyond or before the universe was created.

Further SSM Verification

The following **Figures 9, 10** and **11** illustrate how the Cosmic Background Radiation (CBR) behaves over time. They indicate that even though the SSM universe is closed, it appears, from our "perspective" of the CBR, to be expanding at an ever-faster rate.

Further verification of the SSM hypothesis entails determining if there are bluer shifts in certain spectra than expected. It also entails checking whether there is an increased spread of the spectra lines between ordinary atomic Hydrogen and Deuterium as one gazes ever further into the past. **Figure 12** is illustrative.

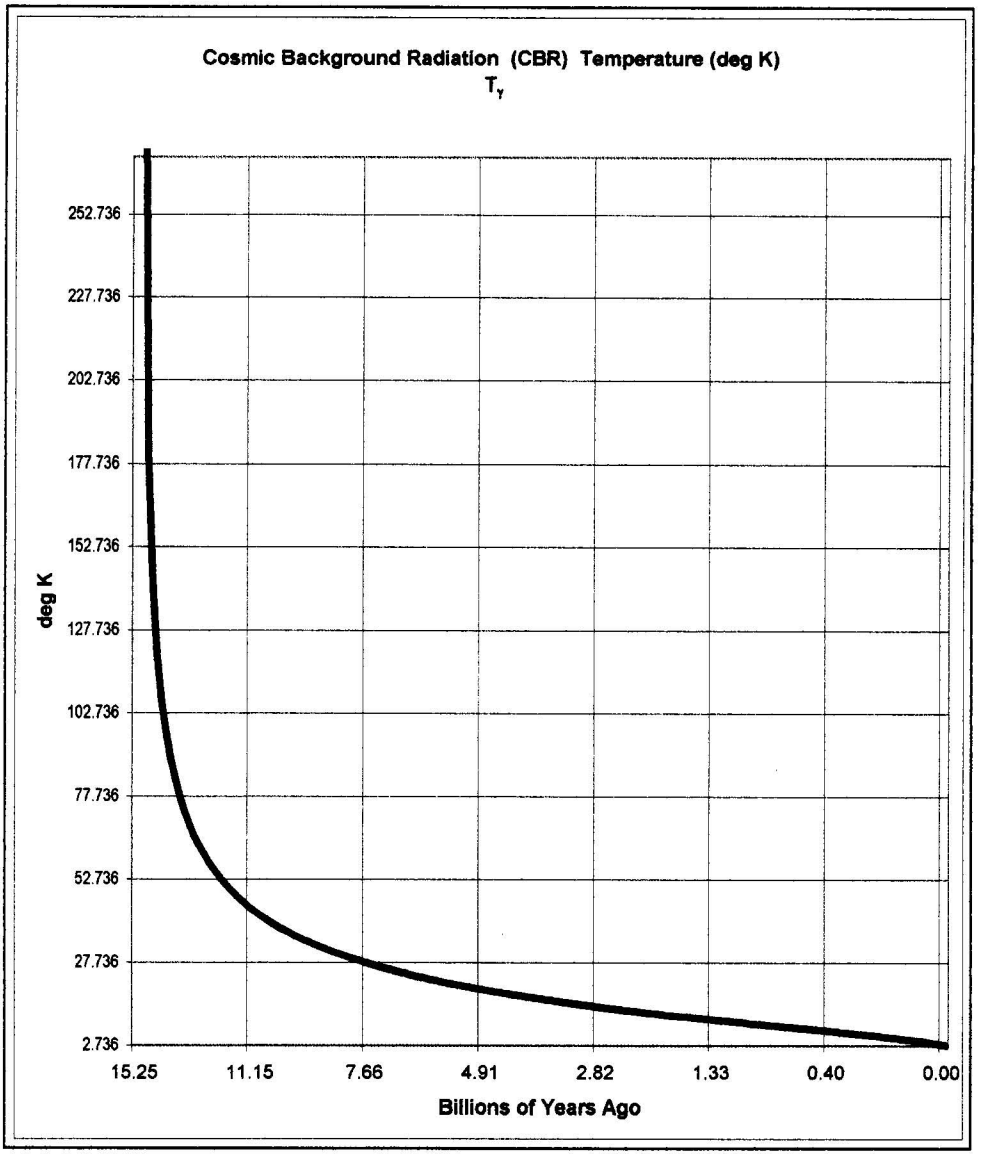


Figure 9 This graph represents the predicted Cosmic Background Radiation Temperature as calculated from the Super Spin Model.

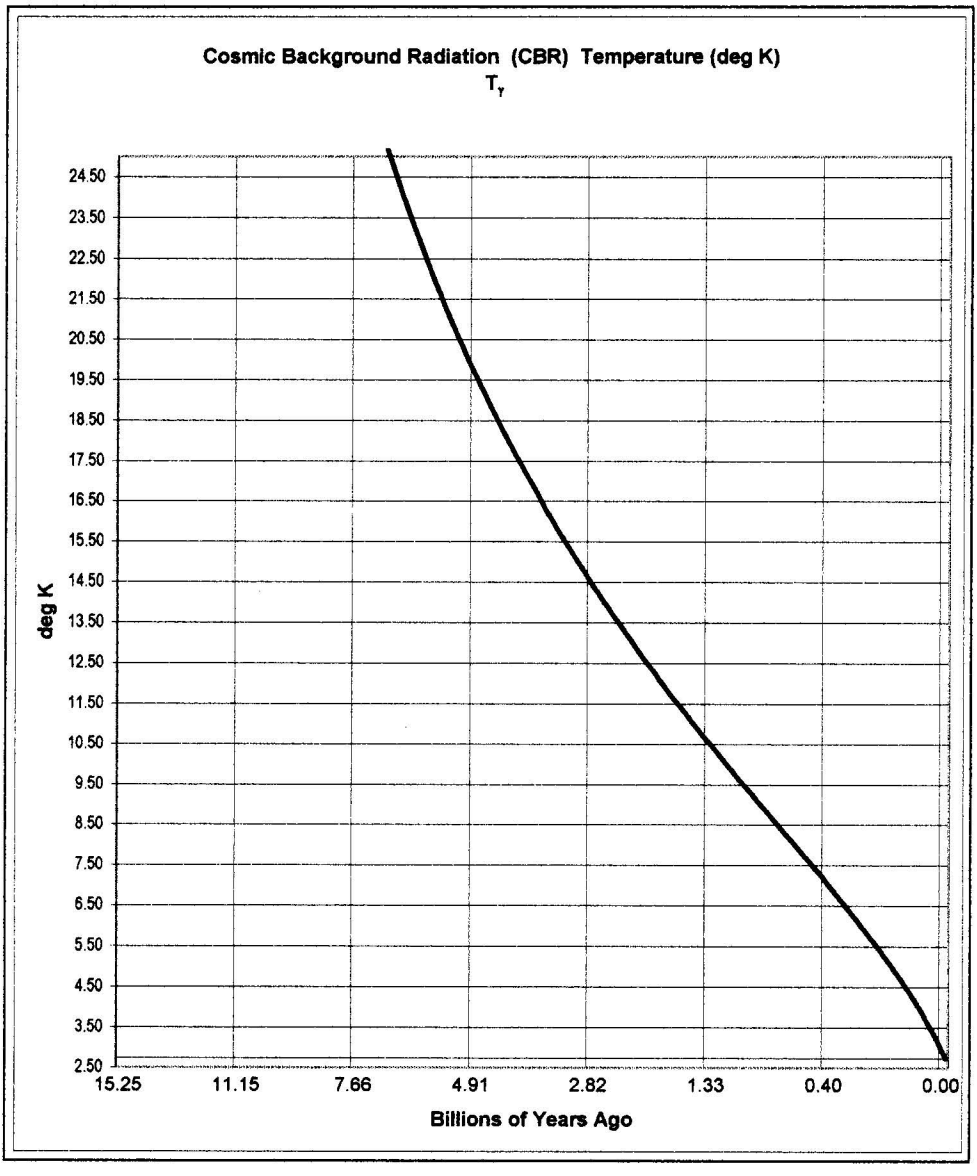


Figure 10 This represents a more recent portion of the predicted Cosmic Background Radiation Temperature as calculated from the Super Spin Model.

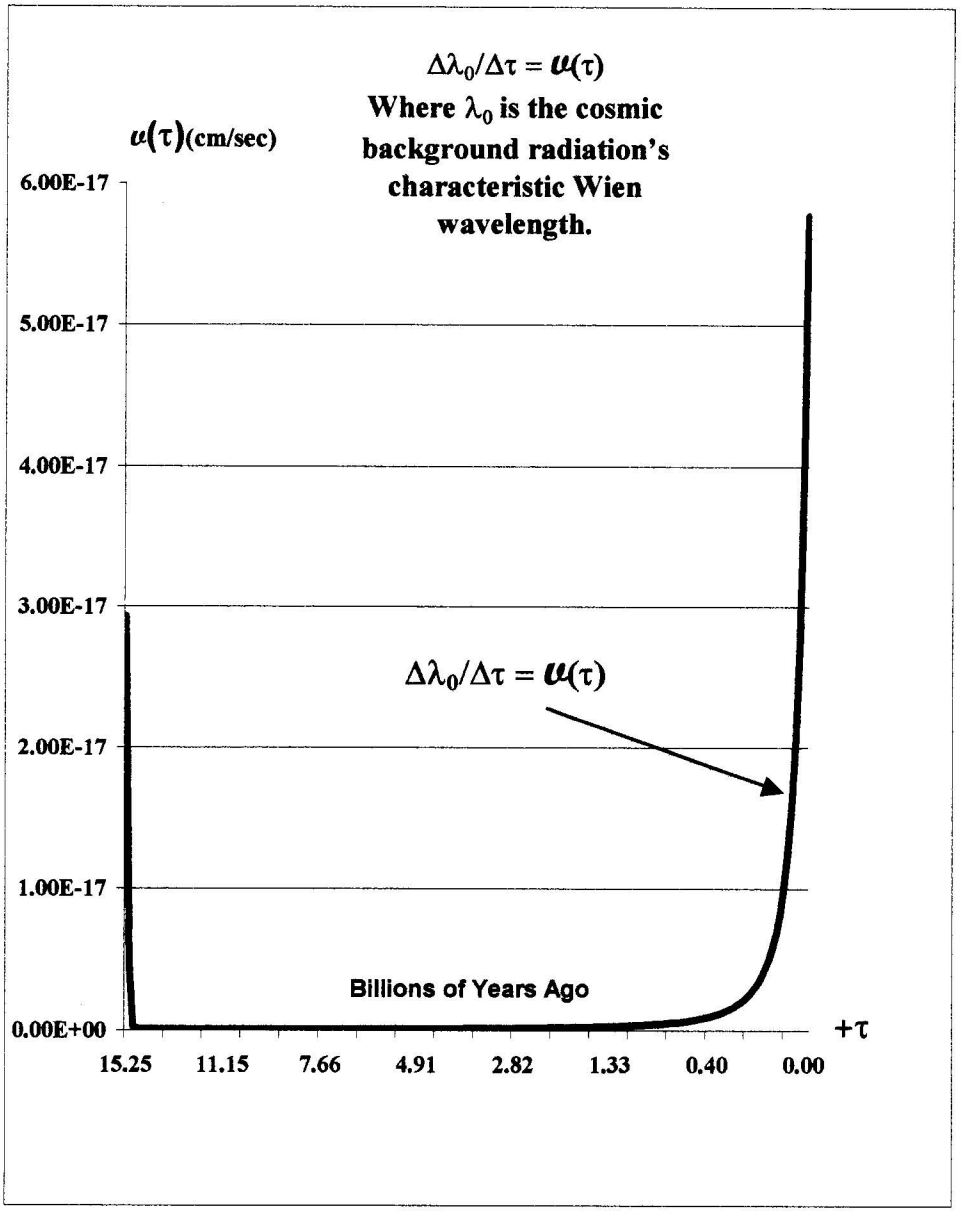


Figure 11. This graph represents the predicted lengthening rate, according to the SSM. of the cosmic background radiation's characteristic Wien wavelength, λ_0.

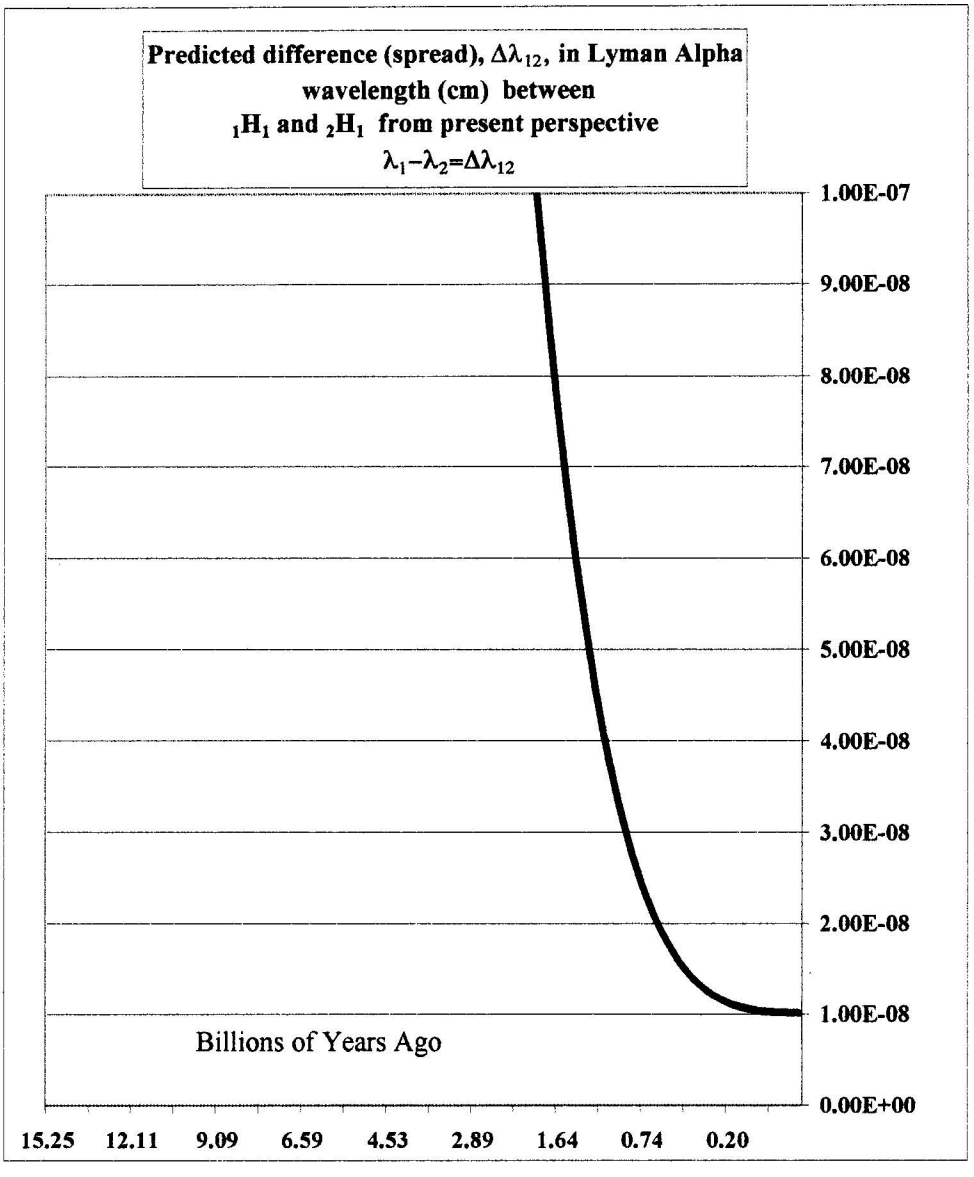


Figure 12. This graph represents the predicted differences between the Lyman alpha wavelengths of Hydrogen 1 and Deuterium as viewed from the present perspective. The Super Spin Model predicts that the Lyman alpha light reaching us now from a common source containing Hydrogen 1 and Deuterium, situated about .75 billion light-years away, may be observed to have the difference between their respective wavelengths amount to over twice as much as is now locally observed in a laboratory frame here on Earth.

ACKNOWLEDGEMENTS

I am very grateful to Professors Behram Kursunoglu and Arnold Perlmutter of the Global Foundation for much helpful advice, to Professor Jeffrey I. Jones, of Queensland Technological University for much of the graphics, and to Dr. Jim I. Jones for productive help and analysis, to Paul E. Schultz for suggesting verification via the H-D spectra, and to my wife Connie for her gracious support and help in getting this paper and presentation together. Above all, I wish to acknowledge and thank the eternal *"God (Who) used beautiful mathematics in Creating the World!"* as P.A.M. Dirac proclaimed.

REFERENCES

Christodoulu, D. 1970. Physical Review Letters, 25, 1596-1597.
Eddington, A.S. 1939. The Philosophy of Physical Science, 170 (Cambridge).
Hartle and Hawking 1976. Physical Review, D13,2188-2203.
Kerr, R. 1963. Physical Review Letters, 11,237.
Krisch, A,, et al. 1976. Physics Letters, 63D, 239.
Kursunoglu, B. 1974. Physical Review, D9,2723-2745.
Kursunoglu, B. 1976. Physical Review, D9, 1539-1560.
Meyer, A.J. 1980 "Primatons, Maximum Energy Density Quanta" in Recent Developments in High Energy Physics (editors A. Perlmutter and L.F. Scott), Plenum Press, New York
Meyer, A.J. 1995 Physics Essays 8 (4), pp. 524-586
Unruh, W.G. 1976. Physical Review, D14,870-892.
Wheeler, J.A. 1955. Physical Review, 97, No. 2,511-536.13.

MAGNETIC MONOPOLES, MASSIVE NEUTRINOS, AND GRAVITATION VIA LOGICAL-EXPERIMENTAL UNIFICATION THEORY (LEUT) AND KURSUNOGLU'S THEORY

Osher Doctorow, Ph.D.

1. INTRODUCTION

The magnetic monopole has not been observed but is predicted by GUTs (grand unified theories (Dirac (1931), 't Hooft (1974) and Polyakov (1974)) contrary to Maxwell's non-magnetic monopole equation (which needs to be revised), whereas the massive neutrino has now been observed contrary to predictions of most theorists (Kursunoglu (1998)), and gravitation is not even theoretically agreed upon by most theorists. These quandaries suggest a fundamental change of emphasis in the foundations of physics away from the usual geometric-algebraic-analytic physics toward logic-based physics, since the quandaries involve deep logical anomalies, paradoxes, and confusions. This direction can already be seen from the related conclusion by the algebraic quantum pioneer R. Haag in his numerous papers that an algebraic interpretation of the Lagrangian (which is the major expression of influence between event/things in theoretical physics) is unlikely to be successful - which is at least as much the case for a geometric or analytic or arithmetic (from which probability/statistics derive) interpretation of the Lagrangian, it may be remarked.

Logic already has entered quantum theory and hence physics via quantum logic, which has been well analyzed by Jammer (1974) up to 1974. However, quantum logic subsequently became bogged down due to its uncritical acceptance of logical anomalies and paradoxes including those involved in the Heisenberg Uncertainty Principle which seemed to imply the non-existence of intersections of canonically conjugate experimental events. The form in which this "bogged down" situation occurred was supposedly the "pinnacle" of quantum logic accomplishments, namely, the isolation of islands of unrelated propositions as non-Boolean lattices. These islands could not be tied down to anything practical in physics and quantum logic became almost completely divorced from the rest of physics including quantum theory.

The return of logic to physics via logical-experimental unified theory (LEUT) takes as its basic assumption the principle that everything must make logical sense, even the definitions when they are asserted to pertain to the real world, so paradoxes and anomalies and incompatible events need to be resolved into meaningful logical and experimental statements in order to be accepted into physics. It is true that definitions may ultimately involve self-definition if carried out for all expressions, but this never precludes requiring that "anomalies" and "paradoxes" be translated into language which compares them with non-anomalous expressions using language understandable by all physicists. In fact, English dictionaries define words in terms of themselves, but this does

Quantum Gravity Generalized Theory of Grav itation and Superstring Theory -Based Unification
Edited by Kursunoglu *et al*. Kluwer Academic / Plenum Publishers. New York 2000

not ordinarily cause trouble because the words that ultimately do not involve some clear mental or physical description are (almost) non-existent.

To be even clearer, LEUT asserts that everything in physics needs to be described either in terms of logical propositions or their set/event analogue. The logical operations are V (or),^(and), ~(not), → (if...then or logical conditional - roughly equivalent to implies) and their set/event theory analogues are U (or), ' (not or "complement"),→ (if..then, also taken to mean "influences"), and "and (intersection of)", which is represented either as an inverted U or, in this paper, by concatenation of set/events, e.g., AB means A and (intersect) B.

The next section gives the main results for monopoles, neutrinos, and gravitons. Derivations of the results is usually left for the remaining sections. String theorists can replace the word "particle" by "string" throughout.

2. RESULTS: DISCRIMINATING MONOPOLES, NEUTRINOS, GRAVITONS, BOSONS, ETC.

1. By logic. Monopoles have one-way influence and so correspond to the logical conditional (if.. .then) →, while dipoles and bosons including gravitons and photons have two-way influence and so correspond to the logical biconditional (if and only if or iff) ←→. The logical picture of bosons is that of an intersection, as mentioned, so it is a two-way rather than a one-way picture.

2. By set/events. Monopoles are generated by perpendicular set/events (the electric versus magnetic "fields"), neutrinos do not interact with ordinary matter and so lack set/event intersections with ordinary matter (thus forming dark matter), and gravitons are uniquely formed by the interaction/intersection of matter with space itself as a set/event other than mere inclusion (curvature of space).. Neutrinos must be massive rather than massless pointlike because point particles arise as the tangential intersection of ordinary masses, e.g., photons arising from tangential electrons, protons, etc.

3. By measures including probabilities as in Doctorow et. al. (1983).. The universe is uniformly distributed, so inhomogeneities can only be produced by collisions of uniform spaces with different dimensions. For example, a black hole regarded as a 2-dimensional line or cone in the Carlip (1998) picture with axis along time penetrates (via its apex) three-dimensional space which either pre-exists in a Kaluza-Klein curled up manner at the Big Bang or is created along with the black hole (as the complement of the black hole), creating inhomogeneity and thus stellar and galactic structures instead of the inflation picture, although uniformity is slowly restored especially in inter-structure space. Thus neutrinos should retain their uniformity in interstellar space (explaining and predicting dark matter), while uniformity predicts that monopoles and dipoles should be uniformly distributed via Kursunoglu's (1996, 1998) containment in elementary particle matter and LEUT's central versus surface magnetic-electrical orthogonal combinations in condensate and large matter structures. Bosons are intersections of two uniformly distributed wave-particles which, similarly on a smaller scale to the Big Bang cross-dimensional intersection creates disturbances which are fundamental forces. The graviton boson or gravity force involves spatial intersection as mentioned, while the photon boson or electromagnetic force may be generated by a uniquely tangential collision of electrons, protons, etc. Finally, neutrinos had an original uniform distribution which was displaced by the central matter structures described above to some degree, so neutrinos should show up outside stellar/galactic structures - precisely where dark matter would be expected. Of course, many neutrinos remain in matter regions because of the low neutrino interaction with most other forms of matter.

4. By transformations. The fundamental forces which increase as distance between particles decreases (e.g., gravitation, electromagnetism) follow the $S(x) = 1/x$

transformation applied across dimensions from the Big Bang: S(f) = 1/r, i.e., f = 1/r without constant of proportionality, where f is force and r is distance, while the other fundamental forces follow the T(x) = x + 1 transformation, i.e., f = r + 1 without constant of proportionality, or considering repeated application, f = r + constant.

3. FURTHER THEORY AND MONOPOLES, NEUTRINOS, GRAVITONS

LEUT has four fundamental properties: logic, measures, set/events, and transformations. Logic has already been discussed, and the remaining three will be discussed below together (using interval continuous random variables) with applications of all four fundamental properties and theorems related to all concepts.

1. Since sets/events are fundamental in LEUT, LEUT immediately notes that measures are a major way to describe and explore and operate on sets, including Lebesgue type measures of set A = m(A), probability measures of set A = P(A), etc. The uniform probability distribution, which is the unique probability distribution whose probability density function is constant, is the fundamental probability distribution of the universe (which can be proven (see Theorem 1) up to a reasonable point by measure + logic arguments or can be derived from the maximum entropy uniform distribution characteristic of Shannon entropy with unspecified mean and variance by ranking unspecified mean and variance higher in entropy terms than specified means and variances which latter restrict things too much), although this can be reformulated in terms of Lebesgue type measures and other measures. This yields isotropy and homogeneity of the universe and solution of the horizon and flatness problem, etc.The uniform distribution on an interval of the nonnegative real line [a, b] has probability density function f(x) = 1/(b-a) and increasing b for fixed a corresponds to effective gauge theory having a higher maximum energy before cutoff (and in fact replaces the need to have an effective quantum gauge field theory at all) and also to a larger influence of (random) variable X or even/set A calculated by P(X-->Y) = P(A-->B) where A = {X <= x} for uniformly distributed X, B = {Y <= y} for any random variable Y.. This is fairly easy to derive from the fact that P(A-->B) is maximized at 1 for P(A) = 0 as well as for A a subset of B (with measure or probability 1), and likewise for finite Lebesgue type measure results., using the fact that A-->B = A' U B so P(A-->B) = 1 - P(A) + P(AB). Wave-particle duality is interpreted in LEUT as two simultaneous measures on objects of the universe: a wave measure and a particle type measure. Unlike Bohr's original claim that physical objects are simultaneously particles and waves, which is logically contradictory, LEUT considers that, in probabilistic (or other measure) terms, there are two simultaneous measures as indicated on physical space. The first measures a wave variable U, the second measures a particle variable V, and the physical object has associated with it the couple (U, V).

Set/events (events are a type of set) when rigorously analyzed help discriminate between monopoles, neutrinos, photons, bosons, and gravitons. The evidence of Kursunoglu (1996) that Big Bang condensates and near zero temperature Bose-Einstein condensates of rubidium-87 gas and lithium-7 gas forming central magnetic versus surrounding (spherical, etc.) surface electric charges (with or without intermediate bands) can be interpreted as evidence that monopole/surface configurations represent our 3+1 dimensional observation of the orthogonality of the electric and magnetic "fields" in 3+3 = 6 spatial dimensions. For example, a one-dimensional line or the apex of a narrow 2-dimensional cone penetrates a 2-dimensional plane or surface or 3-dimensional solid in what usually looks to a "2- or 3-dimensional inhabitant" as a zero-dimensional point or pair of points, analogous to the central monopole point. This also solves the problem of the Maxwell non-magnetic charge equation, since replacing this equation by a magnetic

charge equation similar to the electric charge equation and assuming orthogonality yields the remaining Maxwell equations under quite general conditions. Uniformity and symmetry also indicate that the Maxwell equations should be symmetric with regard to electric and magnetic poles.

The elementary particle theory of bosons as force exchange particles and fermions as particles being related by bosons is too obscure logically, and set/events analysis helps to clarify the situation.. Since wave-particle duality is logically sound via the double probability assignment to masses (wavelike and particle-like) in LEUT, "bosons" need not be interpreted as anything more than intersections in time of two field-particles which generates a wave-particle intersection having a mass and acting upon both original wave-particles as a force in time, followed by separation of the original wave-particles which results in disappearance of the intersection ("boson").

Kursunoglu (1995) points out that the massive spin-2 gauge bosons replace the Higgs Boson. This is correct from the philosophical viewpoint of Cao (1997) also, who points out that Higgs bosons have doubtful philosophical grounding in physics whether from the realistic viewpoint or the instrumental viewpoint (in the latter viewpoint, the Higgs bosons are just regarded as instruments without serious physical embodiment). Higgs boson mass appears to be unpredictable from current theories. If it goes from a massless to a massive state or vice versa, which many bosons have to do to prevent infinities and other anomalies, then it falls under the even more logically obscure Higgs or Higgs-Anderson mechanism which claims that massless objects "acquire mass" through long range forces which recombine massless modes into massive ones.

2. Transformations in LEUT replace much of the eliminated anomalous machinery of effective gauge quantum field theory. Thus, the uncertainty principle is mostly replaced by Carlip's (1998) and others' (2+1)-dimensional quantum gravity modular transformations $S(x) = -1/x$, $T(x) = x+1$, which with the additional generalizations that x can be negative and can be any physical quantity reduce to (with the same symbols) $S(x) = 1/x$, $T(x) = x+1$. As Jammer (1974) points out, it never has been established that the energy and position of any object cannot be simultaneously measured with arbitrary precision since such precision does not exist. As for the form of the uncertainty principle stating that product of standard deviations of two self-adjoint operators on Hilbert space exceeds a constant, the neo-Bohm school has provided convincing evidence of the need to generalize the restrictive Hilbert space framework to rigged Hilbert spaces, lattices of Hilbert spaces, and Banach spaces, where (especially for the last) such forms of the uncertainty principle do not exist. That school shows that the Neumann-Mackey basic Hilbert space needs to be extended at least as far as Rigged Hilbert Spaces (e.g., because former cannot support very singular operators such as unsmeared field , but also because neither delta functions nor plane waves belong to Hilbert L2 space and also eigenvectors of points of the continuous spectrum of self-adjoint operators do not belong to the Hilbert space) and to lattices of Hilbert or Banach spaces (Banach spaces are much more general than Hilbert spaces). The modular transformations play an additional role in LEUT of generating the mass/energy/force/distance relationships of elementary particles such as (to an order of magnitude) $m = 1/E$ for mass m and energy E in combination with the assumption that at the Big Bang all dimensions were united: mass = energy = space [=1, 2, and/or 3 dimensions] = time = force, called dimensional unification. This has the same type of justification as the usual physical principle of unification of the four fundamental forces at the Big Bang.

Several major theorems of LEUT are stated below, difficult ones with proof, easier ones with proof outlines, and simple ones without proof.

THEOREM 1. $E(X \rightarrow Y)$, the expected influence of X on Y, = integral $yfX \rightarrow Y\backslash(x,y)dy$, and is finite iff X and Y are nonzero on a finite interval (like uniform

distribution) and are + infinity for X, Y nonnegative. It is undefined for X, Y symmetric about any point, e.g., Gaussian distribution. The uniform probability distribution is the simplest probability distribution which satisfies the finite E(X→Y) requirement where E(X→Y) is the expected influence of X on Y. The uniform distribution has constant probability density function (pdf) from elementary probability.

Proof. E(X→Y) is constructed analogously to the conditional expectation of Y given X = x, E(Y/X=x) or E(Y/X) which integrates y dy from negative infinity to infinity times the conditional probability density, defined as fY/X(y/x) = f(x,y)/fX(x) where f(x,y) is the joint probability density function (pdf) of random variables X and Y and fX(x) is the marginal probability density function (pdf) of X, provided that fX(x) is not 0.
For E(X→Y), fX→Y(x,y) =1 - fX(x) + f(x,y) for fX(x) the marginal pdf of X and f(x,y) the joint pdf of X and Y. If yf(X→Y)(x,y) is integrated over the real line with respect to y, then the integral of the first term, 1, in the last equation is infinity minus infinity over the real line, whereas the remaining terms are finite from probability theory. If the integral is only taken on the nonnegative real axis, then +infinity is obtained. Only when the interval of integration is finite, meaning that X and Y are defined on a finite interval of the nonnegative real line for example, as with uniform type distributions or truncated/censored distributions, is E(X→Y) finite. Thus, the uniform type distribution (for finite E(X→Y)) and nonnegative type distributions like the gamma (including chi-squared, exponential) distribution are the only types of distributions for which E(X→Y) makes sense. The symmetric distributions like the Gaussian are not usable for analysis by E(X→Y). It should be noted that f(X→Y)(x,y) is not a pdf or a cdf. Of course, neither is fY/X(y/x) a pdf or cdf (in fact, it is a ratio of pdfs). This does not change the usefulness of either expression. Q.E.D.

An interesting and useful theorem is the following.

Theorem 2. $P(A \rightarrow B \rightarrow C) = P(A'B') + P(BC)$ and $P(A \leftrightarrow B \leftrightarrow C) = P(ABC) + P(A'B'C')$, and $P(A \longleftrightarrow B) = P(AB) + P(A'B')$ The Dirac spinor anticommutation relations wuwv + wvwu = 2guv Io and w5wu + wuw5 = 0 for Io 4x4 identity matrix and wu [w with subscript u] Dirac spinor 4x4 complex matrix then correspond in the probability picture to the first equation of the theorem with A = event that 1st matrix in product of 2 matrices is wu, B = event that 2nd matrix is product of 2 matrices is wv, and Io maps to probability 1,0 maps to 0.40.

These theorems greatly simplify logical-real analysis of monopoles, Lagrangians, interactions between particles mediated by bosons (set/event B above would be bosons), symmetry-breaking scenarios from early universe, spinors/tensors/multivectors in Clifford/division algebras, since triple intersections on the left hand sides of the equations reduce to sums of double intersections on the right hand side (which are easier to evaluate and with evaluation similar to what has already been done earlier in the paper). Since multivectors relevant to physics almost never involve more than three products in any term, most physical interpretation of multivectors simplifies enormously via probability/Lebesgue-measure type analyses. The fact that P(A→B) is maximized (= 1) for P(A) = 0 and/or for A a subset of B (with probability 1) has an analogue for $P(A \rightarrow B \rightarrow C)$ since if A is a subset of B and B is a subset of C, then B' is a subset of A' and so A'B' = B' and BC = B, so $P(A'B') + P(BC) = P(B') + P(B) = 1$, so $P(A \rightarrow B \rightarrow C) = 1$, and if $P(A) = P(B) = P(\ C\ ) = 0$, then $P(BC) = 0$ and $P(A'B') = P(A \cup B)' = 1$, so $P(A \not\rightarrow B \not\rightarrow C) = 1$. Thus, for example, scenarios near the Big Bang such as Kursunoglu (1996) monopole → condensate → freezing into confined matter attain maximum influence (somewhat like maximum entropy but more tractable) if all stages involve singularities or at least lower dimensions than 3, and/or if monopoles are a subset of condensates which are a subset of the final "frozen" confined scenario. Both Kursunoglu's and LEUT's theories of monopoles are indicated by this.

Magnetic monopoles have one pole, north or south. This means they have one-way influence rather than the two-way influence of dipoles. Since (using probability measure although Lebesgue-type measures and others can be used) P(A®B) reflects one-way influence and P(A↔B) reflects two-way influence, the theorem below can be proven from the fact that At↔B = (A→B)(B→A) which is a subset of A→B.

Theorem 3. Using the above measures of influence, monopoles have at least as much influence (on other events and/or themselves) as dipoles.

Outline of Proof. E subset of F implies P(E) < = P(F) (monotonicity of probability), any sets E, F. Note that (A→B)(B→A) is the intersection of two sets. Q.E.D.

This theorem justifies both Kursunoglu's theory of Big Bang monopoles entering into all matter via confinement and this author's theory of monopoles centrally located (but screened) in stars, planets, galaxies, etc. Both can be correct in different regions of spacetime or different local scenarios. Many monopoles can be confined, while others become "semi-confined" in central regions of matter.

THEOREM 4. For X, Y nonnegative, E(X→Y) > = E(Y/X=x) and fX→Y(x,y) > = f(Y/X)(y/x) if and only if fX(x) and f(x,y) < = 1 except for the rare "pathological case" where both fX(x) and f(x,y) > 1. Also, P(A→B) > = P(B/A) everywhere and FX→Y > = FY/X=x everywhere where FY/X=x = F(x,y)/FX(x) for FX(x) nonzero cumulative distribution function (cdf) of X, F(x,y) joint cdf of X, Y, and FX→Y(x,y) = 1 - FX(x) + F(x,y). fX(x) > 1 only occurs when the uncertainty as measured by the standard deviation or variance of a distribution is very small, so X approaches a masslike concentration, which is in fact known as a mass or point mass distribution. There are thus two phase regimes: those where fX(x) > 1, and those where fX(x) < = 1. To avoid logical contradictions, however, the two "phases" are described by different random variables U and V with respective pdfs fU and gV.

Proof outline. The second inequality is equivalent to 1 - fX(x) + f(x,y) > = f(x,y)/fX(x) for fX(x) not 0, and this says 1 - fX(x) > = f(x,y)(1/fX(x) - 1) = f(x,y)(1 - f(X(x))/fX(x) for fX(x) not equal to 1 or 0, and if fX(x) < = 1 (the opposite case yields the opposite direction of the inequality as required) this is equivalent to 1 > = f(x,y)/fX(x) which says fX(x) > = f(x,y) which is true always from probability theory.. The third and fourth inequalities hold everywhere because P(A) is never > 1 and FX(x) is never greater than 1 by definition of probabilities and cdfs (unlike pdfs). Also, P(A→B) > = P(B/A) whenever P(A) is not 0 with no exceptions, because the above proof goes through exactly the same except that P(A) and P(AB) are never > 1 by definition of P(A) and P(AB). The same proof as that of the last paragraph holds for the cumulative distribution function FX(x) and F(x,y), and it follows that F(X→Y)(x,y) = 1 - FX(x) + F(x,y) > = F(Y/X=x)(y/x) = F(x,y)/FX(x) wherever FX(x) is not 0. It is even possible to assign only one probability distribution fX(x) to X and then to consider that there are two phases, namely, fX(x) < = 1 versus fX(x) > 1. The same random variable or object X then changes from wave (fX(x) <= 1) to particle (fX(x) > 1). fX(x) attains a maximum, say x = xo, at the particle "center", and the particle is wavelike away from the center. To avoid logical contradictions, it is preferable to regard a physical object as having associated with it two random variables U, V, i.e., the couple (U, V), where U has pdf fU, V has pdf gV, and fU <= 1 always (U is wavelike), gV > 1 near V = vo and gV <= 1 elsewhere (V is particle-like in one region and wavelike in another). Q.E.D.

This explains the Pauli exclusion principle for fermions and its absence for bosons as well as the fact that in the algebraic physics approach two successive creation operators yield zero for fermions but not for bosons (anticommutation relation for fermions verus commutation relation for bosons). Masses cannot intersect except at a point of tangency, but arbitrarily many waves associated with the masses can intersect over nonzero volumes.

The first property is described by and due to the mostly masslike U1, U2, etc. of the different particles, while the second is due to the wavelike VI, V2, etc. (respectively) of the different particles. Bosons are (except possibly at a point of tangency) just wave intersections. Such intersections themselves give rise to a "mostly masslike" part of the intersection as well as a wavelike part of the intersection not so much because of the original physical objects but because the intersection of more and more waves "begins to look like a mass" in the same way that more and more "adjacent" points begin to look like a line and more and more "adjacent" planes begin to look like a solid object. Of course, the order relationship between "adjacent" elements is not algebraic, but it involves no logical contradictions and makes both logical and experimental sense.

4. EXPERIMENTS TO RE PERFORMED

1. Low-temperature results described in Kursunoglu (1996) suggest possibility that not only is there high temperature singularity at Big Bang, but also low temperature singularity at 0 degrees K, also likely because of the one-sidedness of 0 degrees. Decreasing temperatures very close to 0 may initiate a jump "through the singularity" to the Big Bang regime, especially if both singularities coincide or are near each other. 2. Experiment 2 repeats above but alters surface electrical field, and in this version the central magnetic field is considered to be perpendicular in 3+3 or 3+1 + 3+1 = 6+1 dimensions to the surface electrical field, so varying the surface electrical field should tell us how the magnetic field reacts, and with version 1 as a possible supplement, the experiment can confirm the orthogonality at one or both of the temperature regimes. 3. Version 3 is based on recent geophysical results - when the earth's orbit is near the sun, ice ages are most frequent. LRQG explains this as due to the decrease in surface heat generated by electrical fields due to increase in central magnetic pole field strength by attraction to the sun's central magnetic pole, although an alternative scenario is that surface heat decreases due to the same process but with the sun and earth having opposite central magnetic poles. The "experiment" has already been performed since the data are consistent with either approach, planetary orbits around the sun may indicate that, e.g., earth and sun have opposite monopoles. One see far-fetched idea is to use superconducting material and fiber optics to create a very thin stringlike bridge between earth and sun and launch ends of the string toward centers of sun and earth respectively.. Alternatively, surface conduction should affect string conduction similarly for the earth-sun system versus the earth-Jupiter system, oppositely for earth-Mars system. 4. Version 4 is like version 3 but uses earth's deviation from perfect sphere to determine whether magnetic/electrical interaction deviates considerably from that expected with a spherical shape with versus without central monopole. 5. The recent failure of the polar Mars landing suggests version 5 - land a drill on mars and dig to its core or make Mars a testing ground for all other LRQG scenarios, with giant superconductors to cover the large parts of martian surface. 6. Version 6 is to build a space pump via expansion of a sphere due to increased central magnetism of the same or oposite pole signs and then followed by contraction due to gravity or due to an external (concentric or non-concentric) sphere, yielding a spherical space pump basis of a space engine for space travel. 7. Version 7 - earth core penetrating drill or missile (without a warhead, obviously), to pull along or launch super-strong fiber optic cable or superconductor. 8. version 8 is like 5 but on earth using, e.g., unidirectional electric field.

The corporation American Superconductor leads the way in superconductor applications to such a degree that many experiments described are either now or will soon be feasible. With development of high temperature superconducting (HTS) material

(which has a much higher critical temperature below which it superconducts), it is much easier than before to get superconductivity. There have been so many applications, from engines to wires and beyond, that almost anything seems possible. There are even maglev trains (magnetically levitated), with strong magnetic fields created by HTS coils which produce levitation by repulsion or attraction, and these trains are high speed and low cost.

5. CONCLUSION

Magnetic monopoles, massive neutrinos, and gravitation/gravitons are clearly analyzed, discriminated, and categorized by logical experimental unification theory (LEUT), a successor to quantum logic which does not accept anomalies and which replaces effective gauge quantum field theory (the latest version of quantum field theory) by a combination of logic, experiment, set/events, measure, and transformations (especially a generalization of 2+1 dimensional modular transformations). Monopoles are one of the very rare objects which are characterized by only one-way logical-physical influence (single pole) and are obtained in two ways: (1) via Kursunoglu's confinement process: free monopoles $\rightarrow$ condensation $\rightarrow$ confined monopoles constituting fundamental particles, (2) via LEUT's central point magnetic charge versus surrounding (spherical type) surface area electric charge systems which are similar to condensates described by Kursunoglu but which are predicted for stars, possibly planets, and other large scale matter concentrations. Massive neutrinos have of course been discovered recently and are prime candidates for dark matter, but LEUT derives them as the unique particles which do not intersect/interact with ordinary matter which precludes them from having a massless pointlike nature since points arise among fundamental particles exclusively from tangential intersection of ordinary matter (as in photons from electron tangency). Gravitons (and gravitation) are uniquely characterized as the unique objects of the universe formed by the intersection of matter and spatial curvature and, unlike monopoles, involve two-way logical-physical influence. Solar/interstellar experiments are proposed for confirming some predictions, including superconductors.

REFERENCES

Carlip, S., 1998, Quantum Gravity in 2+1 Dimensions, Cambridge University Press, Cambridge.

Cao, T. Y., 1997, Conceptual Developments of 20th Century Field Theories, Cambridge University Press: Cambridge.

Dirac, P. A. M., 1931, Quantized singularities in the electromagnetic field. *Proceedings of the Royal Society of London,* A133, 60-72.

Doctorow, O., and Doctorow, M, 1983, On the nature of causation. *Philosophy of Education Proceedings,* Chapter 8.

Jammer, M., 1974, The Philosophy of Quantum Mechanics. Wiley: New York.

Kursunoglu, B. N., 1995, Unified symmetry in the small and in the large. In Kursunoglu, B. N., Mintz, S. L., and Perlmutter, A. (Eds.), Unified Symmetry in the Small and in the Large, Plenum, New York, 3-30; Innermost structure of matter, In B. N. Kursunoglu, S. L. Mintz, and A. Perlmutter (Eds.), 1996, Neutrino Mass, Dark Matter, Gravitational waves, Monopole Condensation, and Light cone Quantization, Plenum, New York, 2-11; with above editors, 1999, Preface, Confluence of Cosmology, Massive Neutrinos, Elementary Particles, and Gravitation, Plenum, New York, v.

Polyakov, A. M., 1974, Particle spectrum in quantum field theory. *Soviet* Physics, *Journal of Theoretic and Experimental Physics* (*Lett.*) 20, 194-195.
't Hooft, G., 1974, Magnetic monopoles in unified gauge theories. *Nuclear Physics* B79, 276-284.

This page intentionally left blank.

Section IV

Recent Progress on New and Old Ideas II

This page intentionally left blank.

AN UPDATE ON THE PROPERTIES OF THE TOP QUARK

T. Ferbel

University of Rochester, Rochester, NY 14627

Abstract

Properties of the top quark such as its mass, its decay properties, and the $t\bar{t}$ production cross section, have been studied by the CDF and DØexperiments at the Tevatron Collider. Currently, the observed characteristics conform to expectations from the standard model. Nevertheless, all conclusions are limited by statistical uncertainty, and with the anticipated improvement in quality of detectors and the increase by over a factor of 100 in data before the turn-on of the LHC, the enhanced sensitivity may finally reveal the presence of new particle interactions and phenomena.

INTRODUCTION

It has been almost five years since the definitive observation of the top quark by the CDF and DØ experiments [1, 2]. The first hints of a possible signal were gleaned somewhat before then: (i) by DØ in their famous Event 417 [3], and (ii) by CDF in the large excess of events found in their initial data sample, and published in 1994 as "evidence for" top [4]. Event 417 survived the passage of time and withstood greater scrutiny, and is still regarded as one of the best examples of top-antitop production, but the first cross section reported by CDF for top production turned out to be more than a factor of two larger than the currently accepted value. For the early measurements of the mass of the top quark, DØ obtained a rather large value, but CDF got pretty much what is now accepted as the mass of top [1, 2].

Everything we know about top has been learned from studies of $t\bar{t}$ production, which, at the energy of the Tevatron, is dominated by the qq incident channel. With top decaying into $W + b$ in the standard model (SM), the final states with least background arise from events that have $W \rightarrow l + \nu_\ell$ decays. When both W bosons decay leptonically (either e or μ), the events contain two (isolated) leptons of large transverse momentum (p_T). Such events, with their accompanying jets, correspond to "dilepton" channels. When one W decays leptonically and the other one via a quark and antiquark pair, the events comprise the single-lepton channels, and when both

Quantum Gravity, Generalized Theory of Gravitation. and Superstring Theory-Based Unification
Edited by Kursunoglu *et al.*. Kluwer Academic / Plenum Publishers. New York. 2000

W bosons decay via quarks the final state is called the all-jets channel. In addition to the nominal six objects, events can have extra jets arising from gluon emission in the initial or final state. The all-jets channel has the largest yield, but an enormous background from QCD jet production, and is therefore the most difficult to analyze.

During this past year, CDF and DØ joined forces to produce an averaged top mass (M_t) and cross section that would best summarize the results from the analyses at the Tevatron. The averaging of the mass parameters is now complete, and yields M_t = 174.3 ± 5.1 GeV [5], but the results on the $t\bar{t}$ cross section are still not ready (an unofficial value is 6.2 ± 1.2 pb). A summary of the latest measurements of the mass and cross section for all available final states is given in Fig. 1 and 2 [6, 7].

Considering the few events and the difficulty of the analysis, the 3% precision achieved on Mt is quite remarkable. Cross sections obtained from separate channels are consistent with branching fractions expected for $t \rightarrow W + b$ decay. It would be good to establish the electric charges are correct, but the events certainly look like top, feel like top, and, undoubtedly, are top. Although the uncertainties are still quite large, the superb agreement between theory and observed cross section is one of the great triumphs of the SM and QCD [8]. The value of the mass of the top quark is very large, and as a result its Yukawa coupling is close to unity, suggesting that top may hold an especially fundamental position in the SM. Nevertheless, the mass is completely consistent with expectations from electroweak theory. In fact, the top mass, taken with the well measured mass of the W obtained at the Tevatron and at LEP [9], has provided additional constraint on the mass of the Higgs in the standard model, which is now favored to be well below 200 GeV.

With the small sample of top events available from previous runs of the Tevatron, one might wonder whether there are any other important properties of the top quark that could be extracted from the data. Several studies carried out by CDF and D0, although neither as sweeping nor as sensitive as we would have liked, have nevertheless provided some interesting limits and tests of the SM. Recently completed searches and some of the still ongoing analyses are itemized below:

- Spin correlations in $t\bar{t}$ decays.
- Helicity of the W in $t\bar{t}$ final states.
- Extraction of the branching ratio of $t \rightarrow W + b$, and thereby the value of the Cabibbo-Kobayashi-Maskawa matrix element $|V_{tb}|$
- Production of single-top events.
- Flavor-changing decays of the top quark via neutral currents (FCNC).
- The decay of top into a charged Higgs boson: $t \rightarrow H^+ + b$.
- Anomalous contributions to $t\bar{t}$ production from possible tt resonances

We will discuss only several of the above analyses, some of which were intended primarily as vehicles for assessing the eventual sensitivity expected for such studies once data from future runs of the Tevatron become available. The next run is now scheduled to commence in Spring 2001 at a center of mass energy $\sqrt{s}$= 2 TeV, and the first goal is to reach an integrated luminosity of 2 events/fb. With the 10% increase in $\sqrt{s}$ and improvement in both detectors, the 20-fold increase in luminosity will correspond to a far greater increase in signal, especially for the more rare dilepton events and for events that will have b jets tagged either via displaced vertices based on silicon microstrip detectors or through "soft" (not isolated) leptons that often accompany b jets. It has been estimated [10] that an extra factor of at least four in the yield of $t\bar{t}$ events, and an extra factor of more that ten for the more difficult single-top events, will be obtained just from the upgrading of the detectors and increase in $\sqrt{s}$.

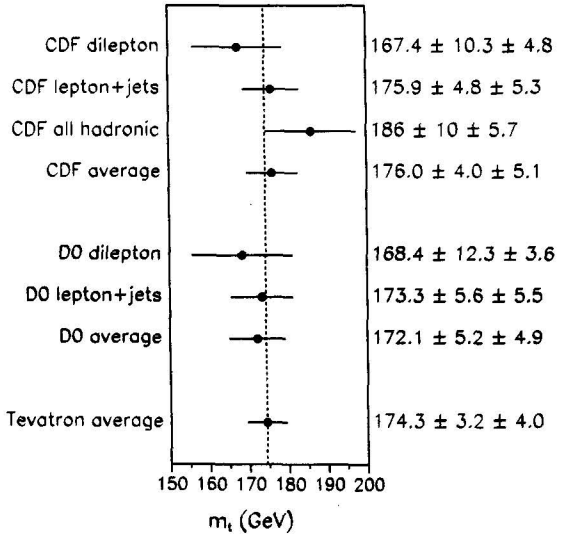


Figure 1. Measured values of the mass of the top quark.

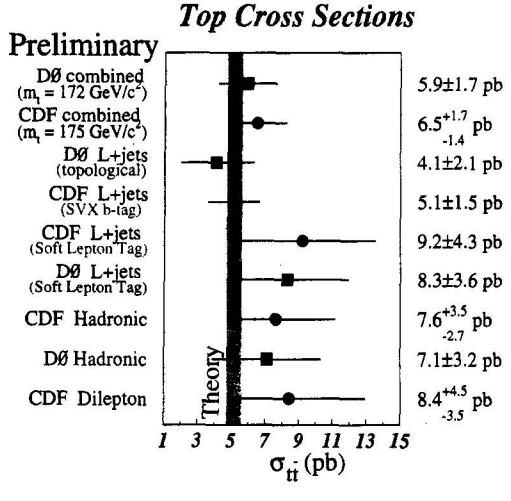


Figure 2. Measured cross sections for $t\bar{t}$ production in different channels.

MORE ON MASS AND CROSS SECTION

Although DØ is still working on the extraction of the mass in the all-jets channel, and the latest values of cross sections from CDF have yet to appear in the journals, most of the results on top mass and cross sections are now relatively well known. In their independent approaches, each group has used both ingenuity and the strengths of their detectors to great advantage. CDF has concentrated on their excellent silicon system, and DØ has relied on its calorimetry and muon coverage, and has pioneered novel approaches in analysis through bold application of neural networks.

For example, DØ has recently re-examined the yield of $e\mu$ dilepton events using a neural network approach rather than more classical means (e.g., random grid search) of implementing cutoffs on variables used to maximize separation between signal and background [11]. A modest improvement has been achieved in the yield of signal, with a simultaneous reduction in background. The net gain corresponds to $\sim$ 18% in statistics or $\sim$40% in running time. These kinds of approaches will be used more often in the next run, and will help reduce uncertainties in many analyses.

In the future, limitations on the accuracy of the top mass will be dominated mainly by the uncertainty in the energy scale used for reconstructing jets, and by ambiguities in the model for production and decay of the top quarks. These are expected to improve by about a factor of two, and bring the total uncertainty down to 2 – 3 GeV. The major improvement in measurements of cross sections will be from an increase in statistics for the individual channels, which will also provide better checks of branching fractions into different final states. The absolute uncertainty will be limited by comparable contributions ($\sim$5%) from absolute luminosity, b–tagging efficiency. statistics, energy scale, and the model used for tt production. Thus, about a 10% uncertainty on the cross section should be within reach [12].

SEARCH FOR DECAY OF TOP INTO A CHARGED HIGGS

The standard model requires a single complex Higgs doublet, which, after symmetry breaking, leaves one neutral Higgs boson. The simplest extensions of the Higgs sector, including supersymmetric theories, involve a two-doublet structure, and point to the existence of a charged Higgs ($H^{\pm}$). If the mass of the charged Higgs ($M_{H^{\pm}}$) is

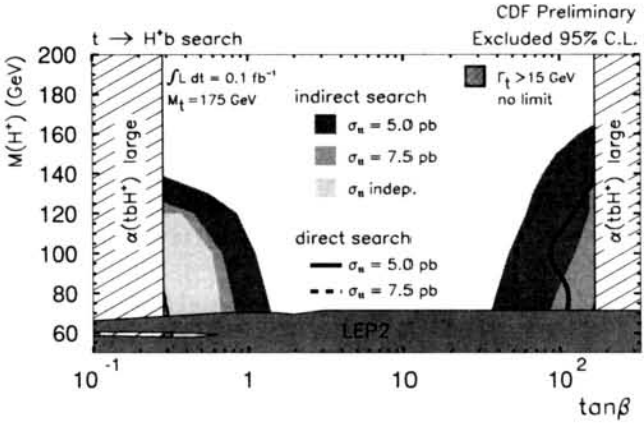


Figure 3. Regions of parameter space for a charged Higgs boson excluded by CDF.

sufficiently small, then the top quark can decay via t $\rightarrow H^+ + b$. Depending on the value of $M_{H^\pm}$ and the parameter tanb (the ratio of the vacuum expectation values of the two Higgs doublets), this decay can compete with the standard mode $t \rightarrow W^+ + b$. The branching fraction of $t \rightarrow H^+ + b$ is largest for both very small and very large tanβ (tanβ < 1 and tanβ > 50), and smallest when tanb = $\sqrt{M_t/M_b} \sim 6$, where the decay is dominated by t → W+ + b. The decay of the $H^\pm$ also depends strongly on tanβ, with the branching to *cs* and t*b → *Wbb* dominating for tanb < 1, and into ττ for tanβ > 1. The relative decay rates into the two hadronic modes are sensitive to $M_{H^\pm}$, especially near the upper edge of allowed kinematics.

The search for t → $H^+ + b$ relies on a violation of lepton universality in Higgs decay, and has proceeded along two lines. First, the more direct approach is based on the appearance of excess tt signal in the t + X channels, where the analyses rely on the specific decay of $H^\pm \rightarrow \tau^\pm \nu_\tau$ (and $t \rightarrow$ hadrons $+\nu\tau$), which is dominant at large tanβ. The other route involves an indirect search, and is based on the disappearance of top signal, because the standard analysis of tt → lepton+jets has selection criteria optimized for the SM modes, and thereby ignores the possibility of a contribution from $H^\pm$. Consequently, if a large fraction of top quarks decay via a $H^\pm$, then, assuming that there are no additional sources of $t\bar{t}$ signal from mechanisms beyond the SM, there will be fewer events observed than expected in channels based purely on the SM. A less model-dependent approach, but one that is not very sensitive at current level of statistics, is used by CDF in searches for an anomaly in the ratio of lepton+jets and dilepton+jets $t\bar{t}$ final states. This indirect method is not affected by uncertainties in the *tt* production cross section [13].

Lower limits on $M_{H^\pm}$ of about 77 GeV, essentially independent of tanb. have been obtained at LEP from searches for direct coupling of $Z \rightarrow H^+H^-$ [14], and a more model-dependent limit of $M_{H^\pm} > 244$ GeV has been extracted from the $b \rightarrow$ sg transition at CLEO [15]. The results from CDF and DØ are given in Fig. 3[13] and 4 [16] as a function of MH± and tanb, and are observed to exclude much of the phase space for tanβ < 1 and tanb > 30. From the connection between tan,!? and the branching fraction of $t \rightarrow Hb$, we can exclude the existence of a charged Higgs with M_H < 120 GeV, for B($t \rightarrow Hb$ > 0.4), at ~95% confidence. The next run of the Tevatron is expected to reduce the unexcluded region of phase space by about a factor of two (as shown in Fig. 4), or, possibly, find the $H^\pm$.

HELICITY OF THE *W* AND SPIN CORRELATIONS IN TOP DECAYS

Spin provides another window for viewing the predictions of, and possible departures from, the standard model. Two areas that have been studied at CDF and DØ involve the helicity of the W boson from top decay, and correlations among the decay products of the two top quarks in *tt* events. Given the V–A form of the weak interaction, a top quark should decay into either a left handed or a longitudinally polarized W+ This implies that leptons from W → *ℓνe* decay will tend to be emitted in a direction opposite to the line of flight of the W. The angular distribution of the lepton in the rest frame of the W, with the axis of quantization defined by the line of flight of the W, will therefore be asymmetric, and characterized by the fraction of left-handed W+ in top decay (with helicity –1), $f_{left} = 2M^2_W/(M^2_t + 2M^2_W) = 1 - f_{long} \sim 0.3$. DØ has made preliminary studies to ascertain prospects for the next run, and CDF has already presented analyses of lepton p_T spectra for *W* decays in *tt* events in lepton and dilepton channels [17]: yielding $f_{long} = 0.91 \pm 0.37 \pm 0.13$ (statistical and systematic uncertainties, respectively), in full agreement with the SM.

The dominance of the $q\bar{q}$ incident channel for $t\bar{t}$ production, guarantees that the two top spins will tend to point along the same direction in the center of mass of the parton-parton collision. Because the lifetime of the top quark is $\sim 4 \times 10^{-25}$sec, and far shorter than hadronization time, the spin information carried by the top quarks is transmitted to their decay products. In fact, any depolarization could provide limits on the lifetime of top, and consequently on $\Gamma(t \rightarrow W + b)$ and $|\mathrm{Vtb}|$

For a polarized top quark, the angular distribution of the decay products in the top rest frame is given by $(1+\alpha\cos\theta)/2$, where a = 1 for the charged lepton or d quark from W decay, and $|\alpha| <- 0.41$ for the other decay products (W, ν, b or the up quark). (The α parameters for t have opposite sign to those for $\bar{t}$.) Because of the difficulty of reconstructing down quarks from W decay, charged leptons would seem to offer the best means for extracting values of α. However, for interactions of unpolarized pp, a cannot be measured in top decay. Nevertheless, a can be determined from the correlated distribution in the decay angles θ_+ and $\theta-$ of the t and $\bar{t}$:

$$\frac{1}{\sigma}\frac{d\sigma}{d\cos\theta_+ d\cos\theta_-} = \frac{1 - \kappa\alpha_+\alpha_-\cos\theta_-\cos\theta_+}{4}$$

The value of κ depends on the axis of quantization chosen for analyzing the decays. The more standard axes of the incident beam ("Gottfried-Jackson" frame) or the lines of flight of the top quarks ("helicity" frames) are not the ones preferred here, but instead there is an optimal axis, or "off diagonal" basis, as defined by the

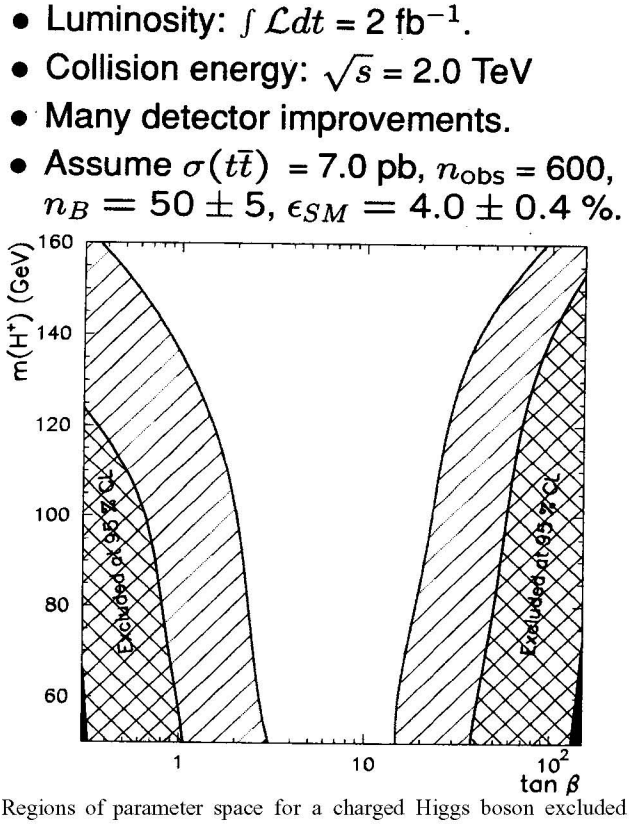


Figure 4. Regions of parameter space for a charged Higgs boson excluded by DØ, and expectations for sensitivity in the next run of the Tevatron.

transformation [18]:

$$\tan\psi = \frac{\beta^{*2}\sin\theta^*\cos\theta^*}{1 - \beta^{*2}\sin^2\theta^*}$$

where ψ and $\theta*$ are, respectively, the angle of the optimal axis and the angle for the line of flight of the top quarks, defined relative to the incident direction of the p in the parton-parton rest frame, and $\beta*$ refers to the velocity of the top quarks in that frame. In the off diagonal basis, the impact

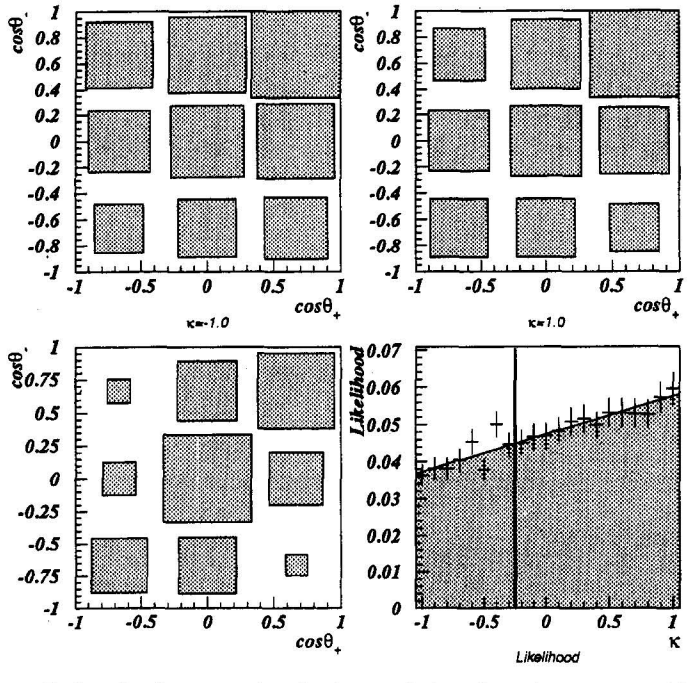


Figure 5. Results from a study of spin correlations in tt decay reported by DØ.

of contributions from opposite spin orientations of the top quarks (e.g., from gluon-gluon production) vanish to leading order in α_{strong}, providing an expected value of k ~ 0.9. To measure the decay angles, requires the full kinematic reconstruction of tt events. Unfortunately, dilepton events are kinematically underconstrained, and a special procedure was therefore developed at DØ [19] to handle the ambiguities and poor resolution brought about by the two missing neutrinos in these channels. Using its 6 dilepton events, DØ calculated all possible neutruno solutions, with smeared resolutions, and obtained a likelihood for each event permutation. These were added for all events, and are shown in the density plot in Fig. 5. A likelihood fit was then performed to signal (based on a spin-correlated $t\bar{t}$ Monte Carlo) and small sources of background, with k as arbitrary parameter, which established that $k > -0.25$ at 68% confidence [20], consistent with production through an intermediary gluon. A value of K ~ –1.0 would correspond to an intermediary Higgs-like $J = 0$ boson.

Clearly, the results of spin studies to date have not been electrifying, however, with the great increase in statistics expected from the next run of the Tevatron, such measurements will provide delicate and sensitive tests of the SM.

CONCLUSION

Considering the small number of events collected thus far, the properties of the top quark are known to remarkable precision. The mass is 174.3 ± 5.1 GeV, the $t\bar{t}$ cross section (unofficial) is 6.2 ± 1.2 pb, the branching modes of the top quark are in line with expectation from t → W + *b* decay, and all observations are consistent with the SM. The upcoming enormous increase in statistical accuracy will hopefully reveal new interactions and the shortcomings of current theory.

ACKNOWLEDGEMENTS

I wish to thank my colleagues on CDF and DØ for their many contributions that have provided the basis for this presentation. I am especially grateful to Dhiman Chakraborty, Suyong Choi, John Conway, Mark Kruse, Ann Heinson, Andrew Robinson, Harpreet Singh, Eric Smith, Kirsten Tollefson, Gordon Watts and John Womersley for their input and helpful comments.

References

[1] F. Abe *et al.,* Phys. Rev. Lett. **74,** 2626 (1995)

[2] S. Abachi *et al.,* Phys. Rev. Lett. **74,** 2632 (1995).

[3] S. Abachi et al., Phys. Rev. Lett. **72,** 2138 (1994).

[4] F. Abe *et al.,* Phys. Rev. Lett. **73,** 225 (1994)

[5] Top Averaging Group, L. Demortier *et al.,* FERMILAB TM 2084 (May 1999)

[6] G. Watts, presentation at 8th Int'l Symposium on Heavy Flavors, Southampton, U.K.(1999).

[7] F. Ptohos, presentation at Int'l Europhysics Conference on High Energy Physics, Tampere, Finland (1999).

[8] E. Laenen, J. Smith, and W. L. Van Neerven, Phys. *Lett.* **B 321,** 254 (1994); E. L. Berger and H. Contopanagos, Phys. Rev. **D 54,** 3085 (1996); S. Catani *et al.,* Phys. Lett. **B 378,** 329 (1996); R. Bonciani *et al.,* Nuc. Phys. **B 529,** 424 (1998).

[9] B. Abbott et al., Phys. Rev. Lett. 84, 222(2000); LEP EW Working Group, CERN-EP/99-15; and for CDF's measurement see the report Fermilab-conf-99-173e.

[10] Report at DØ Workshop, Seattle (1999), and private communication.

[11] H. Singh, presented at conference on Neural Computing in High Energy Physics, Israel(1999).

[12] Thinkshop: Meeting on top-quark physics for Run II (can be accessed at URL http://lutece.fnal.gov/thinkshop/default.html)

[13] F. Abe *et al.,* Phys. Rev. Lett. **79,** 357 (1997). These results are about to be updated because of the recent change in the $t\bar{t}$ cross section measured by CDF.

[14] G Abbiendi *et al.,* Eur. Phys. J. C 7, 407 (1999); M. Acciari *et al.*, Phys. Lett. B 446, 368 (1999); R. Barate, *et al.,* Phys. Lett. **B 450,** 467 (1999).

[15] M.S. Alam *et al.,* Phys. Rev. Lett. **74,** 2885 (1995).

[16] B. Abbott *et al.,* Phys. Rev. Lett. **82,** 4974 (1999), and D. Chakaborty in Proc. of Hadron Collider Physics Meeting at Mumbai, India (1999), World Scientific Pub., B. S. Acharya *et al.,* eds.

[17] For CDF measurements, see their public web page http://www-cdf.fnal.gov /physics/new/top/latest -results. html.

[18] G. Mahlon and S. Parke. Phys. Lett. **B 411,** 173 (1997).

[19] B. Abbott *et al.,* Phys. Rev. **D 60.** 052001 (1999).

[20] S. Choi, PhD Dissertation, Seoul University. 1999 (unpubished).

This page intentionally left blank.

THE SUPERSYMMETRIC MUON ANOMALY

Pran Nath

Department of Physics
Northeastern University
Boston, MA 02115-5005, USA

ABSTRACT

A brief review of the muon anomaly in supersymmetric models is given. The review includes a discussion of the supersymmetric effects on $g_\mu - 2$ in N=1 supersymmetric models and the effect of CP violating phases on the muon anomaly. The effects of Kaluza-Klein excitations of the W and Z bosons and of the photon on $g_\mu - 2$ are also discussed as a possible background to the supersymmetric contribution. In the near future the Brookhaven experiment E821 is expected to increase the sensitivity of the $g_\mu - 2$ measurements by a factor of 20 and test the supersymmetric contribution.

INTRODUCTION

In the near future the Brookhaven experiment E821[1] will improve on the CERN measurement[2] of the muon anomaly $a_\mu=(g_\mu - 2)/2$ and it is hoped that eventually the accuracy of this experiment will go down to the level of 4×10^{-10} for a_μ This result combined combined with the recent reduction of the hadronic error[3] would allow one to test the Standard Model electro-weak correction[4, 5]. However, it was pointed out some time ago that any experiment that tests the Standard Model electro-weak correction, will also test

Quantum Gravity Generalized Theory of Gravitation and Superstring Theory Based Unification
Edited by Kursunoglu *et al* Kluwer Academic / Plenum Publisher New York 2000

the supersymmetric corrections since the supersymmetric correction can be as large or larger than the Standard Model electro-weak correction[6]. In this talk we give a brief review of the current status of the supersymmetric electro-weak correction to the muon anomaly. We also review the recent works analysing the effects of CP violation on a_μ in supersymmetric models[7]. Findly,we discuss the effects of the Kaluza-Klein excitations of the W and Z bosons and of the photon on a_μ in theories with large radius compactifications[8]. While the investigation of Kaluza-Klein contribution to a_μ is important in its own right, it also determines the background to the supersymmetric correction to a_μ. The outline of the paper is as follows. In Sec.2 we give a brief review of the Standard Model electro-weak contribution. In Sec.3 we discuss the supersymmetric electro-weak contribution to a_μ. In Sec.4 we discuss the effects of CP violation on a_μ.In sec.5 we discuss the Kaluza-Klein contributions to a_μ. Conclusions are given in Sec.6.

THE STANDARD MODEL a_μ^{EW}

The Standard Model contribution to a_μ consists of several parts:

$$a_\mu^{SM} = a_\mu^{qed} + a_\mu^{had} + a_\mu^{E_\mu\text{-}W} \tag{1}$$

where a_μ^{qed} has been computed to $O(\alpha^5)$ QED corrections, a_μ^{had} to $O(a^2)$ and $O(\alpha^3)$ [9] hadronic vacuum polarizations, and light-by-light hadronic contributions [10], and $a^{E_\mu\text{-}W}$ is the Standard Model electro-weak contribution. Regarding the electro-weak piece, there are two main contributions to it at the one loop level: these are the one loop W exchange and the one loop Z exchange diagrams which together give the result[4]:

$$a_\mu^{EW}(SM) = a_\mu^{W} + a_\mu^{Z}$$

$$a_\mu^{W} = \frac{5m^2\mu G_F}{12\pi^2 J2'} \qquad a_\mu^{Z} = \frac{m_\mu^2 G_F}{2\sqrt{2}\pi^2}\left(-\frac{5}{12} + \frac{4}{3}(\sin^2\theta w - \frac{1}{4})^2\right) \tag{2}$$

There are important two loop corrections to this formula. Including these one finds[5]

$$a_\mu^{EW}(SM) = 15.1(0.4) \times 10^{-10} \tag{3}$$

As mentioned in Sec.1 the Brookhaven experiment E821 is expected to measure a_μ down to a level of 4×10^{-10}[1], while at the same time the error in the hadronic contributions have been reduced to a level of 6.5×10^{-10}[3]. Clearly

then if the Brookhaven experiment achieves its desired sensitivity, one will then be able to test the Standard Model a_μ^{EW} even with no further reduction in the hadronic error. However, as also mentioned in Sec.1 any experiment that tests the Standard Model electro-weak contribution will also test the supersymmetric correction. Next we discuss the the SUSY contribution.

SUSY CORRECTION TO a_μ^{EW}

Within the framework of the Minimal Supersymmetric Standard Model (MSSM) there are additional contributions to a_μ arising from the chargino-sneutrino exchange and the neutralino-smuon exchange. However, the MSSM has a large number of soft SUSY breaking parameters, and the theory is not very predictive. To reduce the number of parameters one needs a model of supersymmetry breaking and here we use the supergravity unification model with breaking of supersymmetry in the visible sector arising from gravity mediation[11]. In the minimal supergravity model (mSUGRA) the soft SUSY breaking sector is parametrized by the universal scalar mass m_0, the universal gaugino mass m1–2 the universal trilinear coupling A_0 all taken at the GUT scale, and $\tan\beta$ which is the ratio of the Higgs VEVs at the electro-weak scale, i.e., $\tan\beta = < H_2 > / < H_1 >$, where H_2 gives mass to the top quark and H_1 gives mass to the down quark and the leptons. The Higgs mixing parameter μ which enters in the superpotential as $\mu H_1 H_2$ is determined from the constraint of the electro-weak symmetry breaking and is not a free parameter.

Analytic results for the supersymmtric contributions to a_μ were given in Refs.[6] and later analysed by a number of authors under the constraint of the unification of the gauge couplings implied by the LEP data[12, 13]. Two of the general results which do not depend on the details of the numerical analysis are the following. First one finds that a_μ depends approximately linearly on $\tan\beta$. This arises simply because the supersymmetric coupling $\mu\tilde{\nu}\tilde{W}$ has a $1/\cos\beta$ dependence which behaves as $\sim \tan\beta$ over most of large tanb region[13]. A second interesting result that arises is that one finds that there is a strong correlation over most of the parameter space of the model between the sign of μ and the sign of a_μ This phenomenon arises because the supersymmetric contribution to a_μ is dominated by the chiral intereference term which correlates the sign of a_μ with the sign of μ[13]. Thus the a_μ experiment is one of the few experiments which is sensitive to the sign of the μ parameter. We justify now these observations by a more detailed discussion of the supersymmetric contribution.

The supersymmetric Contribution to a_μ at the one loop level is given by

$$a_\mu^{SUSY} = a_\mu^{\tilde{W}} + a_\mu^{\tilde{Z}} \tag{4}$$

where a_μ^W is the chargino-sneutrino exchange contribution and a_μ^Z is the neutralino-smuon exchange contribution. The theoretical evaluation for the chargino-sneutrino contribution to the leading order gives[6]

$$a_\mu^{\tilde{W}} = \frac{m_\mu^2}{48\pi^2}\frac{A_R^{(a)2}}{m_{\tilde{W}_a}^2}F_1(x_a) + \frac{m_\mu}{8\pi^2}\frac{A_R^{(a)}A_L^{(a)}}{m_{\tilde{W}_a}}F_2(x_a) \tag{5}$$

Here $x_a = \left(\frac{m_{\tilde{\nu}}}{m_{\tilde{W}_a}}\right)^2$ (a=1,2), $F1$ and F_2 are form factors as defined in Ref.[6], and A_L and A_R are the left and right chiral amplitudes which are given by[6]

$$A_R^{(1)} = -\frac{e}{\sqrt{2}\sin\theta_W}\cos\gamma_1; \quad A_L^{(1)} = (-1)^\theta\frac{e}{\sqrt{2}\sin\theta_W}\frac{m_\mu\cos\gamma_2}{\sqrt{2}M_W\cos\beta} \tag{6}$$

and

$$A_R^{(2)} = -\frac{e}{\sqrt{2}\sin\theta_W}\sin\gamma_1; \quad A_L^{(2)} = -\frac{e}{\sqrt{2}\sin\theta_W}\frac{m_\mu\sin\gamma_2}{\sqrt{2}M_W\cos\beta} \tag{7}$$

where $\gamma_{1,2}$ are as defined in Ref.[6]. For the neutralino-smuon exchange contribution one has[6]

$$\begin{aligned} a_\mu^{\tilde{Z}} = & -\frac{m_\mu^2}{24\pi^2}\frac{1}{m_{\tilde{Z}_{(k)}}^2}\left[\{s^2(B_k^R)^2 + c^2(B_k^L)^2\}G_1(x_{1k}) + \{c^2(B_k^R)^2 + s^2(B_k^L)^2\}G_1(x_{2k})\right] \\ & + \frac{m_\mu}{8\pi^2}\frac{sc}{m_{\tilde{Z}_{(k)}}}B_k^R B_k^L[G_2(x_{1k}) - G_2(x_{2k})] \\ & - \frac{m_\mu}{8\pi^2}\frac{C_k}{m_{\tilde{Z}_{(k)}}}\left[\{c^2B_k^L - (-1)^{\theta_k}s^2B_k^R\}G_2(x_{1k}) + \{s^2B_k^L - (-1)^{\theta_k}c^2B_k^R\}G_2(x_{2k})\right] \end{aligned} \tag{8}$$

where s = sinδ, c = cosδ, x_{rk} = (mμr/mz(k))2 (r = 1,2;k = 1,2,3,4), G1(x) and G2(x) are form factors, and δ, the co-efficients C_k and the quantities B_k^R and B_k^L and other symbols are as defined in Ref.[6].

In the supersymmetric limit one finds that the chargino contributions reduceto[7]

$$a_\mu^{\tilde{W}} = -\frac{5m_\mu^2 G_F}{12\pi^2\sqrt{2}} \tag{9}$$

which is exactly opposite of what one gets by the W exchange at the one loop level (see Eq.2). Similarly, in the supersymmetric limit one finds that the neutralino exchange contributions limit to[7]

$$a_\mu^{\chi^0} = -\frac{\alpha_{em}}{2\pi} - \frac{m_\mu^2 G_F}{2\sqrt{2}\pi^2}\left(\frac{4}{3}\sin^4\theta_W - \frac{2}{3}\sin^2\theta_W - \frac{1}{3}\right) \qquad (10)$$

Again this result is exactly opposite of the sum of the one loop photon exchange contribution which is $\alpha_{em}/2\pi$ and of the Z boson exchange contribution (see Eq.2). Thus one finds that in the supersymmetric limit one has that the sum of the Standard Model exchange contribution and of the supersymmetric exchange contribution together give zero. This is what is expected on general grounds[15].

Numerical analyses show that the neutralino exchange contributions to a_μ are small over large parts of the parameter space and that it is the chargino exchange contribution that dominates the supersymmetric contribution to a_μ [13]. In the chargino contribution itself, it is the chiral interference term proportional to $A_L A_R$ that is found to dominate, and further it is the lighter chargino exchange contribution that dominates the chiral interference term. As can be seen from Eq.(6) the chiral interference term arising from the light chargino has a front factor of $(-1)^\theta$, where $\theta = 0(1)$ for $\lambda_1 > 0 (< 0)$ where λ_1 is the smaller eigenvalue of the chargino mass matrix which implies that $\lambda_1 < 0$ for $\mu > 0$, and $\lambda_1 > 0$ for $\mu < 0$ for a large part of the parameter space. Because of the above one finds that generally $a_\mu^{SUSY} > 0$ for $\mu > 0$ and $a_\mu^{SUSY} < 0$ for $\mu < 0$ except when $\tan\beta \sim 1$[13].

EFFECTS OF CP VIOLATION ON a_μ

In the above analysis we assumed that there was no violation of CP. However, the soft SUSY breaking parameters bring with them new sources of CP violation since in general these parameters are complex. Thus, for example, in mSUGRA one finds that there are two additional parameters which arise in the presence of CP violation. These can be taken to be the phase of μ (6,) and the phase of A0 (α_{A0}). The CP violating phases must be subject to stringent experimental constraints on the electric dipole moment (EDM) of the electron and of the neutron[14]. To satisfy the EDM constraints the conventional wisdom has been that either the phases are small[16] or the SUSY spectrum is heavy[17]. However, more recently a third possibility has been suggested[18], and that is that the CP phases could be large but there could be internal cancellations to guarantee satisfaction of the EDM constraints, and there have been further developments along this line[19]. In this scenario where the CP

phases are large and the EDM constraints are satisfied via the cancellation mechanism, the effect of CP phases on a_μ could be significant.

Recently, a full one loop analysis of the effects of CP violating phases on a_μ was given within the framework of mSUGRA[7]. It was found that the CP violating phases could generate very significant corrections and further such corrections could be visible in the new Brookhaven experiment. The analysis was then extended to MSSM (see the second paper of Ref.[7]). Here, one has many more CP phases that enter the analysis. Specifically, one finds that the electron EDM depends on theree independent phases, while the neutron EDM depends on eight different phases, and together the electron and the neutron EDMs depend on ten phases. A numerical analysis shows that the effects of CP violation on a_μ can be visible in a significant region of the parameter space[7].

EFFECTS OF LARGE EXTRA DIMENSIONS ON a_μ

Recently there has been considerable interest in the possibility of large extra Kaluza-Klein[20] dimensions which could open up at energies that may become accessible at high energy accelerators in the future[21]. Such large extra dimensions could also affect the value of a_μ. In Ref.[8] an analysis was given for the brane models with several extra dimensions characterized by the mass scale $M_R = 1/R$. In general one finds that in the presence of extra dimensions there are Kaluza-Klein excitations of the W and Z bosons and of the photon (γ) which contribute to the muon anomaly. Thus one has that the total Kaluza-Klein contribution is given by

$$a_\mu^{KK} = a_\mu^{W-ZKK} + a_\mu^{\gamma KK} \tag{11}$$

where a_μ^{W-ZKK} is the contribution from the Kaluza-Klein excitations of the W and Z bosons and $a_\mu^{\gamma KK}$ is contribution of the Kaluza-Klein excitations of the photon. For a_μ^{W-ZKK} one finds for the case of one extra dimension

$$(\Delta a)_\mu^{W-ZKK}(d=1) = \frac{G_F m_\mu^2}{6\sqrt{2}}\left(-\frac{5}{12} + \frac{4}{3}(sin^2\theta_W - \frac{1}{4})^2\right)\left(\frac{M_Z^2 - M_W^2}{M_R^2}\right) \tag{12}$$

Similarly, for the Kaluza-Klein excitations of the photon for the case of one extra dimension one has

$$(\Delta a)_\mu^{\gamma KK}(d=1) = \alpha\frac{\pi}{9}\frac{m_\mu^2}{M_R^2} \tag{13}$$

and there are more complicated expressions for the cases $d > 1$. Numerically, one finds the interesting result that the contribution from the Kaluza-Klein excitations of the W and of the Z boson to a_μ is negative while the photonic Kaluza-Klein contribution to a_μ is positive. Thus one has a partial cancellation between the two contributions. Further, the overall size of the Kaluza-Klein contribution is found to be rather small. The size of these effects increases as we increase the number of extra dimensions. However, even so it turns out that using the constraints on M_R that arise from clashing the accurate experimental determination of G_F and its prediction within the Standard Model[22], one finds that the effect of extra dimensions on a_μ is essentially negligible compared to the supersymmetric contribution. Thus the presence of large extra dimensions does not pose a danger to the observation of the supersymmetric effect in the Brookhaven experiment.[We have not discussed here the corrections to a_μ due to strong gravity. An analysis for this case is given in Ref.[23]].

CONCLUSIONS

In this talk we have given a brief review of the current status of a_μ in supersymmetric theories. One finds that in general the supersymmetric effects can be as larger or larger than the Standard Model electro-weak contribution. The supersymmetric effects are large enough so that they should be observable at the new Brookhaven experiment. However, if no effect is seen one will have stringent bounds on the supersymmetric particle spectrum which could be comparable to the bounds that might arise from the RUN II of the Tevatron. We also discussed the effects of large CP violating phases. Recent analyses show that CP violating effects can generate significant contributions to the supersymmetric anomaly. Thus CP violating effects could also be observable in the new Brookhaven experiment. Finally, we discussed the effects of large extra dimensions on a_μ. These large extra dimensions manifest via Kaluza-Klein modes at low energy and also affect the Fermi constant. The current very accurate determination of the Fermi constant from the $\mu \to e + \nu_e + \nu_\mu$ decay and the theoretical prediction of G_F from the Standard Model put stringent limits on the scale M_R of the extra dimensions. One finds that M_R must at least be 1.6 TeV for d=1. Using these limits one finds a rather negligible contribution to a_μ from one extra dimension. Similar results hold for the case $d > 1$. Thus the contribution from large extra dimensions if they exist does not pose a serious background to the supersymmetric contribution.

Acknowledgements

The content of this talk is based on collaborative work with R. Arnowitt, A.H. Chamseddine, T.C. Yuan, U. Chattopadhyay, M. Yamaguchi, Y. Yamada, and T. Ibrahim. This research was supported in part by NSF grant PHY-9901057.

REFERENCES

1. For recent results from E821 see, R.M. Carey et.al., Phys. Rev. Lett. **82**, 1632(1999). For a review of E821 see, D.W. Hertzog et.al., in Proceedings of the Sixth International Symposium on Particles, Strings and Cosmology, Boston, March 1998 (World Scientific, Singapore).

2. J. Bailey et. al., Nucl. Phys. **B150,** 1(1979).

3. M. Davier and A. Hocker, Phys. Lett. **B419,** 419(1998).

4. K. Fujikawa, B.W. Lee and A. I. Sanda, Phys. Rev. **D6,** 2923(1972); R. Jackiw and S. Weinberg, Phys. Rev. **D5,** 2473(1972); G. Altarelli, N. Cabibbo and L. Maiani, Phys. Lett.**B40,** 415(1972); I. Bars and M. Yoshimura, Phys. Rev. D6, 374(1972); W.A. Bardeen, R. Gastmans and B.E. Lautrup, Nucl. Phys. **B46,** 315(1972).

5. A. Czarnecki, B. Krause and W. Marciano, Phys. Rev. Lett. **76,** 3267(1996); G. Degrassi and G.F. Giudice, Phys. Rev. **D58,** 05007(1998).

6. T. C. Yuan, R. Arnowitt, A.H. Chamseddine and P. Nath, Z. Phys. **C26,** 407(1984); D.A. Kosower, L. M. Krauss, N. Sakai, Phys. Lett. **133B,** 305(1983);

7. T. Ibrahim and P. Nath, hep-ph/9907535; hep-ph/9908443 (to appear in Phys. Rev. D).

8. P. Nath and M. Yamaguchi, hep-ph/9903298; Phys.Rev. **D60,**116006(1999)

9. T. Kinoshita and W.J. Marciano, in *Quantum Electrodynamics,* ed. T. Kinoshita (World Scientific, Singapore).

10. M.Hayakawa and T. Kinoshita, Phys. Rev. **D57,** 465(1998); J. Bijnens, E. Pallante and J. Prades, Nucl. Phys. **B474,** 379(1996).

11. A. Chamseddine, R. Arnowitt and P. Nath, Phys. Rev. Lett. **49,** 970 (1982); For reviews see P. Nath, R. Arnowitt and A.H. Chamseddine, Applied N=1 supergravity, Lecture series,1983 (World Scientific, Singapore); H. P. Nilles, Phys. Rep. **110,** 1(1984).

12. J. Lopez, D.V. Nanopoulos, and X. Wang, Phys. Rev. **D49,** 366(1994).

13. U. Chattopadhyay and P. Nath, Phys. Rev. **D53,**1648(1996); T. Moroi, Phys. Rev. **D53**, 6565(1996); M. Carena, G.F. Giudice and C.E.M. Wagner, Phys. Lett. **B390,** 234(1997); K.L. Chan, U. Chattopadhyay and P. Nath, Proc. Pascos98, World Scientific Singapore, 1999.p. 198;

14. P.G. Harris et.al., Phys. Rev. Lett. **82,** 904(1999); E. Commins, et. al., Phys. Rev. **A50,** 2960(1994); K. Abdullah, et. al., Phys. Rev. Lett. **65**, 234(1990).

15. S. Ferrara and E. Remiddi, Phys. Lett. **B53,** 347(1974); R. Barbieri and G.F. Giudice, Phys. Lett. **B309,** 86(1993).

16. See, e.g., W. Bernreuther and M. Suzuki, Rev. Mod. Phys.**63,** 313(1991).

17. P. Nath, Phys. Rev. Lett.**66,** 2565(1991); Y. Kizukuri and N. Oshimo, Phys.Rev. **D46,** 3025(1992).

18. T. Ibrahim and P. Nath, Phys. Lett.**B 418,** 98(1998).

19. T. Ibrahim and P. Nath, Phys. Rev. **D57,** 478(1998); E ibid **D58,** 019901(1998); Phys. Rev. **D58,** 111301(1998); T. Falk and K Olive, Phys. Lett. **B 439,** 71(1998); M. Brhlik, G.J. Good, and G.L. Kane, Phys. Rev. **D59,** 115004 (1999); A. Bartl, T. Gajdosik, W. Porod, P. Stockinger, and H. Stremnitzer, hep-ph/9903402; S. Pokorski, J. Rosiek and C.A. Savoy, hep-ph/9906206; E. Accomando, R. Arnowitt and B. Datta, hep-ph/9909333; hep-ph/9907446. T. Ibrahim and P. Nath, hep-ph/9910553.

20. Th. Kaluza, Sitzungober. Preuss.Akad.Wiss.Berlin, p.966 (1921); 0. Klein, Z. Phys. **37,** 895(1926).

21. See, e.g., I. Antoniadis, Phys. Lett. **B246,** 377(1990); I. Antoniadis and M. Quiros, Phys. Lett. **B392,** 61(1997).

22. P. Nath and M. Yamaguchi, hep-ph/9902323; Phys.Rev. **D60,**116004(1999); M. Masip and A. Pomarol, hep-ph/9902467; Phys. Rev. **D60,**096005(1999); W. Marciano, hep-ph/9903451; Phys. Rev. **D60,** 093006 (1999); P. Nath, Y. Yamada, M. Yamaguchi, hep-ph/9905415; Phys.Lett.B466:100-106,1999.

23. M.L. Graesser, hep-ph/9902310.

SCHRÖDINGER'S CATAPLEX

Thomas Curtright

Department of Physics
University of Miami
Coral Gables, FL 33124

SUMMARY

We discuss elementary entwiners that cross-weave the variables of certain integrable models: Liouville, sine-Gordon, and sinh-Gordon field theories in two-dimensional spacetime, and their quantum mechanical reductions. First we define a complex time parameter that varies from one energy-shell to another. Then we explain how field propagators can be simply expressed in terms of elementary functions through the combination of an evolution in this complex time and a duality transformation.

IT'S COMPLEX TIME

One hundred years ago at the close of the 19th century, just before Planck's discovery of light quanta, H. M. Macdonald [22] considered the mathematical problem of determining zeroes of Bessel functions in the complex plane. He was led to find the lovely integral identity[1]

$$K_\nu(e^x)\,K_\nu(e^y) = \int_{-\infty}^{+\infty} dz\, S(x,y,z)\; K_\nu(e^z)\;.$$

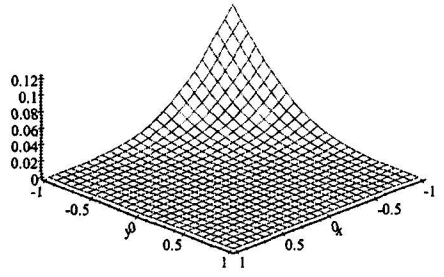
The kernel in the integral is a simple, symmetric exponential of exponentials.

$$\begin{aligned} S(x,y,z) &= \frac{1}{2}\exp\left(-F(x,y,z)\right)\;, \\ F(x,y,z) &= \frac{1}{2}\left(e^{x+y-z}+e^{x-y+z}+e^{-x+y+z}\right)\;. \end{aligned}$$

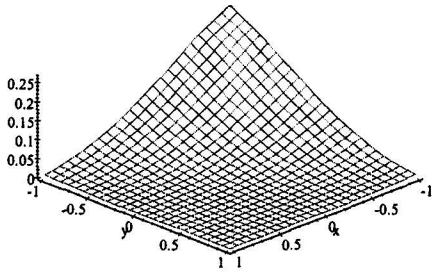
We next plot $S(x, y, z)$ versus x and y for a few values of z.

[1]The most direct way to prove this identity seems to be through the use of the integral transform that expresses modified Bessel functions in terms of plane waves. See §13.71 of [30].

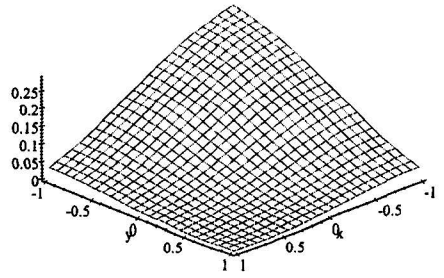
Quantum Gravity. Generalized Theory of Gravitation. arid Superstring\ Theory-Based Unification
Edited by Kursunoglu *et al.*. Kluwer Academic / Plenum Publishers. New York. 2000



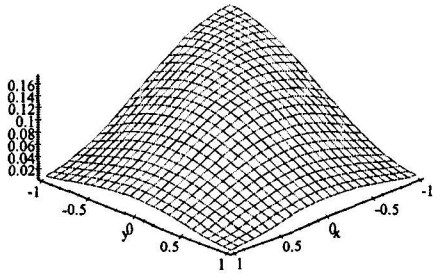
$z = -3$



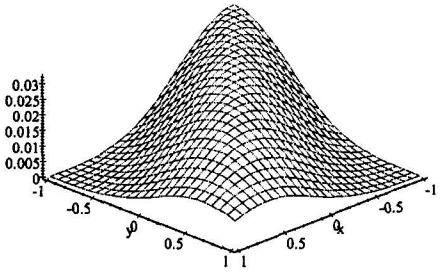
$z = -2$



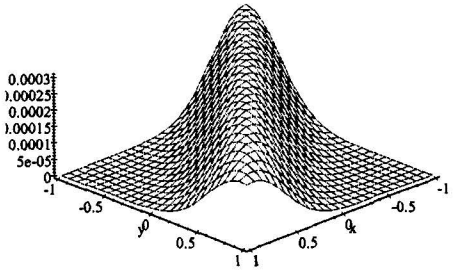
$z = -1$



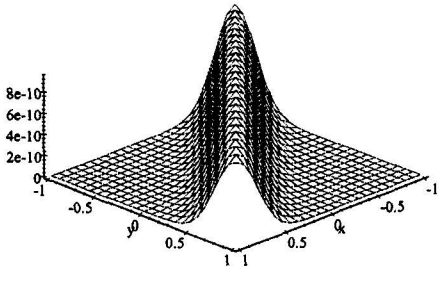
$z = 0$



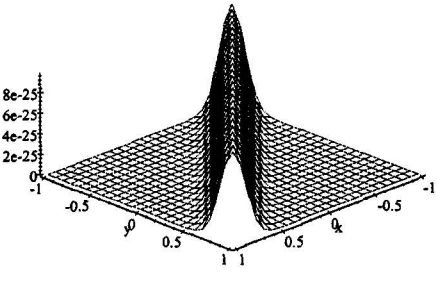
$z = 1$



$z = 2$



$z = 3$



$z = 4$

(Please do *not* try to reproduce these shapes in real time using your table cloth at the conference banquet.)

More recently, the Kelvin (or modified Bessel) functions in Macdonald's identity have appeared in a physical context as solutions of the Liouville quantum mechanics[2]. For Liouville quantum mechanics, the Hamiltonian is $H = p^2 + e^{2x}$. Coordinate space energy eigenfunctions are then solutions of

$$\left(-\frac{d^2}{dx^2} + e^{2x}\right)\psi_E(x) = E\,\psi_E(x)\,.$$

For $0 < E < \infty$, the bounded solutions[3] are

$$\psi_E(x) = N_E\,K_{i\sqrt{E}}(e^x) = \psi_E^*(x)\,,$$

with a normalization factor

$$N_E = \frac{1}{\pi}\sqrt{\sinh\left(\pi\sqrt{E}\right)}\,.$$

As indicated, these ψ_E's are real. There is no solution for $E = 0$, of course [12]. For other values of E, the wave functions are ortho-normalized with our choice for N_E, such that $\int_{-\infty}^{+\infty} dx\,\psi_{E_1}(x)\,\psi_{E2}(x) = d(E1 - E_2)$. They are also complete on the appropriate space of bounded wave functions[4], such that $\int_0^\infty dE\,\psi_E(x)\psi_E(y) = \delta\,(x - y)$.

From the reality and completeness of the Liouville wave functions for real x, y, and z, it follows that another way to state Macdonald's identity is

$$S\,(x, y, z) = \int_0^\infty dE\,K_{i\sqrt{E}}(e^z)\;\psi_E(x)\psi_E^*(y)\,.$$

Upon comparing this expression with the standard form for the propagator as a bilinear in wave functions,

$$G(x, y; t) = \int_0^\infty dE\,e^{-iEt}\;\psi_E(x)\psi_E^*(y)\,,$$

a physical interpretation of Macdonald's identity is immediately apparent.

Proposition: Macdonald's kernel $S\,(x, y, z)$ is precisely the Liouville propagator in the complex time plane, with the identification

$$e^{-iEt} = K_{i\sqrt{E}}(e^z)\,.$$

The parameters t and z are in direct correspondence. That is, the propagator may be written as

$$G\,(x, y; t) \stackrel{\circ}{=} \frac{1}{2}\exp\left(-\frac{1}{2}\left(e^{x+y-z} + e^{x-y+z} + e^{-x+y+z}\right)\right)\,,$$

where $\stackrel{\circ}{=}$ signifies equality[5] on a given energy shell for which $t = \frac{i}{E}\ln\left(K_{i\sqrt{E}}(e^z)\right)$. Real z corresponds to complex t.

---

[2]The Liouville-to-free-particle transformation kernel is obtained by taking the limit of F as y, z $\to$ $-\infty$, with x and $u \equiv y - z$ fixed. This gives F $(x, y, z) \to e^x \cosh u \equiv$ f (x, u), with the variable u acting as the free particle coordinate. Going full circle, f (x, u) then allows Kelvin functions K_{ik} (e^x) to be expressed as integral transforms of plane waves exp (iku), and these transforms can finally be used to derive Macdonald's identity, as in the previous footnote.

[3]There are also unbounded solutions, I_ν, for which Macdonald's integral relation has a "sister" identity: $\theta(y-z)\;\; I_\nu(e^x)K_\nu(\varepsilon^y)+\theta(x-y)\;\; I_\nu(e^y)K_\nu(e^x) \;\; = \int_{-\infty}^{+\infty} dz\,S\,(x, y, z) \;\; I_\nu(e^z)$.

[4]A proof of completeness is given in [18], for example.

[5]One could try replacing E with the operator H, and then properly ordering the terms in the exponential of exponentials. However, this leads to a difficult calculation.

This elementary but nontrivial form for the propagator has the virtue of having explicitly simple x and y coordinate dependence, without being either pathological or tautological[6]. While the time dependence is somewhat mysteriously encoded in the variable z, the coordinate dependence is quite transparent. In principle, such explicit coordinate dependence for any propagator should greatly facilitate extracting the coordinate dependence of the energy eigenstates. Recall that two general methods for extracting such information from the propagator are either to project onto a particular energy by Fourier transforming in the time (that is, construct the Green function and examine the residues of its poles), or to take the deep Euclidean time limit (and, say, isolate a particular exponentially decaying term). Similar general methods should be possible' involving the variable z.

Some care is required, however, since the propagator interpretation of Macdonald's identity implies that the relation between the variable z and the time t is energy dependent, and not just through the combination Et. For example, for large $|e^z|$, so long as $|\arg(ex)| < \frac{3}{2}\pi$, the asymptotic behavior of the Kelvin function is

$$K_\nu(e^z) \sim \sqrt{\frac{\pi}{2e^z}} e^{-e^z} \left\{ 1 + \frac{4\nu^2 - 1}{8} e^{-z} + \frac{1}{2!} \frac{4\nu^2 - 1}{8} \frac{4\nu^2 - 9}{8} e^{-2z} + \cdots \right\} .$$

This means, for deep Euclidean time $t = -iT$, $T \to \infty$ $e^{-iEt} \sim e^{-e^z - \frac{1}{2}z + \ln\sqrt{\frac{\pi}{2}} + \ln\{1+\cdots\}}$. That is

$$T \sim \frac{1}{E}\left(e^z + \frac{1}{2}z - \ln\sqrt{\frac{\pi}{2}} + \frac{1+4E}{8} e^{-z} + O\left(e^{-2z}\right) \right) .$$

Curves in the complex z plane which correspond to real time evolution would be contours of constant modulus for $K_{i\sqrt{E}}(e^z)$ (see graph below). If these are open contours, the corresponding time evolution would be over an interval, perhaps infinite. If these are simple closed contours, the corresponding time variable would be periodic, and the contours might therefore be appropriate to describe Liouville quantum mechanics on closed time-like curves (or perhaps at finite temperature, in the extension to Liouville and other field theories in the following).

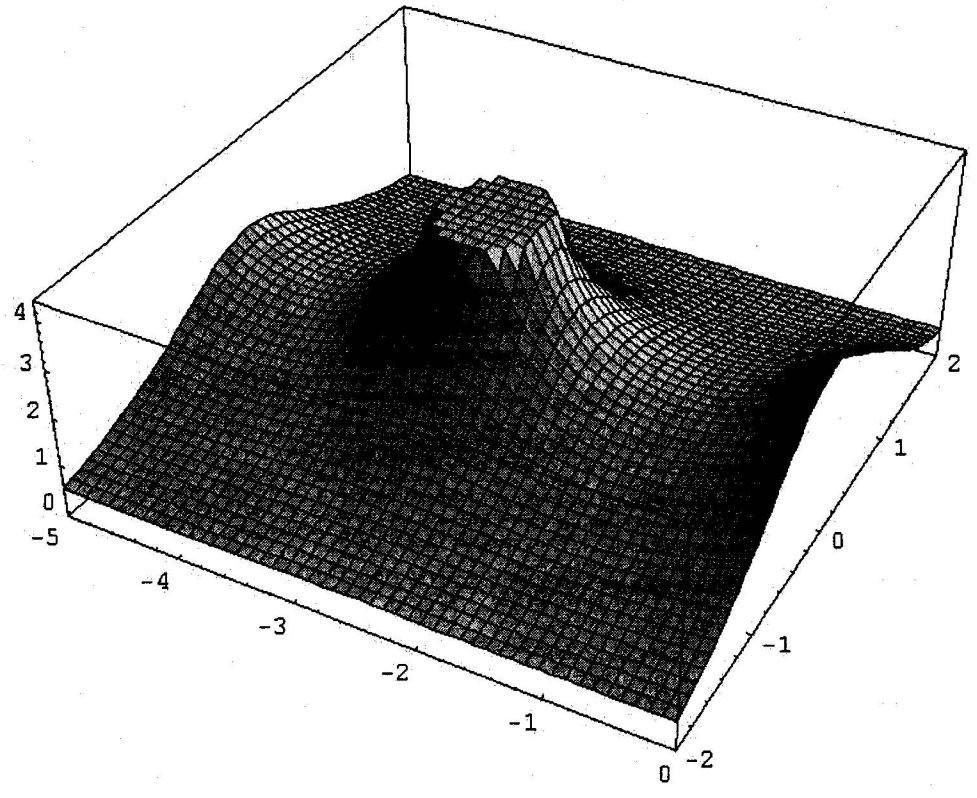
Next we graph $|1/K_i(e^{x+iy})|$ in the complex $z = x + iy$ plane to show that there are both open and closed contours of constant modulus for the Kelvin function. The closed contours circle around the real zeroes of the function on the negative x axis, but note that none of these "rings around the tower" have unit modulus. Somehow this looks familiar[8]

---

[6]By "tautological form" we mean, for example, $G(x, y; t) \triangleq \delta(x - y) \exp(-iw)$, where $w = tE$ on a given energy shell. This is a true statement, but by itself it does not represent much progress in determining the explicit properties of a system, although for at least one simple case it does lead to the familiar form for the propagator. Applying it to the free particle and integrating by parts inside the integral transform, this tautological form immediately yields the well-known result: $\exp\left(it\partial^2/\partial x^2\right) \mathrm{d}(x - y) = \sqrt{\frac{\pi}{it}} \exp(i(x - y)^2/4t)$.

[7]In particular, another way to think of Macdonald's original identity is just as a means of extracting the residues of the Liouville Green function poles.

[8]With apologies to Steven Spielberg, et al.
(http://www. geocities. com/Hollywood/Studio/34 69/encounters. html)



Also note that this relation between z and t is not as strange as it might first appear. Analytic continuation of the time variable is of course a standard practice, but in addition, simple energy dependent (or more generally "state dependent") redefinitions of the time variable are also standard techniques in several areas of physics. For example, in celestial mechanics the use of the various "anomaly" variables (such as the mean anomaly $l\,(t) = a^{-3/2}t$ where a is the semi-major axis for a particular orbit [1]) is just that. The latter is in fact a very old method.

Nonetheless, it would appear that this simple coordinate dependence for the prop agator after energy-dependent time redefinition has not been appreciated previously. For instance, there is no mention of it among the various propagators compiled in [19], although the authors of that compilation did use the previous sister identity to recast the path integral form of the propagator into the standard sum over wave function bilinears [18]. As far as I can tell, the $t \leftrightarrow z$ correspondence is not realized either in the work of Anderson, et al., [2, 3, 4]. All in all, it would seem that a more careful and thorough analysis of the $t \leftrightarrow z$ correspondence is warranted.

DUALITY ENTWINES

When this correspondence is extended to the field theory case, a more compelling collection of ideas emerges. In 1 + 1 field theory, the correspondence between z and complex time is retained, but conjoined with a duality transformation. This follows from replacing the x and y variables in the exponentials of Macdonald's kernel with local fields $\phi\,(\sigma)$ and $\psi\,(\sigma)$, integrating over the spatial coordinate σ, and adding the

elementary duality generator $\int \phi \partial_\sigma \psi d\sigma$ as follows.

$$\mathfrak{S}(\phi,\psi,z) \equiv \exp i \int d\sigma \left(\phi \partial_\sigma \psi + \frac{1}{2} \left(e^{\phi+\psi-z} - e^{\phi-\psi+z} - e^{-\phi+\psi+z} \right) \right) .$$

We have also adjusted the phases in the exponential to conform to those in the usual Schrödinger equation, shifting $z \rightarrow z + i\pi/2$.

The kernel $\mathfrak{S}$ "entwines" or "cross-weaves" various field theory operators for the ϕ and ψ fields within the Schrödinger wave-functional framework[9], as we now explain. We first observe that

$$\begin{aligned} -i \frac{\delta}{\delta\phi(\rho)} \mathfrak{S}(\phi,\psi,z) &= \left(\partial_\rho \psi + \frac{1}{2} \left(e^{\phi+\psi-z} - e^{\phi-\psi+z} + e^{-\phi+\psi+z} \right) \right) \mathfrak{S}(\phi,\psi,z) , \\ -i \frac{\delta}{\delta\psi(\rho)} \mathfrak{S}(\phi,\psi,z) &= \left(-\partial_\rho \phi + \frac{1}{2} \left(e^{\phi+\psi-z} + e^{\phi-\psi+z} - e^{-\phi+\psi+z} \right) \right) \mathfrak{S}(\phi,\psi,z) , \end{aligned}$$

where we have assumed that $\frac{\delta}{\delta\psi}(\phi\psi) = 0$ at the ends of the σ integration range. These results immediately allow us to show that the kernel relates local momentum density operators for the two fields.

By definition these momentum operators are $P_\phi(\rho) = -2if\pi\phi \frac{\delta}{\delta\phi(\rho)}$ and $P_\psi(\rho) = -2i\partial_\rho\psi \frac{\delta}{\delta\psi(\rho)}$

$$\begin{aligned} \mathcal{P}_\phi(\rho)\,\mathfrak{S}(\phi,\psi,z) &= 2\partial_\rho\phi \left(\partial_\rho \psi + \frac{1}{2} \left(e^{\phi+\psi-z} - e^{\phi-\psi+z} + e^{-\phi+\psi+z} \right) \right) \mathfrak{S}(\phi,\psi,z) , \\ \mathcal{P}_\psi(\rho)\,\mathfrak{S}(\phi,\psi,z) &= 2\partial_\rho\psi \left(-\partial_\rho \phi + \frac{1}{2} \left(e^{\phi+\psi-z} + e^{\phi-\psi+z} - e^{-\phi+\psi+z} \right) \right) \mathfrak{S}(\phi,\psi,z) . \end{aligned}$$

Combining these and assuming that z is *not* also a local field, so that $\partial_{\rho z} = 0$, we obtain

$$(\mathcal{P}_\phi(\rho) + \mathcal{P}_\psi(\rho))\,\mathfrak{S}(\phi,\psi,z) = \mathfrak{S}(\phi,\psi,z)\; 2i\partial_\rho F(\phi,\psi,z+i\pi/2) .$$

We now integrate this last equation over r to obtain the total, global momentum operators for the two fields: $P_\phi = \int d\rho P_\phi(\rho)$, $P_\psi = \int d\rho P_\psi(\rho)$.

If we impose boundary conditions in ρ such that $0 = \int d\rho \partial\rho F(\phi,\psi,z+i\pi/2)$ then we have

$$\mathbf{P}_\phi \mathfrak{S}(\phi,\psi,z) = -\mathbf{P}_\psi \mathfrak{S}(\phi,\psi,z) .$$

Using functional integration by parts, this implies that the two momenta are exchanged by, or entwined with the kernel in an integral transform. That is, the momenta of ϕ

[9]Hence the title of this talk. From Liddell-Scott-Jones Lexicon of Classical Greek: καταπλεκω (kataplekô) - *entwine, plait.* Or from Herodotus *Histories* (Loeb) [3.98.4]:

> Houtoi men dê tan Indôn phoreousi esthêta phloïnên: epean ek tou potamou phloun amêsôsi kai kopôsi, to entheuten phormou tropon **kataplexantes** hôs thôrêka en-dunousi.
>
> (These Indians wear clothes of bullrushes; they mow and cut these from the river, then **having woven them crosswise** like a mat, wear them like a breastplate.)

Note that kataplexantes is the plural of the active participle of kataplekô, which we have chosen to distill for obvious reasons to a more contemporary "cataplex". Of course, as scholars of classical Greek will note, there is also: καταπληξ (kata-plêx) - *stricken, struck,* usu. metaph., *stricken with amazement, astounded.* However, this too is an appropriate meaning for the situation under discussion, in our opinion.

and ψ wave functionals become cross-weaved with one another when these functionals are related through the use of (ϕ, ψ, z) in a functional integral transform. More explicitly, let[10]

$$\Phi(\phi) = N \int D\psi \, \mathfrak{S}(\phi, \psi, z) \, \Psi(\psi) \ .$$

Then

$$\mathbf{P}_\phi \Phi(\phi) = N \int D\psi \, \mathbf{P}_\phi \mathfrak{S}(\phi, \psi, z) \, \Psi(\psi) = N \int D\psi \, \mathfrak{S}(\phi, \psi, z) \, \mathbf{P}_\psi \Psi(\psi) \ ,$$

where we have discarded the surface terms arising from the functional integration by parts. This last relation is precisely what we mean by the kernel entwining or cross-weaving the momentum operators.

A perspicacious observer would notice that the momenta of ϕ and ψ theories are entwined in precisely the same way for any choice $6 = \exp i \int d\sigma \, (\phi f \sigma \psi + f(\phi\psi))$ regardless of the form of $f(\phi,\psi)$. The crucial behavior is provided solely by the elementary duality generator $\int d\sigma \phi f \sigma \psi$, which by itself would interchange spatial derivatives of the fields with their canonically conjugate variables (realized as functional derivatives here) just as in the classical theory. So, cross-weaving spatial momentum operators inside the functional integral transform is a relatively trivial task that places only minor restrictions on the kernel. In a much less trivial way, the previous kernel $6(\phi,\psi z)$ also entwines with the energy operators for the ϕ and ψ fields.

To demonstrate this, we need to take second functional derivatives. Rewrite the previous first functional derivatives as

$$-i\left(\frac{\delta}{\delta\phi(\rho)} + \frac{\delta}{\delta\psi(\rho)}\right)\mathfrak{S}(\phi,\psi,z) = \left\{\partial_\rho(\psi-\phi) + e^{-z+\phi(\rho)+\psi(\rho)}\right\}\mathfrak{S}(\phi,\psi,z) \ ,$$

$$-i\left(\frac{\delta}{\delta\phi(\rho)} - \frac{\delta}{\delta\psi(\rho)}\right)\mathfrak{S}(\phi,\psi,z) = \left\{\partial_\rho(\psi+\phi) + e^{z}\left(e^{-\phi(\rho)+\psi(\rho)} - e^{\phi(\rho)-\psi(\rho)}\right)\right\}\mathfrak{S}(\phi,\psi,z) \ ,$$

and combine these to get the second derivative

$$(-i)^2\left(\frac{\delta}{\delta\phi(\rho_1)} - \frac{\delta}{\delta\psi(\rho_1)}\right)\left(\frac{\delta}{\delta\phi(\rho_2)} + \frac{\delta}{\delta\psi(\rho_2)}\right)\mathfrak{S}(\phi,\psi,z) = \left\{2i\partial_{\rho_2}\delta(\rho_2-\rho_1)\right\}\mathfrak{S}(\phi,\psi,z)$$
$$+\left\{\partial_{\rho_2}(\psi-\phi) + e^{-z+\phi(\rho_2)+\psi(\rho_2)}\right\}\left\{\partial_{\rho_1}(\psi+\phi) + e^{z}\left(e^{-\phi(\rho_1)+\psi(\rho_1)} - e^{\phi(\rho_1)-\psi(\rho_1)}\right)\right\}\mathfrak{S}(\phi,\psi,z) \ .$$

Taking the $1 \cap 2$ symmetric, $\rho_1 \to \rho$, $\rho_2 \to \rho$ limit of this gives

$$\begin{aligned}
&(-i)^2\left(\frac{\delta^2}{\delta\phi(\rho)^2} - \frac{\delta^2}{\delta\psi(\rho)^2}\right)\mathfrak{S}(\phi,\psi,z) \\
&\equiv \frac{1}{2}\lim_{\rho_1,\rho_2\to\rho}(-i)^2\left(\frac{\delta}{\delta\phi(\rho_1)} - \frac{\delta}{\delta\psi(\rho_1)}\right)\left(\frac{\delta}{\delta\phi(\rho_2)} + \frac{\delta}{\delta\psi(\rho_2)}\right)\mathfrak{S}(\phi,\psi,z) + (1 \longleftrightarrow 2) \\
&= \left\{\partial_\rho(\psi-\phi) + e^{-z+\phi(\rho)+\psi(\rho)}\right\}\left\{\partial_\rho(\psi+\phi) + e^{z}\left(e^{-\phi(\rho)+\psi(\rho)} - e^{\phi(\rho)-\psi(\rho)}\right)\right\}\mathfrak{S}(\phi,\psi,z) \\
&= \left\{(\partial_\rho\psi)^2 - (\partial_\rho\phi)^2 + e^{2\psi(\rho)} - e^{2\phi(\rho)}\right\}\mathfrak{S}(\phi,\psi,z) + 2\mathfrak{S}(\phi,\psi,z)\ \partial_\rho F(\phi,\psi,z) \ .
\end{aligned}$$

[10]The Liouville-to-free-field transformation kernel is obtained by taking the limit of F as ψ, $z \to -\infty$ with ϕ and $\varphi \equiv \psi - z$ fixed. This gives $F(\phi, \psi, z + i\pi/2) \to -ie^{\phi} \sinh\varphi$, with the variable φ acting as the free field. The corresponding functional integral transforms of free field energy eigenfunctionals were first used in [7].

Now the local energy density operators for the ϕ and ψ fields are of the same form for either:

$$\mathcal{H}_\phi(\rho) = -\frac{\delta^2}{\delta\phi(\rho)^2} + (\partial_\rho\phi)^2 + e^{2\phi(\rho)}\ , \qquad \mathcal{H}_\psi(\rho) = -\frac{\delta^2}{\delta\psi(\rho)^2} + (\partial_\rho\psi)^2 + e^{2\psi(\rho)}\ .$$

In view of these, the previous second derivative relation is

$$\mathcal{H}_\phi(\rho)\,\mathfrak{S}(\phi,\psi,z) = \mathcal{H}_\psi(\rho)\,\mathfrak{S}(\phi,\psi,z) + 2\mathfrak{S}(\phi,\psi,z)\ \partial_\rho F(\phi,\psi,z)\ .$$

If we once again integrate over ρ to obtain the total energy operators for either field, $\mathbf{H}\phi = \int d\rho H\phi(\rho)$ and $\mathbf{H}_\psi = \int d\rho \mathrm{H}\psi,(\mathrm{r})$, and if we again impose boundary conditions in r such that $0 = \int d\rho\partial\rho F(\phi,\psi, z)$, we finally obtain

$$\mathbf{H}_\phi\mathfrak{S}(\phi,\psi,z) = \mathbf{H}_\psi\mathfrak{S}(\phi,\psi,z)\ .$$

Acting on wave functionals, this leads to

$$\mathbf{H}_\phi\Phi(\phi) = N\int D\psi\,\mathbf{H}_\phi\mathfrak{S}(\phi,\psi,z)\ \Psi(\psi) = N\int D\psi\,\mathfrak{S}(\phi,\psi,z)\ \mathbf{H}_\psi\Psi(\psi)\ .$$

The energy operators are therefore also cross-woven by the kernel 6 $(\phi,\psi z)$.

All this entwined structure is present in other models besides the Liouville. For example, the sinh-Gordon and sine-Gordon theories in 1 + 1 dimensions also have simple entwining kernels[11] explicitly given by exponentials of exponentials. This is not surprising. These models are well-known [24,29] to be the only ones (besides quadratic Hamiltonians) involving a single variable which have first-order differential equations involving both fields whose consistency requires the same field equations for either field separately (i.e. auto-Bäcklund transformations, as discussed in [27]). In that purely classical context, the parameter z above is known as a "Bäklund parameter". Exponentiation of the corresponding classical generators for use in quantum theories follows from Dirac's correspondence rule [13]. The fact that the naive correspondence works exactly, without the need for local quantum corrections, for the Liouville, sinh-Gordon, and sineGordon theories, is in our view the essence of the integrability of these models[12]. However, it should be stressed that the exact propagator for *any* theory provides an exact entwining kernel[13], even if that propagator has extensive quantum corrections, and even if those corrections are non-local. This point has been noted previously [7] with somewhat different emphasis.

Let us summarize the results for exponential potentials. The general form of the kernel is:

$$\mathfrak{S}(\phi,\psi,z) \equiv \exp i\int d\sigma\,\mathfrak{F}(\phi(\sigma),\psi(\sigma),z)$$

The explicit forms of the generators, the local energy densities, and their effects on the kernel are:

[11] I obtained kernels for the sine-Gordon and sinh-Gordon theories in the late 1980's, after having spent two earlier years working on the quantization of the classical Bäcklund transformation connecting Liouville and free fields, initially in an operator framework [5] and subsequently using functional methods in collaboration with Ghassan Ghandour and my student Thomas McCarty. The latter work was not published until 1991 [7, 23]. Also see [16].

[12] Recently, Davis and Ghandour [10] have shown that there are no other models involving a single variable for which the classical generators can be used in Dirac's correspondence to obtain valid kernels.

[13] We leave it as a straightforward exercise for the student to show that the usual propagators for the linear potential and the harmonic oscillator are indeed entwiners in the above sense, and for these cases the correspondence between t and z is in fact energy independent.

Liouville

$$\mathcal{H}_\phi = -\frac{\delta^2}{\delta\phi(\rho)^2} + (\partial_\rho\phi)^2 + e^{2\phi(\rho)}$$

$$\mathfrak{F} \equiv \phi\partial_\sigma\psi + \tfrac{1}{2}\left(e^{-z+\phi+\psi} - e^{z-\phi+\psi} - e^{z+\phi-\psi}\right)$$

$$\mathcal{H}_\phi\mathfrak{S} = \mathcal{H}_\psi\mathfrak{S} + \mathfrak{S}\,\partial_\rho\left\{e^{-z+\phi+\psi} + e^{z-\phi+\psi} + e^{z+\phi-\psi}\right\}$$

sinh-Gordon

$$\mathcal{H}_\phi = -\frac{\delta^2}{\delta\phi(\rho)^2} + (\partial_\rho\phi)^2 + 2\cosh 2\phi\,(\rho)$$

$$\mathfrak{F} \equiv \phi\partial_\sigma\psi + e^{-z}\cosh(\phi+\psi) - e^{+z}\cosh(\phi-\psi)$$

$$\mathcal{H}_\phi\mathfrak{S} = \mathcal{H}_\psi\mathfrak{S} + 2\mathfrak{S}\,\partial_\rho\{e^{-z}\cosh(\phi+\psi) + e^{+z}\cosh(\phi-\psi)\}$$

sine-Gordon

$$\mathcal{H}_\phi = -\frac{\delta^2}{\delta\phi(\rho)^2} + (\partial_\rho\phi)^2 - 2\cos 2\phi\,(\rho)$$

$$\mathfrak{F} \equiv \phi\partial_\sigma\psi - e^{-z}\cos(\phi+\psi) + e^{+z}\cos(\phi-\psi)$$

$$\mathcal{H}_\phi\mathfrak{S} = \mathcal{H}_\psi\mathfrak{S} + 2\mathfrak{S}\,\partial_\rho\{-e^{-z}\cos(\phi+\psi) - e^{+z}\cos(\phi-\psi)\}$$

The above generators for the sinh-Gordon and sineGordon theories have been used in a classical context for a long time[14]. They appear in textbooks as the generators of (auto) Bäcklund transformations [27, 31], where for the sineGordon case their functional derivatives are most often employed to generate classical $(N+1)$-soliton solutions starting from N-soliton solutions, with $\phi = 0$ as the trivial $N = 0$ soliton [28,20]. In that classical situation the Bäcklund parameter z is related to the rapidity of the soliton's center of mass.

Now let us reconsider those total divergence terms that axe produced by entwining the densities with $\mathfrak{S}(\phi, \psi, z)$ and show that they are just the usual conformal improvements for the energy-momentum tensor. We find in all three cases:

$$\left(\mathcal{H}_\phi - 2\partial_\rho^2\phi\,(\rho) + \mathcal{P}_\phi - 2\partial_\rho\left(-i\frac{\delta}{\delta\phi\,(\rho)}\right)\right)\mathfrak{S} = \left(\mathcal{H}_\psi + 2\partial_\rho\left(-i\frac{\delta}{\delta\psi\,(\rho)}\right) - \mathcal{P}_\psi - 2\partial_\rho^2\psi\,(\rho)\right)\mathfrak{S}$$

$$\left(\mathcal{H}_\phi - 2\partial_\rho^2\phi\,(\rho) - \mathcal{P}_\phi + 2\partial_\rho\left(-i\frac{\delta}{\delta\phi\,(\rho)}\right)\right)\mathfrak{S} = \left(\mathcal{H}_\psi + 2\partial_\rho\left(-i\frac{\delta}{\delta\psi\,(\rho)}\right) + \mathcal{P}_\psi + 2\partial_\rho^2\psi\,(\rho)\right)\mathfrak{S}$$

The pattern clearly shows that the densities for the two fields undergo dual improvements.

$$\mathcal{H}_\phi \to \mathcal{H}_\phi - 2\partial_\rho^2\phi\,(\rho)\ , \quad \mathcal{P}_\phi \to \mathcal{P}_\phi - 2\partial_\rho\left(-i\frac{\delta}{\delta\phi\,(\rho)}\right)\ ,$$

$$\mathcal{H}_\psi \to \mathcal{H}_\psi + 2\partial_\rho\left(-i\frac{\delta}{\delta\psi\,(\rho)}\right)\ , \quad \mathcal{P}_\psi \to \mathcal{P}_\psi + 2\partial_\rho^2\psi\,(\rho)\ .$$

[14]The Liouville generator follows from the sinh-Gordon generator as a contraction: shift $\phi \to \phi + w$, $\psi \to \psi + w$, $z \to z + w$, rescale $\sigma \to e^{-w}\sigma$, and take $w \to \infty$

Expressing this covariantly for classical densities, using $T_{\mu\nu}$ for the conventional unmodified energy-momentum tensor and $\theta_{\mu\nu}$ for the conformally improved one, we would have the on-shell relations

$$\begin{aligned}\theta_{\mu\nu}(\phi) &= T_{\mu\nu}(\phi) + 2(g_{\mu\nu}\Box - \partial_\mu\partial_\nu)\phi = T_{\mu\nu}(\phi) + 2\varepsilon_{\mu\alpha}\varepsilon_{\nu\beta}\partial^\alpha\partial^\beta\phi \\ \theta_{\mu\nu}(\psi) &= T_{\mu\nu}(\psi) + (\varepsilon_{\mu\alpha}\partial^\alpha\partial_\nu + \varepsilon_{\nu\alpha}\partial^\alpha\partial_\mu)\psi\end{aligned}$$

So, with these local modifications, the energy and momentum densities are entwined without left-over total derivatives. In the case of the Liouville theory, at least. this means that the full Virasoro algebra entwines with $\mathfrak{S}$.For an earlier quantum mechanical example of this situation, see [6].

WISHFUL THOUGHTS

Perhaps other models can be found to have simple propagators using the approach discussed here. An interesting case would be the nonlinear σ model, and its supersymmetric siblings, which can be entwined with a dual σ model at the expense of deforming the field manifold and introducing torsion [9,8]. It is not yet known how to incorporate the parameter *z,* and by correspondence the time, into this transformation.

Perhaps this approach to propagators is also useful when the $(\tau,\sigma) = (\zeta^0, \zeta^1)$ manifold is not intrinsically flat. For example, classical relations *at fixed time* between the Liouville field ϕ and a "free" field ψ have been discussed before [26] (also see [11]). These fields satisfy

$$D^\mu D_\mu\phi = \frac{1}{2g}R - \frac{4m^2}{g}e^{2g\phi}, \qquad D^\mu(\partial_\mu\psi - \frac{1}{g}\omega_\mu) = 0,$$

where zweibein $e\mu a$ connection $w\mu = \eta_{ab}e^a_\mu\epsilon^{\nu\lambda}\partial_\nu e^b_\lambda$, and scalar curvature $R = -2\varepsilon^{\mu\nu}f_\mu w_\nu$ are given functions that depend on (ζ^0,ζ^1). Canonical equivalence of the ϕ and ψ fields in this curved surface situation again' follows from a generating function, which here depends explicitly on ζ^0 even before evolution is included.

$$F[\phi,\psi;\zeta^0] = \int d\zeta^1 \left(\phi\left(\partial_1\psi - \frac{1}{g}\omega_1(\zeta)\right) - \frac{2m}{g^2}e^{g\phi}e^a_1(\zeta)V_a(\psi)\right) .$$

The tangent space vector V is given by $(V_0,V_1\ ) = (\cosh(g\psi),\sinh(g\psi))$.

To generalize these decade-old results and find the analogue of MacDonald's century-old propagator, we seek a generating function that yields exponential potentials for both fields, and that allows for evolution in ζ^0 through an explicit z parameter. Indeed, such a generalization is needed to make contact with other studies of propagators and correlation functions for the Liouville and sine/sinh-Gordon models, since these other studies almost invariably consider the underlying spacetime to be a sphere. For example, see [17, 14, 32, 21, 15, 25]. It remains to entwine all these other studies.

Acknowledgements

I thank Cosmas Zachos and Ghassan Ghandour for informative exchanges. I also thank Behram Kursunoglu and the other organizers of the 1999 Orbis Scientiae meeting for an opportunity to present this paper.

References

[1] R. Abraham and J. E. Marsden, *Foundations of Mechanics,* Perseus Books, 1994 (http://www.perseusbooks.com).

[2] A. Anderson, "Operator method for finding new propagators from old", Phys. Rev. **D37** (1988) 536-539; "Canonical Transformations in Quantum Mechanics", Ann. Phys. (NY) **232** (1994) 292 (*hep-th/9305054*).

[3] A. Anderson and R. Camporesi, "Intertwining operators for solving differential equations with applications to symmetric spaces", Commun. Math. Phys. **130** (1990) 61.

[4] A. Anderson, B.E. Nilsson, C.N. Pope and K.S. Stelle, "The Multivalued free field maps of Liouville and Toda gravities," Nucl. Phys. **B430** (1994) 107 (*hep-th/9401007*).

[5] E. Braaten, T. Curtright, and C. Thorn, "Quantum Bäcklund Transformation for the Liouville Theory", Phys. Lett. **118B** (1982) 115; E. Braaten, T. Curtright, G. Ghandour, and C. Thorn, "Nonperturbative Weak Coupling Analysis of the Quantum Liouville Field Theory", Ann. Phys. (NY) **153** (1984) 147.

[6] T. Curtright, "Quantum Bäcklund Transformations and Conformal Algebras", talk given at 18th Int. Conf. on Differential Geometric Methods in Theoretical Physics: Physics and Geometry, Tahoe City, CA, Jul 2-8, 1989. In *Davis 1989, Proceedings, Differential geometric methods in theoretical physics* 279-289 (*http://phyvax.ir.miami.edu:8001/curtright/tahoe89.html*) .

[7] T.L. Curtright and G.I. Ghandour, "Using Functional Methods to Compute Quantum Effects in the Liouville Model", based on talks given at NATO Advanced Workshop: Quantum Field Theory..., Coral Gables, FL, Jan 7-12, 1991. Published in Coral Gables QFT 1991:333-346 (QC174.45:N21:1991) (*hep-th/9503080*).

[8] T. Curtright, T. Uematsu, and C. Zachos, "Geometry and duality in supersymmetric a-models", Nucl. Phys. **B469** (1996) 488–512 (*hep-th/9601096*).

[9] T. Curtright and C. Zachos, "Currents, charges, and canonical structure of pseude dual chiral models", Phys. Rev. **D49** (1994) 5408-5421 (*hepth/9401006*); "Canonical nonabelian dual transformations in supersymmetric field theories", Phys. Rev. D52 (1995) R573-R576 (*hep-th/9502126*).

[10] E. D. Davis and G. I. Ghandour, "Implications of invariance of the Hamiltonian under canonical transformations in phase space" (*quant-ph/9905002).*

[11] E. D'Hoker, "Generalized Lax and Bäcklund equations for Liouville and super-Liouville theory", Phys. Lett. **264B** (1991) 101-106.

[12] E. D'Hoker and R. Jackiw, "Liouville Field Theory", Phys. Rev. **D26** (1982) 3517.

[13] P. A. M. Dirac, "The Lagrangian in Quantum Mechanics", Phys. Zeit. der Sowjetunion **3** (1933) 64-72.

[14] H. Dorn and H.-J. Otto, "On correlation functions for non-critical strings with $c \leq 1$ but $d \geq 1$", Phys. Lett. **291B** (1992) 39-43. (hepth/9206053); "Two and three-point functions in Liouville theory", Nucl. Phys. **B429** (1994) 375-388. (hep th/9403141)

[15] V. Fateev, D. Fradkin, S. Lukyanov, A. B. Zamolodchikov and Al. B. Zamolodchikov, "Expectation values of descendent fields in the sine-Gordon model", Nucl. Phys. **B540** (1999) 587. (hep-th/9807236)

[16] G. Ghandour, "Effective generating functions for quantum canonical transformations", Phys. Rev. **D35** (1987) 1289.

[17] M. Goulian and M. Li, "Correlation functions in Liouville theory", Phys. Rev. Lett. **66** (1991) 2051-2055.

[18] C. Grosche and F. Steiner, "The Path Integral On The Poincare Upper Half Plane And For Liouville Quantum Mechanics,".Phys. Lett. **A123** (1987) 319.

[19] C. Grosche and F. Steiner, *Handbook of Feynman Path Integrals,* Springer Tracts in Modern Physics, Volume 145, 1998 (http://www.springer-ny.com/).

[20] G. L. Lamb, Jr., "Analytical descriptions of ultrashort optical pulse propagation in a resonant medium", Rev. Mod. Phys. **43** (1971) 99-124.

[21] S. Lukyanov and A. B. Zamolodchikov, "Exact expectation values of local fields in quantum sine-Gordon model", Nucl. Phys. **B493** (1997) 571-587. (hep th/9611238)

[22] H.M. Macdonald, "Zeroes of the Bessel Functions", *Proc. London Math. Soc.* XXX (1899) pp 165-179.

[23] T. McCarty, University of Florida doctoral thesis, 1991 (unpublished).

[24] D. W. McLaughlin and A. C. Scott, "A Restricted Bäcklund Transformation", J. Math. Phys. **14** (1973) 1817-1828.

[25] L. O'Raifeartaigh, J. M. Pawlowski, and V. V. Sreedhar, "Duality in quantum Liouville theory", Annals Phys. **277** (1999) 117. (hep–th/9811090)

[26] C. Preitschopf and C.B. Thorn, "The Bäcklund transform for the Liouville field in a curved background", Phys. Lett. **250B** (1990) 79-83.

[27] C. Rogers and W. F. Shadwick, *Bäcklund Transformations and Their Applications,* Academic Press, 1982 (http://www.apnet.com/).

[28] A. Seeger, H. Donth, and A. Köchendörfer, "Theorie der Versetzungen, in Eindimensionalen Atomreihen: III. Versetzungen, Eigenbewegungen und Ihre Wechselwirkung", Z. Phys. **134** (1953) 173-193.

[29] W. F. Shadwick, "The Bäcklund Problem for the Equation $\partial^2 z/\partial x^1 \partial x^2 = f(z)$", J. Math. Phys. **19** (1978) 2312-2317.

[30] G. N. Watson, *A Treatise on the Theory of Bessel Functions,* 2nd Ed., Cambridge University Press, 1995 (http://www.cup.cam.ac.dc/).

[31] G. B. Whitham, *Linear and Nonlinear Waves,* Wiley-Interscience, 1999 (http://www.wiley.com/).

[32] A. B. Zamolodchikov and Al. B. Zamolodchikov, "Structure constants and conformal bootstrap in Liouville field theory", Nucl. Phys. **B477** (1996) 577-605. (hep-th/9506136)

THE WEAK PRODUCTION OF NEUTRAL HYPERONS IN ELECTRON PROTON SCATTERING

S.L. Mintz

Physics Department
Florida International University
Miami, Florida 33199

INTRODUCTION

The weak non-strangeness changing current has been studied in at least some detail in nuclei and nucleons. At low energies ($q^2 \simeq 0$) a substantial number of beta decay process are available. At $q^2 \simeq -m_\mu{}^2$ both inclusive and exclusive muon capture reactions are observed. Above this q^2 range , neutrino reactions in nuclei and nucleons offer some promise. Finally polarized parity violating electron scattering experiments on nuclei and nucleons are currently being undertaken and are planned for the future. At accelerators such as TJNAF these experiments will allow weak processes to be studied at intermediate energies up to the several GeV level.

The same situation does not prevail for the weak strangeness changing current. The only low and intermediate energy processes which have been studied in detail are hyperon decays such as $\Lambda \rightarrow p + e_- + \nu e$ and $\Sigma_- \rightarrow n + e_- + \nu e$. However the advent of accelerators such as TJNAF with electron beams available from 0.5 GeV to 6.0 GeV have made it feasible to begin examining other strangeness changing processes. In particular the processes $e_- + p \rightarrow \Lambda + \nu e$ and $e_- + p \rightarrow \Sigma_o + \nu e$ might be explored with this type of machine.

These processes would enable several different questions to be studied. It is generally asumed that the strangeness changing weak current is an isospin 1/2 current. In the first process because the Λ is an isospin 0 particle, there would be no contribution from possible I= 3/2 parts of the current. However because the Σ^o particle is an I=1 particle, possible I= 3/2 parts of the current could connect the Σ^o state with the initial proton state. Thus the latter reaction might be useful in testing the structure of the weak strangeness changing current.

Furthermore, both of these reactions might be useful in testing SU(3) relations. These are used to relate baryon data in a similar way to which SU(2) relations can be used. However SU(3) symmetry is more badly broken than SU(2) symmetry. In the calculations which follow we make use of SU(3) relations and phenomenological results to calculate cross sections for these two processes in as model independent a

Quantum Grav ity Generalized Theory of Gravitation and Superstring Theory -Bused Unification
Edited by Kursunoglu *et al* Kluwer Academic / Plenum Publishers New York 2000

way as possible. For hyperon decays, the SU(3) relations produce accurate results but at higher energies we expect that they will break down. It would be very useful to determine where and how this breakdown might occur.

Finally both of these reactions will help in studying possible nucleon models. This should be true in the range of energy at which SU(3) symmetry begins to break down. These processes however will not permit us to look at PCAC. For this a muon beam would be needed because all terms proportional to the pseudoscalar form factor in the cross sections for these processes are proportional to the lepton mass squared and hence not presently observable at an electron accelerator. We therefore leave this question to a later time. In the next two sections we consider first the reaction $e^- + p \rightarrow \Lambda + \nu e$ and then the reaction $e^- + p \rightarrow \Sigma_0 + \nu e$ to determine what might be learned from each of them and magnitudes of the differential cross sections which might be expected from them. We then will present some general conclusions.

THE REACTION $e^- + p \rightarrow \Lambda + \nu_e$

There has been an interest among some of the experimentalists at the Thomas Jefferson National Accelerator Facility, TJNAF1, for studying the reaction $e^- + p \rightarrow \Lambda + \nu e$ and consequently a desire for a more phenomenologically based calculation which might give an indication of the practicality of such an experiment. Such an experiment would be very interesting because it might be possible to obtain the contributions from the F_A, and F_V form factors and hence to test microscopic models of baryonic transitions and to test the Cabibbo model at higher energies.

In this section we calculate the differential cross section for the process, $e^- + p \rightarrow \Lambda + \nu e$ for energies from 0.5 GeV to 6.0 GeV. We shall as noted above where possible make use of the Cabibbo model to obtain the form factors necessary for the calculation and of experimental results[2] to obtain the the axial current form factor at $q^2 = 0$. The Cabibbo model has worked well for Λ beta decay which takes place at $|q_2|$ up to approximately 0.1 GeV^2 , and it would be interesting to see at what energy range the Cabibbo model might break down.

There is also an interesting kinematical effect near the maximal angle of the outgoing hyperon which leads to a mild singularity in the differential cross section and hence apparently unbounded results. This can be corrected by an appropriate wave packet for the outgoing hyperon as will be discussed later.

The processes we are considering can be well described as a first order weak interaction. Although values of q^2 as high as 30 GeV^2/c^2 are possible for the energies being considered here, this is still small compared to the mass squared of the intermediate vector boson and so we are justified in writing the interaction as:

$$< \nu_e \ \Lambda|H_w|e^- \ p >= \frac{G}{\sqrt{2}} \sin\theta_C \bar{u}_\nu \gamma^\lambda (1 - \gamma_5) u_e < \Lambda|J_\lambda^\dagger(0)|p > . \qquad (1)$$

if the quantity $<\Lambda|J_\lambda^\dagger(0)|\ p>$ were known it would be immediately possible to obtain a differential cross section. We note that here the hadronic current,$J\mu(0)$ is written as:

$$J_\mu(0) = V_\mu(0) - A_\mu(0) \qquad (2)$$

where V_μ and A_μ are the vector and axial vector parts of the weak strangeness changing hadronic current. We have written this matrix for an outgoing Λ but they

work equally well for an outgoing Σ^0. There are almost as many notations as papers concerning the p $\leftrightarrow$ Λ transition. We use here a notation similar to that used for $p \leftrightarrow n$ transitions. In this notation, the weak current matrix elements may be written as follows:

$$< \Lambda|V_\mu^\dagger(0)|p >= \bar{u}_f[\gamma_\mu F_V(q^2) + i\frac{F_M(q^2)\sigma_{\mu\nu}q^\nu}{2m_p} - F_S(q^2)\frac{q_\mu}{2m_p}]u_i \qquad (3a)$$

and

$$< \Lambda|A_\mu^\dagger(0)|p >= \bar{u}_f[\gamma_\mu\gamma_5 F_A(q^2) + \frac{q_\mu\gamma_5 F_P(q^2)}{m_\pi} + \frac{iF_E(q^2)\sigma_{\mu\nu}q^\nu\gamma_5}{2m_p}]u_i \qquad (3b)$$

where i is the initial particle and f is the final particle, p and Λ respectively. The structure of the particles is contained, of course, in the six form factors describing the Currents, $F_V(q^2)$, $F_M(q^2)$, $F_S(q^2)$, $F_A(q^2)$, $F_P(q^2)$, and $F_E(q^2)$.

We note that the form factors F_S and F_E would be due to contributions from second class currents. Thus if we are able to determine these six form factors we can write and evaluate a transition matrix element for the $p \leftrightarrow \Lambda$ transition.

Because this is an electron induced process, and all terms of the transition matrix element squared containing either F_P or F_S are proportional to the lepton mass squared, we shall not be able to observe these contributions. Thus only the form factors F_V,F_M,F_A, and F_E need be determined. Unlike the case of of the non-strangeness changing weak current, SU(3) relations rather than SU(2) relations must be used to obtain the unknown form factors. These results are well known and we may in general express the form factors as:

$$F_r^{ijk} = -if^{ijk}\tilde{F}_r + d^{ijk}\tilde{D}_r \qquad (4)$$

where we use a tilde to distinguish the SU(3) functions from the form factors used in Eqs. (3a) and (3b). Here i refers to the current octet number,k and j refer to the initial and final baryon octet numbers and r stands for V,M,A, E, or 1,2,and 3 if an electromagnetic current is being described. For our process Eq.(4) reduces to:

$$F_r = \frac{-1}{\sqrt{6}}(3\tilde{F}_r + \tilde{D}_r) \qquad (5)$$

where we have suppressed the q^2 behavior of the form factors in Eq.(4) and Eq.(5).

Making use of Eq.(5) for the electromagnetic current,$V_\mu^3 + \frac{1}{\sqrt{3}}V_\mu^8$, and for first the proton and then the neutron cases one obtains:

$$\tilde{D}_V = 0 \qquad (5a)$$

$$\tilde{F}_V = F_1^p \qquad (5b)$$

$$\tilde{D}_M = \frac{3}{2}F_2^n \qquad (5c)$$

$$\tilde{F}_M = -F_2^p - \frac{1}{2}F_2^n \qquad (5d)$$

where we have again suppressed the q^2 dependence of the form factors. Using these relations,and Eq.(5) we obtain the following expressions for the vector form factors:

$$F_V(q^2) = F_V(0)/(1 - q^2/M_V^2)^2 \qquad (6a)$$

with Fv(0) = 1.2247 and Mv = .98GeV/c^2 and

$$F_M(q^2) = F_M(0)/(1 - q^2/M_M^2)^2 \tag{6b}$$

with $F_M(0)$ = 1.793/2m_p and M_M = .71GeV/c^2. This completely determines the vector current matrix element for the purposes of this calculation.

The axial current matrix element is more difficult to obtain. Although there exists relations given by Eq.(5), there is no corresponding electromagnetic current of course. However there is very useful experimental data[2] from Λ beta decay, $\Lambda \rightarrow p + e^- + \nu_e$ which gives in the notation used here:

$$\frac{F_A(0)}{F_V(0)} = 0.718 \pm 0.015. \tag{7}$$

Furthermore,these measurementss[3,4,5,6] are consistent with a dipole fit given by:

$$F_A(q^2) = F_A(0)/(1 - q^2/M_A^2)^2 \tag{8}$$

with M_A = 1.25GeV/c^2 and from Eqs.(6a) and (7),$F_A(0)$ = .8793.

Finally we estimate a value for F_E. From a theoretical reference' we obtain an estimate for $F_E(0)$ = .705/2m_p in the notation used here. Making use of our experience that8 F_E and F_M have similar q^2 dependence, we write:

$$F_E(q^2) = F_E(0)/(1 - q^2/M_M^2)^2 \tag{9}$$

where M_M is given in Eq.(6b) and $F_E(0)$ is given above.

Thus we have obtained all of the necessary form factors for evaluating the dif-

ferential cross section which is given by:

$$
\begin{aligned}
|M|^2 = \frac{1}{m_e m_\nu}\Bigg[& \frac{4|F_V|^2}{m_i m_f}[p_f \cdot \nu p_i \cdot e + p_f \cdot e p_i \cdot \nu - e \cdot \nu m_i m_f] + \\
& \frac{4|F_A|^2}{m_f m_i}[p_f \cdot \nu p_i \cdot e + p_f \cdot e p_i \cdot \nu + e \cdot \nu m_i m_f] + \\
& \frac{2|F_M|^2}{m_p^2 m_i m_f}[e \cdot \nu(p_i \cdot e p_f \cdot e + p_i \cdot \nu p_f \cdot \nu + e \cdot \nu m_i m_f)] + \\
& \frac{8F_V F_A}{m_i m_f}[p_f \cdot \nu p_i \cdot e - p_i \cdot \nu p_f \cdot e] + \\
& \frac{4F_M F_V}{m_p m_f}[e \cdot \nu(p_f \cdot \nu - p_f \cdot e)] + \\
& \frac{4F_M F_V}{m_p m_i}[e \cdot \nu(p_i \cdot e - p_i \cdot \nu)] + \\
& \frac{4F_A F_M}{m_p m_f}[e \cdot \nu(p_f \cdot e + p_f \cdot \nu)] + \\
& \frac{4F_A F_M}{m_p m_i}[e \cdot \nu(p_i \cdot e + p_i \cdot \nu)] + \\
& \frac{|F_E|^2}{m_p^2 m_i m_f}[e \cdot \nu(2(p_f \cdot e p_i \cdot e + p_f \cdot \nu p_i \cdot \nu) + q^2 p_f \cdot p_i] + \\
& \frac{4F_E F_V}{m_p m_i}[e \cdot \nu(p_i \cdot \nu + p_i \cdot e)] - \\
& \frac{4F_E F_V}{m_p m_f}[e \cdot \nu(p_f \cdot \nu + p_f \cdot e)] + \\
& \frac{4F_E F_A}{m_p m_f}[e \cdot \nu(p_f \cdot \nu - p_f \cdot e)] + \\
& \frac{4F_E F_A}{m_p m_i}[e \cdot \nu(p_i \cdot \nu - p_i \cdot e)]\Bigg]
\end{aligned}
$$

In the above equation we use m_i to denote the mass of the initial hadron, here the proton and m $_f$ to denote the final hadron which is the Λ. We use m_p to denote the proton mass which occurs in the definition of current matrix elements so that Eq.(10) may be more readily adapted to other processes. We note that every term in this matrix element squared is proportional to the neutrino and to the electron energy. The differential cross section can now be calculated by standard methods. The result is:

$$\frac{d\sigma}{d\Omega} = \frac{m_e m_\nu G^2 m_f p_f |M|^2}{(2\pi)^2 E 8|m_i + E - \frac{E E_f \cos\theta}{p_f}|} \tag{11}$$

where p$_f$ and E_f are here the magnitude of the three momentum and the energy of the the final state Λ respectively. We note here the presence of E in the denominator of Eq.(14) which cancels much of the direct dependence of the matrix element squared ,Eq.(11), on the incoming electron energy. The differential cross sections may now be readily obtained by evaluating Eq.(11)

We do so for incoming electron energies avaailable at TJNAF, namely 0.5 GeV,1.0 GeV,2.0 GeV,4.0 GeV and 6.0 GeV. The results for the differential cross section as a function of the Λ laboratory angle are shown in figure 1. As examples we show in

greater detail the 0.5 GeV and 4.0 GeV cases in figures 2 and 3 respectively. We plot the differential cross section for these energies as a function of the Λ laboratory angle and for these energies we also show the contributions of the individual form factors to the differential cross section by setting all of the others to zero.

In figure 4 we show the the behavior of the differential cross section for the 2.0 GeV case near its peak. Finally in figures 5 and 6 we show the absolute value of the space momentum of the final state Λ particle and the absolute value of q_2 for the reaction for an incident electron energy of 2.0 GeV, both as functions of the Λ laboratory angle.

Before proceeding with our discusion there is an interesting kinematical effect which should be discussed. The energy of the outgoing hyperon may be written as:

$$E_f = \frac{\rho\eta + |\mathbf{p_e}|\cos(\theta)[\eta^2 - 4m_f^2\rho^2 + 4|\mathbf{p_e}|^2 m_f^2\cos^2(\theta)]^{1/2}}{2[\rho^2 - |\mathbf{p_e}|^2\cos(\theta)]} \tag{12}$$

where $\rho = mi + E, \eta = \alpha + 2m_iE$, and $a = m^2_i + m^2_f + m^2_e$. We note that we have written an exact expression here. However at the electron energies being considered here, $|\mathbf{p_e}|$ may be replaced by E, the incident electron energy. This expression for for *Ef* leads to a maximal laboratory angle for the outgoing[9] hyperon given by:

$$\sin^2(\theta_{max}) = 1 - \frac{2\delta}{m_f} - \frac{2\delta}{E} + \frac{3\delta^2}{m_f E} + \frac{\delta^2}{E^2} + \frac{\delta^2}{m_f^2} - \frac{\delta^3}{m_f E^2} - \frac{\delta^3}{m_f^2 E} + \frac{\delta^4}{4m_f^2 E^2} \tag{13}$$

where $\delta = mf - mi$. As can be noted from figure 1, all of the differential cross sections begin to rise rapidly near the maximal angle. This is because there is a mild singularity[9] in the denominator of Eq.(11) which may be written for θ in the neighborhood of θ_{max} as:

$$|m_i + E - \frac{E_f E\cos(\theta)}{p_f}| \approx \frac{[\rho^2 - E^2\cos^2(\theta_{max})]2m_f\sin^2(\theta_{max})}{\eta\cos(\theta_m ax)}\epsilon^{1/2} \tag{14}$$

where $\varepsilon = \theta_{max} - \theta$. Thus as θ approaches θ_{max} the denominator given by Eq.(14) approaches zero and the differential cross section approaches infinity. This has been previously noted in nuclear processes in which the final state nucleus is observed[8,9], but does not occur for observation of the outgoing lepton for which there is no maximal angle.

The singularity in Eq.(14) is very mild, and disappears if a wave packet is used to describe the outgoing hyperon. Following reference 9, we use a Gaussian wave packet . After. integrating over the space parts, we obtain an expression for the differential cross section given by:

$$\frac{d\sigma}{d\Omega_{\bar{f}}} = N\int \chi(p_{fo}, p)\frac{d\sigma}{d\Omega_f}d^3p \tag{15}$$

where quantities described by the *f* are averaged over the wave packet ,pf_o is the momentum of the outgoing hyperon corresponding to the maximal angle, N is a normalization factor, and *x* is the Gaussian wave packet. We choose a wave packet sharply peaked at *pfo*. When there is little overlap between the wave packet and θ_{max}, the averaging has no measurable effect, but when this overlap is large very near the maximal angle, the singularity is integrated out and the infinity disappears. This unbounded increase can be seen in other calculations[7] at the maximal angle and this is the reason for it.

From figure 1 it can be seen that as the incoming electron energy increases from 0.5 GeV to 6.0 GeV, the maximal angle increases from 30.95 degrees to 54.46 degrees and that as the energy of the incoming electron increases, the change in the maximal angle becomes smaller. This is because the terms in Eq.(13) with energy denominators become less important as the incident electron energy becomes large and Eq.(13) approaches:

$$\sin^2(\theta_{max}) = 1 - \frac{2\delta}{m_f} + \frac{\delta^2}{m_f^2} \tag{16}$$

which yields a maximal angle of 57.24 degrees as a limiting value for the Λ case.

From figure 1 it may also be noted that for small angles,the differential cross section falls substantially with increasing incident electron energy. This is not surprising as the largest values of q^2 occur for the smallest angles as can be seen in figure 6, and $|q^2|$increases as the incident electron energy increases. Because the form factors here are dipole, the larger values of q^2 cause a suppression of the form factors and therefore a diminished differential cross section.

Finally from figure 1, it may be seen that the differential cross sections have larger peaking values for larger incident energies. This again is not surprising as the peaks occur at low q^2 values (see figure 6) so the form factors are large. In addition, all terms in Eq.(10), are proportional to at least the first power of the neutrino energy which is largest for small q2. Finally *pf,* the outgoing Λ momentum, increases as the incident electron energy increases and from Eq.(11), the differential cross section is proportional to *pf.* It should be noted that in all cases, the increase in the differential cross section is very rapid near the maximal angle. For the 4.0 GeV case for example, in the region within .05 degrees of the maximal angle, the differential cross section is increasing by at least 10 percent for each increase of .01 degrees. Thus very good angular resolution would be required to obtain an accurate measurement in this region. If one looks at the region about .15 degrees below the maximal angle the increase is much smaller, being of the order of two percent per hundreth of a degree coupled with a decrease in differential cross section of roughly a factor of three from the peak. It would therefore probably be best to take measurements in the region a little below the peak. We also note, from figure 8, that the outgoing space momentum of the Λ near the peak is still large enough to observe.

From figures 2 and 3, it is clear that the contribution from F_E to the differential cross section is small and probably not observable. The contribution from F_M is largest at small angles but this is where the the differential cross section is smallest. Even under the most favorable conditions it contributes at or below the 10 percent level. Thus in the region where the differential cross is largest, the major contributions come from F_V and F_A and these contributions are similar in magnitude. This is actually useful because it should be possible to vary the kinematical conditions so that q^2 remains the same and thus to separate the two form factors. This would be extremely useful for testing microscopic models for the form factors as well as testing the efficacy of the Cabibbo model in a q^2 region not previously available, and for determining F_A (q^2).

A previous theoretical calculation has been done for this reaction[7]. However the purpose of that calculation was to test two microscopic models ,the MIT bag model, and a Dirac harmonic oscillator model. Thus this calculation should usefully complement the earlier work. With regard to comparing results for the two calculations, there is reasonable agreement at 0.5 GeV between our results and the results of the earlier calculation in which CVC was invoked. At higher energy our results are

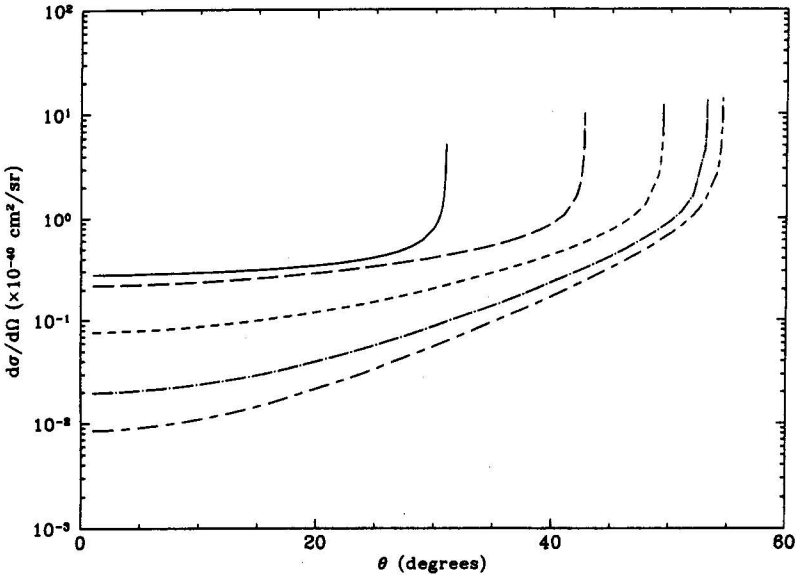


Fig.1 Differential cross section for the reaction,e– + p $\rightarrow$ Λ + *ve* as a function of outgoing Λ laboratory angle. The solid,dashed, small dashed,dot dashed, and double dashed curves correspond to incoming electron energies of 0.5 GeV,1.0 GeV,2.0 GeV,4.0 GeV, and 6.0 GeV respectively.

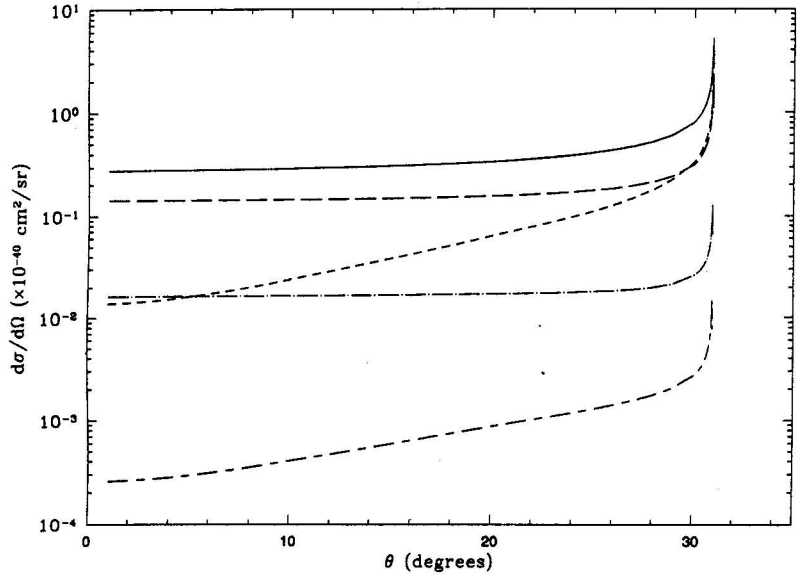


Fig.2 Plot showing the contributions of the form factors to the differential cross section as a function of outgoing A laboratory angle for an incident electron energy of 0.5 GeV. The solid,dashed,small dashed, dot dashed and double dashed curves are the contributions of the whole cross section, *FA,FV, FM,* and *FE* respectively. The curves are obtained by setting all form factors but one to zero.

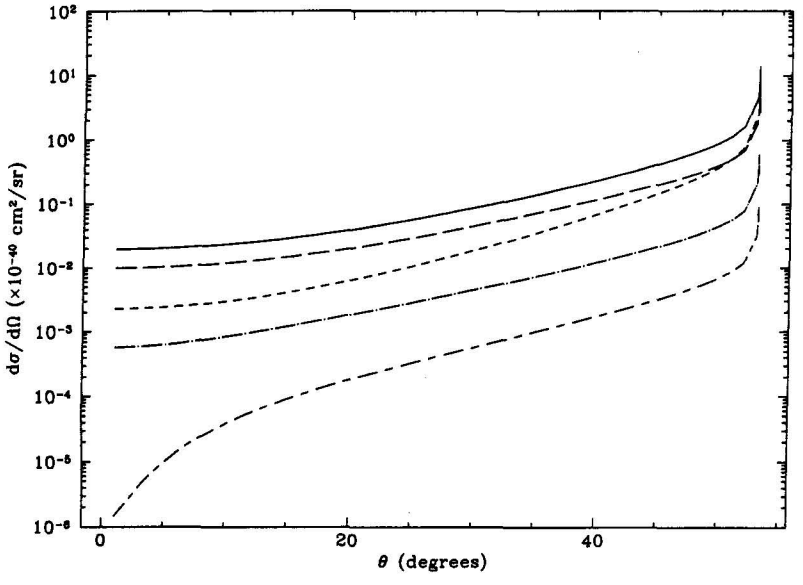


Fig.3 Plot showing the contributions of the form factors to the differential cross section as a function of outgoing Λ laboratory angle for an incident electron energy of 4.0 GeV. The solid,dashed,small dashed, dot dashed and double dashed curves are the contributions of the whole cross section, *FA,Fv, FM,* and *FE* respectively. The curves are obtained by setting all form factors but one to zero.

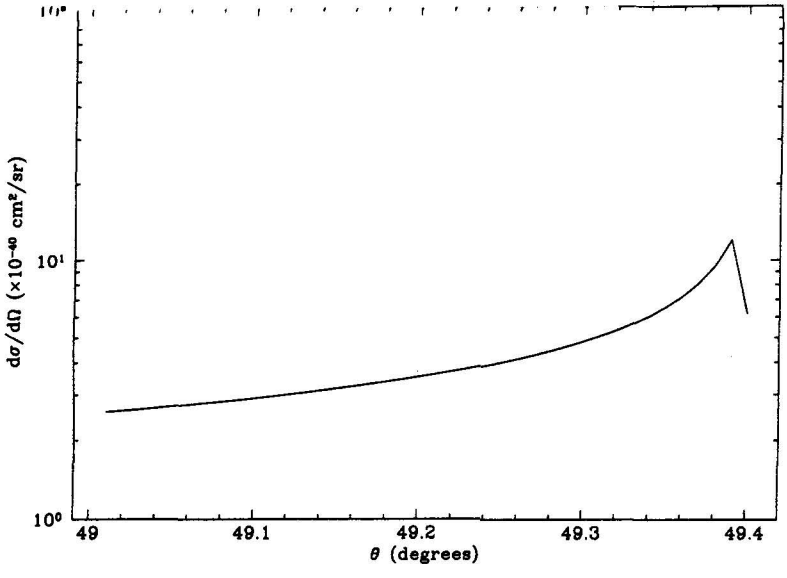


Fig.4 The differential cross section for an incident electron of energy 2.0 GeV for the reaction e– +p $\rightarrow$ Λ + ν_e as a function of outgoing Λ laboratory angle clearly showing the maximum.

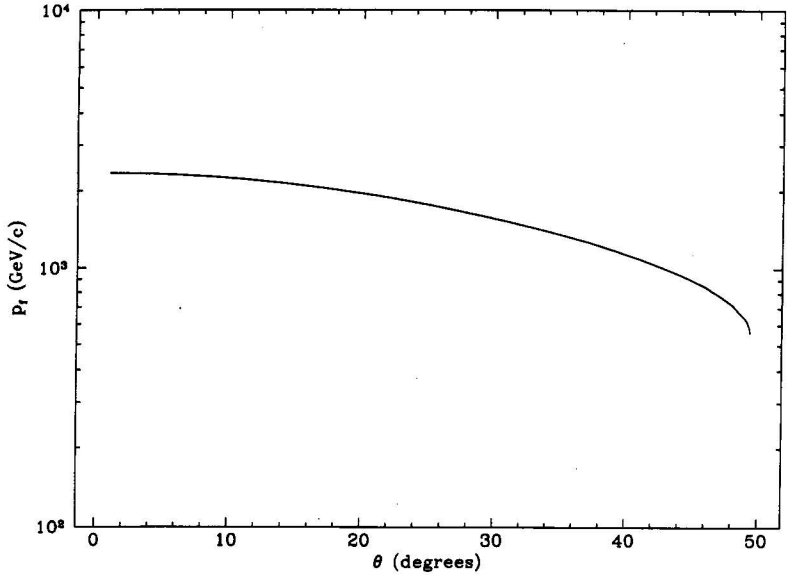


Fig.5 Plot of the absolute value of the three-momentum of the outgoing Λ as a function of laboratory angle for an incident electron of energy 2.0 GeV.

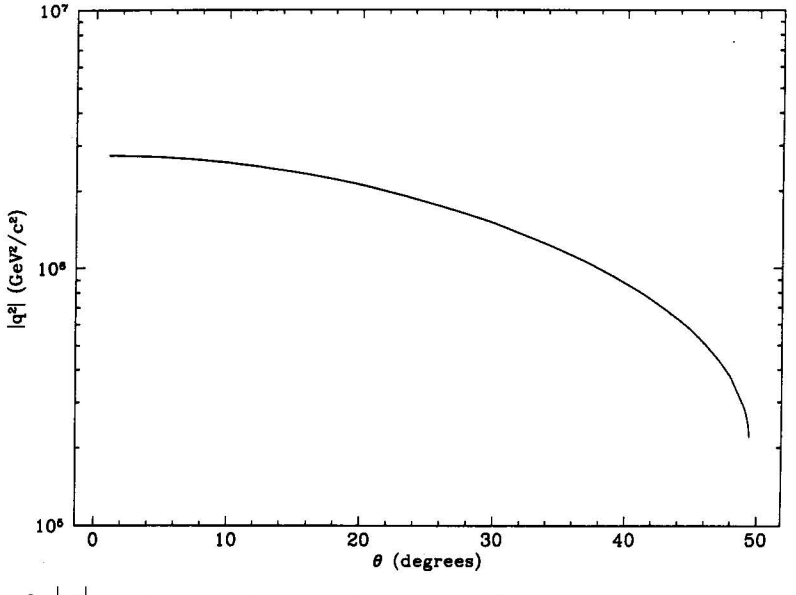


Fig.6 Plot of $|q^2|$ as a function of outgoing laboratory angle of the Λ for an incident electron energy of 2.0 GeV.

similar to the earlier results near the maximal angle (ours peak for the reasons given earlier). At higher q^2, our results are generally larger than those of the earlier calculation. This is not surprising as the MIT bag model produces results which behave as a damped harmonic oscillator and the Dirac harmonic oscillator model becomes rapidly damped as q^2 approaches $1/R^2$ where R is the confinement distance[7].

Some mention should be made concerning possible errors. As it is not known at what values of q^2 the dipole form factors cease to be realistic it is difficult to give a quantitative error in this range. To a large extent the answer to this question depends upon the usefulness of the Cabibbo model under these conditions. The Cabibbo model relates electromagnetic form factors to weak vector form factors. It is known that the electromagnetic nucleon form factors work over a wide range of q^2. In the region of the maximal angle, q^2 is smaller (of the order of 5 times that of beta decay for the 4.0 GeV case) and the Cabibbo model may well produce reasonable results. The agreement between the earlier calculation based on microscopic models and this one near the maximal angle give some credence to this view. If the Cabibbo model were assumed to be correct, the errors in the form factors which are at the few percent level would give a result for the differential cross section accurate to better than 10 percent.

Finally the question of observability of this reaction arises. The differential cross section for this reaction is relatively large for a weak strangeness changing process, with values near the maximum of 10^{-39} cm^2/sr. Making use of parameters appropriate[10] to CEBAF,namely a 15 cm liquid hydrogen target and a current of 200 μA,one obtains a luminosity of L = 7.88 x 1038 cm–2sec–1. This combined with the above cross section yields an event rate of approximately 1 *Hz/sr* or about 0.1 *Hz* assuming a 0.1 sr detector. This would result in over 300 events per hour and discussions with a number of experimentalists indicate that this is feasible[10,11]

A general problem for observing this reaction is the presence of background. This is a much smaller problem here than for non-strangeness changing reactions. The largest background is likely to be electroproduction of K's and Λ's ,i.e., $e_- + p \rightarrow K^+ + \Lambda + e_-$. A missing mass analysis performed in reference 7, indicated that with even only one degree of angular resolution, events from the above background can readily be separated from those of interest. The reaction $e_- + p \rightarrow \Lambda + \nu e$, can also be run below threshold for K^+, Λ production thereby removing this background. There are also possible backgrounds from processes such $e_- + p \rightarrow e_- + p + \pi^+ + \pi^-$. The two pion case can be most readily separated from the one pion case in hall B. However we have been informed by the experimentalists[10,11] that the Λ production process described here can also be performed in halls A and C for limited kinematical ranges for which the two pion production case can effectively be separated by missing mass considerations. They also point out that in principle hall D could also be used although it is set up primarily for photon experiments.

Although no one would claim that the reaction described here is easy to observe, it would be very useful for studying the form factors to test both microscopic models and the Cabibbo model in under circumstances not otherwise easily obtainable, and to provide guidance in determining the axial current form factor.

THE REACTION $e^- + p \rightarrow \Sigma^0 + \nu e$

We have just discussed the reaction[12] ,$e_- + p \rightarrow \Lambda + \nu e$- We found that this reaction might be observable and would be a useful way to study the weak strangeness

changing nuclear current. The reaction $e^- + p \rightarrow \Sigma^0 + \nu e$ might be even more interesting. The weak strangeness changing current is assumed to be an $I = 1/2$ current. This cannot be tested in the reaction $e_- + p \rightarrow \Lambda + \nu e$ because the final state Λ is an I = 0 particle. Thus isospin contributions to the weak strangeness changing current greater than one-half cannot connect the proton to the Λ particle. However for the transition p $\rightarrow$ S0, because the isospin of the S0 is $I = 1$, an $I = 3/2$ contribution to the weak strangeness changing current could connect the two states. Thus the reaction $e^- + p \rightarrow \Sigma^0 + \nu e$ is potentially a better test of the isospin structure of the weak strangeness changing current.

Also there has been a continuing interest among some of the experimentalists at the Thomas Jefferson National Accelerator Facility, TJNAF[1,2] for studying the reaction $e_- + p \rightarrow \Sigma_0 + \nu e$ along with the previously described $e_- + p \rightarrow \Lambda + \nu e$ and consequently a desire for ,in so far as possible,a phenomenologically based calculation which might give realistic chances of observing these reactions. If observable experiments on these reactions might be interesting . It might be possible to obtain the contributions from the form factors as already noted for the Λ case. For the Σ_0 case it will turn out that most of the contributions to the differential cross section will come from the F_V form factor. Thus it might be possible to test microscopic models of baryonic transitions and to test the Cabibbo model at higher energies.

We therefore calculate the differential cross section for the process, $e^- + p \rightarrow \Sigma^0 + \nu e$ for energies from 0.5 GeV to 6.0 GeV. We shall again make our treatment as phenomenological as possible and shall make extensive use of the Cabibbo model to obtain the form factors necessary for the calculation. For the axial current form factor we shall make use of experimental result[13] for a related process as will be discussed. However it will turn out that the differential cross section is not sensitive to the axial current form factor.

The Cabibbo model has worked well for Λ and Σ^- beta decay which take place at $|q^2|$ up to approximately 0.1 GeV^2, and it would be useful to see at what energy range the Cabibbo model might break down. It would also be useful to see if various microscopic models accurately represent this process. Another reason for studying this reaction is that strangeness changing weak processes have not been systematically studied particularly at intermediate energies and this particular reaction offers that possibility.

As before, process we are considering is well described as a first order weak interaction and we may therefore write the transition matrix element as in Eq. (1) with Λ replaced by Σ^0. The structure of the particles is contained, of course, as before in the six form *factors*,$F_V(q^2)$,$F_M(q^2)$,$F_S(q^2)$,$F_A(q^2)$, $F_P(q^2)$,and $F_E(q^2)$ of which the form factors F_S and F_E would be due to contributions from second class currents. Thus as for the Λ case we must determine these form factors.

Again as this is an electron induced process ,all terms of the transition matrix element squared containing either F_P or F_S are proportional to the lepton mass squared these form factors will not be observable. As before we shall thus make use of SU(3) relations to obtain the vector current form factors. We can do this via Eq.(4). For the Σ^0 process Eq.(4) reduces to:

$$F_r = \frac{1}{\sqrt{2}}(F_r - D_r) \tag{17}$$

where we have suppressed the q^2 behavior of the form factors in Eq.(17)

We make use of Eq.(17) for the electromagnetic current,$V_\mu^3 + \frac{1}{\sqrt{3}}V_\mu^8$, and for first the proton and then the neutron cases to obtain in a similar way to the Λ case

$$\bar{D}_V = 0 \tag{18a}$$

$$\tilde{F}_V = F_1^p \tag{18b}$$

$$\tilde{D}_M = \frac{3}{2}F_2^n \tag{18c}$$

$$\tilde{F}_M = -F_2^p - \frac{1}{2}F_2^n. \tag{18d}$$

From Eqs(17) and (18a,b,c,d) we obtain for the vector form factors:

$$F_V(q^2) = F_V(0)/(1 - q^2/M_V^2)^2 \tag{19a}$$

with Fv(0) = –.707 and $M_V = .98GeV/c^2$ and

$$F_M(q^2) = F_M(0)/(1 - q^2/M_M^2)^2 \tag{19b}$$

with $F_M(0) = -1.437/2m_p$ and $M_M = .71\text{GeV/c}^2$. Thus the vector current matrix element for the purposes of this calculation is determined.

The axial current matrix element is more difficult to obtain. There exists no data for the weak decay of Σ^0. However there is beta decay data[13] for the transition $\Sigma^- \leftrightarrow n$. From the isospin relation:

$$[I^+, J_\lambda] = 0 \tag{20}$$

we obtain:

$$< p|[I^+, J_\lambda]|\Sigma^0 >= 0 \tag{21}$$

which implies that:

$$\frac{1}{\sqrt{2}} < n|J_\lambda|\Sigma^- >=< p|J_\lambda|\Sigma^0 > . \tag{22}$$

From the measured value[2] for $F_A^{\Sigma^-}/F_V^{\Sigma^-}$ we find:

$$\frac{F_A^{\Sigma^0}}{F_V^{\Sigma^0}} = \frac{F_A^{\Sigma^-}}{F_V^{\Sigma^-}} = -.34 \pm .017 \tag{23}$$

and finally obtain:

$$F_A = F_A(0)/(1 - q^2/M_A^2)^2 \tag{24}$$

with $M_A = 1.25\text{GeV/c}^2$ and from above $F_A(0) = .24$. We note that experimental data for the Σ^- beta decay is consistent with the above dipole fit.

Finally we estimate a value for F_E. From a theoretical reference' we obtain an estimate for $F_E(0) = .705/2m_p$ in the notation used here. Making use of our experience that8 F_E and F_M have similar q^2 dependence, we write:

$$F_E(q^2) = F_E(0)/(1 - q^2/M_M^2)^2 \tag{25}$$

where M_M is given in Eq.(19b) and FE(0) is given above. Thus we have obtained all of the necessary form factors for evaluating the differential cross section which may be calculated via Eq.(14) and results obtained.

In figure 7 we plot the differential cross section in the laboratory frame for the reaction, $e^- + p \rightarrow \Sigma^0 + ve$, for incident electron energies of 0.5, 1.0,2.0,4.0 and 6.0 GeV. In figure 8 for purposes of comparison we show for an incident electron energy of 4.0 GeV, the differential cross sections for Λ and Σ^0 production.

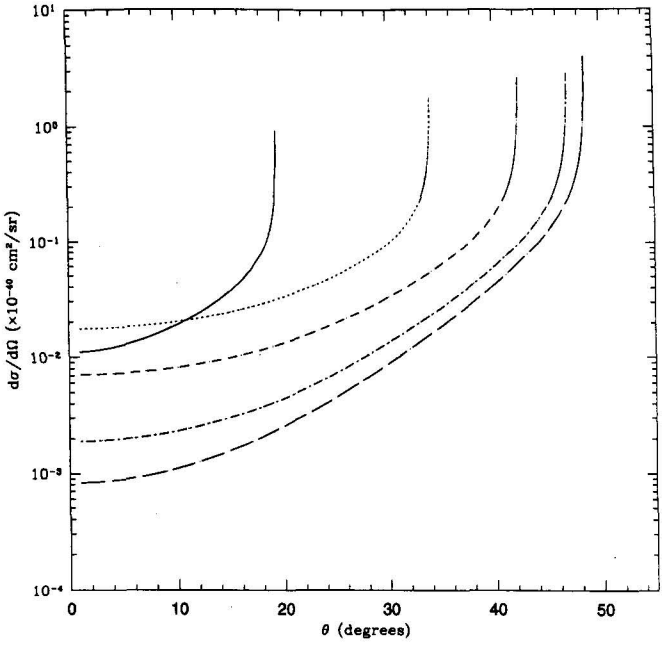


Fig.7 Differential cross section for the reaction,e– $+p \rightarrow \Sigma^0$ + ve as a function of outgoing Σ^0 laboratory angle. The solid,dashed, small dashed,dot dashed, and double dashed curves correspond to incoming electron energies of 0.5 GeV,1.0 GeV,2.0 GeV,4.0 GeV, and 6.0 GeV respectively.

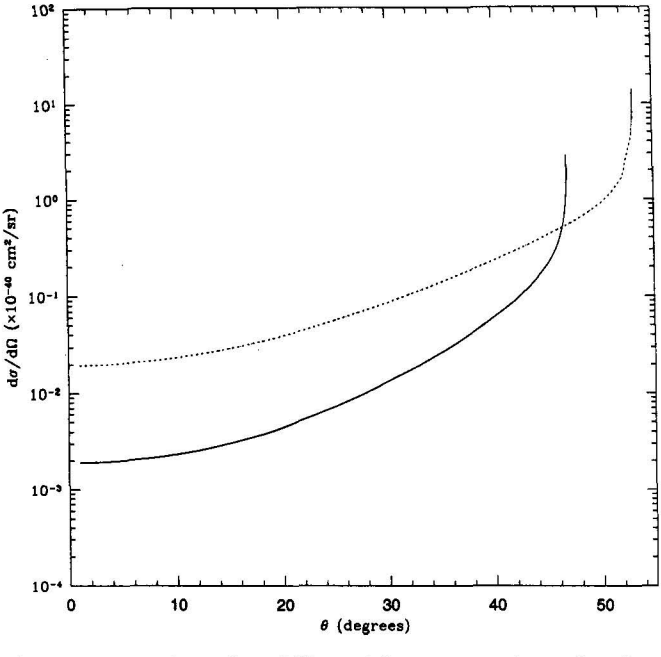


Fig.8 Plot showing a comparison for differential cross sections for the reactions,e– + $p \rightarrow$ S0 + ν_e, and e– +p $\rightarrow \Lambda + \nu_e$, in the laboratory frame for an incident electron of 4.0 GeV. The solid line is for the Σ^0 result and the short dashed line is for the Λ result.

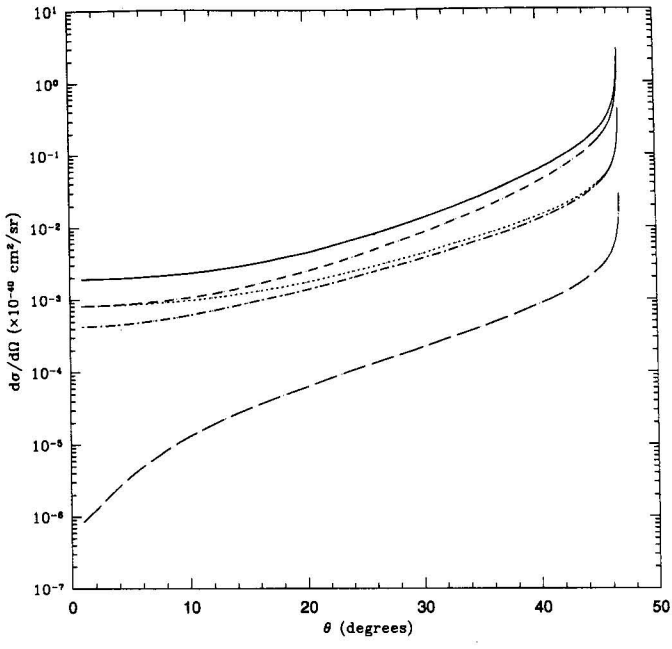


Fig.9 Plot showing the contributions of the form factors to the differential cross section as a function of outgoing Σ^0 laboratory angle for an incident electron energy of 4.0 GeV. The solid,dashed,small dashed, dot dashed and double dashed curves are the contributions of the whole cross section, $F_V, F_A, F_M,$ and F_E respectively. The curves are obtained by setting all form factors but one to zero.

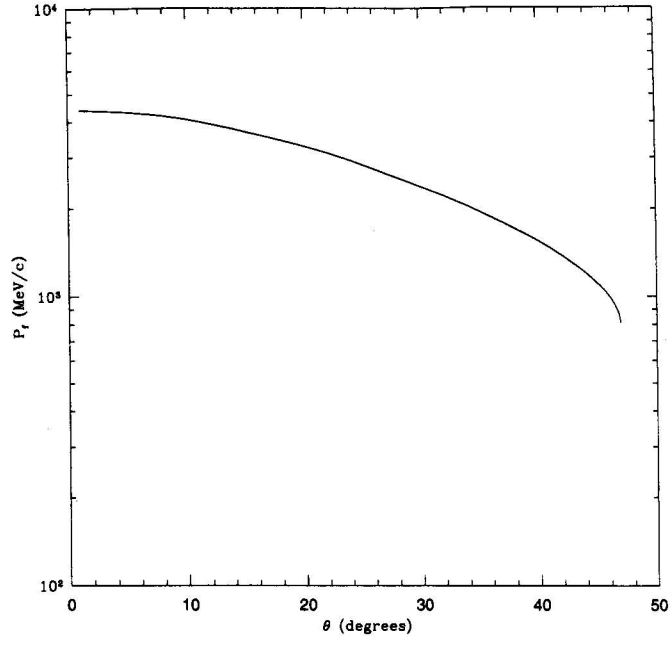


Fig.10 Plot of the absolute value of the three-momentum of the outgoing Σ^0 as a function of laboratory angle for an incident electron of energy 4.0 GeV.

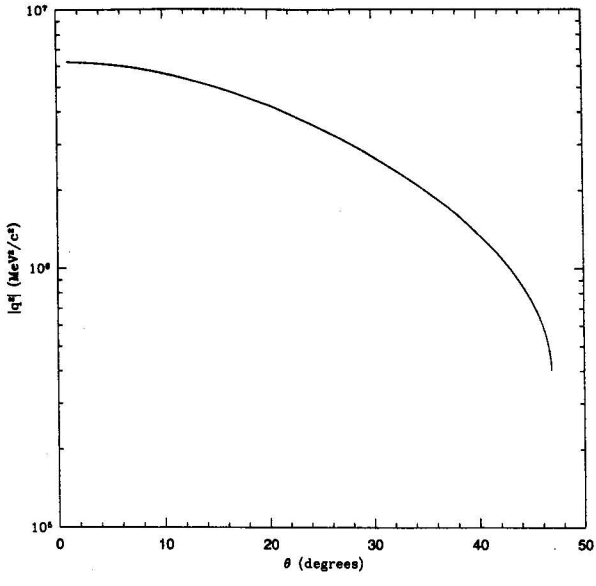


Fig.11 Plot of $|q^2|$ as a function of outgoing laboratory angle of the Σ^0 for an incident electron energy of 4.0 GeV.

Because we shall be interested in the possibility of obtaining the various form factors which appear in the weak currents, we plot for the 4.0 GeV case the contributions of the indiviual form factors to the differential cross section in figure 9. Finally in figures 10, and 11 we plot the three momentum of the outgoing Σ^0 as a function of laboratory angle and $|q^2|$ as a function of the outgoing Σ^0 laboratory angle for an incident electron energy of 4.0 GeV.

The first thing that we note is that in general, differential cross sections for for the reaction $e- + p \rightarrow \Sigma^0 + ve$ are substantially smaller than those for $e- + p \rightarrow \Lambda + ve$. The immediate reason for this is that the axial current form factor is very small, approximately .24 versus .8793 for the Λ case for $q^2 = 0$. This is a factor of almost 4 smaller and leads to a value for $|F_A(0)|^2$ which is less than 8 percent of the Λ value. Thus as can be seen from figure 8, the differential cross section for the process $e- + p \rightarrow \Sigma^0 + ve$ near the maximal angle depends almost entirely on the vector current from factor. This was also noted in a model dependent calculation done earlier[7].

The small size of the axial current form factor and the fact that the other form factors are also smaller leads to much smaller differential cross sections near the maximal angle for the Σ^0 case than for the Λ case. For the 4.0 GeV case, at an angle about 2 degrees below the maximal angle, the cross, section for the Σ^0 process is about 1.8×10^{-40} cm2/sr versus 1.0×10^{-39} cm^2/sr for the Λ case. This leads to reduced expectations for observing this reaction at TJNAF. For the same conditions as were supposed for the Λ case approximately 50 to 60 events might be observed per hour for the Σ^0 case instead of the 300 expected for the Λ case. Although small this number is not an impossible one to observe. Finally the backgrounds are similar for the Σ^0 case to the Λ case. However the break-up of the Σ^0 into a Λ and a γ virtually 100 percent of the time may make the background easier to handle. Thus these two processes offer real possibilities for studying the weak strangeness changing current which should be pusued.

CONCLUSIONS

As we remarked at the beginning of this paper. The study of hyperon production opens a window on the weak strangeness changing current. For the reaction $e^- + p \rightarrow \Lambda + \nu e$ there is an opportunity to look at the hadronic current form factors and for the reaction $e^- + p \rightarrow \Sigma^0 + \nu e$ there is the opportunity to focus on one form factor F_V and to look for the presence of $I = 3/2$ components of the strangeness changing weak hadronic current. This would be the first time that it would be possible to study the weak strangeness changing current at low to intermediate q^2 in a systematic fashion.

Processes of this type would also allow the testing of SU(3) symmetry as incorporated into the Cabibbo over a range of q^2 not generally available. This is particularly true for the case of Σ^0 production where in the region of the maximal angle, the cross section depends effectively on only one form factor for which the Cabibbo model makes definite predictions.

Furthermore, the processes described here would be useful in testing microscopic models of the nucleons. There are many open questions still remaining about the internal structure of nucleons including the contributions of the sea quarks and gluons to nucleon properties such as spin and the extent to which strange quarks contribute to the nucleon sea quarks. It is possible that accurate measurement of these processes might shed some light on this latter question.

Finally one aspect of weak Λ and Σ^0 production which cannot be answered by the processes considered here is the validity of PCAC relations for the weak hadronic strangeness changing current. This is because the pseudoscalar form factor is suppressed by the small size of the electron mass squared. However if muon beams were available the lepton mas squared would be sufficiently large, so that in the low q^2 region it might be possible to observe the pseudoscalar form factor,F_P. This region occurs near the maximal angle as can be seen from figures 6 and 10. This is a very interesting question which we shall save for a later paper.

REFERENCES

1 J.M. Finn,private communication.
2 Particle Data Group,Eur. Phys.J C **3,**1(1998).
3 J. Dworkin et al.,Phys. Rev. D **41,**780(1990).
4 J. Wise et al., Phys. Lett. **98 B**,123(1981).
5 M. Bourquin et al.,Z. Phys. **C 12**,307(1982).
6 Larry J. Carson,Robert J. Oakes, and Charles R. Wilcox, Phys. Rev. **D 37,**3197(1988).
7 W-Y. P. Hwang and E.M. Henley,Phys. Rev. D **38**,798(1988).
8 S.L. Mintz,M.A. Barnett,G.M. Gerstner, and M. Pourkaviani, Nucl. Phys. **A 598**,367(1996).
9 S.L. Mintz and M. Pourkaviani,Phys. Rev C **37**,2249(1988).
10 W. Boeglin,private communication
11 P. Markowitz,private communication
12 S.L. Mintz,Nucl. Phys. **A 657**,303(1999).

This page intentionally left blank.

Section V

CPT, Lorentz Symmetry and Neutrino Oscillation

This page intentionally left blank.

TORSION BALANCE TEST OF SPIN COUPLED FORCES

Blayne R. Heckel, Eric G. Adelberger, Jens H. Gundlach,
Michael G. Harris, and H. Erik Swanson

Department of Physics, Box 351560
University of Washington
Seattle, WA 98195

INTRODUCTION

The extraordinary sensitivity of the torsion balance has made it a valuable tool to test symmetries in nature and to search for new weak macroscopic forces. Most torsion balance experiments employ unpolarized test bodies either of different composition to test the universality of free fall or of special geometry to test for violations of the $1/r^2$ law of gravity.[1] There are several motivations, however, to perform similar torsion balance measurements with spin polarized test bodies: to help elucidate the role of spin in gravitation, to search for new forces mediated by pseudoscalar bosons, and to perform a precise test of Lorentz (rotational) and CPT invariance.

We have constructed an electron spin polarized test body and have completed a first round of measurements with this test body mounted on our EotWash II torsion balance[2] In this paper, we present our results and interpret them as new limits on the strength and range of macroscopic spin coupled interactions and as a new limit on Lorentz and CPT invariance violation.

Moody and Wilczek[3] have shown that the exchange of a mixed parity boson (such as the axion, a proposed 0^- particle with a small admixture of 0^+) leads to a CP-violating potential between two point particles of the form:

$$V_{1,2}(\vec{r},\vec{\sigma}_1) = \frac{g_1^P g_2^S}{8\pi m_1 c}\frac{\exp(-r/\lambda)}{r}(\vec{\sigma}_1\cdot\hat{r})\left[\frac{1}{\lambda}+\frac{1}{r}\right] \qquad (1)$$

where σ_1 and m_1 are the Pauli spin and mass of particle 1, λ is the Compton wavelength of the exchanged boson, and $g^{S(p)}$ is the scalar (pseudoscalar) coupling constant. An interaction of the form of Eq. (1) can be detected as a non-magnetic torque on a spin in the presence of an unpolarized attractor mass.

Kostelecky and Colladay[4,5] have developed a general Lorentz invariance-violating extension of the standard model that includes CPT-even and CPT-odd terms. When applied to electrons, the Lorentz-violating lagrangian terms are [6]:

Quantum Gravity, Generalized Theory of Gravitation, and Superstring Theory-Based Unification
Edited by Kursunoglu *et al.*. Kluwer Academic / Plenum Publishers. New York. 2000

$$L^e = -a^e_\mu \bar{\Psi}\gamma^\mu\Psi - b^e_\mu \bar{\Psi}\gamma_5\gamma^\mu\Psi - H^e_{\mu\nu}\bar{\Psi}\sigma^{\mu\nu}\Psi/2$$
$$+ ic^e_{\mu\nu}\bar{\Psi}\gamma^\mu \vec{D}^\nu\Psi/2 + id^e_{\mu\nu}\gamma_5\gamma^\mu \vec{D}^\nu\Psi/2 \quad (2)$$

where a^e_μ and $b_\mu{}^e$ are CPT-odd terms and the others CPT-even. For non-relativistic electrons, the lagrangian in Eq. (2) gives rise to a coupling to the electron spin given by [6]:

$$V = \tilde{b}^e_j \sigma^j_e, \quad j = 1,2,3 \quad (3)$$

where $\tilde{b}_j{}^e = b_j{}^e - m_e d^e{}_{j0} - \varepsilon_{jkl} H^e{}_{kl}/2$. The Lorentz and CPT symmetry violation appears as a pseudo-magnetic field, $\tilde{b}_j{}^e$, that couples to spin, along an axis fixed in space.

By monitoring the torque on a spin-polarized torsion pendulum as a function of the orientation of the spin relative to both local sources of mass and axes fixed in space, we are able to detect interactions of the forms given by both Eq. (1) and Eq. (3).

SPIN-POLARIZD TEST MASS

To detect anomalous coupling to spin, it is essential to minimize magnetic interactions. Ideally, one would employ a test mass with a non-vanishing spin dipole moment and a vanishing magnetic moment. We approximate this ideal case by constructing an 8-sided ring out of four Alnico magnets and four SmCo magnets, as shown in Figure 1. Eight soft-iron comer pieces allow the magnet sections to be assembled as an octagon, with the Alnico 5 magnets on one side and the Sm_2Co_{17} magnets on the other side. After assembly, a coil is wrapped temporarily around the magnet sections and current pulses are sent through the coil to magnetize the Alnico to the same magnetization as the SmCo. The result is a toroidal distribution of magnetization that has essentially the entire magnetic flux enclosed within the octagon.

The net spin polarization comes from the fact that in Alnico, electron spin polarization provides approximately 94% of the magnetization while in $Sm2Co_{17}$ electron spin polarization provides only approximately 63% of the magnetization (the remaining fraction comes from the orbital angular momentum of the Sm ions).[2] Four octagonal rings are stacked with the two center rings rotated by 180° about the net spin axis, giving an A-B-B-A pattern with a common spin axis, as shown in Figure 2. We estimate that the 64 g of magnets provide a net spin dipole of $(7.8 \pm 0.6) \times 10^{22}$ electron spins that points perpendicular to the central axis of the magnet stack.[2]

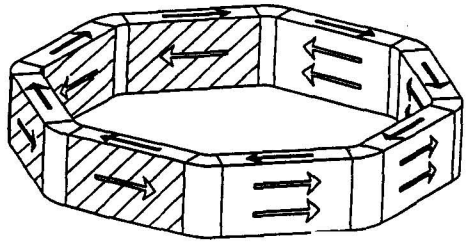


Figure 1. Magnet ring of the spin pendulum. The shaded sections are SmCo magnets and the unshaded are Alnico. The solid arrows on top of the ring show the direction of magnetization. The open arrows on the sides of the ring show the electron spin polarization in each section.

The remaining components of the spin pendulum are a high permeability cylindrical magnetic shield that surrounds the stack of magnet rings and four right-angle mirrors equally spaced around the midplane of the shield for use by the optical readout system. The dipolar component of the magnetic flux that leaks out the magnetic shield surrounding the stack of magnets is less than 0.2 mGauss at a distance of 6 cm from the center of the rings, corresponding to a magnetic dipole moment of 0.02 erg/Gauss.

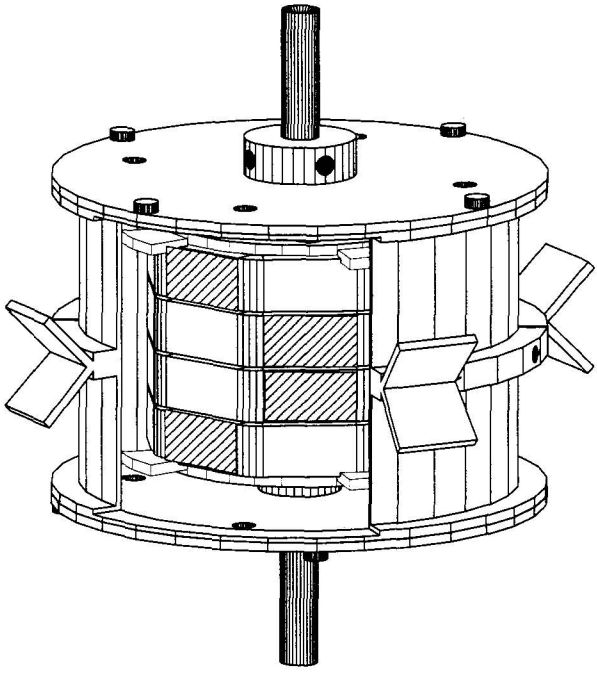


Figure 2. Assembled spin pendulum showing the stack of four magnet rings mounted inside of a magnetic shield. The screws are adjusted to minimize residual gravitational moments.

TORSION BALANCE APPARATUS

The spin pendulum is mounted within the EotWash II torsion balance apparatus shown in Figure 3. Because this apparatus is described in detail elsewhere,[7] only a brief description will be given here. The pendulum is suspended from an 80 cm long, 50 μm diameter tungsten fiber, having a torsion constant of 1.29 erg/rad, and centered within four layers of high permeability magnetic shields. The innermost shield is gold-coated to minimize electrostatic coupling. The pendulum and shields are located within a vacuum vessel that is held to approximately 10^{-6} torr by an ion pump. The vacuum vessel is mounted on a turntable that rotates at a constant rate, $\omega \approx 2p$ rad/hr. A feedback loop locks the output of a precise rotary encoder that is attached below the rotating vacuum vessel to the frequency of a crystal oscillator.

Other important components of the apparatus include tilt monitors that allow the rotation axis to be monitored and aligned vertically, constant temperature water-cooled Cu shields that provide thermal isolation, and nearby machined Pb compensator masses that are used to cancel the Y_{21}, Y_{22}, Y_{31}, Y_{41}, and , and Y_{44} spherical multipole components of the local gravitational field. A set of three-axis Helmholtz coils surround the apparatus and are adjusted to cancel the local magnetic field to 1%.

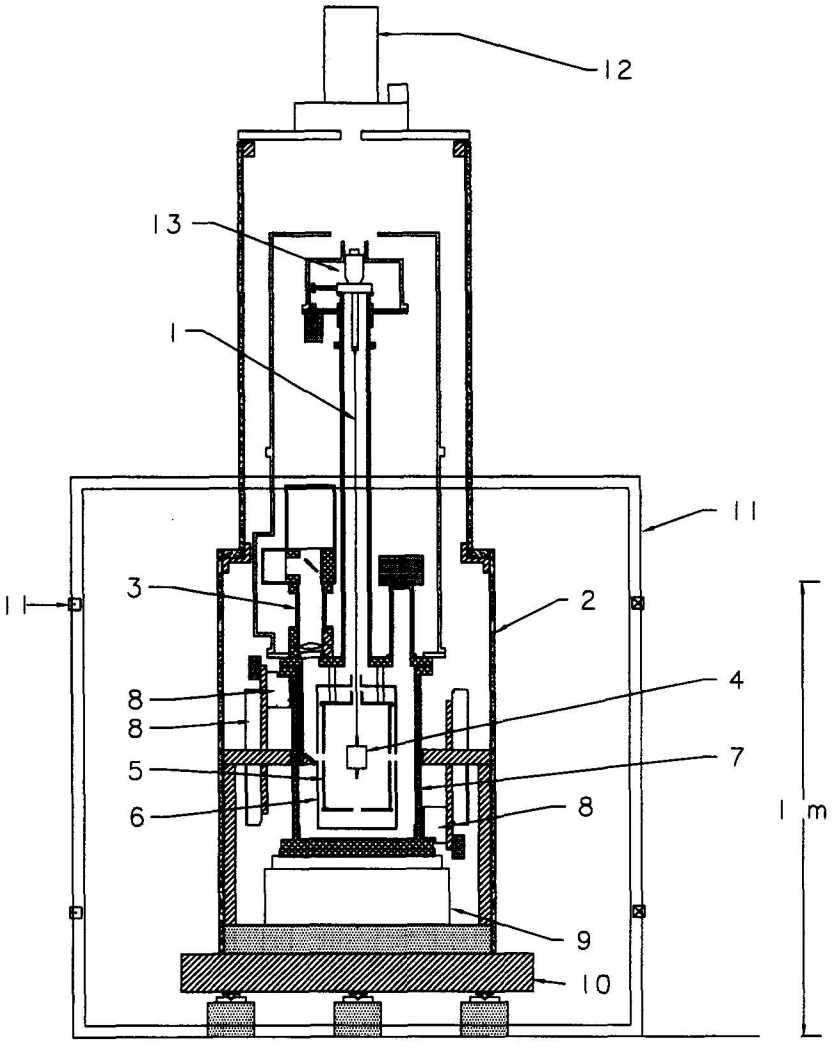


Figure 3. Torsion balance apparatus: 1. Fiber 2. Thermal shield 3. Optical readout system 4. Spin pendulum 5,6. Magnetic shields 7. Vacuum vessel 8. Compensation masses 9. Turntable 10. Baseplate with leveling feet 11. Helmholtz coils 12. Rotary feedthrough 13. Fiber suspension

As the vacuum vessel and pendulum rotate relative to the laboratory at an angle $\varphi = \omega t$, an external potential, V, that couples to spin will produce a torque, $\tau = -\partial V/\partial\varphi$, causing the spin pendulum to twist by an angle, θ, relative to the rotating vessel:

$$\theta(\varphi) = V_H \sin(\varphi_0 - \varphi)/K \tag{4}$$

where K is the torsion constant of the fiber, V_H is the horizontal component of the coupling to spin, and φ_0 is the angle in the horizontal plane at which the coupling is largest. Collimated diode laser light is reflected from one of the four mirrors mounted on the pendulum and the reflected beam is focused onto a linear position sensitive photodiode to monitor the angular position of the pendulum, θ. A rotary stage at the top of the torsion

fiber allows the light to be centered onto any one of the four symmetrically placed mirrors. As different mirrors are used, φ_o in Eq. (4) is altered by 90°, 180°, or 270°. By adjusting the speed of the turntable at the appropriate times, it was possible to damp the free torsion oscillation of the pendulum, leaving the pendulum essentially at rest in the rotating frame. A magnetic damper plate near the top of the fiber damped most of the other fiber modes.

SIGNAL EXTRACTION

The free torsional period, T_o, of the spin pendulum was 213 s. The rotation period of the turntable was chosen to be either $14T_o$ or $20T_o$. At each rotation rate, data was taken on all four mirrors of the pendulum, comprising eight data sets. An example of typical raw data recorded by the optical readout system is shown in Figure 4. The two dominant features are a linear drift of the equilibrium position of the fiber (as the tungsten fiber slowly unwinds) and residual free torsional oscillations. We divide the raw data into 'cuts' that consist of three complete revolutions of the turntable. Each cut is then filtered to remove the free torsional oscillation (by averaging the data over 213 s) and fit to a Fourier series out to the fourth harmonic of the turntable frequency in addition to an offset and linear drift term.[7]

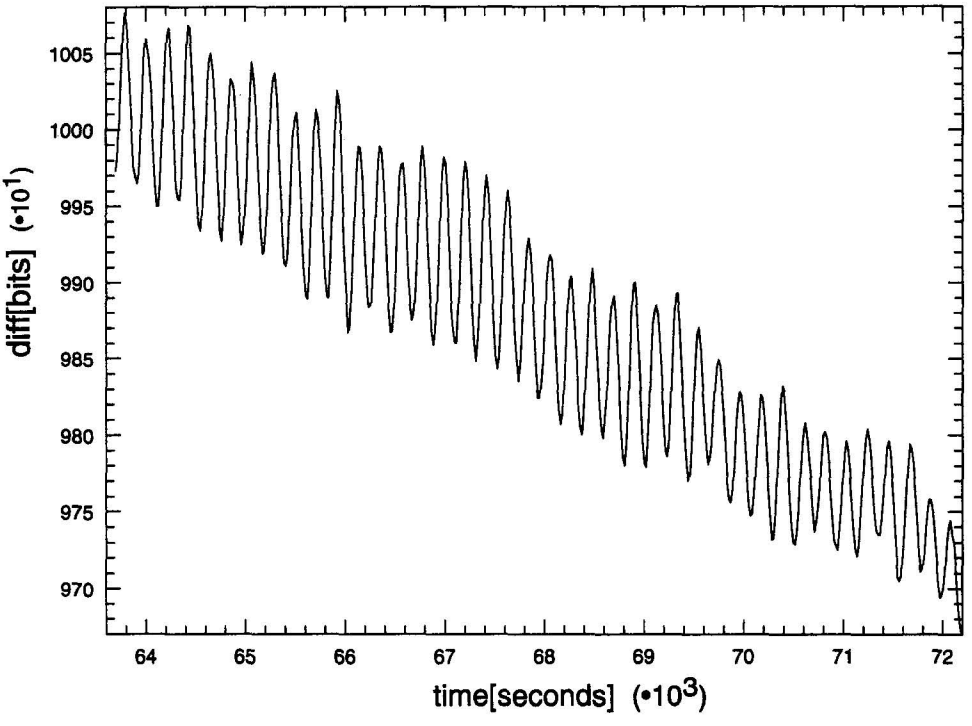


Figure 4. Raw signal from the optical readout system for one data cut. The free torsional oscillation amplitude is approximately 800 nrad.

An external coupling to spin will appear in the first harmonic of the Fourier series. The higher harmonics (due to imperfections in the turntable rotation rate and gravity gradient couplings) are monitored for stability. The cuts from each data run are then averaged and the scatter of the results provides an estimate of the error.

Only two corrections were made to the results. The first is an attenuation correction that accounts for the effects of the pendulum inertia, electronic time constants, and signal averaging on the amplitudes and phases of the harmonic signals.[7] The second correction is for tilt: if the rotation axis is not exactly vertical, the bending of the fiber at its upper attachment point leads to a fiber twist that varies as the first harmonic of the turntable frequency. Because the tilt of the floor changes by several μad each day, it is necessary to remove the tilt feed-through from our signal. We do so by deliberately tilting the apparatus in orthogonal directions to calibrate the fiber's sensitivity to tilt. The readings of the tilt monitors for each cut are then used with the measured tilt sensitivity to derive a correction.[7]

Between data sets, additional measurements were made to examine sources for systematic errors: temperature effects, magnetic coupling to the pendulum, and gravitational gradients. In each case, the driving term was greatly exaggerated. The temperature of the apparatus, normally constant to 0.1 mK, was made to vary by 1 K at the turntable rotation frequency. The current in the Helmholtz coils was reversed, increasing the static magnetic field at the apparatus by a factor of 200. The machined Pb gravity gradient compensators were rotated to add to the local gradients rather than cancel them, increasing the gradients by a factor of typically 100. Surprisingly, the magnetic coupling with the Helmholtz coils reversed was almost undetectable, leading to a systematic error of only 0.03 nrad. Gravity gradients and temperature effects were larger sources for systematic error, both at the level of 0.5 mad.

The largest systematic error was associated with tilt. Although we could reliably correct for slowly varying tilts of the rotation axis, the turntable bearing introduced a reproducible wobble of the rotation axis. Because we could not exaggerate the size of the wobble, we were unable to measure its contribution to the first harmonic component of θ. Our measured sensitivity to tilt times the magnitude of the wobble leads to a systematic error of 4 nrad.

RESULTS FOR LORENTZ SYMMETRY VIOLATION

To search for a pseudo-magnetic field that violates Lorentz and possibly CPT invariance, as described in Eq. (3), we follow the convention of Bluhm and Kostelecky[6] to define the nonrotating coordinate axes of $\tilde{b}^e_j$. The $\hat{z}$ axis is taken to lie along the rotational north pole of the earth: a coupling of the spin pendulum to $\tilde{b}^e_z$ will produce a signal that does not vary as the earth rotates. The $\hat{x}$ axis points from the earth towards the sun at the vernal equinox. Both the amplitude, V_H, and phase, φ_o, of the spin coupling in Eq. (4) will vary as the laboratory coordinates rotate relative to the $\tilde{b}^e_x$ and $\tilde{b}^e_y$ celestial axes.

Table 1. Spin pendulum results for Lorentz symmetry violation

Data Set	Period	Mirror	$\tilde{b}^e_x$ (10^{-20} eV)	$\tilde{b}^e_y$ (10^{-20} eV)	$\tilde{b}^e_z$ (10^{-20} eV)
1	$14T_o$	1	-6.7 ± 6.5	5.5 ± 6.5	-6.1 ± 8.9
2	$14T_o$	2	4.0 ± 6.2	1.7 ± 6.2	-15.3 ± 7.1
3	$14T_o$	3	4.1 ± 7.6	0.4 ± 7.6	-20.5 ± 9.4
4	$14T_o$	4	3.8 ± 5.3	-2.2 ± 5.3	8.4 ± 7.4
5	$20T_o$	1	-0.2 ± 5.4	-0.4 ± 5.4	1.3 ± 7.8
6	$20T_o$	2	-9.5 ± 6.4	14.5 ± 6.4	-18.4 ± 9.6
7	$20T_o$	3	-0.3 ± 5.2	-5.5 ± 5.2	-16.3 ± 6.8
8	$20T_o$	4	5.7 ± 6.0	-0.7 ± 6.0	-15.4 ± 8.8
Averaged results			0.1 ± 2.1	1.7 ± 2.3	-10.3 ± 3.9
Systematic error			± 0.8	± 0.8	± 7.1

For each cut within a data set, we compute the angular coordinates of our spin pendulum relative to the celestial axes. We then fit all of the first harmonic signals from the cuts to a function that describes the amplitude and phase of a coupling to any of the celestial axes (see, for example, Eq. (5) of ref. 8). The results of the fits for each of the eight data sets are shown in Table 1.

The systematic errors for $\tilde{b}^e_x$ and $\tilde{b}^e_y$ in Table 1 are smaller than that for $\tilde{b}^e_z$ because only the components of temperature, magnetic field, gravity gradients, and turntable wobble that vary over the course of a sidereal day contribute to $\tilde{b}^e_x$ and $\tilde{b}^e_y$ while their average values contribute to $\tilde{b}^e_z$

We therefore find no evidence for Lorentz or CPT symmetry violation and quote our results as:

$$\tilde{b}^e_x = (0.1 \pm 2.1 \pm 0.8) \times 10^{-20} \text{ eV} \quad (5)$$

$$\tilde{b}^e_y = (1.7 \pm 2.3 \pm 0.8) \times 10^{-20} \text{ eV} \quad (6)$$

$$\tilde{b}^e_z = -(10.3 \pm 3.9 \pm 7.6) \times 10^{-20} \text{ eV} \quad (7)$$

where the first error is statistical and the second systematic. Upper limits derived from Eqs. (5)-(7) provide the most sensitive test, to date, for Lorentz symmetry violation in the electron sector.

RESULTS ON NEW SPIN-COUPLED FORCES

We can also analyze the spin pendulum results as a test for new spin-coupled forces due to, for example, the exchange of a mixed parity boson from a local source mass as described in Eq. (1). To do so, we integrate Eq. (1) over the mass distribution of the local topography and large scale structure of the earth as a function of λ, the range of the interaction. Such a spin-coupled force will produce a first harmonic signal that does not vary in time, like a coupling to $\tilde{b}^e_z$ in the previous section. The phase of the signal will change by increments of 90°, however, as different mirrors on the pendulum are aligned with the optical readout system. (It was important to take data on all four mirrors because imperfections in the turntable rotation rate lead to a first harmonic signal of approximately 20 nrad. This turntable offset signal was independent of the orientation of the spin pendulum relative to the optical readout system, and could be removed by comparing data sets where the spin axis was reversed with respect to the rotating vacuum vessel.)

Combining the eight data sets after removing the turntable offset, we find a first harmonic signal that tracks the orientation of the spin pendulum of[2]:

$$\theta = 8.9 \pm 2.0 \pm 4.6 \text{ nrad} \quad (8)$$

where the first error is statistical and the second systematic. This leads to a 95% confidence level upper limit on the first harmonic signal of:

$$|\theta| < 17 \text{ nrad} \quad (95\% \text{ CL}) \quad (9)$$

We use this upper limit with Eqs. (1) and (4) to set limits on the coupling constant, $|g_e g^{ps}_N|$, the mixed parity coupling of electrons to nucleons. These limits are shown in Figure 5. The gap in our Eot-Wash limits between the ranges of 10^4 to 10^6 m reflects our ignorance of the source mass topography at those distances. Also shown in Figure 5 are the limits obtained

by Ritter *et al.* using a torsion balance with a different type of polarized mass[9] and the limits obtained by Youdin *et al.* through the comparison of the precession frequencies of optically pumped Hg and Cs atoms.[10]

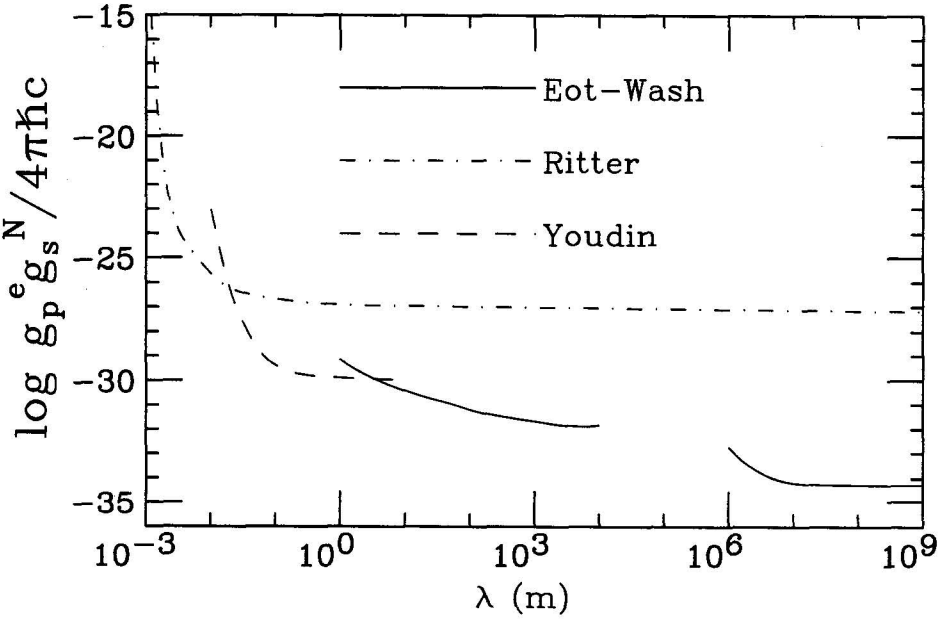


Figure 5. 95% confidence limits on the σ_e r interaction. The horizontal axis shows the interaction range; the vertical axis the limit on the interaction strength.

ACKNOWLEDGEMENTS

We gratefully acknowledge the financial support for this work provided by the NSF (Grant PHY-9602494) and the DOE.

REFERENCES

1. E. G. Adelberger, B. R. Heckel, C. W. Stubbs, and W. F. Rogers, Searches for new macroscopic forces, *Annu. Rev. Nucl. Part. Sci.* **41**,269-320 (1991).
2. M. G. Harris, A search for a macroscopic CP violating interaction, using a spin-polarized torsion pendulum, Ph.D. thesis, Univ. of Washington, unpublished (1998).
3. J. E. Moody and F. Wilczek, New macroscopic forces?, *Phys. Rev D* **30**(1), 130-138 (1984).
4. D. Colladay and V. A. Kostelecy, CFT violation and the standard model, *Phys. Rev. D* **55**(1 1), 6760-6774 (1997).
5. D. Colladay and V. A. Kostelecky, Lorentz-violating extension of the standard model, *Phys. Rev. D* **58** (116002), 1-23 (1998).
6. R. Bluhm and V. A. Kostelecky, Lorentz and CPT tests with spin-polarized solids, *Phys. Rev. Lett.* (accepted for publication).
7. Y. Su, B. R. Heckel, E. G. Adelberger, J. H. Gundlach, M. Harris, G. L. Smith, and H. E. Swanson, New tests of the universality of free fall, *Phys. Rev.* D **50**(6), 3614-3636 (1994).
8. S. Baeßler, B. R. Heckel, E. G. Adelberger, J. H. Gundlach, U. Schmidt, and H. E. Swanson, Improved test of the equivalence principle for gravitational self-energy, *Phys. Rev. Lett.* **83**(18) 3885-3588 (1999).
9. R. C. Ritter, L. I. Winkler, and G. T. Gillies, Search for anomalous spin-dependent forces with a polarized-mass torsion pendulum, *Phys. Rev. Lett.* **70**(6), 701-704 (1993).
10. A. N. Youdin, D. Krause Jr., K. Jagannathan, L. R. Hunter, and S. K. Lamoreaux, *Phys. Rev. Lett.* **77**(1 1), 2170-2173 (1996).

RECENT RESULTS IN LORENTZ AND CPT TESTS

V. Alan Kostelecky

Physics Department
Indiana University
Bloomington, IN 47405
U.S.A.

INTRODUCTION

At a fundamental level, nature appears invariant under Lorentz transformations. This symmetry, which includes rotations and boosts, is incorporated into the standard model of particle physics. Like other local relativistic field theories of point particles, the standard model is also invariant under the CPT transformation, which is formed from the combination of charge conjugation C, parity reflection P, and time reversal T. Numerous experimental tests of Lorentz and CPT symmetry have been performed [1, 2]. The exceptional sensitivity of these tests and the cornerstone role of Lorentz and CPT symmetry in established theory make studies of possible Lorentz and CPT violation of interest in the context of physics beyond the standard model [3].

Talks at previous conferences in this series (Orbis Scientiae 1997-I [4], 1997-11 [5], and 1998) have presented the idea that Lorentz and CPT symmetry might be spontaneously broken in nature by effects emerging from a fundamental theory beyond the standard model, such as string theory [3]. They also have outlined the low-energy description of the resulting effects and have described a candidate consistent standard-model extension incorporating Lorentz and CPT violation [6]. In this talk, I summarize some of the recent experimental constraints on the standard-model extension that that have been obtained since the previous conference. New constraints on Lorentz and CPT violation are also being announced for the first time at this meeting, as reported in other contributions to the proceedings [7, 8].

Quatum Gravity Generalized Theory of Gra vitation and Superstring Theory Based Unification
Edited by Kursunoglu *et al* Kluwer Academic / Plenum Publishers New York 2000

Since the natual dimensionless suppression factor for observable Lorentz or CPT violation is the ratio r ~ 10^{-17} of the low-energy scale to the Planck scale, relatively few experimental tests are capable of detecting any associated effect. Among those with the necessary sensitivity and placing interesting constraints on parameters in the standard-model extension are studies of neutral-meson oscillations [9, 10, 11, 12, 13,141, comparative tests of QED in Penning traps [15,16,17,18,19], spectroscopy of hydrogen and antihydrogen [20, 8, 21], measurements of muon properties [22], clock-comparison experiments [23, 24, 8], observations of the behavior of a spin-polarized torsion pendulum [25, 7], measurements of cosmological birefringence [26, 6, 27, 28], and observations of the baryon asymmetry [29]. Effects on cosmic rays have also been investigated in a restricted version of the standard-model extension [30, 31]. In this contribution to the proceedings, I limit considerations to recent results directly relevant to the standard-model extension and obtained in kaon oscillations and in clock-comparison experiments.

EXPERIMENTS WITH NEUTRAL KAONS

Neutral-meson oscillations provide a sensitive tool for studies of Lorentz and CPT symmetry. In the kaon system, experiments already constrain the CPT figure of merit $r_K \equiv |m_K - m_{\bar{K}}| / m_K$ to better than a part in 1018 [9, 14, 32], with improvements expected in the near future [33].

The standard analysis [34, 35] of possible CPT violation in the kaon system is purely phenomenological, introducing a complex parameter δ_K in the standard relationships between the physical meson states and the strong-interaction eigenstates. However, in the context of the standard-model extension with Lorentz and CPT violation, the parameter δ_K is calculable rather than purely phenomenological. Thus, a meson with velocity b in the laboratory frame and associated boost factor γ displays CPT-violating effects given by [13]

$$\delta_K \approx i \sin\phi \; e^{i\phi}\gamma(\Delta a_0 - \beta \; \Delta a)/\Delta m \quad . \tag{1}$$

In this expression, $\phi \equiv \tan^{-1}(2\Delta m/\Delta\gamma)$, where Δm and $\Delta\gamma$ are the mass and rate differences between the physical eigenstates, and the four components of the quantity Δa_μ, control certain specific Lorentz- and CPT-violating couplings in the standard-model extension.

Equation (1) exhibits several unexpected features, including dependence on momentum magnitude and orientation. These imply various observable consequences including, for example, time variations of the measured value of dK with the Earth's sidereal (not solar) rotation frequency $\Omega \cong 2\pi/(23$ h 56 min) [13]. To display explicitly the time dependence of dK arising from the rotation of the Earth, one can introduce a convenient nonrotating frame. Denote the nonrotating-frame basis as $(\hat{X}, \hat{Y}, \hat{Z})$. The natural choice for Z

is the rotation axis of the Earth, and celestial equatorial coordinates can be used to fix the $\hat{X}$ and $\hat{Y}$ axes [24].

For the general case of a kaon with three-velocity $\vec{\beta}$ in the laboratory frame, an expression for the parameter δ_K in the nonrotating frame can be found. However, for simplicity in what follows I restrict attention to the special case of experiments involving highly collimated uncorrelated kaons with nontrivial momentum spectrum and large mean boost, such as the E773 and KTeV experiments [9, 36] where the average boost factor $\overline{\gamma}$ is of order 100. General theoretical expressions and a discussion of issues relevant to other classes of experiment can be found in Ref. [13].

In experiments with boosted collimated kaons, the z axis for the laboratory frame can be chosen along the kaon three-velocity, $\hat{\beta} = (0, 0, \beta)$. The general expression for δ_K in the nonrotating frame then reduces to

$$\delta_K(\vec{p}, t) = \frac{i \sin\hat{\phi}\, e^{i\hat{\phi}}}{\Delta m}\gamma[\Delta a_0 + \beta\Delta a_Z \cos\chi + \beta \sin\chi(\Delta a_Y \sin\Omega t + \Delta a_X \cos\Omega t)], \tag{2}$$

where $\cos\chi = \hat{z} \cdot \hat{Z}$ Note that this equation shows that each component of Δa_μ, in the nonrotating frame is associated with momentum dependence through the boost factor γ but only the coefficients of Δa_X and Δa_Y vary with sidereal time.

Experiments are performed over extended time periods, so a conventional analysis for CPT bounds disregarding the momentum and time dependence is sensitive to a time and momentum average over the data momentum spectrum given by

$$|\overline{\delta_K}| = \frac{\sin\hat{\phi}}{\Delta m}\overline{\gamma}(\Delta a_0 + \overline{\beta}\Delta a_Z \cos\chi) \quad , \tag{3}$$

where $\overline{\beta}$ and $\overline{\gamma}$ are averages of β and γ. This expression allows the derivation of a bound on a combination of the quantities Δa_0 and Δa_Z [13]:

$$|\Delta a_0 + 0.6\Delta a_Z| \lesssim 10^{-20}\ \text{GeV} \tag{4}$$

In practice, the experimental constraints on δ_K are obtained via measurements on other observables such as the mass difference Δm, the Ks lifetime $\tau_S = 1/\gamma_S$ and the ratios η_{+-}, h_{00} of amplitudes for 2π decays. Analysis shows that only the phases ϕ_{+-} and ϕ_{00} of the latter vary with momentum and sidereal time at leading order [13]. For example, the phase f_{+-} is given by

$$\phi_{+-} \approx \hat{\phi} + \frac{\sin\hat{\phi}}{|\eta_{+-}|\Delta m}\gamma[\Delta a_0 + \beta\Delta a_Z \cos\chi + \beta \sin\chi(\Delta a_Y \sin\Omega t + \Delta a_X \cos\Omega t)]. \tag{5}$$

This expression shows that distinct bounds on the components of Δa_μ, can

in principle be obtained in experiments with boosted collimated kaons if the momentum spectrum is sufficiently resolved.

The KTeV collaboration has recently placed a constraint $A_{+-} \lesssim 0.5°$ on the amplitude A_{+-} of time variations of the phase ϕ_{+-} with sidereal periodicity [14]. This gives the limit

$$\sqrt{(\Delta a_X)^2 + (\Delta a_Y)^2} \lesssim 10^{-20}\ \text{GeV} \quad , \tag{6}$$

which represents the first bound obtained on the parameters Δa_X and Δa_Y.

It should be noted that experiments with neutral mesons are presently the only ones known to be capable of detecting effects associated with the Lorentz- and CPT-violating parameter Δa_μ, [13]. Note also that the two bounds (4) and (6) discussed here are independent constraints on possible CPT violation. Relative to the kaon mass, both bounds compare favorably with the ratio of the kaon mass to the Planck scale.

CLOCK-COMPARISON EXPERIMENTS

Among the most sensitive tests of Lorentz and CPT symmetry are the clock-comparison experiments [23]. These provide limits on possible spatial anisotropies and hence on violations of rotation symmetry by bounding the relative frequency change between two hyperfine or Zeeman transitions as the Earth rotates. Data from these experiments can be interpreted in the context of the standard-model extension [24]. In this section, I provide a brief outline of the primary results of this study.

The standard-model extension allows for flavor-dependent effects. Since distinct species of atoms and ions have different compositions in terms of elementary particles, the corresponding signals in clock-comparison experiments can crucially depend on the chosen species. The complexity of most atoms and ions makes it impractical to perform a complete *ab initio* calculation of energy-level shifts arising from Lorentz-violating terms in the standard-model extension. Fortunately, since any Lorentz-violating effects must be minuscule, it suffices to determine leading-order effects in a perturbative calculation. The leading perturbative contribution to Lorentz-violating energy-level shifts consists of a sum of shifts originating from each elementary particle in the atom, generated through the expectation value of the nonrelativistic Lorentz-violating hamiltonian in the multiparticle unperturbed atomic state.

The appropriate single-particle nonrelativistic hamiltonian is known [37], and its perturbation component δh for Lorentz violation has the form

$$\delta h = (a_0 - mc_{00} - me_0) + \left(-b_j + md_{j0} - \tfrac{1}{2}m\varepsilon_{jkl}g_{kl0} + \tfrac{1}{2}\varepsilon_{jkl}H_{kl}\right)\sigma^j + \ldots \tag{7}$$

Here, m is the single-particle mass, each Lorentz index is split into a timelike

component 0 and spacelike cartesian components $j = 1,2,3$, ε_{jkl} is the totally antisymmetric rotation tensor, and the Pauli matrices are denoted by σ^j. The other quantities are parameters for Lorentz and CPT violation arising in the standard-model extension. A complete expression for dh is given in Refs. [24, 37].

The multiparticle Lorentz-violating perturbative hamiltonian describing an atom W is formed as the sum of the perturbative hamiltonians for each of the N_w particles of type ω comprising W:

$$h' = \sum_w \sum_{N=1}^{N_w} \delta h_{w,N} \quad . \tag{8}$$

Here, w is p for the proton, n for the neutron, and e for the electron. The perturbative hamiltonian δh_{wN} for the Nth particle of type w has the form given in Eq. (7), except that the dependence of the parameters for Lorentz violation is shown by a superscript w.

The perturbative Lorentz-violating energy shift of the state $|F, m_F\rangle$ of W is derived as the expectation value $\langle \Phi, m_F|h'|F, m_F\rangle$ of the perturbative hamiltonian (8) in the appropriate unperturbed quantum state. After some calculation, one finds [24]

$$\langle F, m_F|h'|F, m_F\rangle = \widehat{m}_F E_d^W + \widetilde{m}_F E_q^W \quad . \tag{9}$$

Here, $\widehat{m}_F$ and $\widetilde{m}_F$ are ratios of Clebsch-Gordan coefficients [24]. The dipole and quadrupole energy shifts E_d^W and E^W_q are explicitly given in Ref. [24], and they involve components of the parameters for Lorentz violation defined in the laboratory frame.

Since the laboratory frame rotates with the Earth, the laboratory-frame components change cyclically with the Earth's sidereal rotation frequency W It is therefore more convenient to work in a nonrotating frame. Denote the nonrotating-frame basis by $(\hat{X},\hat{Y},\hat{Z})$ as in the previous section, and let the laboratory-frame basis be $(\hat{x},\hat{y},\hat{z})$. The z axis here is taken as the quantization axis of W for the given experiment, and the angle $\chi \in (0,\pi)$ given by $\cos\chi = \hat{z} \cdot \hat{Z}$ is assumed nonzero.

To express the results in a relatively compact form, it is convenient to introduce nonrotating-frame combinations of Lorentz-violating parameters, denoted $\tilde{b}_j$, $\tilde{c}_Q$ $\tilde{c}_{Q,J}$, $\tilde{c}_-$, $\tilde{c}_{XY}$, $\tilde{d}_J$, $\tilde{g}_{D,J}$, $\tilde{g}_Q$ $\tilde{g}_{Q,J}$, $\tilde{g}_-$, $\tilde{g}_{XY}$. Their definitions in terms of quantities in the nonrelativistic hamiltonian h can be found in Ref. [24]. As one example,

$$\tilde{b}_J^w := b_J^w - m d_{J0}^w + \tfrac{1}{2} m \epsilon_{JKL} g_{KL0}^w - \tfrac{1}{2} \epsilon_{JKL} H_{KL}^w \tag{10}$$

which involves a combination of CPT-odd and CPT-even couplings in the

standard-model extension. Here, spatial indices in the nonrotating frame are denoted by $J = X, Y, Z$, the time index is denoted 0, and ϵ_{JKL} is the nonrotating-frame antisymmetric tensor.

Substituting the above into the expression for the energy-level shift Rives

$$\langle F, m_F|h'|F, m_F\rangle = E_0+E_{1X}\cos\Omega t+E_{1Y}\sin\Omega t+E_{2X}\cos 2\Omega t+E_{2Y}\sin 2\Omega t \quad . \tag{11}$$

The energy E_0 is constant in time and is therefore irrelevant for clock-comparison experiments. The four other energies are given explicitly in terms of the Lorentz-violating parameters and other quantities in Ref. [24]. In clock-comparison experiments, the result is typically a bound on the amplitude of the time variation of a transition frequency, determined here as the difference between two energy-level shifts of the form $\langle F, m_F|h^1|\ F\, m_F\rangle$.

In the remainder of this section, I consider the clock-comparison experiments performed by Prestage *et al.*, Lamoreaux *et al.*, Chupp *et al.*, and Berglund *et al*, [23]. Each of the bounds from each of these experiments fits one of the following forms:

$$\begin{aligned}
&\Big|\sum_w [u_0^A(\beta_w^A\tilde{b}_X^w + \delta_w^A\tilde{d}_X^w + \kappa_w^A\tilde{g}_{D,X}^w) + u_1^A(\gamma_w^A\tilde{c}_{Q,X}^w + \lambda_w^A\tilde{g}_{Q,X}^w)] \\
&-v\sum_w [u_0^B(\beta_w^B\tilde{b}_X^w + \delta_w^B\tilde{d}_X^w + \kappa_w^B\tilde{g}_{D,X}^w) + u_1^B(\gamma_w^B\tilde{c}_{Q,X}^w + \lambda_w^B\tilde{g}_{Q,X}^w)]\Big| \lesssim 2\pi\varepsilon_{1,X}, \\
&\Big|\sum_w [u_0^A(\beta_w^A\tilde{b}_Y^w + \delta_w^A\tilde{d}_Y^w + \kappa_w^A\tilde{g}_{D,Y}^w) + u_1^A(\gamma_w^A\tilde{c}_{Q,Y}^w + \lambda_w^A\tilde{g}_{Q,Y}^w)] \\
&-v\sum_w [u_0^B(\beta_w^B\tilde{b}_Y^w + \delta_w^B\tilde{d}_Y^w + \kappa_w^B\tilde{g}_{D,Y}^w) + u_1^B(\gamma_w^B\tilde{c}_{Q,Y}^w + \lambda_w^B\tilde{g}_{Q,Y}^w)]\Big| \lesssim 2\pi\varepsilon_{1,Y}, \\
&\Big|\sum_w u_2^A(\gamma_w^A\tilde{c}_-^w + \lambda_w^A\tilde{g}_-^w) - v\sum_w u_2^B(\gamma_w^B\tilde{c}_-^w + \lambda_w^B\tilde{g}_-^w)\Big| \lesssim 2\pi\varepsilon_{2,-}, \\
&\Big|\sum_w u_2^A(\gamma_w^A\tilde{c}_{XY}^w + \lambda_w^A\tilde{g}_{XY}^w) - v\sum_w u_2^B(\gamma_w^B\tilde{c}_{XY}^w + \lambda_w^B\tilde{g}_{XY}^w)\Big| \lesssim 2\pi\varepsilon_{2,XY}.
\end{aligned} \tag{12}$$

In these expressions, the coefficients u_0, u_1, u_2, and v contain the dependences on quantities such as m_F, m_F, $\mathcal{X}$, and gyromagnetic ratios. The quantities β δ, k, γ, λ with superscripts and subscripts are special matrix elements described in Ref. [24]. The parameter $v = g_A/g_B$ is the ratio of gyromagnetic ratios for the atomic species A and B involved in the particular experiment. The associated bounds on the amplitudes of frequency shifts are denoted $\varepsilon_{1,X}$, $\varepsilon_{1,Y}$, $\varepsilon_{2,-}$, $\varepsilon_{2,XY}$, corresponding to sidereal or semi-sidereal variations as $\cos\Omega t$, $\sin\Omega t$, $\cos 2\Omega t$, $\sin 2\Omega t$, respectively. All the quantities in the above experiment are tabulated in Ref. [24] for each of the experiments in question.

It turns out that the experimental results all constrain distinct linear combinations of parameters for Lorentz violation. A useful tool for studying specific sensitivities is the nuclear Schmidt model [38]. In this context, the Prestage *et al.*, Lamoreaux *et al.*, and Chupp *et al.* experiments are sensi-

tive to neutron parameters for Lorentz violation, while the Berglund *et al.* experiment is sensitive to electron, proton, and neutron parameters. In fact, only a subset of the allowed parameter space is constrained [24] by all these experiments. However, the bounds obtained are impressive and represent sensitivity to Planck-scale physics.

The relatively complicated form of the results (12) can be simplified under certain assumptions. If one supposes both no appreciable cancellation of effects between the species A and B and no cancellations among different terms in the sums appearing in Eq. (12), then the numerical value of each bound can be applied to each term in the sum, producing individual constraints on the parameters for Lorentz violation appearing in Eq. (12). To obtain specific values, one can work within the context of the Schmidt model and make some crude dimensional estimates of the unknown matrix elements. The results of this procedure are tabulated in Ref. [24]. For example, one finds that the Lorentz- and CPT-violating parameters bwj are most tightly constrained by the experiment of Berglund *et al.*, which gives $|\tilde{b}_J^n| \lesssim 10^{-30}$ GeV, $|\tilde{b}_J^e| \lesssim 10^{-27}$ GeV, $|\tilde{b}_J^p| \lesssim 10^{-27}$ GeV. The experiments in Ref. [23] also bound other parameters, as described in Ref. [24].

Experiments producing both calculable and clean bounds would evidently be of particular theoretical interest. One possibility for improving both calculability and cleanliness is to use species W for which the Lorentz-violating energy shifts depend predominantly on a single valence particle w. For example, in the case where w is an electron, substances of nuclear spin zero could be used. For the case where w is a nucleon, a list of nuclei theoretically expected to yield relatively calculable and clean bounds is provided in Ref. [24].

NEW RESULTS REPORTED AT THIS CONFERENCE

In other presentations to this conference [7, 8], new experimental results are reported that provide relatively calculable and clean bounds on certain Lorentz-violating parameters in the standard-model extension. In this final section, I provide a brief summary placing these results in the context of the preceding discussion.

Neutron parameters. An interesting limit on neutron parameters for Lorentz violation is attainable using a dual nuclear Zeeman ^{3}He-^{129}Xe maser [39] because the $I = \frac{1}{2}$ nucleus ^{129}Xe is sensitive to dipole energy shifts from neutron parameters. Within the Schmidt model, the description of the ^{3}He and ^{129}Xe systems are related, which leads to a relatively clean bound [24]. At this conference, Walsworth discusses [8] an experiment producing a bound of 80 nHz on sidereal variations of the free-running ^{3}He frequency using ^{129}Xe as a reference. In the context of the Schmidt model and the

assumptions described in the previous section, this can be interpreted as a bound on equatorial components of $|\tilde{b}_J|$ of approximately 10^{-31} GeV [8].

Electron parameters. High-sensitivity tests of Lorentz symmetry in the electron sector can be performed by searching for Lorentz-violating spin couplings with macroscopic materials having a net spin polarization generated by the effects of many electrons [25]. The most sensitive apparatus of this type at present is the spin-polarized torsion pendulum used with the Eöt-Wash II instrument at the University of Washington [40,41,7], which involves stacked layers of toroidal magnets producing a large net electron spin but negligible magnetic moment. At this conference, Heckel describes [7] an analysis of data taken with this apparatus that places a strong constraint on the components $|\tilde{b}^e_J|$ at the level of about 10^{-29} GeV for the equatorial components and about 10^{-28} GeV for the component along Z

Proton parameters. Since hydrogen is theoretically well understood, it is a good candidate for a substance producing a calculable bound in a clock-comparison experiment. In fact, the reference transition in the Prestage *et al.* experiment was a hydrogen maser. In the context of the standard-model extension, analyses of experiments with hydrogen and antihydrogen have been performed [16, 20, 21]. The standard H-maser line involves atomic states with $m_F = 0$ and is insensitive to Lorentz violation, but the other ground-state hyperfine lines involve states with $m_F = \pm 1$ and therefore are sensitive to Lorentz violation. The sidereal variations of these lines are determined at leading order by the combinations $\tilde{b}^e_J \pm \tilde{b}^p_J$ At this conference, Walsworth describes [8] an experiment with hydrogen masers that places a bound of 0.7 mHz on the magnitude of sidereal variations in these frequencies. Combined with the above constraints on $\tilde{b}^e_J$ in the electron sector announced by Heckel [7], this can be interpreted as a bound on the equatorial components of $|\tilde{b}^p_J|$ of approximately 4×10^{-27} GeV [8].

ACKNOWLEDGMENTS

This work is supported in part by the United States Department of Energy under grant number DE-FG02-91ER40661.

REFERENCES

1. See, for example, *Review of Particle Properties,* Eur. Phys. J. C 3 (1998) 1.
2. See, for example, V.A. Kostelecký ed., CPT *and Lorentz Symmetry,* World Scientific, Singapore, 1999.

3. V.A. Kostelecký and S. Samuel, Phys. Rev. D **39** (1989) 683; *ibid.* **40** (1989) 1886; Phys. Rev. Lett. **63** (1989) 224; *ibid.* **66** (1991) 1811; V.A. Kostelecký and R. Potting, Nucl. Phys. B **359** (1991) 545; Phys. Lett. B 381 (1996) 89; V.A. Kostelecký M. Perry, and R. Potting, Indiana University preprint IUHET 413 (1999), hep-th/991243.
4. V.A. Kostelecký in B.N. Kursunoglu, S.L. Mintz, A. Perlmutter, eds., *High-Energy Physics and Cosmology,* Plenum, New York, 1997 (hep-ph/9704264).
5. V.A. Kostelecký in B.N. Kursunoglu, S.L. Mintz, A. Perlmutter, eds., *Physics ofMass,* Plenum, New York, 1999 (hep-ph/9810239).
6. D. Colladay and V.A. Kostelecký Phys. Rev. D 55 (1997) 6760; *ibid.* 58, 116002 (1998).
7. B. Heckel *et al.,* these proceedings.
8. R. Walsworth *et al.,* these proceedings.
9. E773 collaboration, B. Schwingenheuer *et al.,* Phys. Rev. Lett. **74** (1995) 4376. See also E731 collaboration, L.K. Gibbons et al., Phys. Rev. D 55 (1997) 6625; R. Carosi et al., Phys. Lett. B **237** (1990) 303.
10. V.A. Kostelecký and R. Potting, Phys. Rev. D **51** (1995) 3923.
11. V.A. Kostelecký and R. Potting, in D.B. Cline, ed., *Gamma Ray–Neutrino Cosmology and Planck Scale Physics* (World Scientific, Singapore, 1993) (hep-th/9211116); D. Colladay and V.A. Kostelecký Phys. Lett. B **344** (1995) 259; Phys. Rev. D **52** (1995) 6224; V.A. Kostelecký and R. Van Kooten, Phys. Rev. D **54** (1996) 5585.
12. OPAL Collaboration, R. Ackerstaff *et al.,* Z. Phys. C **76** (1997) 401; DELPHI Collaboration, M. Feindt *et al.,* preprint DELPHI 97-98 CONF 80 (July 1997).
13. V.A. Kostelecký Phys. Rev. Lett. **80** (1998) 1818; Phys. Rev. D **61** (2000)16002.
14. KTeV Collaboration, presented by Y.B. Hsiung at the KAON 99 conference, Chicago, June 1999.
15. P.B. Schwinberg, R.S. Van Dyck, Jr., and H.G. Dehmelt, Phys. Lett. A 81 (1981) 119; Phys. Rev. D **34** (1986) 722; L.S. Brown and G. Gabrielse, Rev. Mod. Phys. **58** (1986) 233; R.S. Van Dyck, Jr., P.B. Schwinberg, and H.G. Dehmelt, Phys. Rev. Lett. 59 (1987) 26; G. Gabrielse *et al., ibid.,* **74** (1995) 3544.
16. R. Bluhm, V.A. Kostelecký and N. Russell, Phys. Rev. Lett. **79** (1997) 1432; Phys. Rev. D **57** (1998) 3932.
17. G. Gabrielse *et al.,* in Ref. [2]; Phys. Rev, Lett. **82** (1999) 3198.

18. H. Dehmelt *et al.*, Phys. Rev. Lett. **83** (1999) 4694.
19. R. Mittleman, I. Ioannou, and H. Dehmelt, in Ref. [2]; R. Mittleman *et al.*, Phys. Rev. Lett. **83** (1999) 2116.
20. R. Bluhm, V.A. Kostelecký and N. Russell, Phys. Rev. Lett. **82** (1999) 2254.
21. R. Bluhm *et al.*, these proceedings.
22. V.A. Kostelecký and C.D. Lane, Phys. Rev. D **60** (1999) 116010.
23. V.W. Hughes, H.G. Robinson, and V. Beltran-Lopez, Phys. Rev. Lett. 4 (1960) 342; R.W.P. Drever, Philos. Mag. **6** (1961) 683; J.D. Prestage *et al.*, Phys. Rev. Lett. **54** (1985) 2387; S.K. Lamoreaux *et al.*, Phys. Rev. Lett. 57 (1986) 3125; Phys. Rev. A 39 (1989) 1082; T.E. Chupp *et al.*, Phys. Rev. Lett. **63** (1989) 1541; C.J. Berglund *et al.*, Phys. Rev. Lett. **75** (1995) 1879.
24. V.A. Kostelecký and C.D. Lane, Phys. Rev. D **60** (1999) 116010.
25. R. Bluhm and V.A. Kostelecký Phys. Rev. Lett. **84** (2000) 1381.
26. S.M. Carroll, G.B. Field, and R. Jackiw, Phys. Rev. D **41** (1990) 1231.
27. R. Jackiw and V.A. Kostelecký Phys. Rev. Lett. **82** (1999) 3572.
28. M. Pérez-Victoria, Phys. Rev. Lett. **83** (1999) 2518; J.M. Chung, Phys. Lett. B **461** (1999) 138.
29. 0. Bertolami *et al.*, Phys. Lett. B **395** (1997) 178.
30. S. Coleman and S. Glashow, Phys. Rev. D **59** (1999) 116008.
31. **O.** Bertolami and C.S. Carvalho, gr-qc/9912117.
32. CPLEAR collaboration, presented by P. Bloch, at the KAON 99 conference, Chicago, June 1999.
33. P. Franzini, in G. Diambrini-Palazzi, C. Cosmelli, L. Zanello, eds., *Phenomenology of Unification from Present to Future,* World Scientific, Singapore, 1998; P. Franzini and J. Lee-Franxini, Nucl. Phys. Proc. Suppl. **71** (1999) 478.
34. See, for example, T.D. Lee and C.S. Wu, Annu. Rev. Nucl. Sci. **16** (1966) 511.
35. See, for example, R.G. Sachs, *The Physics of Time Reversal,* University of Chicago Press, Chicago, 1987.
36. J. Adams *et al.*, Phys. Rev. Lett. **79** (1997) 4093.
37. V.A. Kostelecký and C.D. Lane, J. Math. Phys. **40** (1999) 6245.
38. T. Schmidt, Z. Physik **106** (1937) 358.
39. R.E. Stoner *et al.*, Phys. Rev. Lett. **77** (1996) 3971.

40. E.G. Adelberger *et al.,* in P. Herczeg *et al.,* eds., *Physics Beyond the Standard Model,* p. 717, World Scientific, Singapore, 1999.
41. M.G. Harris, Ph.D. thesis, Univ. of Washington, 1998.

This page intentionally left blank.

SEARCHING FOR LORENTZ VIOLATION IN THE GROUND STATE OF HYDROGEN [1]

Robert Bluhm[a], V. Alan Kostelecký[b] and Neil Russell[c]

[a]Physics Department
ColbyCollege
Waterville, ME 04901 USA

[b]Physics Department
Indiana University
Bloomington, IN 47405 USA

[c]Physics Department
Northern Michigan University
Marquette, MI 49855 USA

INTRODUCTION

The hydrogen atom has a rich history as a testing ground of fundamental physics where small differences between theory and experiment have led to major advances [1]. With the advent of optical high-resolution spectroscopy and tunable dye lasers, new tests of quantum electrodynamics in hydrogen have become possible. The two-photon 1S-2S transition is especially suitable for high-precision tests and metrology because of its small natural linewidth of only 1.3 Hz. This transition has been measured in a cold atomic beam of hydrogen [2] with a precision of 3.4 parts in 10^{14}. It has also been observed in trapped hydrogen [3] with a precision of about one part in 10^{12} As experimental techniques advance, the measurement of the line center to one part in 10^{3} becomes plausible with an ultimate resolution of one part in 10^{18}, making new tests of fundamental theory possible.

The recent production of antihydrogen in experiments [4] ushers in a new era for testing fundamental physics by allowing direct high-precision comparisons of hydrogen and antihydrogen [5]. Since the CPT theorem predicts that all local relativistic quantum field theories of point particles are invariant under the combined

[1]Presented by R.B. at Orbis Scientiae 1999, Ft. Lauderdale, Florida, December 1999

Quantum Gravity, Generalized Theory of Gravitation, and Superstring Theory Based Unification
Edited by Kursunoglu *et al.*. Kluwer Academic / Plenum Publishers. New York. 2000

operations of charge conjugation C, parity reversal P, and time reversal T [6, 7], comparisons of the 1S-2S transition in hydrogen and antihydrogen should provide a new high-precision test of CPT. Indeed, two future experiments at CERN [8] are aimed at making high-resolution spectroscopic comparisons of the 1S-2S transitions in spin-polarized hydrogen and antihydrogen confined within a magnetic trap. The comparisons of the 1S-2S transition should have relative figures of merit comparable to that of the neutral meson system, which places a bound on the mass difference between the K_0 and $\bar{K}_0$ at less than 2 parts in 10^{18} [9].

In this proceedings, we first review a recent theoretical analysis we made of CPT and Lorentz tests in hydrogen and antihydrogen, which was published in Ref. [10]. This included investigations of on-going experiments in hydrogen as well as the proposed experiments at CERN comparing hydrogen and antihydrogen. We showed that these experiments can provide tests of both CPT-preserving and CPT-violating Lorentz symmetry. In addition to examining comparisons of 1S-2S transitions, we suggested other possible experimental signatures that are sensitive to CPT or Lorentz breaking, including measurements of the Zeeman hyperfine levels in the ground state of hydrogen. Some of these measurements are currently being made and preliminary results are presented for the first time in Walsworth's talk [11].

THEORETICAL FRAMEWORK

Our analysis uses a theoretical framework that describes CPT- and Lorentz-violating effects in an extension of the SU(3)×SU(2)×U(1) standard model and quantum electrodynamics (QED) [12]. The framework originates from the idea of spontaneous CPT and Lorentz breaking in a more fundamental theory such as string theory [13, 14]. Within this framework, possible violations of CPT and Lorentz symmetry are included which maintain desirable features of quantum field theory, including gauge invariance, power-counting renormalizability, and microcausality. The model is highly constrained, and only a small number of terms are possible. These terms are controlled by parameters that can be bounded by experiments. This framework has been used to analyze neutral-meson experiments [13,15,16, 17], baryogenesis [18], photon properties [12, 19], Penning-trap experiments [20, 21, 22], atomic clock comparisons [23], muon experiments [24], and experiments in spin-polarized matter [25].

To investigate experiments in hydrogen and antihydrogen, it suffices to work in the context of the QED extension. The modified Dirac equation for a four-component spinor field ψ describing electrons and positrons of mass me and charge $q = -|e|$ in a Coulomb potential A^μ is

$$\left(i\gamma^\mu D_\mu - m_e - a^e_\mu\gamma^\mu - b^e_\mu\gamma_5\gamma^\mu - \tfrac{1}{2}H^e_{\mu\nu}\sigma^{\mu\nu} + ic^e_{\mu\nu}\gamma^\mu D^\nu + id^e_{\mu\nu}\gamma_5\gamma^\mu D^\nu\right)\psi = 0 \quad . \tag{1}$$

Here, natural units with $h = c = 1$ are used, $iD\mu$ ..$i\partial_\mu - qA\mu$, and $A^\mu = (|e|/4\pi r, 0)$. The two terms involving the effective coupling constants a^e_μ and b^e_μ violate CPT, while the three terms involving $H^e_{\mu\nu}$, $c^e_{\mu\nu}$, and $d^e_{\mu\nu}$ preserve CPT. All five of these terms break Lorentz invariance. Since no CPT or Lorentz violation has been observed, these parameters are assumed to be small. Free protons are also described

by a modified Dirac equation involving the corresponding parameters a^p_μ, b^p_μ, $H^p_{\mu\nu}$, $c^p_{\mu\nu}$ and $d^p_{\mu\nu}$

A perturbative treatment in the context of relativistic quantum mechanics is used to examine the bound states of hydrogen and antihydrogen. In this approach, the unperturbed hamiltonian $\hat{H}_0$ and its energy eigenfunctions are the same for hydrogen and antihydrogen. All of the perturbations in free hydrogen described by conventional quantum electrodynamics are identical for both systems. However, the interaction hamiltonians for hydrogen and antihydrogen including the effects of possible CPT- and Lorentz-breaking are not the same. These are obtained in several steps [21], involving charge conjugation to obtain the Dirac equation for antihydrogen, a field redefinition to eliminate additional time derivatives in the Dirac equation, and the use of standard relativistic two-fermion techniques [26].

EXPERIMENTS WITH FREE HYDROGEN

We first consider free hydrogen and antihydrogen in the absence of external trapping potentials. Using a description in terms of the basis states $|m_J, m_I\rangle$, with $J = 1/2$ and $I = 1/2$ describing the uncoupled atomic and nuclear angular momenta, the leading-order energy corrections can be computed. The energy shifts at the 1S and 2S levels are found to be the same. For hydrogen they are given by

$$\Delta E^H(m_J = \pm\tfrac{1}{2}, m_I = \pm\tfrac{1}{2}) = (a_0^e + a_0^p - c_{00}^e m_e - c_{00}^p m_p) + \frac{m_J}{|m_J|}(-b_3^e + d_{30}^e m_e + H_{12}^e) + \frac{m_I}{|m_I|}(-b_3^p + d_{30}^p m_p + H_{12}^p) \quad (2)$$

where m_e and m_p are the electron and proton masses, respectively. The corresponding energy corrections for the 1S and 2S states of antihydrogen $\Delta E^{\bar{H}}$ are obtained from these by letting $a_\mu \rightarrow -a_\mu$, $d_{\mu\nu} \rightarrow -d_{\mu\nu}$, and $H_{\mu\nu} \rightarrow -H_{\mu\nu}$ for both the electron-positron and proton-antiproton coefficients.

The hyperfine interaction couples the electron and proton or positron and antiproton spins. The appropriate basis states are then $|F, m_F\rangle$ which are linear combinations of the states $|m_J, m_I\rangle$. The selection rules for the two-photon 1S-2S transition are $\Delta F = 0$ and $\Delta m_F = 0$. These selection rules require that the 1S-2S transitions in free hydrogen and antihydrogen occur between states of the same spin configurations. As a result, the leading-order energy shifts are equal, and there are no observable leading-order shifts in frequency in either hydrogen or antihydrogen.

There are, however, subleading-order shifts in the 1S-2S frequencies. These are due to small relativistic corrections of order a2 times the CPT- or Lorentz-breaking parameters which are different at the 1S and 2S levels. For example, the term proportional to be3 results in a frequency shift in the mF = 1 $\rightarrow m_F = 1$ transition relative to that of the $m_F = 0 \rightarrow m_F = 0$ line (which remains unshifted) equal to $\delta\nu^H_{1S-2S} \approx -\alpha^2 b^e_3/8\pi$. However, electron bounds obtained in g – 2 experiments [22] suggest that b^e_3 is sufficiently small so that $\delta\nu^H_{1S-2S}$ would be below the expected 1S-2S line resolution.

EXPERIMENTS WITH TRAPPED HYDROGEN

The experiments to be performed at CERN will use trapped hydrogen and antihydrogen in a magnetic field B. We use the conventional labels $|a\rangle_n$, $|b\rangle_n$, $|c\rangle_n$ and $|d\rangle_n$ in order of increasing energy to denote the four S-state hyperfine levels of hydrogen with principal quantum number n. The $|b\rangle_n$ and $|d\rangle_n$ states have proton and electron spins that are aligned, while the remaining two states have mixed spin configurations given by

$$|c\rangle_n = \sin\theta_n|-\tfrac{1}{2},\tfrac{1}{2}\rangle + \cos\theta_n|\tfrac{1}{2},-\tfrac{1}{2}\rangle \quad , \tag{3}$$

$$|a\rangle_n = \cos\theta_n|-\tfrac{1}{2},\tfrac{1}{2}\rangle - \sin\theta_n|\tfrac{1}{2},-\tfrac{1}{2}\rangle \quad . \tag{4}$$

The mixing angles depend on n and obey $\tan 2\theta_n \cup (51\ \mathrm{mT})/n^3 B$.

The states $|c\rangle$ n and $|d\rangle_n$ are low-field seeking states that remain confined in the trap. However, collisional effects lead to a loss of population over time of the $|c\rangle_n$ states. One possible measurement would therefore be to compare the frequencies ν_d^H and ν_d^H for transitions between $|d\rangle_n$ states at the 1S and 2s levels. These measurements are particularly attractive because the 1S-2S $|d\rangle_1 \rightarrow |d\rangle_2$ transitions are field-independent for small values of B. However, since the spin configurations of the 1S $|d\rangle_1$ and 2S $|d\rangle_2$ states are the same, we find no observable frequency shifts to leading order in this case, i.e., $\delta\nu_d^H = \delta\nu_d^H \simeq 0$.

An alternative experiment would look at transitions involving the mixed states $|c\rangle_n$ and $|a\rangle_n$. Here, the n dependence in the hyperfine splitting leads to a difference in the amount of spin mixing at the 1S and 2S levels. This gives rise to a nonzero frequency shift in 1S-2S transitions between $|c\rangle_n$ hyperfine states:

$$\delta\nu_c^H \simeq -(\cos 2\theta_2 - \cos 2\theta_1)(b_3^e - b_3^p - d_{30}^e m_e + d_{30}^p m_p - H_{12}^e + H_{12}^p) \quad , \tag{5}$$

The corresponding transition for antihydrogen can be computed as well. The hyperfine states in antihydrogen in the same magnetic fields have opposite spin assignments for the positron and antiproton compared to those of the electron and proton in hydrogen. The resulting shift $\delta\nu_c^H$ for antihydrogen is the same as for hydrogen except that the signs of b^e_3 and b^p_3 are changed.

Two possible experimental signatures for CPT and Lorentz breaking follow from these results. The first involves looking for sidereal time variations in the frequencies ν_c^H and ν_c^H The second involves measuring the instantaneous 1S-2S frequency difference in hydrogen and antihydrogen in the same magnetic trapping fields. In either case, the strength of the signal would depend on the difference in the amount of spin mixing at the 1S and 2S levels. The optimal experiment would be one that maximizes the 1S-2S spin-mixing difference, which is controlled by the magnetic field B. Since the 1S-2S $|c\rangle_1 \rightarrow |c\rangle_2$ transition in hydrogen and antihydrogen is field dependent, these experiments would need to overcome line broadening effects due to field inhomogeneities in the trap.

EXPERIMENTS ON THE GROUND-STATE HYPERFINE LEVELS

The best tests of CPT and Lorentz symmetry in atomic systems are those that have the sharpest frequency resolutions. It is therefore natural to consider other transitions in hydrogen and antihydrogen besides the 1S-2S transition that can be measured with high precision. One candidate set involves measurements of the ground-state hyperfine levels in hydrogen and antihydrogen. For example, hydrogen maser transitions between $F = 0$ and $F' = 1$ hyperfine states can be measured with accuracies of less than 1 mHz. High-resolution radio-frequency measurements can also be made on transitions between Zeeman hyperfine levels in a magnetic field.

To examine these types of experiments, we compute the energy shifts of the four hydrogen ground-state hyperfine levels in a magnetic field. The spin-dependent contributions to the energy are

$$\Delta E_a^H \simeq \hat{\kappa}(b_3^e - b_3^p - d_{30}^e m_e + d_{30}^p m_p - H_{12}^e + H_{12}^p) \quad , \tag{6}$$

$$\Delta E_b^H \simeq b_3^e + b_3^p - d_{30}^e m_e - d_{30}^p m_p - H_{12}^e - H_{12}^p \quad , \tag{7}$$

$$\Delta E_c^H \simeq -\Delta E_a^H \quad , \tag{8}$$

$$\Delta E_d^H \simeq -\Delta E_b^H \quad , \tag{9}$$

where k ..cos2θ1.

In a very weak or zero magnetic field k ≃ 0 and the energies of the states ⏐a□ and |c⟩1 are unshifted while the states ⏐b⟩1 and |ıdñ1 acquire equal and opposite shifts. The degeneracy of the three $F = 1$ levels is therefore lifted. A conventional hydrogen maser operates on the field-independent transition |c⟩1 → ⏐a⟩1 in the presence of a small (B ≲ 10–6 T) magnetic field. Since $k \lesssim 10^{-4}$ in this case, the leading-order effects due to CPT and Lorentz violation are suppressed. However, the frequencies of the Zeeman hyperfine transitions between $F = 1$ levels are affected by CPT and Lorentz violation and have unsuppresed corrections. For example, the correction to the |c⟩1 → |ıd⟩1 transition frequency in a very weak field is given by

$$\delta\nu_{c\to d}^{\text{H maser}} \simeq (-b_3^e - b_3^p + d_{30}^e m_e + d_{30}^p m_p + H_{12}^e + H_{12}^p)/2\pi \quad . \tag{10}$$

A signature of CPT and Lorentz violation would thus be sidereal time variations in the frequency $\nu_{c\to d}^{\text{H master}}$.

The transition |c⟩1 → ⏐d⟩1 in a hydrogen maser is field-dependent, and one would expect field broadening to limit the resolution of frequency measurements. However, as described by Walsworth [11], it is possible to perform a double-resonance experiment [27] in which variations of the |ıc⟩1 → |ıd⟩1 transition are determined by monitoring their effect on the usual |a⟩1 → |c⟩1 maser line. This then permits a search for sidereal variations in the frequency $\nu_{c\to d}^{\text{Hmaster}}$. Walsworth's group at the Harvard-Smithsonian Center has begun this experiment, and their preliminary results indicate that the sidereal variations in $\nu_{c\to d}^{\text{Hmaster}}$ can be bounded at a level of approximately 0.7 mHz. This corresponds to a bound on the combination of parameters in $\delta\nu_{c\to d}^{\text{H master}}$ in Eq. (10) at a level of 10^{-27} GeV. Defining a figure of

merit as the ratio of the amplitude of the sidereal variations of the energy relative to the energy itself, i.e., r^{H}_{hf} ...$(\Delta Ehf)_{sidereal}/Ehf$ one obtains from the results of Walsworth's experiment the value

$$r^{H}_{hf} \lesssim 10^{-27} \quad . \tag{11}$$

This now gives one of the sharpest bounds on CPT and Lorentz violation for protons and electrons.

In principle, measurements of this kind can also be made on the Zeeman hyperfine levels in antihydrogen. Since only in a direct comparison of matter and antimatter can the CPT-violating effects be isolated, it is hoped that the technical obstacles of performing radio-frequency spectroscopy in trapped antihydrogen can be overcome. As an alternative to measurements in a very weak magnetic field, which might be hard to maintain in a trapping environment, one could perform a comparison of $|c\rangle 1 \rightarrow |d\rangle 1$ transitions in hydrogen and antihydrogen at the field-independent transition point $B \simeq 0.65$ T. At this field strength, the electron and proton spins in the $|c\rangle 1$ state are highly polarized with $mJ = \frac{1}{2}$ and $mI = -\frac{1}{2}$. The transition $|c\rangle 1 \rightarrow |d\rangle 1$ is effectively a proton spin-flip transition. The instantaneous difference in this transition for hydrogen and antihydrogen is found to be $\Delta\nu_{c\rightarrow d} \simeq -2b^{p}_{3}/\pi$. A measurement of this difference would provide a direct, clean, and accurate test of CPT for the proton.

CONCLUSIONS

In summary, we find that by using a general framework we are able to analyze proposed tests of CPT in hydrogen and antihydrogen. We find that in addition to testing CPT, these experiments will also test Lorentz symmetry. Our analysis shows that in comparisons of 1S-2S transitions in hydrogen and antihydrogen, control of the spin mixing at the 1S and 2S levels is an essential feature in designing an effective test of CPT and Lorentz symmetry. We also find that high-resolution radio frequency experiments in hydrogen or antihydrogen offer the possibility of new and precise tests of CPT and Lorentz symmetry. One very recent experiment using a double-resonance technique in a hydrogen maser has obtained a new CPT and Lorentz bound at the level of 10^{-27} for electrons and protons.

ACKNOWLEDGMENTS

This work was supported in part by the National Science Foundation under grant number PHY-9801869.

REFERENCES

1. See, for example, G.F. Bassani, M. Inguscio, and T.W. Hänsch, eds., *The Hydrogen Atom* (Springer-Verlag, Berlin, 1989).
2. T. Udem et al., Phys. Rev. Lett. **79** (1997) 2646.
3. C.L. Cesar et al., Phys. Rev. Lett. **77** (1996) 255.

4. G. Baur et al., Phys. Lett. B **368** (1996) 251; G. Blanford et al., Phys. Rev. Lett. **80** (1998) 3037.
5. M. Charlton, J. Eades, D. Horvath, and C. Zimmermann, Phys. Reps. **241** (1994) 65; J. Eades, ed., *Antihydrogen* (J.C. Baltzer, Geneva, 1993).
6. See, for example, R. G. Sachs, *The Physics of Time Reversal,* University of Chicago,Chicago,1987.
7. V.A. Kostelecký, ed., CPT *and Lorentz Symmetry* (World Scientific, Singapore,1999).
8. B. Brown et al., Nucl. Phys. B (Proc. Suppl.) **56A** (1997) 326; M.H. Holzscheiter et al., Nucl. Phys. B (Proc. Suppl.) **56A** (1997) 336.
9. See, for example, R.M. Barnett et al., Review of Particle Properties, Phys. Rev. D **54** (1996) 1.
10. R. Bluhm, V.A. Kostelecký and N. Russell, Phys. Rev. Lett. **82** (1999) 2254.
11. R. Walsworth et al, in preparation; see also this volume.
12. D. Colladay and V.A. Kostelecký, Phys. Rev. D **55** (1997) 6760; Phys. Rev. D **58,** 116002 (1998).
13. V.A. Kostelecký and R. Potting, Nucl. Phys. B **359** (1991) 545; Phys. Lett. B 381 (1996) 389.
14. V.A. Kostelecký and S. Samuel, Phys. Rev. Lett. **63** (1989) 224; ibid. **66** (1991) 1811; Phys. Rev. D **39** (1989) 683; ibid. **40** (1989) 1886.
15. V.A. Kostelecký and R. Potting, in D.B. Cline, ed., *Gumma Ray–Neutrino Cosmology and Planck Scale Physics* (World Scientific, Singapore, 1993) (hep-th/9211116); Phys. Rev. D **51** (1995) 3923; D. Colladay and V. A. Kostelecký Phys. Lett. B **344** (1995) 259; Phys. Rev. D **52** (1995) 6224; V.A. Kostelecký and R. Van Kooten, Phys. Rev. D **54** (1996) 5585.
16. B. Schwingenheuer *et al.,* Phys. Rev. Lett. **74** (1995) 4376; L.K. Gibbons et al., Phys. Rev. D **55** (1997) 6625; KTeV Collaboration, presented by Y.B. Hsiung at the KAON99 conference, Chicago, June 1999; OPAL Collaboration, R. Ackerstaff et al., Z. Phys. C **76** (1997) 401; DELPHI Collaboration, M. Feindt et al., preprint DELPHI 97-98 CONF 80 (July 1997).
17. V.A. Kostelecký, Phys. Rev. Lett. **80** (1998) 1818; Phys. Rev. D **61,** 016002 (2000).
18. 0. Bertolami et al., Phys. Lett. B **395,** 178 (1997).
19. S.M. Carroll, G.B. Field, and R. Jackiw, Phys. Rev. D **41** (1990) 1231; R. Jackiw and V.A. Kostelecký, Phys. Rev. Lett. **82** (1999) 3572; M. Pérez-Victoria, Phys. Rev. Lett. **83** (1999) 2518; J.-M. Chung, Phys. Lett. B **461** (1999)138.
20. P.B. Schwinberg, R.S. Van Dyck, Jr., and H.G. Dehmelt, Phys. Lett. A **81** (1981) 119; R.S. Van Dyck, Jr., P.B. Schwinberg, and H.G. Dehmelt, Phys. Rev. D **34** (1986) 722; L.S. Brown and G. Gabrielse, Rev. Mod. Phys. **58** (1986) 233; R.S. Van Dyck, Jr., P.B. Schwinberg, and H.G. Dehmelt, Phys. Rev. Lett. **59** (1987) 26; G. Gabrielse et al., Phys. Rev. Lett. **74** (1995) 3544;

21. R. Bluhm, V.A. Kostelecký and N. Russell, Phys. Rev. Lett. **79** (1997) 1432; Phys. Rev. D **57** (1998) 3932.
22. R.K. Mittleman, 1.1. Ioannou, H.G. Dehmelt, and N. Russell, Phys. Rev. Lett. **83** (1999) 2116; H.G. Dehmelt, R.K. Mittleman, R.S. Van Dyck, Jr., and P. Schwinberg, Phys. Rev. Lett. **83** (1999) 4694.
23. V.A. Kostelecký and C.D. Lane, Phys. Rev. D **60,** 116010 (1999).
24. R. Bluhm, V.A. Kostelecký and C.D. Lane, Phys. Rev. Lett. **84** (2000) 1098.
25. R. Bluhm and V.A. Kostelecký, Phys. Rev. Lett. **84** (2000) 1381.
26. See, for example, H.A. Bethe and E.E. Salpeter, *Quantum Mechanics of One- and Two-Electron Atoms* (Plenum, New York, 1957).
27. H.G. Andresen, Z. Phys. **210** (1968) 113.

NEUTRINO OSCILLATIONS: SOME THEORETICAL IDEAS

Stephen M. Barr

Bartol Research Institute
University of Delaware
Newark, DE 19711

INTRODUCTION

Over the years, and especially since the discovery of the large mixing of ν_μ seen in atmospheric neutrino experiments, there have been numerous models of neutrino masses proposed in the literature. In the last two years alone, as many as one hundred different models have been published. One of the goals of this talk is to give a helpful classification of these models. Such a classification is possible because in actuality there are only a few basic ideas that underlie the vast majority of published neutrino mixing schemes. After some preliminaries, I give a classification of three-neutrino models, and then in the last part of the talk I discuss in more detail one category of models — those with "lopsided" charged-lepton mass matrices. Finally, I talk about a specific very predictive model based on lopsided mass matrices that I have worked on with Albright and Babu.

THE DATA

There are four indications of neutrino mass that guide recent attemps to build models: (1) the solar neutrino problem, (2) the atmospheric neutrino anomaly, (3) the LSND experiment, and (4) dark matter. Several excellent reviews of the evidence for neutrino mass have appeared recently.'

(1) The three most promising solutions to the solar neutrino problem are based on neutrino mass. These are the small-angle MSW solution (SA), the large-angle MSW solution (LA), and the vacuum oscillation solution (VO). All these solutions involve ve oscillating into some other type of neutrino — in the models we shall consider predominantly ν_μ. In the SA solution the mixing angle and mass-squared splitting between ve and the neutrino into which it oscillates are roughly $\sin^2 2\theta \sim 5.5 \times 10^{-3}$ and $\delta m^2 \sim 5.1 \times 10^{-6}\text{eV}^2$. For the LA solution one has $\sin^2 2\theta \sim 0.79$, and $\delta m^2 \sim 3.6 \times 10^{-5}\text{eV}'$. (The numbers are best-fit values from a recent analysis.') And for the VO solution $\sin^2 2\theta \sim 0.93$, and $\delta m^2 \sim 4.4 \times 10^{-10}\text{eV}^2$. (Again, these are best-fit values from a

Quantum Gravity Generalized Theory of Gravitation and Superstring Theory-Based Unification
Edited by Kursunoglu *et al* Kluwer Academic / Plenum Publishers New York 2000

recentanalysis.[3])

(2) The atmospheric neutrino anomaly strongly implies that ν_μ is oscillating with nearly maximal angle into either ν_τ or a sterile neutrino, with the data preferring the former possibility.[4] One has $\sin^2 2\theta \sim 1.0$, and $\delta m2 \sim 3 \times 10{-}3eV^2$.

(3) The LSND result, which would indicate a mixing between νe and ν_μ with $\delta m^2 \sim 0.1 - 1eV^2$ is regarded with more skepticism for two reasons. The experimental reason is that KARMEN has failed to corroborate the discovery. The theoretical reason is that to account for the LSND result and also for both the solar and atmospheric anomalies by neutrino oscillations would require three quite different mass-squared splittings, and that can only be achieved with *four* species of neutrino. This significantly complicates the problem of model-building. In particular, it is regarded as not very natural, in general, to have a fourth sterile neutrino that is extremely light compared to the weak scale. For these reasons, the classification given in this talk will assume that the LSND results do not need to be explained by neutrino oscillations, and will include only three-neutrino models.

(4) The fourth possible indication of neutrino mass is the existence of dark matter. If a significant amount of this dark matter is in neutrino mass, it would imply a neutrino mass of order several eVs . In order then to achieve the small δm^2's needed to explain the solar and atmospheric anomalies one would have to assume that νe ν_μ and ν_τ were nearly degenerate. We shall not focus on such models in our classification, which is primarily devoted to models with "hierarchical" neutrino masses. However, in most models with nearly degenerate masses, the neutrino mass matrix consists of a dominant piece proportional to the identity matrix and a much smaller hierarchical piece. Since the piece proportional to the identity matrix would not by itself give oscillations, such models can be classified together with hierarchical mass models in most instances.

In sum, the models we shall classify are those which assume (a) three flavors of neutrino that oscillate (νe, ν_μ, and ν_τ), (b) a hierarchical pattern of neutrino masses, (c) the atmospheric anomaly explained by ν_μ-ν_τ oscillations with nearly maximal angle, and (d) the solar anomalies explained by νe oscillating primarily with ν_μ with either small angle (SA) or large angle (LA, VO).

MAJOR DIVISIONS

There are several major divisions among models. One is between models in which the neutrino masses arise through the see-saw mechanism,[5] and those in which the neutrino masses are generated directly at low energy. In see-saw models, there are both left- and right-handed neutrinos. Consequently, there are five fermion mass matrices to explain: the four Dirac mass matrices, U, D, L, and N of the up quarks, down quarks, charged leptons, and neutrinos, respectively, and the Majorana mass matrix M_R of the right-handed neutrinos. The four Dirac mass matrices are all roughly of the weak scale, while M_R is many orders of magnitude larger than the weak scale. After integrating out the superheavy right-handed neutrinos, the mass matrix of the left-handed neutrinos is given by $M_\nu = -N^T M_R^{-1} N$. Typically, in see-saw models, the four Dirac mass matrices are closely related to each other, either by grand unification or by flavor symmetries. That means that in see-saw models neutrino masses and mixings are just one aspect of the larger problem of quark and lepton masses, and are likely to shed great light on that problem, and perhaps even be the key to solving it. On the other hand, in most see-saw models M_R is either not related or is tenuously related to the Dirac mass matrices of the quarks and leptons. The freedom in M_R is the major obstacle to making precise

predictions of neutrino masses and mixings in most see-saw schemes.

In non-see-saw schemes, there are no right-handed neutrinos. Consequently, there are only four mass matrices to consider, the Dirac mass matrices of the quarks and charged leptons, *U, D,* and *L,* and the Majorana mass matrix of the light left-handed neutrinos M_ν. Typically in such schemes M_ν has nothing directly to do with the matrices *U, D,* and *L,* but is generated at low-energy by completely different physics.

The three most popular possibilities in recent models for generating M_ν at low energy in a non-see-saw way are (a) triplet Higgs, (b) variants of the Zee model,[6] and (c) R-parity violating terms in low-energy supersymmetry. (a) In triplet-Higgs models, Mv arises from a renormalizable term of the form $\lambda_{ij}\nu_i\nu_j H^0_T$ where H_T is a Higgs field in the (1,3,+1) representation of SU(3) × SU(2) × U(1). (b) In the Zee model, the Standard Model is supplemented with a scalar, *h,* in the (1,1, $1) representation and having weak-scale mass. This field can couple to the lepton doublets L_i as L_iL_jh and to the Higgs doublets ϕ_a (if there is more than one) as $\phi_a\phi_b h$. Clearly it is not possible to assign a lepton number to *h* in such a way as to conserve it in both these terms. The resulting lepton-number violation allows one-loop diagrams that generate a Majorana mass for the left-handed neutrinos. (c) In supersymmetry the presence of such R-parity-violating terms in the superpotential as $L_iL_jD^c_k$ and $Q_iD^c_jL_k$, causes lepton-number violation, and allows one-loop diagrams that give neutrino masses.

It is clear that in all of these schemes the couplings that give rise to neutrino masses have nothing to do with the physics that gives mass to the other quarks and leptons. While this allows more freedom to the neutrino masses, it would from one point of view be very disappointing, as it would mean that the observation of neutrino oscillations is almost irrelevant to the burning question of the origin of quark and charged lepton masses.

Another major division among models has to do with the kinds of symmetries that constrain the forms of mass matrices and that, in some models, relate different mass matrices to each other. There are two main approaches: (a) grand unification, and (b) flavor symmetry. Many models use both.

(a) The simplest grand unified group is *SU(5)*. In minimal SU(5) there is one relation among the Dirac mass matrices, namely $D = L^T$, coming from the fact that the left-handed charged leptons are unified with the right-handed down quarks in a $\bar{\mathbf{5}}$ while the right-handed charged leptons and left-handed down quarks are unified in a **10.** In *SU*(5) there do not have to be right-handed neutrinos, though they may be introduced. In *SO*(10), which in several ways is a very attractive group for unification, the minimal model gives the relations $N = U \propto D = L$. In realistic models these relations are modified in various ways, for example by the appearance of Clebsch coefficients in certain entries of some of the mass matrices. It is clear that unified symmetries are so powerful that very predictive models are possible. Most of the published models which give sharp predictions for masses and mixings are unified models.

(b) Flavor symmetries can be either abelian or non-abelian. Non-abelian symmetries are useful for obtaining the equality of certain elements of the mass matrix, as in models where the neutrino masses are nearly degenerate, and in the so-called "flavor democracy" schemes. Abelian symmetries are useful for explaining hierarchical mass matrices through the so-called Froggatt-Nielson mechanism.[7] The idea is that different fermion multiplets can differ in charge under a *U*(1) flavor symmetry that is spontaneously broken by some "flavon" expectation value (or values), ñfiñ. Thus, different elements of the fermion mass matrices would be suppressed by different powers of ⟨fi⟩/M ≡ ∈*i* « 1, where *M* is the scale of flavor physics. This kind of scheme can explain small mass ratios and mixings in the sense of predicting them to arise at certain orders in the small

quantities ϵ_i. A drawback of such models compared to many grand unified models, is that actual numerical predictions, as opposed to order of magnitude estimates, are not possible. On the other hand, models based on flavor symmetry involve less of a theoretical superstructure built on top of the Standard Model than do unified models, and could therefore be considered more economical in a certain sense. Unified models put more in but get more out than flavor symmetry.

THE PUZZLE OF LARGE $\nu\mu - \nu t$ MIXING

The most significant new fact about neutrino mixing is the largeness of the mixing between $\nu\mu$ and $\nu\tau$. This comes as somewhat of a surprise from the point of view of both grand unification and flavor symmetry approaches. Since grand unification relates leptons to quarks, one might expect lepton mixing angles to be small like those of the quarks. In particular, the mixing between the second and third family of quarks is given by Vcb, which is known to be 0.04. That is to be compared to the nearly maximal mixing of the second and third families of leptons: $U\mu 3 \cong 1/\sqrt{2} \cong 0.7$. It is true that even in the early 1980's some grand unified models predicted large neutrino mixing angles. (Especially noteworthy is the remarkably prophetic 1982 paper of Harvey, Ramond, and Reiss,[8] which explicitly predicted and emphasized that there should be large $\nu\mu - \nu\tau$ mixing. However, in those days the top mass was expected to be light, and Ref. 8 chose it to be 25 GeV. That gave Vcb in that model to be about 0.22. The corresponding lepton mixing was further boosted by a Clebsch of 3. With the actual value of m_t that we now know, the model of Ref. 8 would predict $U\mu 3$ to be 0.12). What makes the largeness of $U\mu 3$ a puzzle in the present situation is the fact that we now know that both Vcb and mc/mt are exceedingly small.

The same puzzle exists in the context of flavor symmetry. The fact that the quark mixing angles are small suggests that there is a family symmetry that is only weakly broken, while the large mixings of some of the neutrinos suggests that family symmetries are badly broken.

The chief point of interest in looking at any model of neutrino mixing is how it explains the large mixing of $\nu\mu$ and νt. This will be the feature that I will use to organize the classification of models.

CLASSIFICATION OF THREE-NEUTRINO MODELS

Virtually all published models fit somewhere in the simple classification now to be described. The main divisions of this classification are based on how the large $\nu\mu - \nu\tau$ mixing arises. This mixing is described by the element $U\mu 3$ of the so-called MNS matrix (analogous to the CKM matrix for the quarks).

The mixing angles of the neutrinos are the mismatch between the eigenstates of the, neutrinos and those of the charged leptons, or in other words between the mass matrices L and Mv. Thus, there are two obvious ways of obtaining large $U\mu 3$: either Mv has large off-diagonal elements while L is nearly diagonal, or L has large off-diagonal elements and Mv is nearly diagonal. Of course this distinction only makes sense in some preferred basis. But in almost every model there is some preferred basis given by the underlying symmetries of that model. This distinction gives the first major division in the classification, between models of what I shall call class I and class II. (It is also possible that the large mixing is due almost equally to large off-diagonal elements in L

and M_ν, but this possibility seems to be realized in very few published models. I will put them into class II.)

If the large $U_{\mu 3}$ is due to M_ν (class I), then it becomes important whether M_ν arises from a non-see-saw mechanism or the see-saw mechanism. We therefore distinguish these cases as class 1(1) and class I(2) respectively. In the see-saw models, M_ν is given by $-N^T M_R^{-1} N$, so a further subdivision is possible: between models in which the large off-diagonal elements are in M_R and those in which they are in N. We call these class I(2A) and I(2B) respectively.

If $U_{\mu 3}$ is due to large off-diagonal elements in L, while M_ν is nearly diagonal (class II), then the question to ask is why, given that L has large off-diagonal elements, there are not also large off-diagonal elements in the Dirac mass matrices of the other charged fermions, namely U and D, causing large CKM mixing of the quarks. In the literature there seem to be two ways of answering this question. One way involves the CKM angles being small due to a cancellation between large angles that are nearly equal in the up and down quark sectors. We call this class II(1). The main examples of this idea are the so-called "flavor democracy models". The other idea is that the matrices L and D^T (related by unified or flavor symmetry) are "lopsided" in such a way that the large off-diagonal elements only affect the mixing of fermions of one handedness: left-handed for the leptons, making $U_{\mu 3}$ large, and right-handed for the quarks, leaving V_{cb} small. we call this approach class II(2).

Schematically, one then has

$$
\begin{array}{ll}
I & \text{Large mixing from } M_\nu \\
 & \quad (1)\ \text{Non see saw} \\
 & \quad (2)\ \text{Seesaw} \\
 & \qquad \text{A. Large mixing from } M_R \\
 & \qquad \text{B. Large mixing from } N \\
II & \text{Large mixing from } L \\
 & \quad (1)\ \text{CKM small by cancellation} \\
 & \quad (2)\ \text{lopsided } L.
\end{array}
\tag{1}
$$

Now let us examine the different categories in more detail, giving examples from the literature.

I(1) Large mixing from M_ν, non-see-saw.

This kind of model gives a natural explanation of the discrepancy between the largeness of $U_{\mu 3}$ and the smallness of V_{cb}. V_{cb} comes from Dirac mass matrices, which are all presumably nearly diagonal like L, whereas $U_{\mu 3}$ comes from the matrix U_ν; and since in non-see-saw models M_ν comes from models the matrix M_ν comes from completely different physics than do the Dirac mass matrices it is not at all surprising if it has a very different form from the others, containing some large off-diagonal elements. While this basic idea is very simple and appealing, these models have the drawback that in non-see-saw models the form of M_ν, since it comes from new physics unrelated to the origin of the other mass matrices, is highly unconstrained. Thus, there are few definite predictions, in general, for masses and mixings in such schemes. However, in some schemes constraints can be put on the new physics responsible for M_ν.

As we saw, there are a variety of attractive ideas for generating a non-see-saw M_ν at low energy, and there are published models of neutrino mixing corresponding to all these ideas.[9-13] M_ν comes from triplet Higgs in Ref. 9; from the Zee mechanism in Ref. 10; and from R-parity and lepton-number-violating terms in a SUSY model in Ref. 11. In Ref. 12 a "democratic form" of M_ν is enforced by a family symmetry. Several other models in class I(1) exist in the literature.13

I(2A) See-saw M_ν, large mixing from M_R

In these models, M_ν comes from the see-saw mechanism and therefore has the form $-N^T M_R^{-1} N$. The large off-diagonal elements in M_ν are assumed to come from M_R, while the Dirac neutrino matrix N is assumed to be nearly diagonal and hierarchical like the other Dirac matrices L, U, and D. As with the models of class I(1), these models have the virtue of explaining in a natural way the difference between the lepton angle $U_{\mu 3}$ and the quark angle V_{cb}. The quark mixings all come from Dirac matrices, while the lepton mixings involve the Majorana matrix M_R, which it is quite reasonable to suppose might have a very different character, with large off-diagonal elements.

However, there is a general problem with models of this type, which not all the examples in the literature convincingly overcome. The problem is that if N has a hierarchical and nearly diagonal form, it tends to communicate this property to M_ν. For example, suppose we take N = diag(e1, E, 1)M, with 1 » ϵ » ϵ'. And suppose that the ij^{th} element of M_R^{-1} is called a_{ij}. Then the matrix Mv will have the form

$$M_\nu \propto \begin{pmatrix} \epsilon'^2 a_{11} & \epsilon' \epsilon a_{12} & \epsilon' a_{13} \\ \epsilon' \epsilon a_{12} & \epsilon^2 a_{22} & \epsilon a_{23} \\ \epsilon' a_{13} & \epsilon a_{23} & a_{33} \end{pmatrix}. \tag{2}$$

If all the non-vanishing elements aij were of the same order of magnitude, then obviously M_ν is approximately diagonal and hierarchical. The contribution to the leptonic angles coming from Mv would therefore typically be proportional to the small parameters e and ϵ'. This suggests that to get a value of $U_{\mu 3}$ that is of order 1, it is necessary to have the small parameter coming from N get cancelled by a correspondingly large parameter from M_R^{-1} The trouble is that to have such a conspiracy between the magnitudes of parameters in N and M_R is unnatural, in general, since these matrices have very different origins. This problem has been pointed out by various authors.[14] We shall call it the Dirac-Majorana conspiracy problem.

There are several models in the literature that fall into class I(2A).[15–17] Of these, an especially interesting paper is that of Jezabek and Sumino,[15] because it shows that a Dirac-Majorana conspiracy can be avoided. Jezabek and Sumino consider the case that the Dirac and Majorana matrices of the neutrinos have the forms

$$N = \begin{pmatrix} x^2 y & 0 & 0 \\ 0 & x & x \\ 0 & O(x^2) & 1 \end{pmatrix} m_D, \quad M_R = \begin{pmatrix} 0 & 0 & A \\ 0 & 1 & 0 \\ A & 0 & 0 \end{pmatrix} m_R, \tag{3}$$

where x is a small parameter. If one computes $M_\nu = -N^T M_R^{-1} N$ one finds that

$$M_\nu = -\begin{pmatrix} 0 & O(x^4 y/A) & x^2 y/A \\ O(x^4 y/A) & x^2 & x^2 \\ x^2 y/A & x^2 & x^2 \end{pmatrix} m_D^2/m_R. \tag{4}$$

Note that this gives a maximal mixing of the second and third families, without having to assume any special relationship between the small parameter in N (namely x) and the parameter in M_R (namely A). Altarelli and Feruglio[16] generalize this example, showing that the same effect occurs if M_R is taken to have a triangular symmetric form.

An interesting point about the form of M_ν in Eq. (4) is that it gives bimaximal mixing. This is easily seen by doing a rotation of π/4 in the 2-3 plane, bringing the matrix to the form

$$M'_\nu = \begin{pmatrix} 0 & z & z' \\ z & 0 & 0 \\ z' & 0 & 2x^2 \end{pmatrix}. \qquad (5)$$

In the 1-2 block this matrix has a Dirac form, giving nearly maximal mixing of ν_e.

Other published models that fall into class I(2) are given in Ref. 17.

I(2B) See-saw M_ν, large mixing from N

At least at first glance, this seems to be a less natural approach. the point is that if the large $U_{\mu 3}$ is due to large off-diagonal elements in N, it might be expected that the other Dirac mass matrices, U, D, and L, would also have large off-diagonal elements, giving large CKM angles. There are ways around this objection, and a few interesting models that fall into this class have been constructed. However, experience seems to show that this approach is harder to make work than the others, and fewer models of this type exist in the literature.[18]

II(1) Large mixing from L, CKM small by cancellation

If the large value of $U_{\mu 3}$ comes from large off-diagonal elements in the mass matrix L of the *charged* leptons, then it is most natural to assume that the other Dirac mass matrices have large off-diagonal elements also. Why, then, are the CKM angles small? One possibility is that the CKM angles are small because of an almost exact cancellation between large angles needed to diagonalize U and D. That, in turn, would imply that U and D, even though highly non-diagonal, have nearly identical forms. This is the idea realized in so-called "flavor democracy" models.

In flavor democracy models, a permutation symmetry $S_3 \times S_3$ among the left- and right-handed fermions causes the Dirac mass matrices L, D, and U to have the form

$$L, D, U \propto \begin{pmatrix} 1 & 1 & 1 \\ 1 & 1 & 1 \\ 1 & 1 & 1 \end{pmatrix}. \qquad (6)$$

Smaller contributions that break the permutation symmetry cause deviations from this form. These flavor-democratic forms are of rank 1, explaining why one family is much heavier than the others. On the other hand, the mass matrix of the neutrinos M_ν is assmed to have, by an S_3 symmetry acting on the left-handed neutrinos, the approximate form

$$M_\nu \propto \begin{pmatrix} 1 & 0 & 0 \\ 0 & 1 & 0 \\ 0 & 0 & 1 \end{pmatrix}. \qquad (7)$$

If M_ν were *exactly* proportional to the identity, then the basis of neutrino mass eigenstates would be undefined, and so then would be the MNS angles. However, once the small S3-violating effects are taken into account, a neutrino basis is picked out. It is not surprising that, typically, the neutrino angles that are predicted are of order unity. On the other hand, the fact that U and D are nearly the same in form leads to a cancellation that tends to make the quark mixing angles small.

Exactly what angles are predicted for the neutrinos depends on the form of the small contributions to the mass matrices that break the permutation symmetries. There are many simple forms that might be assumed, and the possibilities are rich. There exists a large and growing literature on these models.[19]

The idea of flavor democracy is an elegant one, especially in that it uses one basic idea to explain the largeness of the leptonic angles, the smallness of the quark angles,

and the fact that one family is much heavier than the others. On the other hand, it requires the very specific forms given in Eqs. (6) and (7), which come from very specific symmetries. It is in this sense a narrower approach to the problem of fermion masses than some of the others I have mentioned.

It would be interesting to know whether models of class II(1), in which the CKM angles are small by cancellations of large angles, can be constructed using ideas other than flavor democracy.

II(2) Large mixing from "lopsided" L

We now come to what I regard as the most elegant way to explain the largeness of $U_{\mu 3}$: "lopsided" L. The basic idea is that the charged-lepton and down-quark mass matrices have the approximate forms

$$L \sim \begin{pmatrix} 0 & 0 & 0 \\ 0 & 0 & \epsilon \\ 0 & \sigma & 1 \end{pmatrix} m_D, \quad D \sim \begin{pmatrix} 0 & 0 & 0 \\ 0 & 0 & \sigma \\ 0 & \epsilon & 1 \end{pmatrix} m_D. \tag{8}$$

The "~" sign is used because in realistic models these σ and ϵ entries could have additional factors of order unity, such as from Clebsches. The fact that L is related closely in form to the transpose of D is a very natural feature from the point of view of SU(5) or related symmetries, and is a crucial ingredient in this approach. The assumption is that $\epsilon \ll 1$, while $\sigma \sim 1$. In the case of the charged leptons ϵ controls the mixing of the second and third families of *right*-handed fermions (which is not observable at low energies), while s controls the mixing of the second and third families of *left*-handed fermions, which contributes to $U_{\mu 3}$ and makes it large. For the quarks the reverse is the case because of the "$SU(5)$" feature: the small $O(\epsilon)$ mixing is in the left-handed sector, accounting for the smallness of V_{cb}, while the large $O(\sigma)$ mixing is in the right-handed sector, where it cannot be observed and does no harm.

In this approach the three crucial elements are these: (a) Large mixing of neutrinos (in particular of ν_μ and ν_t) caused by large off-diagonal elements in the *charged*-lepton mass matrix L; (b) this off-diagonal element appearing in a highly asymmetric or lopsided way; and (c) L being similar to the transpose of D by $SU(5)$ or a related symmetry.

To my knowledge the first place that all the elements of this approach appear is in a paper by Babu and Barr[20] and a sequel by Barr.[21] In those papers the emphasis was on a particular mechanism (in $SU(5)$ and $SO(10)$) by which the lopsidedness of L and D can arise. So perhaps it was not noticed by some readers that the scheme described in those papers was an instance of a more general mechanism.

The next time that this general idea can be found is in three papers that appeared almost simultaneously: Sato and Yanagida,[22] Albright, Babu, and Barr,[23] and Irges, Lavignac, and Ramond.[24]

It is interesting that the same mechanism was arrived at independently by these three groups from completely different points of view. In Sato and Yanagida the model is based on Et, and the structure of the matrices is determined by the Froggatt-Nielson mechanism. In Albright, Babu, and Barr, the model was based on $SO(10)$, and does not use the Froggett-Nielson approach. Rather, the constraints on the form of the mass matrices come from assuming a "minimal" set of Higgs for $SO(10)$ and choosing the smallest and simplest set of Yukawa operators that can give realistic matrices. Though both papers assume a unified symmetry larger than $SU(5)$, in both it is the $SU(5)$ subgroup that plays the critical role in relating L to D^T. The model of Irges, Lavignac, and Ramond, like that of Sato and Yanagida, uses the Froggatt-Nielson idea, but is not based on a grand unified group. Rather, the fact that L is related to D^T

follows ultimately from the requirement of anomaly cancellation for the various $U(1)$ flavor symmetries of the model. However, it is well known that anomaly cancellation typically enforces charge assignments that can be embedded in unified groups. So that even though the model does not contain an explicit $SU(5)$, it could be said to be "$SU(5)$-like".

In the last two years, the same mechanism has been employed by a large number of authors using a variety of approaches.25

A PREDICTIVE SO(10) MODEL WITH LOPSIDED L

The model that I shall now describe briefly was not constructed to explain neutrino phenomenology; rather it emerged from the attempt to find a realistic model of the masses of the charged leptons and quarks in the context of $SO(10)$, In particular, the idea was to take the Higgs sector of $SO(10)$ to be as minimal as possible, and then to find what this implied for the mass matrices of the quarks and leptons. In fact, in the first paper we wrote, we did not pay any attention to the neutrino spectrum. Then we noticed that the model in that paper actually predicted a large mixing of ν_μ with ν_τ and published a follow-up paper.[23] The reason for the large mixing of the mu and tau neutrinos was precisely the fact that the charged lepton mass matrix has a lopsided form.

The reason this lopsided form was built into this model (which I shall refer to as the ABB model henceforth) was that it was necessary to account for certain well-known features of the mass spectrum of the quarks. In particular, the mass matrix entry that is denoted s in Eq. (8) above plays three crucial roles in the ABB model that have nothing to do with neutrino mixing. (1) It is required to get the Georgi-Jarlskog[26] factor of 3 between m_μ and m_s. (2) It explains the value of V_{cb} (3) It explains why $m_c/m_t \ll m_s/m_b$. Remarkably, it turns out not only to perform these three tasks, but also gives mixing of order 1 between ν_μ and ν_τ. Not often are four birds killed with one stone!

In constructing the model, several considerations guided us. First, we assumed the "minimal" set of Higgs for $SO(10)$. It has been shown[27] that the smallest set of Higgs that will allow a realistic breaking of $SO(10)$ down to SU(3) x SU(2) x U(1), with natural doublet-triplet splitting,[28] consists of a single adjoint (**45**), two pairs of spinors ($16 + \overline{16}$), a pair of vectors (**10**), and some singlets. The adjoint, in order to give the doublet-triplet splitting, must have a VEV proportional to the $SO(10)$ generator $B - L$. This fact is an important constraint. Second, we assumed that the qualitative features of the quark and lepton spectrum should not arise by artificial cancellations or numerical accidents. Third, we required that the Georgi-Jarlskog factor arise in a simple and natural way. Fourth, we assumed that the entries in the mass matrices should come from operators of low-dimension that arise in simple ways from integrating out small representations of fermions.

Having imposed these conditions of economy and naturalness on the model we were led to a structure coming from just six effective Yukawa terms (just five if m_μ is allowed to vanish). These gave the following mass matrices:

$$U^0 = \begin{pmatrix} \eta & 0 & 0 \\ 0 & 0 & \frac{1}{3}\epsilon \\ 0 & -\frac{1}{3}\epsilon & 1 \end{pmatrix} m_U, \qquad D^0 = \begin{pmatrix} 0 & \delta & \delta' \\ \delta & 0 & \sigma + \frac{1}{3}\epsilon \\ \delta' & -\frac{1}{3}\epsilon & 1 \end{pmatrix} m_D$$

$$N^0 = \begin{pmatrix} \eta & 0 & 0 \\ 0 & 0 & -\epsilon \\ 0 & \epsilon & 1 \end{pmatrix} m_U, \qquad L^0 = \begin{pmatrix} 0 & \delta & \delta' \\ \delta & 0 & -\epsilon \\ \delta' & \sigma + \epsilon & 1 \end{pmatrix} m_D. \tag{9}$$

(The first papers[23] gave only the structures of the second and third families, while this was extended to the first family in a subsequent paper.[29]) Here $\sigma \cong 1.8$, $\epsilon \cong 0.14$, $\delta \cong |\delta'| \cong 0.008$, $\eta \cong 0.6 \times 10^{-5}$. The patterns that are evident in these matrices are due to the SO(10) group-theoretical characteristics of the various Yukawa terms. Notice several facts about the crucial parameter σ that is responsible for the lopsidedness of L and D. First, if s were not present, then instead of the Georgi-Jarlskog factor of 3, the ratio m_μ/m_s would be given by 9. (That is, the Clebsch of $\frac{1}{3}$ that appears in D due to the generator $B - L$ gets squared in computing m_s.) Since the large entry σ overpowers the small entries of order ϵ, the correct Georgi-Jarlskog factor emerges. Second, if σ were not present, U and D would be proportional, as far as the two heavier families are concerned, and V_{cb} would vanish. Third, by having $\sigma \sim 1$ one ends up with V_{cb} and m_s/m_b being of the same order (ϵ) as is indeed observed. And since σ does not appear in U (for group-theoretical reasons) the ratio m_c/m_t comes out much smaller, of order ϵ^2, also as observed. In fact, with this structure, the mass of charm is predicted correctly to within the level of the uncertainties.

Thus, for several reasons that have nothing to do with neutrinos one is led naturally to the very lopsided form that we found gives an elegant explanation of the mixing seen in atmospheric neutrino data!

From the very small number of Yukawa terms, and from the fact that $SO(10)$ symmetry gives the normalizations of these terms, and not merely order of magnitude estimates for them, it is not surprising that many precise predictions result. In fact there are altogether nine predictions.[29] Some of these are post-dictions (including the highly non-trivial one for m_c). But several predictions will allow the model to be tested in the future, including predictions for V_{ub}, and the mixing angles U_{e2} U_{e3}.

In the first papers it appeared that the model only gave the small-angle MSW solution to the solar neutrino problem. In fact, if $\eta = 0$, or if forms for M_R are chosen that do not involve much mixing of the first-family right-handed neutrino with the others, then a very precise prediction for U_{e2} results that is beautifully consistent with the small-angle MSW solution.[29] However, in a subsequent paper[30] we showed that for other simple forms of M_R the model gives bi-maximal mixing. (This happens in a way similar to what we saw above in Eqs. (4) and (5) for the Jezabek-Sumino model.)

For more details of the ABB model and its predictions I refer you the papers I have mentioned.

REFERENCES

1. J.W.F. Valle, Neutrino physics at the turn of the millenium (hep-ph/9911224); S.M. Bilenky, Neutrino masses, mixings, and oscillations, Lectures at the 1999 European School of High Energy Physics, Casta Papiernicka, Slovakia, Aug. 22-Sept. 4, 1999 (hep-ph/0001311).

2. M.C. Gozalez-Garcia, P.C. de Holanda, C. Peña-Garay, and J.C.W. Valle, Status of the MSW solutions to the solar neutrino problem, hep-ph/9906469

3. V. Barger and K. Whisnant, Seasonal and energy dependence of solar neutrino vacuum oscillations, hep-ph/9903262

4. M.C. Gonzalez-Garcia, talk at International Workshop on Particles in Astrophysics and Cosmology: From Theory to Observation, Valencia, Spain, May 3-8, 1999.

5. M. Gell-Mann, P. Ramond, and Slansky, in *Supergravity, Proc. Supergravity Workshop ut Stony Brook,* ed. P. Van Nieuwenhuizen and D.Z. Freedman (North-Holland, Amsterdam, 1979); T. Yanagida, *Proc. Workshop on Unified theory and the baryon number of the universe,* ed. 0. Sawada and A. Sugamota (KEK, 1979).

6. A. Zee, Phys. Lett. **B93** (1980) 389; Phys. Lett. **B161** (1985) 141.

7. C. Froggatt and H.B. Nielson, Nucl. Phys. **B147** (1979) 277.

8. J.A. Harvey, D.B. Reiss, and P. Ramond, Mass relations and neutrino oscilations in an SO(10) model, Nucl. Phys. **B199** (1982) 223-268.

9. R.N. Mohapatra and S. Nussinov, Bimaximal neutrino mixing and neutrino mass matrix, Phys. Rev. **D60** (1999) 013002 (hep-ph/9809415).

10. C. Jarlskog, M. Matsuda, S. Skadhauge, and M. Tanimoto, Zee mass matrix and bimaximal neutrino mixing, Phys. Lett. **B449** (1999) 240-252 (hep-ph/9812282).

11. M. Drees, S. Pakvasa, X. Tata, T. terVeldhuis, A supersymmetric resolution of solar and atmospheric neutrino puzzles, Phys. Rev. **D57** (1998) 5335-5339 (hep-ph/9712392).

12. K. Fukuura, T. Miura, E. Takasugi, and M. Yoshimura, Maximal CP violation, large mixings of neutrinos and democratic type neutrino mass matrix, Osaka Univ. preprint, OU-HET-326 (hep-ph/9909415).

13. G.K. Leontaris and J. Rizos, New fermion mass textures from anomalous $U(1)$ symmetries with baryon and lepton number conservation, CERN-TH-99-268 (hep-ph/9909206).

14. M. Jezabek and Y. Sumino, Neutrino mixing and seesaw mechanism, Phys. Lett. **B440** (1998) 327-331 (hep-ph/9807310); G. Altarelli and F. Feruglio, Neutrino mass textures from oscillations with maximal mixing, Phys. Lett. **B439** (1998) 112-118 (hep-ph/9807353).

15. M. Jezabek and Y. Sumino, Neutrino mixing and seesaw mechanism, Phys. Lett. **B440** (1998) 327-331 (hep-ph/9807310).

16. G. Altarelli and F. Feruglio, Phys. Lett. **B439** (1998) 112-118 (hep-ph/9807353).

17. B. Stech, Are the neutrino masses and mixings closely related to the masses and mixings of quarks?, talk at 23rd Johns Hopkins Workshop on Current Problems in Particle Theory: Neutrinos in the Next Millenium, Baltimore, MD, 10-12 June 1999 (hep-ph/9909268). M. Bando, T. Kugo, and K. Yoshioki, Neutrino mass textures with large mixing, Phys. Rev. Lett. **80** (1998) 3004-3007 (hep-ph/9710417).

M. Abud, F. Buccella, D. Falcone, G. Ricciardi, and F. Tramontano, Neutrino masses and mixings in $SO(10)$, DSF-T-99-36 (hep-ph/9911238).

18. Q. Shafi and Z. Tavartkiladze, Proton decay, neutrino oscillations and other consequences from supersymmetric $SU(6)$ with pseudogoldstone Higgs, BA-99-39 (hep-ph/9905202); D.P. Roy, talk at 6th Topical Seminar on Neutrino and AstroParticle Physics, San Miniato, Italy, 17-21 May 1999 (hep-ph/9908262).

19. M. Fukugita, M. Tanimoto, and T. Yanagida, Atmospheric neutrino oscillation and a phenomenological lepton mass matrix, Phys. Rev. **D57** (1998) 4429-4432 (hep-ph/9709388); M. Tanimoto, Vacuum neutrino oscillations of solar neutrinos and lepton mass matrix, Phys. Rev. **D59** (1999) 017304 (hep-ph/9807283); H. Fritzsch and Z.-z. Xing, Large leptonic flavor mixing and the mass spectrum of leptons, Phys. Lett. **B440** (1998) 313-318 (hep-ph/9808272); S.K. Kang and C.S. Kim, Bimaximal lepton flavor mixing and neutrino oscillation, Phys. Rev. **D59** (1999)091302(hep-ph/9811379).

20. K.S. Babu and S.M. Barr, Large neutrino mixing angles in unified theories, Phys. Lett. **B381** (1996) 202-208 (hep-ph/9511446).

21. S.M. Barr, Predictive models of large neutrino mixing angles, Phys. Rev. **D55** (1997)1659-1664(hep-ph/9607419).

22. J. Sato and T. Yanagida, Large lepton mixing in a coset space family unification on E(7)/SU(5) x U(1)3, Phys. Lett. **B430** (1998) 127-131 (hep-ph/9710516).

23. C.H. Albright, K.S. Babu, and S.M. Barr, A minimality condition and atmospheric neutrino oscillations, Phys. Rev. Lett. **81** (1998) 1167-1170 (hep-ph/9802314); C.H. Albright and S.M. Barr, Fermion masses in SO(10) with a single adjoint Higgs field, Phys. Rev. **D58** (1998) 013002 (hep-ph/9712488).

24. N. Irges, S. Lavignac, and P. Ramond, Predictions from an anomalous V(1) model of Yukawa hierarchies, Phys. Rev. **D58** (1998) 035003 (hep-ph/9802334).

25. Y. Nomura and T. Yanagida, Bimaximal neutrino mixing in SO(10) (GUT), Phys. Rev. **D59** (1999) 017303 (hep-ph/9807325); Z. Berezhiani and A. Rossi, Grand unified textures for neutrino and quark mixings, JHEP 9903:002 (1999) (hep-ph/9811447); K. Hagiwara and N. Okamura, Quark and lepton flavor mixings in the SU(5) grand unification theory, Nucl. Phys. **B548** (1999) 60-86 (hep-ph/9811495); G. Altarelli and F. Feruglio, A simple grand unification view of neutrino mixing and fermion mass matrices, Phys. Lett. **B451** (1999) 388-396 (hep-ph/9812475); K.S. Babu, J. Pati, and F. Wilczek, Fermion masses, neutrino oscillations and proton decay in the light of SuperKamiokande, (hep-ph/9812538); R. Barbieri, L.J. Hall, G.L. Kane, and G.G. Ross, Nearly degenarate neutrinos and broken flavor symmetry, OUTP-9901-P (hep-ph/9901228); K.I. Izawa, K. Kurcsawa, Y. Nomura, and T. Yanagida, Grand unification scale generation through anomalous V(1) breaking, Phys. Rev. **D60** (1999) 115016 (hep-ph/9904303); E. Ma, Permutation symmetry for neutrino and charged lepton mass matrices, Phys. Rev. **D61** (2000) 033012 (hep-ph/9909249); Q. Shafi and Z. Tavartkiladze, Bimaximal neutrino mixings and proton decay in SO(10) with anomalous flavor U(1), BA-99-63 (hep-ph/9910314); P. Frampton and A. Rasin, Non-abelian discrete symmetries, fermion mass textures and large neutrino mixing, IFP-777-UNC (hep-ph/9910522).

26. H. Georgi and S.L. Glashow, Phys. Lett. **B86** (1979) 297.

27. S.M. Barr and S. Raby, Minimal SO(10) unification, Phys. Rev. Lett. **79** (1998) 4748-4751.

28. S. Dimopoulos and F. Wilczek, report No. NSF-ITP-82-07 (1981), in *The unity of fundamental interactions* Proceedings of the 19th Course of the International School of Subnuclear Physics, Erice, Italy, 1981 ed. A. Zichichi (Plenum Press, New York, 1983); K.S. Babu and S.M. Barr, Natural suppression of Higgsino mediated proton decay in supersymmetric SO(10), Phys. Rev. **D48** 5354-5364.

29. C.H. Albright and S.M. Barr, A model of quark and lepton masses, Phys. Lett. **B452** (1999) 287-293.

30. C.H. Albright and S.M. Barr, Bimaximal mixing in an SO(10) minimal Higgs model, Phys. Lett. **B461** (1999) 218-223.

This page intentionally left blank.

Section VI

Recent Progress on New and Old Ideas III

This page intentionally left blank.

SIMP (Strongly Interacting Massive Particle) Search*

Vigdor L. Teplitz,[1] Rabindra N. Mohapatra,[2] Fred Olness,[1] and Ryszard Stroynowski[1]

[1]Department of Physics, Southern Methodist University, Dallas, TX 75275
[2]Department of Physics, University of Maryland, College Park, MD 20742.

Introduction

Strongly Interacting Massive Particle (SIMPS), by which we will always mean neutral, stable SIMPs, are of current interest for at least three reasons:

- They could be a dark matter constituent as suggested some time ago by Dover, Gaisser and Steigman [1] and by Wolfram [2]. Starkman et al.,[3] show SIMPs would be restricted to rather narrow mass ranges if they were to exhaust $\Omega = 1$. We will not make this assumption and will consider SIMPs outside the regions allowed by the analysis of ref. [3].
- It is possible that the lightest SUSY particle (LSP) is strongly interacting and hence, if R-parity is conserved, would form a colorless SIMP. Possibilities, such as a $\tilde{g}g$ bound state are discussed in ref. [4].
- An explanation of the ultra high energy cosmic ray events (UHECRs) proposed by Farrar, Kolb and co-workers [5] is that they are due to interactions of SIMPs with a mass below 50 GeV and a cross section for interactions with nucleons on the order of a (few) millibarns.

This summary will review two laboratory experiments that might detect SIMPs. For more detail, the reader is encouraged to examine with care ref. [6] and the paper on which it is based [7].

In Section 2 we consider the possibility of finding SIMPs bound in ordinary nuclei by searching for anomalously heavy isotopes of high-Z nuclei. It is a pleasure to note that the accelerator mass spectrometry (AMS) group at Purdue is in the process of performing the experiment† suggested in ref. [6] In Section 3, we address the extent to which production and detection of SIMP–anti-SIMP ($S\bar{S}$) pairs might be performed at the Tevatron.

*Presented by Vigdor L. Teplite

†We are grateful to Professor Ephraim Fischbach for keeping us informed as to progress on this crucial experiment.

Our results, in brief, are that the AMS experiment should be sensitive to SIMPs over a wide range of parameter space: (σ_{SN}, Ms), where Ms is the SIMP mass and σ_{SN} is its cross section for scattering off nucleons. The Tevatron, on the other hand is likely only to produce and to detect SIMPs in a much more restricted range, but one that includes much of the mass range for which the SIMP could be the UHECR explanation. It would be only fitting, since much of the work on that possibility [5] was done at Fermilab, if SIMPs were to be detected at Fermilab and we encourage those with influence in the collaborations to explore vigorously that possibility. Finally, we note that we proceed without committing to a specific SIMP model. We parameterize the experimental predictions in terms of the two parameters σ_{SN} and Ms.

SIMPs in Nuclei

We know a fair amount about SIMP binding in nuclei from the phenomenology of hyper-fragments. See, for example, Povh [8] for a readable review. Based on that experience, we can write for the binding B of the SIMP in a nucleus A the relation:

$$B = |V_{SN}| - \pi^2/(2\mu R^2) \qquad (1)$$

where μ is the reduced mass of the S-A system, R is the radius of the nucleus A, and V is the S-N potential averaged over the volume of the nucleus X. We expect the low energy potential, V_{SN}, to be always attractive. This is true if exchange of vacuum quantum numbers dominates. We assume this to be the case, and have not found a model to the contrary. Under this assumption, the SIMP can be bound in a nucleus for which μ and $R^2 \sim A^{2/3}$ are large enough to make the kinetic energy less than the (average) magnitude of the attractive potential.

From equation (1) we see that the best chance of finding SIMPs is to search in high Z (large) nuclei which minimize the kinetic energy term. Capture by light elements at the time of cosmic nucleosynthesis has been studied in ref. [9]. Atomic Mass Spectrometer (AMS) searches to date are reviewed in the careful study of Hemmick et al., [10] where one learns the somewhat surprising fact that previous searches have only been conducted up to sodium (Z = 11, A = 23). This makes the current Purdue AMS experiment particularly exciting. They are looking in gold (Z = 79, A = 100). At the risk, however, of sounding greedy, we would be interested in anyone with AMS equipment, a supply of Lawrencium (Z = 103, A = 262), and an affinity for maximal experiments. However, as will become clear below, we do not want any such calls from interested parties to be collect.

How big is the potential V_{XN}? We take this as a parameter, but we can put an approximate LOWER bound on it from the requirement that primordial S and S, left over from the early universe, not overclose the universe so that it couldn't have continued expanding until today (late 1999). The classic book of Kolb and Turner [11] tells us that the number density of primordial SIMPs behaves as

$$n_S \sim (Ms\, \sigma_{SS})^{-1} \quad . \qquad (2)$$

Equation (2) says that too small an annihilation cross section means too many SIMPs will be left over from the early universe, and Kolb and Turner collect together the numerical recipes for computing how small is too small. We still need, however, to relate the annihilation cross section, σ_{SS} to the SIMP-nucleon cross section, σ_{SN} and to the $S - N$ potential in Equation (1). We make the simple ansatz

$$V_{SN} = V_{NN}\, (\sigma_{SN}/\sigma_{NN})^{1/2} \qquad (3)$$

$$\sigma_{SN}^2 = \beta \sigma_{NN} \sigma_{S\overline{S}}$$

where β should be on the order of one. Note that V_{SN} goes as $\beta^{1/4}$ so that our results for binding will not be highly dependent on the precision of Equation (3).

Now that we know, for each point in the *MS*, σ_{SN} parameter space, the primordial S abundance and the binding energy in nuclei, we are almost ready to compute for our friends at Purdue, the abundance of anomalous gold–gold with a SIMP bound in it. First, however, we need a scenario for how the SIMPs get bound into the gold. Our picture is as follows:

- We assume that the ratio of SIMPs to protons in the galaxy is the same as the cosmic ratio, but that most of the SIMPs are in the galactic halo (*i.e.,* that their density distribution is $\rho \sim R^{-2}$), not in stars. We can then calculate the SIMP flux on the Earth, since we know that the Earth is traveling through the galaxy with a velocity of about *200km/s* which not too different from the galactic virial velocity.

- We assume that when the SIMP hits the Earth, it is slowed by scattering with all nucleons and nuclei at a rate determined by σ_{SN}, but can only be captured by a nucleus that is large enough.

- Gold must compete, for SIMP capture, with the most abundant nuclei large enough to bind the SIMP. Our comparative estimates use, as the most abundant elements:, aluminum (A = 27), barium (A = 137), and lead (A = 206).

Our procedure is then as follows:

- We chose values for *MS* and σ_{SN} and then determine whether, for that point in parameter space, there is binding in gold.

- Assuming that there is binding, we then determine (a) the mean free path in Earth from the galactic virial velocity and σ_{SN}, and (b) which of the 3 elements above is gold's chief competitor for SIMP capture.

- From the ratio of the abundance of gold to its chief competitor, the mean free path, and the average density of Earth, we then compute the chance of a particular gold nucleus within a mean free path to capture an incident SIMP. Multiplying by the flux (see above) of SIMPs and the time for which the sample being put in the AMS target has been exposed (which is why we don't want collect calls from those long in Lawrencium) gives us the fraction of gold nuclei in the sample that should have a SIMP if they exist at that point in parameter space.

Finally, we assume‡ that the exposure time is 10 million years because there are regions that are geologically inactive over such periods and have had for example "placer" gold in the beds of streams for a longer period than that§.

The results are shown in the table. It gives $\log_{10}$ of the ratio of normal to anomalous gold nuclei. The dashes indicate parameter values for which there is either no binding in gold or overclosure of the universe. One sees that smaller values of σ_{SN} give larger ratios of anomalous to normal gold. This is because smaller values imply that only lead

†We appreciate conversations with Professor E. T. Herrin on searching for old exposed gold.

§Purdue is, we believe, taking collect calls from people who have pieces of gold with such provenance; they give all but a small fraction of a mole back at the end of the run.

Table 1. M_X (vertical) is in units of GeV, and σ_{XN} (horizontal) is in units of *mb*. Table entries are *log10(1/f)*, and the – indicates those cases for which X does not bind at all.

	0.0005	0.0042	0.012	0.032	0.25	0.69	1.9	5.3	15	41	110	860
1.0	–	–	–	–	–	–	–	6.3	8.3	8.7	12.5	13.4
1.6	–	–	–	–	–	–	6.1	8.1	8.5	12.3	12.7	13.6
2.7	–	–	–	–	–	5.9	7.9	8.3	12.1	12.5	12.9	13.8
4.3	–	–	–	–	5.7	7.7	8.1	11.1	12.3	12.7	13.1	14.0
7.1	–	–	–	–	7.5	7.9	10.9	12.1	12.5	12.9	13.4	14.2
12	–	–	–	5.6	8.1	8.5	12.2	12.7	13.1	13.5	13.9	14.8
19	–	–	–	7.5	8.3	11.3	12.5	12.9	13.3	13.8	14.2	15.0
31	–	–	7.4	7.8	8.6	12.4	12.8	13.2	13.6	14.1	14.5	15.3
50	–	5.7	7.7	8.1	11.5	12.7	13.1	13.6	14.0	14.4	14.8	15.7
81	5.7	7.7	8.1	8.5	11.9	13.1	13.5	14.0	14.4	14.8	15.2	16.1
132	7.7	8.1	8.5	8.9	12.2	13.5	13.9	14.3	14.7	15.2	15.6	16.4
220	8.0	8.4	8.9	9.3	12.6	13.9	14.3	14.7	15.1	15.5	16.0	16.8
350	8.4	8.8	9.3	9.7	13.8	14.3	14.7	15.1	15.5	15.9	16.4	17.2
570	8.8	9.2	9.7	10.1	14.3	14.7	15.1	15.5	15.9	16.4	16.8	17.6
930	9.3	9.7	10.1	10.5	14.7	15.1	15.5	16.0	16.4	16.8	17.2	18.1

has a nucleus large enough to compete with gold for SIMP capture and because the smaller cross section means more primordial abundance. The important thing to take away from hours of table study is the fact that the relative abundance entries are all considerably higher (for anomalous to normal) than the limits of 10^{-20} that have been set in AMS work on some of the light elements. This provides reason to expect that, if the SIMPs are there, the Purdue AMS people will find them.

SIMPs at Fermilab

Next we consider $S\bar{S}$ production at the Tevatron. Since we are talking neutral SIMPs, we expect little or no signal in the central tracker and in the electromagnetic calorimeter. However, in the hadron calorimeter, we expect to detect SIMP signals if σ_{SN} is large enough. The detection of SIMPs is possible if one triggers on two back-to-back hadron calorimeter showers, accompanied by little else. We will use 10 GeV for the minimum size showers for which such triggering might be done. Our task now is to determine:

- For what values of {Ms,σs} will the SIMP interact in the steel plates of the hadron calorimeter?
- For what values of these parameters will we get calorimeter showers greater than 10 GeV or more?
- Can one recognize a SIMP shower if one sees one?
- How many such events should we expect?

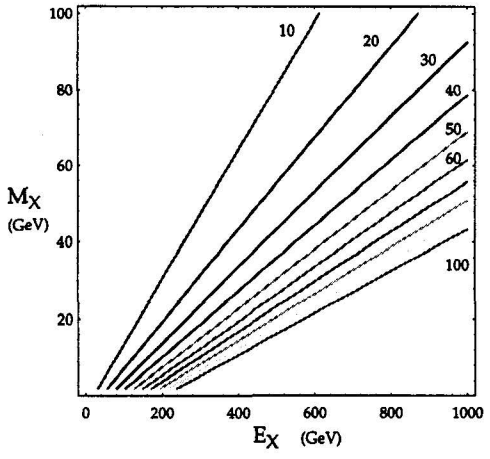


Figure 1. Contours for energy loss as a function of {Mx, Ex}. The contours displayed are in steps of 10 GeV.

First we look at the region of parameter space for which there will be interaction. The minimum annihilation cross section permitted by the cosmology argument is ~ 3 x 10^{-13} *barns,* which corresponds through Equation (3) to about a microbarn for the S-N cross section. SIMPs with such small cross sections won't shower in 1 meter of steel, but for a higher cross section of a few millibarns, we would expect 10 or more interactions with the 10^{27} *nucleons/cm*^{2} in the 1 meter.

To estimate the energy we expect in a shower resulting from a SIMP interaction in the steel plates of a hadron calorimeter we use a cosmic ray rule of thumb kindly provided by G. Yodh[¶] who says that, in a high energy strong interaction, about half the center of mass energy goes into inelasticity. In the figure, we give the (laboratory) energy released in the calorimeter as we vary the mass and energy of the SIMP; the straight lines are constant shower energies. One sees that the bigger the SIMP lab energy, the greater a SIMP mass will result in a given shower energy.

Consider now the question of whether we would recognize a SIMP shower if we saw one. The background for SIMP showers would likely be neutron showers and *K* decays. The distinguishing feature would be shower opening angle. A pion moving transverse in the c.m. system would have a lab angle given by tanq = 1/γ. Comparing the angle for a SIMP with that from a neutron of the same energy, the SIMP shower should be wider by roughly the ratio of the masses.

Finally, we turn to the number of SIMP pairs the Tevatron might produce. We scale the (known) production rate of jets by the ratio of the S-N cross section to that of Meson-N, which we take to be on the order of 30 millibarns. So long as the SIMP energy is a few times its mass, we don't worry about phase space suppression. We assume conservatively a cross section of about *3pb* for any one parton in the region E > 200GeV. This implies about 6000 events in Run II. The estimate of [5] is that the Nucleon-UHECR cross section needs to be over a tenth the Meson-Nucleon cross section, so we estimate 600 events in the Tevatron run if SIMPs are the explanation for the UHECR events.

[¶]This useful approximation from Professor Gaurang Yodh made the whole trip to Paris (where the conversation took place) well worthwhile (and the food was OK too).

Summary

For the Table we see that there is SIMP binding in gold for $M_8^2 \sigma_{SN} > 5 mb GeV^2$, and that AMS experiments sensitive to one part in 1020 can detect the existence of SIMPs of mass less than a TeV, while the region of interest for explaining UHECRs can be explored with a sensitivity of one part in 10^{16} or less. Looking for SIMPs at the Tevatron is more difficult, but over half the region of interest for explaining UHECRs could be searched in the upcoming Run II by looking for (wide) back to back jets with no signal in the central tracker or EM calorimeter. Interested people are urged to send any gold in their possession for which they can prove 10^7 (or more) years of exposure to Purdue. Almost all nuclei will be returned intact [‖].

We thank D. Berley, K. Brockett, K. De, D. Dicus, M.A. Doncheski, R. Ellsworth, G. Farrar, E. T. Herrin, D. Rosenbaum, R. Scalise, and G. Yodh. The work of RNM has been supported by the National Science Foundation grant under no. PHY-9802551 The work of Olness, Stroynowski, and Teplitz is supported by DOE.

REFERENCES

1. C. Dover, T, Gaisser, and G. Steigman, Phys. Rev. Lett. 42, 1117 (1979).
2. S. Wolfram, Phys. Lett. 82B, 65 (1979).
3. G. Starkman et al., Phys. Rev. D41 2388 (1990).
4. H. Baer, K. Cheung and J. F. Gunion, Phys. Rev. D59, 075002 (1999); S. Raby and K. Tobe, Nucl. Phys. B539, 3 (1999); A. Mafi and S. Raby, hep-ph/9912436, and references therein.
5. D. Chung, G. Farrar, and E. W. Kolb, Phys. Rev. D57,4606 (1998) and I. F. M. Albequerque, G. Farrar, and E. W. Kolb, Phys. Rev. D59 015021 (1999).
6. R. N. Mohapatra, F. Olness, R. Stroynowski, and V. L. Teplitz, Phys. Rev. D60, 115013 (1999).
7. R. N. Mohapatra and V. L. Teplitz, Phys. Rev. Lett. 81, 3079 (1998).
8. Z. Povh, Ann. Rev. Nuc. Sci. 28, 1 (1978).
9. D. A. Dicus and V. L. Teplitz, Phys. Rev. Lett. 44, 218 (1980).
10. T. K. Hemmick et al., Phys. Rev. D41 2074 (1990).
11. E. W. Kolb and M. Turner, *The Early Universe* (Addison Wesley, Reading, MA, 1990).

[‖]Sorry, but neither Purdue, SMU, or Maryland can be responsible for nuclei lost or damaged in transit (by either AMS or Fedex)

WHITHER HADRON SUPERSYMMETRY?

D. B. Lichtenberg

Physics Department
Indiana University
Bloomington, IN 47405, USA

INTRODUCTION

Physicists have applied the concept of supersymmetry to a number of different areas. To particle physicists, the most familiar supersymmetry is a spontaneously broken supersymmetry between particles and sparticles, for which at present no experimental evidence exists. However, there is experimental evidence for dynamically broken supersymmetries in the areas of atomic physics, nuclear physics, and hadron physics.

One of the oldest of these applications of supersymmetry was to hadron physics, discussed by Miyazawa[1] in 1966. Almost a decade later, Catto and Gürsey[2] macle plausible that dynamically broken hadron supersymmetry is a consequence of QCD. They also showed that one consequence of the supersymmetry is that Regge trajectories of mesons and baryons have approximately the same slope.

The reason for hadron supersymmetry is most transparent in the approximation to QCD known as the constituent quark model. In this model, the reason for hadron supersymmetry can be seen as follows: According to QCD an antiquark belongs to a $\bar{\mathbf{3}}$ multiplet of color SU(3). A two-quark system, which I call a diquark. can be in either a $\mathbf{6}$ or $\bar{\mathbf{3}}$ multiplet. Any two constituent quarks in a baryon must belong to the $\bar{\mathbf{3}}$ so that the baryon can be an overall color singlet. Now a meson contains a constituent quark and a constituent antiquark. If we replace the antiquark (a fermion) by a 3 diquark (a boson), we make a supersymmetric transformation of a meson into a baryon. This transformation does not change the color configuration. Because, in first approximation, the QCD interaction depends only on the color configuration, the force between the quark and diquark in a baryon should be approximately the same as the force between quark and antiquark in a meson. Hence, we should be able to use supersymmetry to relate the properties of baryons to the properties of mesons.

If we replace antiquarks by diquarks in normal hadrons, we can obtain exotic hadrons. For example, if we replace $Q\bar{Q}$ (a bar on the symbol for a particle denotes the antiparticle) by $D\bar{D}$, where Q is a quark and D is a diquark, we obtain an exotic meson from a normal one. Making use of supersymmetry, we can relate properties of exotic hadrons to similar properties of normal ones. In exotic hadrons. a diquark can

Quantum Gravity Generalized Theory of Gravitation and Superstring Theory Bused Unification
Edited by Kursunoplu *et al* Kluwer Academic / Plenum Puhlishers New York 2000

be either in a $\bar{\mathbf{3}}$ or a **6** multiplet of color. The interactions of the **6** cannot be related by supersymmetry to the interactions of an antiquark, and so we must neglect the 6. We justify this neglect as follows: When two quarks are close together, QCD says that their Coulomb-like interaction is attractive in a $\bar{\mathbf{3}}$ and repulsive in a **6.** It is then plausible that the $\bar{\mathbf{3}}$ lies lower in energy than the **6.** If we confine ourselves to low-mass exotics we hope that we may safely neglect the contribution of color-6 diquarks.

The difficulty with applying supersymmetry to hadrons is that the supersymmetry is badly broken, or the pion and proton would have the same mass. Miyazawa[1] was already aware of this difficulty in 1966. Supersymmetry breaking arises from at least three differences between a diquark and a quark (or antiquark): 1) they have different sizes; 2) they have different masses; and 3) they have different spins. We briefly discuss these differences.

1) Obviously, a diquark is not a point particle, but neither is a constituent quark, as it consists of a pointlike quark surrounded by a cloud of gluons and quark antiquark pairs. I have not seen any paper discussing how supersymmetry is broken by size differences between quark and diquark, and I have made no progress on this problem myself, so I have to neglect the effects of diquark size.

2) Mass effects can be taken into account in several ways. One particularly simple method is to relate mass differences between mesons to mass differences between baryons in such a way that the effect of the diquark-quark mass difference is most likely to cancel out. Another method is to make use of the fact that the quark-antiquark binding energy in mesons depends smoothly on the constituent quark masses.[3] In this method, the binding energy of a quark with a diquark can be estimated by treating the diquark as a fictitious antiquark with the diquark mass.

3) There are spin-dependent forces in QCD. One way to minimize their effect is to take appropriate averages over spin. Another way is to assume that the spin-dependent interaction energy between two quarks in a diquark is independent of the hadrons in which the diquark is embedded. This assumption is not strictly correct,4 but it is a good approximation. Then the spin-dependent contribution to the interaction energy can be approximately extracted[4] from the experimentally known masses of baryons. In both spin averaging and extracting spin-dependent forces from baryons, it is assumed that the spin-dependent force in ground-state hadrons is the usual chromomagnetic force arising from one-gluon exchange.[5] This assumption has been challenged by Glozman and Riska,[6] and I have discussed the arguments in favor of one-gluon exchange in a talk at the last Orbis meeting.[7]

I have been working on the consequences of broken hadron supersymmetry for several years and have spoken about it at two previous Orbis meetings.[8,9] In the present talk I shall update the conclusions of my two earlier talks and discuss possible directions for future work in hadron supersymmetry.

RELATIONS BETWEEN MESON AND BARYON MASSES

From here on, I will sometimes call an antiquark a quark and an antidiquark a diquark. In this language, for example, a meson is a two-quark state and an exotic meson is a four-quark or two-diquark state. I have nothing to say about glueballs and other exotic mesons that axe not made of two diquarks.

We use the notation that Q denotes any quark, q denotes a light u or d quark, and D (QQ) denotes a color 3 diquark. Also M (QQ) is a normal meson, *ME*

($QQ\bar{Q}\bar{Q}$ or $D\bar{D}$) is an exotic meson, B (QQQ or QD) is a normal baryon, B_E ($QQQQ\bar{Q}$ or $DD\bar{Q}$) is an exotic baryon, and B_2 ($QQQQQQ$ or DDD) a dibaryon.

As a consequence of hadron supersymmetry, we can make the transformations

$$\bar{Q} \rightarrow D, \quad Q \rightarrow \bar{D}. \tag{1}$$

Applying either the first or second of eqs. (1) one or more times, we obtain

$$M = Q\bar{Q} \rightarrow B = QD, \tag{2}$$

$$B = QD \rightarrow M_E = \bar{D}D \tag{3}$$

$$B = \bar{Q}\bar{Q}\bar{Q} \rightarrow B_E = DD\bar{Q}, \tag{4}$$

$$B = \bar{Q}\bar{Q}\bar{Q} \rightarrow B2 = DDD. \tag{5}$$

We next consider how to take into account supersymmetry breaking. One way to minimize the effects of spin-dependent forces is to average over spins in such a way that perturbatively the spin-dependent forces cancel out. In order to do this, we must make an assumption about the nature of these spin-dependent forces. Following De Rújula et al.,[5] we assume that the spin-dependent forces arise from one-gluon exchange. Then the spin averaging of ground-state hadrons is given by the prescription of Anselmino et al.[4] One way to minimize the effects of mass differences between quarks and diquarks is to let one quark in the diquark be a light quark q. We do this by confining ourselves (in this section) to the transformations

$$\bar{Q} \rightarrow D, = Qq, \quad Q \rightarrow \bar{D}q = \bar{Q}\bar{q}. \tag{6}$$

We also take differences in masses such that the mass of the light quark in the diquark will tend to cancel out.

In the following, we let the symbol for a hadron denote its mass, and we sometimes write the constituent quarks of a hadron in parentheses following the hadron symbol. We are led by the considerations of the previous paragraph to consider the difference of two meson masses: $M(\bar{Q}_2 q) - M(\bar{Q}_1 q)$. Applying the transformation of eq. (6), we get

$$M(\bar{Q}_2 q) - M(\bar{Q}_1 q) = B(Q_2 qq) - B(Q_1 qq). \tag{7}$$

The masses in eq. (7) are to be thought of as spin averages, i.e.

$$M(\bar{q}q) = (3\rho + \pi)/4, \quad M(\bar{s}q) = (3K^* + K)/4,$$

$$M(c\bar{q}) = (3D^* + D)/4, \quad M(\bar{b}q) = (3B^* + B)/4, \tag{8}$$

$$B(qqq) = (\Delta + N)/2, \quad B(sqq) = (2\Sigma^* + \Sigma + \Lambda)/4,$$

$$B(cqq) = (2\Sigma_c^* + \Sigma_c + \Lambda_c)/4, \quad B(bqq) = (2\Sigma_b^* + \Sigma_b + \Lambda_b)/4, \tag{9}$$

where the symbols for the mesons and baryons are those of the Particle Data Group.[10] Using eqs. (8) and (9) in (7), we obtain the sum rules[8]

$$(3K^* + K)/4 - (3\rho + \pi)/4 = (2\Sigma^* + \Sigma + \Lambda)/4 - (N + \Delta)/2, \tag{10}$$

$$(3D^* + D)/4 - (3K^* + K)/4 = (2\Sigma_c^* + \Sigma_c + \Lambda_c)/4 - (2\Sigma^* + \Sigma + \Lambda)/4, \tag{11}$$

$$(3B^* + B)/4 - (3D^* + D)/4 = (2\Sigma_b^* + \Sigma_b + \Lambda_b)/4 - (2\Sigma_c^* + \Sigma_c + \Lambda_c)/4. \quad (12)$$

These same sum rules were obtained earlier[11] by a method not using hadron suger-symmetry. However, the assumption of one-gluon exchange was needed for averaging over spin states.

We can test the sum rules with the experimental values of the known hadron masses.[10] The left-hand side of eq. (10) is 182 ± 1 MeV, while the right-hand side is 184± 1 MeV, in good agreement with experiment. Similarly, the left-hand side of eq. (11) is 1179 ± 1 MeV, while the right-hand side is 1174 ± 1 MeV, also in satisfactory agreement with the data. In a 1996 talk,[8] I noted that eq. (12) was consistent with preliminary data on baryons containing b quarks, but the 1998 tables of the Particle Data Group[10] do not confirm those data. Therefore, the sum rule of eq. (12) remains to be tested by measurements of the masses of the Σ_b and Σ^*_b baryons. Once the mass of the Σ_b is measured, the sum rule (12) will give a prediction for the mass of the Σ^*_b.

The fact that the sum rules of eqs. (10) and (11) agree with the data constitutes evidence in support of spin-dependent forces arising from one-gluon exchange. These sum rules do not follow from the spin-dependent forces postulated by Glozman and Riska.[6] In their work, the spin-dependent forces in baryons containing only light quarks arise from pseudoscalar meson exchanges. However, I don't see how the same mechanism can apply to mesons or to baryons containing heavy quarks. If I would need two or three different mechanisms to account for the spin-dependent forces in hadrons (or a linear combination of them), then I would not know how to obtain sum rules.

EXOTIC HADRONS

We do not need to restrict ourselves to spin-averaged hadron masses or to di-quarks containing at least one light quark, as we can explicitly take into account mass and spin effects. I discussed this problem at a previous Orbis,[9] and so will only briefly review the method.

We start with the spin-averaged hadron masses, but include spin effects explicitly at a later stage. We assign constituent masses to the quarks such that the binding energy of a quark and antiquark in a meson is a smooth function of the reduced mass of the two constituent.[3] We can use this "meson curve" to read off the binding energy of a fictitious hadron made of a fictitious quark and antiquark of any given masses.

We consider a spin-averaged baryon made of a quark and a diquark, treating the diquark as a fictitious antiquark. Our first guess for the diquark mass is that it equals the sum of its two constituent quark masses. We obtain the reduced mass of the quark and diquark and read off the binding energy from the meson curve. We add this binding energy to the masses of the quark and diquark to obtain a calculated spin-averaged baryon mass. In general, this mass does not equal the experimental mass of a baryon, averaged over spin. However, by repeatedly adjusting the mass of the diquark, we can obtain the correct spin-averaged baryon mass. We are thus able to obtain the spin-averaged diquark masses for constituent quarks of any flavors.

Next we obtain diquark properties from observed baryon masses rather than from spin-averaged masses. We extract the spin-dependent interaction energies of two quarks in a diquark from the observed baryon masses.[4] Adding these terms to the spin-averaged diquark mass, we obtain the masses of spin-one and spin-zero diquarks.

We are now ready to calculate the masses of ground-state exotic hadrons. We first consider exotic mesons containing at least one diquark of spin zero. In such mesons, there are no spin-dependent forces between the diquarks. Therefore, we only have to calculate the reduced mass of the constituents and add the binding energy from the meson curve to the diquark masses in order to obtain the exotic meson mass. (If both diquarks have spin one, there are additional spin-dependent forces, but their effects can be calculated.)

The results of these calculations is that diquark-antidiquark exotic mesons have sufficiently large masses to decay rapidly into two normal mesons. Because we expect production cross sections to be small and decay widths large, it is unlikely that such exotic mesons will be observed. A possible exception is that an exotic meson containing a bb diquark might be stable against strong decay, but its production cross section will be extremely small. Our conclusion is in agreement with the fact that no exotic mesons composed of a diquark and antidiquark have yet been seen.

The same method can be applied to exotic baryons and to dibaryons. However, there is the complication that, except in the limit of point-like diquarks, the Pauli principle is not strictly satisfied for quarks in different diquarks. The results are similar to the results for mesons: exotic baryons and dibaryons (other than the deuteron) are not likely to be observed. Again, this conclusion is in agreement with observations to date.

THE FUTURE

The predictions of the previous sections follow from broken hadron supersymmetry plus spin-dependent forces arising from one-gluon exchange. It is gratifying that we have not obtained any predictions in serious disagreement with experiments done so far, but it is disappointing that our model says that diquark exotics will probably not be observed.

Although enough has been established so far to give me confidence that hadron supersymnetry is a useful concept, open questions remain to be answered. Among them are:

(1) A diquark may be almost as large as the hadron that contains it. How do we correct for the non-negligible size of a diquark?

(2) Is there any way to take into account the contribution from color-sextet diquarks to exotic hadrons?

(3) If the spin-dependent forces in some hadrons are not given by one-gluon exchange but rather by the mechanism of Glozman and Riska, how do the results change? Are the changes large enough to destroy the good agreement with experiment?

(4) How can we take the Pauli principle into account in exotic baryons and dibaryons?

(5) Exotic hadrons containing diquarks can mix with other hadrons having the same quantum numbers. For example, quantum numbers permitting, a diquark–antidiquark meson can mix with normal mesons, hybrids, and glueballs. Can we take this mixing into account?

(6) Are there any other useful predictions to be obtained from broken hadron supersymmetry?

In conclusion, if physicists can successfully tackle the preceding open questions. hadron supersymnetry will rest on a much sounder foundation than it does now.

However, if answers are not forthcoming, it may be time for physicists to store in their minds that broken hadron supersymmetry exists and go on to other topics.

Acknowledgments

Some of this work was done with Enrico Predazzi and Renato Roncaglia. I should like to thank Floarea Stancu for helpful discussions.

References

1. H. Miyazawa, Baryon number changing currents, *Prog. Theor. Phys.* 36:1266 (1966).
2. S. Catto and F. Gürsey, Algebraic treatment of effective supersymmetry, *Nuovo Cimento* 86:201 (1985).
3. R. Roncaglia, A.R. Dzierba, D.B. Lichtenberg, and E. Predazzi, Predicting the masses of heavy hadrons without an explicit Hamilatonian, *Phys. Rev.* D 51:1248 (1995).
4. M. Anselmino, D.B. Lichtenberg, and E. Predazzi, Quark color-hyperfine interactions in baryons, Z. *Phys.* C48:605 (1990).
5. A. De Rújula, H. Georgi, and S. L. Glashow, Hadron masses in a gauge theory, *Phys. Rev.* D 12:147 (1975).
6. L.Ya Glozman and D.O. Riska, The spectrum of the nucleons and the strange hyperons and chiral dynamics, *Phys. Rep.* 268:263 (1996).
7. D. B. Lichtenberg, Spin-dependent forces between quarks in hadrons, in: *Confluence of Cosmology, Massive Neutrinos, Elementary Particles, and Gravitataon,* B.N. Kursunoglu, S.L. Mintz and A. Perlmutter eds. Klewer Academic/Plenum Publishers, New York (1999). p. 101.
8. D. B. Lichtenberg, Hadron Supersymmetry and relations between meson and baryon masses, in: *Neutrino Mass, Dark Matter, Gravitational Waves, Monopole Condensation and Light Cone Quantization,* B.N. Kursunoglu, S.L. Mintz, and A. Perlmutter, eds., Plenum Press, New York (1996), p. 319.
9. D.B. Lichtenberg, Exotic hadrons, in: *High Energy Physics and Cosmology: Celebrating the Impact of 25 Gables Conferences* B.N. Kursunoglu, S.L. Mintz, and A. Perlmutter, eds. Plenum Press, New York (1997), p. 59.
10. Particle Data Group: C. Caso et al., Review of particle physics, *Euro. Phys.* J. C 3:1 (1998).
11. D.B. Lichtenberg and R. Roncaglia, New formulas relating the masses of some baryons and mesons, *Phys. Lett.* B 358:106 (1995).

THE MYSTERY OF NUCLEON SPIN

W. Lorenzon

Randall Laboratory of Physics
University of Michigan
Ann Arbor, MI 48109-1120

INTRODUCTION

Understanding the underlying composition of the nucleon's spin has proven to be a significant challenge both theoretically and experimentally. Even though protons and neutrons, which were among the first sub-atomic particles discovered this century, have been studied for almost ninety years, some of their fundamental properties still hold puzzles and surprises. For the past ten years, physicists have tried to resolve a particular puzzle known as the "spin crisis".

The crisis emerged from the highly successful quark model of sub-atomic particles. Gell-Mann and Zweig developed this model in 1964 as a compact description of the zoo of new particles detected in the the 1950s and 1960s. In their constituent quark model, the proton consists of three spin-1/2 $\hbar$ quarks of mass 350 MeV moving in an S-orbit. The spin of the proton entirely comes from the spin of its quarks: two of the quarks have opposite spins which cancel, and the spin of the remaining quark produces precisely the observed spin of the proton. This appeared to be a reasonable assumption based on the idea that many of the nucleon's properties could be derived by combining properties of their constituent quarks in a simple way. It worked very well for the electric charge of the proton, for example, which is exactly the sum of its quarks' fractional charges. It also worked well in explaining the static magnetic moments of the lowest mass baryons. For the ratio of the magnetic moment of the neutron to that of the proton, $\mu n/\mu p$, the quark model predicted a value of –2/3, very close to the experimental value of –0.685.

The spin of a fundamental particle is crucial to determine how the particle behaves. For example, if electrons did have any spin other than 1/2 $\hbar$, the way electrons stack into orbitals around an atomic nucleus would be radically changed, and the periodic table of elements would look very different. Also, the spin structure of composite particles can have a big impact on their mass. Whereas aligning the spins of the proton and the electron in a hydrogen atom increases its mass (0.9 GeV) by only a few μeV, aligning the spin of all three quarks in a proton turns the proton into a $\Delta+$ particle which is 30% heavier than the proton. Computing the spin of an atom by adding up the angular momenta of its components, even for an atom with dozens of electrons, is well understood. Unfortunately, the analogous computation for quarks and gluons that make up the protons and neutrons has been unsuccessful so far.

Quantum Gravity. Generalized Theory of Gravitation. and Superstring Theory-Based Unification
Edited by Kursunoglu *et al.,* Kluwer Academic / Plenum Publishers. New York. 2000

The problem lies with Quantum Chromodynamics (QCD). Its equations have been known since the 1970s, but they have several features that make them very hard to work with. Even today, with the most advanced mathematical techniques and the fastest super computers, physicists have not succeeded in exactly solving the equation for a nucleon.

The strong force arises when quarks exchange gluons, a process similar to the electromagnetic force which arises when electrically charged particles exchange photons. However, there are two crucial differences that make computations in QCD much harder to deal with than in electromagnetism. First, the strong force is about 100 times stronger than the electromagnetic force, and second, in contrast to photons which are electrically neutral and thus do not interact with other photons directly, gluons carry color charge and therefore do interact with one another. Moreover, QCD is a quantum field theory, implying that virtual quarks and gluons are constantly being created and annihilated. Their brief interactions have to be taken into account. And to add even more, the uncertainty principle dictates that the quarks must in be in motion, at close the speed of light. In summary, according to QCD, the proton is a strongly coupled, relativistic, infinite-body system that has never been solved before. The only direct method to solve it is using the techniques of lattice calculations which might give reliable results in the near future.

THE EARLY EXPERIMENTS

The spin structure of nucleons is typically investigated by scattering polarized leptons off polarized targets. The method of choice in the past has been deep-inelastic scattering (DIS) to measure the polarized quark density $g_1(x)$ in a polarized nucleon. The basic interaction between the lepton and the target quark in DIS is the exchange of a photon. If the lepton beam is longitudinally polarized, meaning that the spin axis of the lepton beam points along the beam, the leptons will exchange photons with quarks having the opposite spin due to conservation of total angular momentum. Therefore, measurements first made with one polarization and then with the beam or target polarization reversed reveal the asymmetry in the distribution of quarks polarized parallel to the nucleon spin minus the distribution of quarks polarized antiparallel to the nucleon spin.

The pioneering experiments were performed in the late 1970s at the Stanford Linear Accelerator (SLAC) with modest polarization of beam and target. They were followed in the mid-1980s by more precise measurements from the European Muon Collaboration (EMC) at CERN, which, while consistent with the SLAC data, suggested that the strange quark sea makes a significant negative contribution to the proton's spin and that the amount of the proton's spin attributable to the quarks was only about 12%[1] in contradiction to expectations of a much higher fraction. This was the birth of the "spin crisis".

This result spurred a new generation of experiments at SLAC, CERN, and DESY (Deutsches Elektronen Synchrotron) with significant improvements in precision. At the same time, an intense theoretical effort was launched to reconcile theory and experiment.

SUMMARY OF EXPERIMENTAL DATA

The new experiments at SLAC, CERN, and DESY over the last decade have concentrated mainly on high precision measurements of the structure function g_1 over a large kinematic range to extract information on the spin structure. In a simple quark parton model the spin of the nucleon can be decomposed schematically as

$$\frac{1}{2}\hbar = \frac{1}{2}\Delta\Sigma + \Delta G + L_q + L_G, \tag{1}$$

Table 1. Summary of experiments at SLAC, CERN, and DESY to measure spin-dependent deep inelastic scattering.

Lab	Experiment	Year	Beam	Target
SLAC	E80	75	23 GeV e^-	H–butanol
	E130	80	23 GeV e^-	H–butanol
	E142	92	25 GeV e^-	^{3}He
	E143	93	29 GeV e^-	NH3/ND3
	E154	95	49 GeV e^-	^{3}He
	E155	97	49 GeV e^-	NH3/LiD
	E155x	99	49 GeV e^-	NH3/LiD
CERN	EMC	85	100-200 GeV $\mu-$	NH3
	SMC	92	100 GeV $\mu+$	D–butanol
	SMC	93	190 GeV $\mu+$	H–butanol
	SMC	94/95	190 GeV $\mu+$	D–butanol
	SMC	96	190GeV $\mu+$	NH_3
DESY	HERMES	95	28GeVe+	^{3}He
	HERMES	96/97	28GeVe+	H
	HERMES	98/99	28GeVe–	D

where $\Delta\Sigma$ denotes the contribution of the quark spins, ΔG the contribution from the gluon spin, and L_g and L_G the contributions of the orbital angular momenta of the quarks and gluons. It is important to remember that this equation is schematic; for example, only in the case of quarks can one decompose the spin and orbital angular momentum contributions in a gauge-invariant manner[2], although only the sum $\Delta\Sigma+L_q$ is independent of the factorization scheme.

A summary of spin structure function measurements is shown in Table 1, where the beams, targets, and energies are listed for each experiment. Those were very difficult experiments that needed a tremendous effort to measure tiny asymmetries. Since the EMC measurements in the mid-1980s, enormous progress had been made in achieving highly polarized beams and targets. At SLAC, for example, electron beam polarizations of 85% had been obtained routinely using strained GaAs electron sources. Using standard GaAs electron sources, previous experiments at SLAC and elsewhere had achieved electron beam polarizations of 45% at most. At CERN, where the Spin Muon Collaboration (SMC) took over the earlier apparatus from EMC, the 72-cm target was replaced with a 1.2-m target (the longest ever built). Using cryogenic polarized ammonia (NH_3 / ND_3) and butanol (C_4H_9OH / C_4D_9OD) targets, the SLAC and CERN experiments achieved target polarizations of 90% for hydrogen targets and 40% for deuterium targets. At DESY, the HEMS collaboration employed low-density gaseous targets of pure atomic hydrogen, deuterium or ^{3}He. They achieved typically target polarizations of 90% for H and D, and about 50% for ^{3}He.

The Inclusive Results

The results of all the second-generation experiments agree remarkably well with one another, as shown in Fig. 1, thus demonstrating that the experimental uncertainties are well understood. These results have strongly confirmed the earlier EMC result that only about 30% of a proton's spin is produced by its quarks' spin, and that the strange quark sea is negatively polarized.

Though it was pointed out more than a decade ago[3], it had only recently become widely recognized that this result had to be reinterpreted, and that the simple parton interpretation of g_1 was too naive. The reason was that the measured polarized structure function can contain significant contributions from processes involving gluons via the axial anomaly. The gluonic contribution tends to reduce the contribution of the quarks if the gluons make up a sizeable

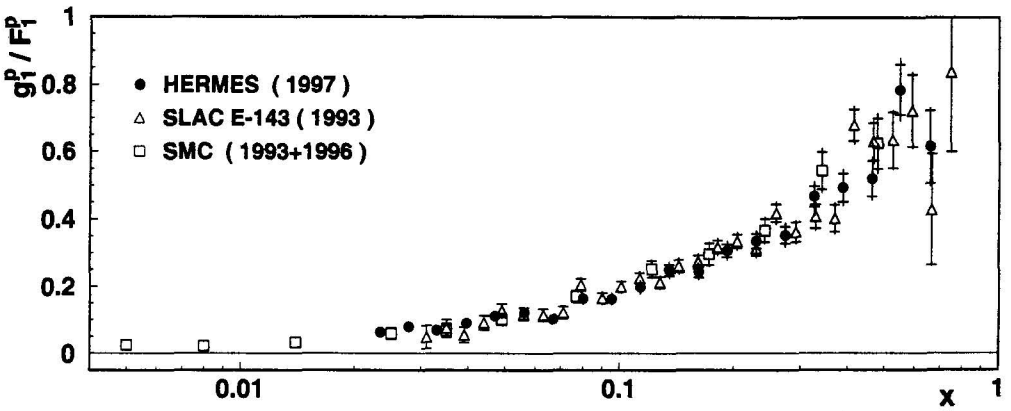


Figure 1. The structure function ratio g_1^p/F_1^p of the proton as a function of x from HERMES[4] is compared with recent results for g_1^p/F_1^p measured at SLAC (E143)[5] and A_1^p at CERN (SMC)[6]. The inner error bars show the statistical uncertainties and the outer ones the quadratic sum of the statistical and total systematic uncertainties.

positive contribution to the nucleon spin. One can redefine $\Delta\Sigma$ to $\Delta\Sigma' = \Delta\Sigma - n_f \frac{\alpha_s}{2\pi} \Delta G(Q2)$. This would explain the low value of $\Delta\Sigma'$ and increase the deduced contribution of the quarks..

However, the separation of $\Delta\Sigma$ and ΔG becomes dependent on the factorization scheme used. Nonetheless, given a choice of scheme, one can use QCD via the Altarelli-Parisi evolution equations to form a globally consistent picture of the polarized quark and gluon distribution functions, with

$$\Delta\Sigma' \simeq 0.3 \pm 0.1$$

$$\Delta G \simeq 1.2 \pm 1.0$$

$$\Rightarrow \quad L_z = -0.9 \qquad (\text{at } Q^2 = 3\ (\text{GeV/c})^2).$$

Thus, is this the end of the spin crisis? The missing 70% of the spin no longer constitutes a "crisis" since it can come from gluon spins and from the orbital angular momentum from the motion of all the quarks and gluons within the nucleon. That such large quantities are present within a nucleon of total spin 1/2 $\hbar$ is quite counterintuitive. We therefore have to ask how we can verify these surprisingly large gluon and orbital contributions separately. At present, no one has proposed a practical way to measure the orbital contribution. There are however several next-generation experiments planned to the measure the gluon contribution, among which are the RHIC-SPIN[7] experiments STAR and PHENIX at the Brookhaven National Laboratory (BNL), and the COMPASS[8] experiment at CERN. If the measured gluon contribution turned out to be too small, however, we would face a far more drastic spin crisis than ever before.

A new Approach – Semi-Inclusive Scattering

At this stage, many contributions to the nucleon spin remain poorly constrained or unknown. Information from inclusive scattering is inherently limited by the domination of scattering from up quarks, since the cross sections scale as the square of the electric charge, which is twice as large for up quarks as for down or strange quarks. To distinguish the contributions of the quark flavors and in particular of the sea quarks, it is necessary to use more sophisticated experimental techniques than so far. Semi-inclusive scattering offers a new approach by

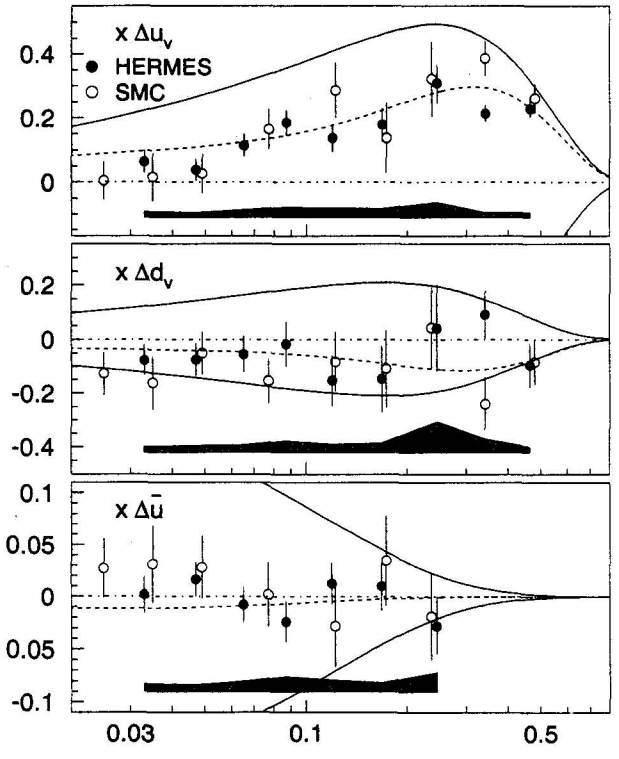


Figure 2. The polarized valence and sea quark distributions measured at HERMES (1995-97) and SMC (all data).

detecting a leading hadron in coincidence with the scattered lepton. The essential principle behind this method is the likelihood of the leading hadron to 'contain' the quark originally struck by the virtual photon from the lepton. Scattering asymmetries with various leading hadrons in the final state can be analyzed to determine the fractional contributions of the various quark flavors to the nucleon spin. Such an analysis uses data-constrained models for the fragmentation functions, which give the probability of a given flavor of quark to produce a given type of leading hadron.

First efforts to use semi-inclusive scattering to distinguish the polarizations of the various quark flavors were performed by the SMC experiment[9] at CERN. Using its unique undiluted targets, HERMES has performed the world's most precise determination to date of the separate contributions of the up, down and sea quarks to the nucleon spin[10]. By applying the quark parton model to the combined inclusive and semi-inclusive data on hydrogen and ^{3}He, the polarized quark distributions have been extracted. Their results are shown in Fig. 2 in comparison to those of SMC.

The resulting up quark polarizations are positive and the down quark polarizations are negative over the measured range of x. The sea polarization is compatible with zero over the measured range of x. Whereas the sea quark contribution is found to be close to zero in this semi-inclusive analysis, the strange quark sea is significantly negative in the inclusive analysis. However, neither result represents a direct measurement of Δs, but rather depends on the assumptions of $SU(3)_f$ symmetry for the inclusive case and on the sea symmetry condition for the semi-inclusive case. A newly installed Ring Imaging Cherenkov (RICH) counter at the HERMES experiment offers the possibility of a direct measurement of Δs through kaon identification.

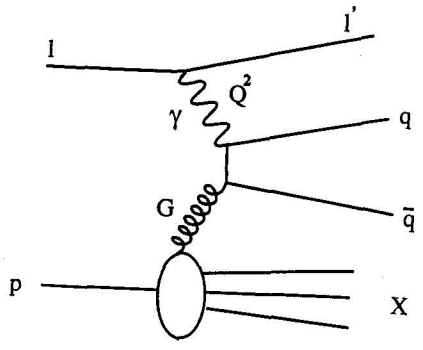


Figure 3. The Photon-Gluon fusion process.

How to measure ΔG?

The precise inclusive and semi-inclusive polarized deep-inelastic scattering data from SLAC, CERN and HERMES have clearly shown that the integral of $g1(x)$ is much smaller than expected from the naive quark parton model. Given the axial anomaly, one can interpret this deficit in terms of a possible large positive polarization of the gluon field in the proton. Clearly it is important to test this hypothesis by measuring the gluon helicity distribution, $\Delta G(xG)$. Even a determination of the algebraic sign of this distribution is of interest given that some theoretical models predict a negative contribution to the nucleon spin[11, 12]. One way to probe $\Delta G(xG)$ is by a measurement of the scaling violation of the polarized structure functions. However, the presently available data only poorly constrain $\Delta G(xG)$, although there is some indication for the integral to be positive.

A more promising prospect is a direct measurement of $\Delta G(xG)$ using scattering processes in which the gluon enters in leading order. Such a lepto-production process is photon-gluon fusion (PGF), indicated in the diagram shown in Fig. 3. Two useful experimental signatures of this process are charm production and the productions of jets with high transverse momentum pT. Both charm production and high-pT jet production have resulted in direct measurements of the unpolarized gluon structure function G[13, 14, 15]. The energies available at present fixed target experiments are however not high enough to produce jets; therefore, high-pT. hadrons must serve in place of jets[16] for HERMES and the COMPASS experiment at CERN.

At HERMES the spin asymmetry in the polarized photo-production of pairs of hadrons with opposite charge and high-pT has been studied[17]. Under certain kinematical conditions, this signal is dominated by PGF, which has a strong negative polarization analyzing power. A negative asymmetry has been observed which is in contrast to the positive asymmetries typically measured in deep-inelastic scattering from protons, and in the absence of any background process known to give a negative asymmetry, indicates a significant positive gluon polarization. When these data are interpreted in a model which takes into account leading order QCD processes and vector meson dominance contributions to the cross section, a value for $\Delta G(x)/G(x)$ of $0.41 \pm 0.18(\text{stat.}) \pm 0.03(\text{syst.})$ has been determined at $\langle xG \rangle = 0.17$. Possible higher order QCD processes or contributions from anomalous photon structure have been neglected, since no spin-dependent analyses of these processes are currently available. If such processes were important, but have no significant spin asymmetry, the extracted value of $\langle DG/G \rangle$ would increase, but still differ from zero by 2.3σ. To alter the conclusion that $\langle DG/G \rangle$ is positive, a significant contribution from a process with a large negative asymmetry would be needed. The HERMES result is compared in Fig. 4 with several phenomenological LO QCD fits to the data on $g_1\langle x, Q2 \rangle$.

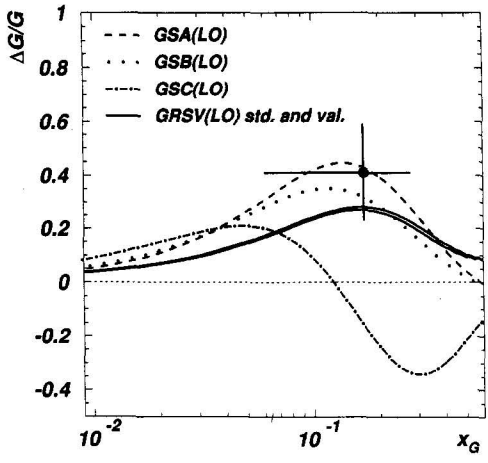


Figure 4. The extracted value of $\Delta G(x)/G(x)$ compared with phenomenological QCD fits to a subset of the world's data on $g_1^{p,n}(x, Q2)$. The curves are from Refs. [18, 19], evaluated at a scale of 2 $(GeV/c)^2$. The indicated error represents statistical and experimental systematic uncertainties only; no theoretical uncertainty is included.

More theoretical support is needed to reduce the model dependent uncertainties that arise when extracting $\Delta G(x_G)$ from data based on light $q\bar{q}$ pair production. Some of these theoretical uncertainties are avoided when the PGF process is identified by observing mesons containing charmed quarks, based on the assumption that intrinsic charm in the nucleon is negligible. In this case, the perturbative hard scale is provided by the charm quark mass, rather than transverse momentum. HERMES might be the first experiment to be able to derive some constraints on the gluonic polarization by using charm mesons to tag the PGF process, both with open (D^0, D^*) and hidden (J/ψ) charm mesons. However, the available statistics on J/ψ and D0 from the 1996/97 data set on a polarized hydrogen target is only of the order of 20 events for each channel. The 1998 charm upgrade to the HERMES detector did increase the acceptance by a factor of four, but no results are available yet from their 1998/99 running period.

FUTURE

Great progress has been made since the EMC experiment in experimentally determining the polarized structure function g_1 for the nucleon over the range of $0.005 \leq x \leq 0.7$. At present, however, many contributions to the nucleon spin remain unknown, as the orbital contribution, or are poorly constrained, as the strange quark and the gluon contributions. While attempts to extract the polarized gluon distribution $\Delta G(xG)$ from inclusive data have suggested a positive contribution of the gluons to the nucleon spin, it is clear that a direct measurement of the gluon spin contribution is very important. A first such measurement has been reported by the HERMES experiment at DESY, also indicating a significant positive gluon polarization. However, these data might contain substantial model uncertainties. Several other experimental efforts are underway to probe the gluons via the photon-gluon fusion reaction. These include the COMPASS experiment at CERN[8], and the SLAC proposal E156[20]. In addition, the RHIC-SPIN[7] experiments at BNL plan to probe the gluon spin by direct photon production. Further, it has been shown that HERA, with polarized protons in collider mode and with significantly increased luminosity, can probe gluon spin at low x[21]. Table 2 summarizes the likely sensitivities of these experiments.

Table 2. Summary of planned experiments at BNL, CERN, DESY, and SLAC to directly probe gluon spin.

Experiment	Results expected by	Kinematic range	$\delta\left(\frac{\Delta G}{G}\right)$
HERMES	running	$xg \sim 0.2 - 0.3$	~ 0.2 by 2002
COMPASS	~2002/3	$xg \sim 0.15$	~ 0.1
RHIC-SPIN	~2002/3	$xg \sim 0.05 - 0.3$	~ 0.01 – 0.3
SLACE-156	deferred	$xg \sim 0.1 - 0.5$	~ 0.02
pol. HERA	notapproved	$xg \sim 0.01 - 0.1$	~ 0.1

It is expected that by May 2000, HERMES will provide precise knowledge of the valence and sea quark polarizations, and report on the first direct measurement of the strange quark polarization, It is hoped that their results on $\Delta G/G$ obtained from pairs of hadrons with high-p_T can be improved in precision and confirmed from charm production data. The planned experiments at CERN, RHIC, and SLAC should be able to provide significantly more precise information on both, the gluon and the strange quark contribution to the nucleon spin by the middle of the next decade.

REFERENCES

1. EMC, J. Ashman et al., *Phys. Lett.* B 206,364 (1988); *Nucl. Phys.* B **328,** 1 (1989).
2. Xiangdong Ji, *Phys. Rev. Lett.* **78,**610 (1997).
3. R. L. Jaffe, *Phys. Lett.* B **193,**101 (1987).
4. HERMES, A. Airapetian et al., "Measurement of the Proton Spin Structure Function g_1^p with a Pure Hydrogen Target", *Phys. Lett.* B 442,484 (1998).
5. E143, K. Abe *et al., Phys. Rev. Lett.* **74,**346 (1995); *Phys. Lett.* B **364,**61 (1995); Phys. Rev. D **58,** 112003 (1998).
6. SMC, D. Adams et al., Phys. Lett. B **329,** 399 (1994); *Phys. Rev.* D **56,** 5330 (1997); B. Adeva *et al., Phys. Lett.* B **412,**414 (1997).
7. RHIC, PHENIX, BNL-PROPOSAL-R5, Aug. 1992; STAR, S.E. Vigdoret al., hep-ex/9905034.
8. COMPASS, The COMPASS Collaboration, CERN/SPSLC 96-14 (1996).
9. SMC, B. Adeva *et al., Phys. Lett.* B **420,**180 (1998).
10. HERMES, K. Ackerstaff *et al.,* "Flavor Decomposition of the Polarized Quark Distributions in the Nucleon from Inclusive and Semi-Inclusive Deep-inelastic Scattering". *Phys. Lett* B **464,** 123 (1999).
11. R.L. Jaffe, *Phys. Lett.* B **365,**359 (1996).
12. V. Barone, T. Calarco, A. Drago, *Phys. Lett.* B **431,**405 (1998).
13. H1, S. Aid et al., *Nucl. Phys.* B **472,**3 (1996); **B472,**32 (1996); **B449,**3 (1995).
14. ZEUS, 1. Breitweg *et al., Z Phys.* C 76,599 (1997); *Phys. Lett.* B **407,**402 (1997).
15. NMC, D. Allasia *at al., Phys. Lett.* B **258,**493 (1991).
16. COMPASS, A. Bravar et al., *Phys. Lett. B* **421,**349 (1998).
17. HERMES, A. Airapetian et al., "Measurement of the Spin Asymmetry in the Photoproductionof Pairs of High-pT Hadrons at HERMES", *Phys. Lett. B* (in press), hep-ex/9907020.
18. T. Gehrmann, W.J. Stirling,*Phys. Rev.* D 53,6100 (1996).
19. M. Glück et al., *Phys. Rev.* D 53,4775 (1996).
20. E156, SLAC Proposal E156, March 15,1997.
21. A. De Roeck *et al.,* Proceedings of the Workshop on Future Physics at HERA 1995/96, volume 2, page 803, September 1996.

PERFORMANCES AND FIRST RESULTS FROM BABAR

Giampiero Mancinelli[1]

Rutgers University
Piscataway, New Jersey 08855

INTRODUCTION

The Universe is observed to be made up mostly of matter. The Standard Model allows for such an asymmetry through the CP violation mechanism[2]. CP violation was discovered in the kaon system in 1964 at Brookheaven[3], but CP violation in the kaon system is not enough to account for the observed asymmetry and this phenomenon is still, after so many years, the least understood (or, better, the least constrained) subject in high energy physics. One of the main motivations for the BA$\bar{B}$AR experiment is to investigate whether or not the Standard Model completely explains CP violation.

In fact, CP violation is also expected in the B meson system. Since the processes where it is expected are very rare, we need to be able to produce many B mesons. This is the reason why B-factories have been built at SLAC (California, USA) and KEK (Japan). Some of the channels are very clean, in particular the so called "golden" mode $B^0 \rightarrow J/\psi K^0_S$. In this case the final state is CP invariant and can be reached from either a B^0 or a $\overline{B^0}$. The Standard Model predicts that, because of $B^0\overline{B^0}$ mixing, the CKM phase will produce a time dependent asymmetry in the decay of B^0 and $\overline{B^0}$ to this final state and that this asymmetry will vary sinusoidally.

We can have two possible outcomes of the B-factory experiments: 1) all measurements fully determine the CKM matrix elements and these are consistent with the Standard Model; 2) there is not going to be a single choice of the CKM parameters and this would indicate the existence of new physics. To reach either conclusion, we can exploit the unitariety of the CKM matrix, trying to over constrain the unitariety triangle, measuring the angles α, β and γ, via ,e.g., the following B decays: $B^0 \rightarrow J/\psi K^0_S$ ($BR \sim 3 \times 10^{-4}$, sin2b), $B^0 \rightarrow \pi\pi$ ($BR \sim 2 \times 10^{-5}$ sin 2α), Bs $\rightarrow \phi K^0_S$ (BR $\sim 10^{-6}$, sin 2γ).

The measurement of sin2β is the least difficult to perform. These are the necessary ingredients for this measurement[4]:

- measurement of the time between the decay of the B into a CP eigenstate and the decay of the other B. For this reason we need good vertexing and use asymmetric beams to boost the center of mass along the beam direction[5];

Quantum Gravity Generalized Theory of Gravitation and Superstring Theory Bused Unificartoin
Edited by Kursunoglu *et al.* Kluwer Academic / Plenum Publishers New York 2000

- exclusive reconstruction of the CP mode; this requires good tracking efficiency, solid angle coverage and particle identification;
- reconstruction of the flavor of the other B meson, for example via the charge of the leptons or kaons from its decay; particle identification is essential also for this task.

The low branching ratios for the most interesting channels constitute a formidable challenge, since we need to deal with large combinatoric background and continuum events.

BABAR will also perform other interesting measurements (V_{ub}, rare B decays, charm, τ, $\gamma\gamma$ physics), but at this time it is still too early for physics results.

THE ACCELERATOR PEPII

To get the millions of B mesons we need, a B-factory, PEPII, has been built at the Stanford Linear Acceleration Center (SLAC)[6]. The collider operates at the $\Upsilon(4S)$ resonance with a design luminosity of $3.0 \times 10^{33} cm^{-2}s^{-1}$ and $\beta\gamma = 0.56$. The high luminosity is achieved through many bunches (1658) and a short bunch spacing (4.2 ns) with head-on collisions. At the peak of this resonance, ~ 25% of all hadronic events are $B\bar{B}$ events, and of these, approximately half are $B^0\bar{B}^0$. To allow for different energies for the electron and positron beams, two rings are necessary: the high energy ring (HER) is a refurbished PEPI, while the low energy ring (LER) was recently built specifically for BABAR . It collides 9.0 GeV/c electrons with 3.1 GeV/c positions. PEPII delivered the first hadronic event on May 26th 1999 and it has reached very quickly a peak luminosity of 1.4×10^{33} $cm^{-2}s^{-1}$ (about half of design). It has delivered 20 fb^{-1} (1.7 recorded by BABAR , including 0.2 off the $\Upsilon(4S)$ peak) as of November 1999. This data sample includes ~1.6 million $\Upsilon(4S)$ decays and 5.5 million continuum hadronic events. The beams have been reasonably clean, delivering to the BABAR detector less than the budgeted radiation dose. The processing rate has been steadily improving and has recently been very close to matching the arriving data from PEPII.

THE BABAR DETECTOR

The BABAR detector is composed of 5 main subsystems[7].

The Silicon Vertex Tracker (SVT) has 5 layers of double-sided silicon microstrip detectors, the first of which is located ~3 cm from the beam line. This device is completely radiation hard (it can sustain up to 2 Mrad). The resolution in z and ϕ is represented in Fig. 1 for Bhabha events; the Monte Carlo (MC) simulation reproduces the data quite well, considering that it assumes perfect alignment. The expected resolution of 15 μm at 0° has been achieved.

The Drift Chamber (DCH) has 40 layers (10 alternating axial and stereo superlayers). It uses a low density 80% He, 20% isobutane gas mixture and gold plated aluminum wires. The achieved single hit resolution shown in Fig. 2 is in average 125 μm which is better than design. The momentum resolution for high momentum tracks, where the multiple scattering is negligible, is 0.45% of the momentum and improves to 0.3%, when the tracking information from the SVT is included. Besides tracking, another goal of the DCH (and also of the SVT) is to provide particle identification at low momenta via the measurement of dE/dx. This is particularly important for kaon identification when used for tagging, since the expected K/π separation is greater

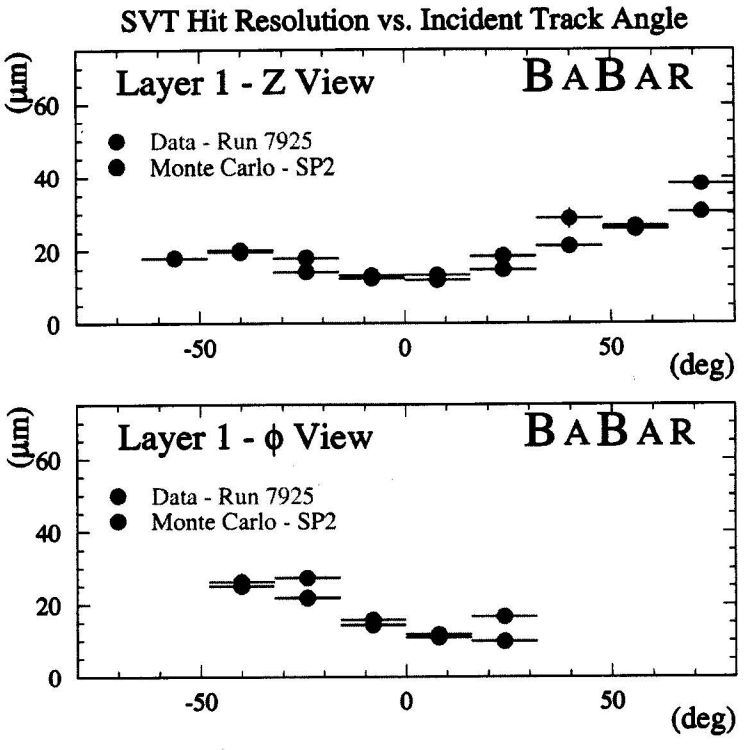


Figure 1. Resolution of the SVT in z and ϕ.

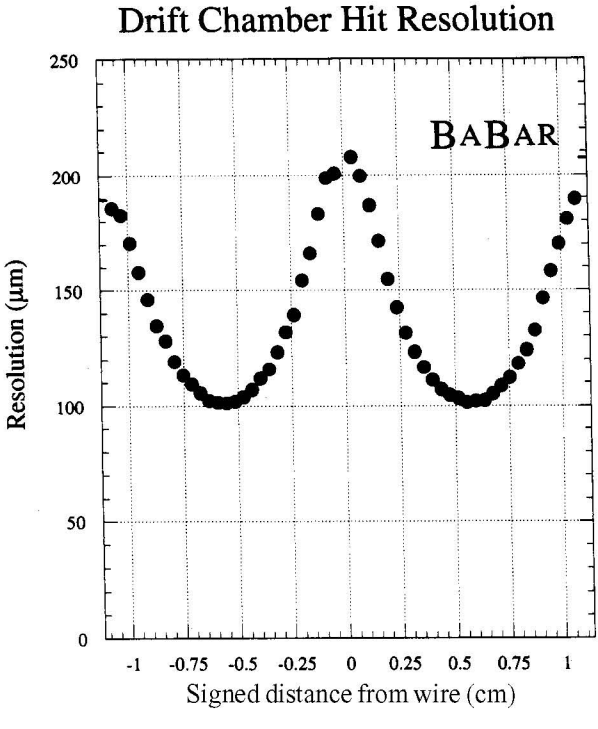


Figure 2. Single hit resolution in the DCH.

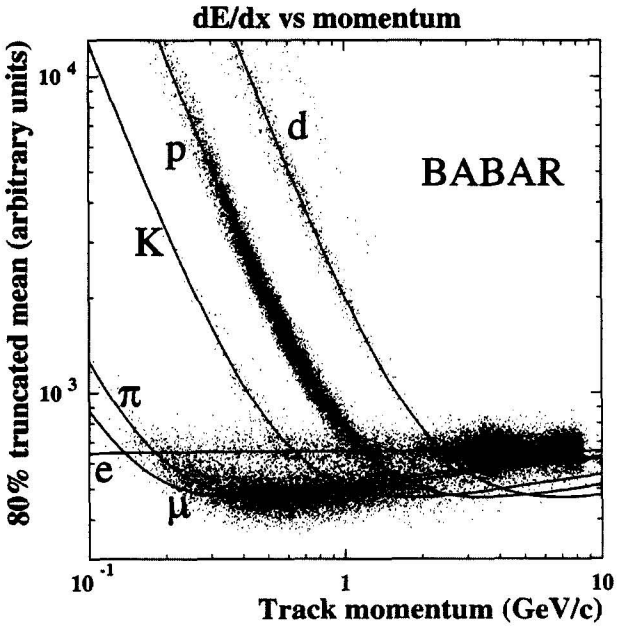


Figure 3. DCH dE/dx measurement: Bethe-Bloch expected curves for different particle types and measurements from data.

than 3 s up to 0.7 GeV/c. In Fig. 3 the Bethe-Bloch expected curves are represented for different particle types, together with the measurements from data. The achieved resolution is ~7.5% for Bhabhas (very close to the expected performance).

The particle identification subsystem is called DIRC (which stands for Detection of Internally Reflected Cherenkov light). This device exploits a new concept of CRID (Cherenkov imaging detector) and it constitutes one of the main differences between the BABAR and Belle (at KEK, which uses aerogel counters) detectors. As shown in Fig. 4, tracks traversing the thin quartz bars (the entire detector material contributes only 0.14 radiation lengths radially) emit Cherenkov photons, most of which are totally reflected, trapped inside the quartz. Finally they reach a grid of 10572 photomultiplier tubes on one side of the BABAR detector, where they form rings (or parts thereof). The angle of an individual photon with respect to the charged track is determined by tracing its trajectory backwards, assuming it emerged from the center of the quartz bar and hit the center of the phototube. Five out of 12 sectors were installed at the beginning of the run, but as of October 1999 the detector is complete and fully functional. The DIRC is reaching design performance. The achieved time resolution is 1.8 ns (design: 1.4 ns) for dimuon events and the Cherenkov angle resolution is 3.0 mrad (design: 2.3 mrad) for Bhabhas. Each track above Cherenkov threshold emits —50photons and the single photon resolution is 9 mrad. Fig. 5 shows how the D^0 signal improves using the information from the DIRC; we can estimate the kaon identification efficiency to be about 80% with a rejection factor of —5.We can estimate such efficiency also from pure samples of kaons and pions from kinematically selected D^* decays: the result is ~ 84%, which is consistent with the previous method, with a pion misidentification rate of the order of 1 to 2 %.

The Electromagnetic Calorimeter (EMC) is made up of ~7000 CsI crystals (doped with thallium atoms). It is designed to reconstruct photons down to 20 MeV/c and electrons down to 500 MeV/c. The measured energy is in agreement with expectations

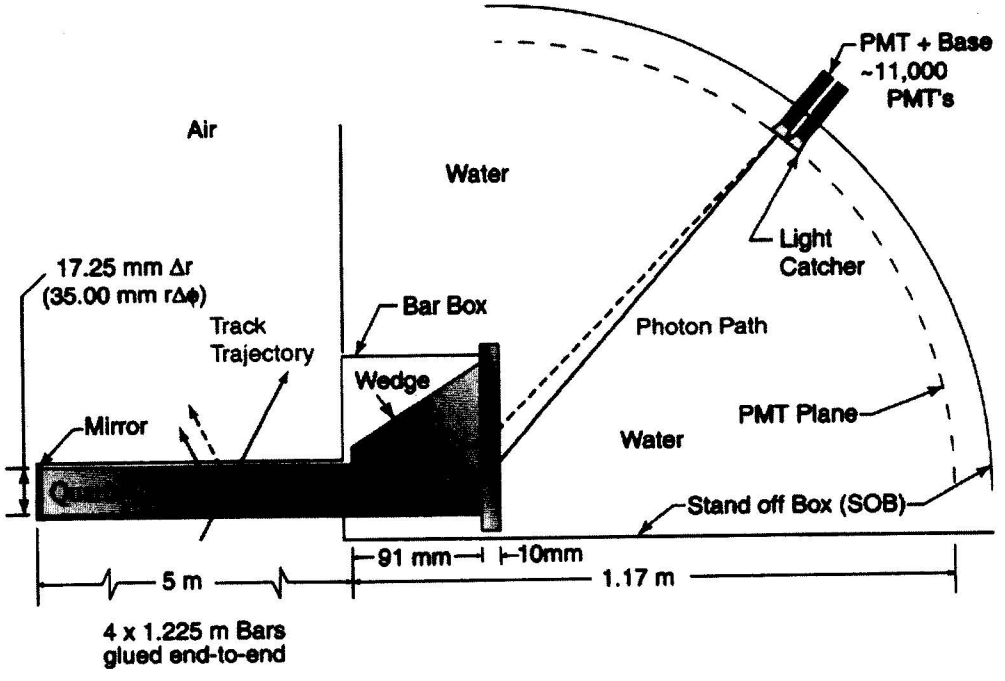


Figure 4. Schematic view of the DIRC principle of operation.

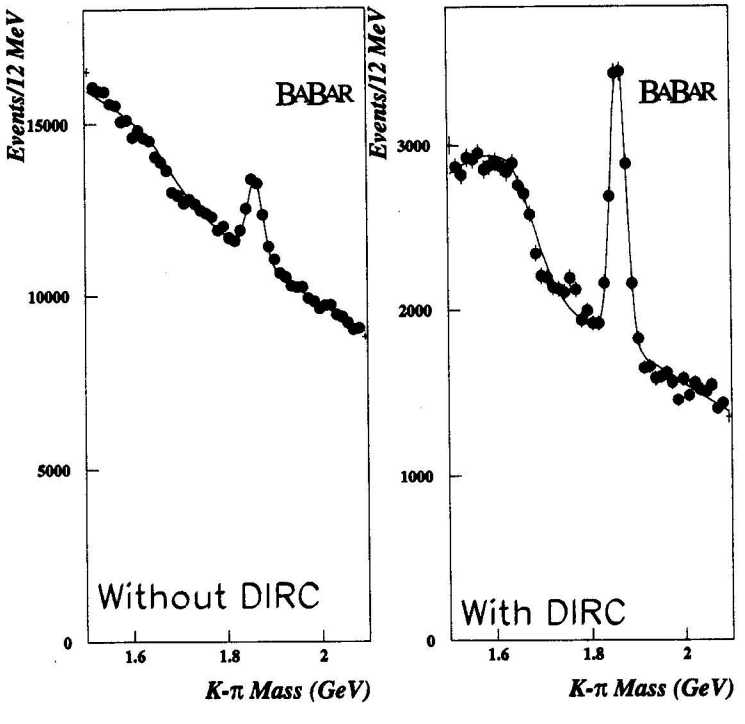


Figure 5. The D^0 signal without and with the information from the DIRC.

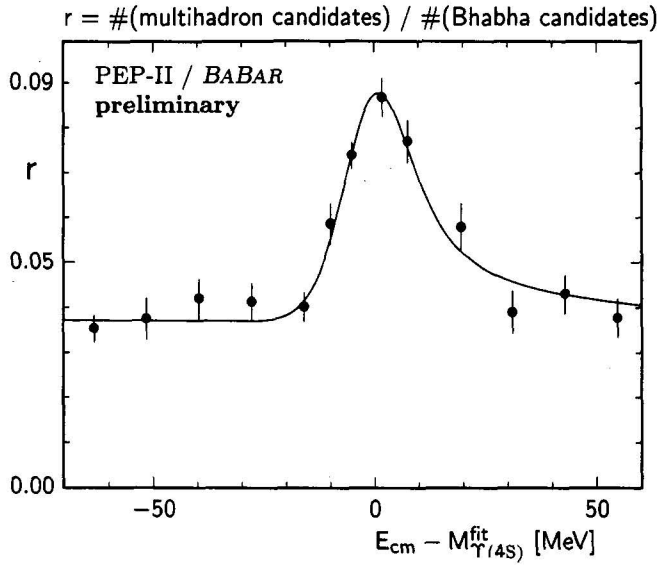


Figure 6. Resonance energy scan preliminary results.

and the π^0 mass resolution is about 7.7 MeV/c^2, still worse than the expected value. The electromagnetic calorimeter is located inside a 1.5 T superconducting solenoid.

Finally, the Instrumented Flux Return (IFR), for muon and neutral hadron identification, is made up of resistive plate chambers (RPC) interleaved with the iron which constitutes the flux return of the magnetic field. The RPC's use an argon-freon gas mix with aluminum strips for signal pickup. The IFR is designed to detect muons with momentum as low as 500 MeV/c. A significant part of the detector was off for most of the pre-October data, but the IFR is now fully functional. The muon identification efficiency for dimuon events is about 80% with a pion misidentification level of ~5%) in good agreement with the Monte Carlo predictions.

PRELIMINARY RESULTS

As mentioned previously, it is still too early for physics results. We are concentrating instead on understanding our detector response and on studying the key ingredients for the measurement of sin 2β.

Resonance Energy Scan

The resonance energy scan was performed June 15–17 1999, running on 13 points. The data from each center-of-mass energy point is used to measure the ratio, *r*, of multihadron candidates to Bhabha candidates. We expect an approximately flat background from Bhabha and continuum events, with a resonant contribution from Υ(4S) decays superimposed. Hadronic events were selected using event shape cuts to enhance the Υ(4S) contribution. Fig. 6 shows the values of *r* measured at each point together with the theoretically expected shape fitted to the data itself. We fit these values to a model which takes into account the Υ(4S) lineshape and the spread in the PEP-II center-of-mass energy. About 30% of the data has been analyzed, with the following

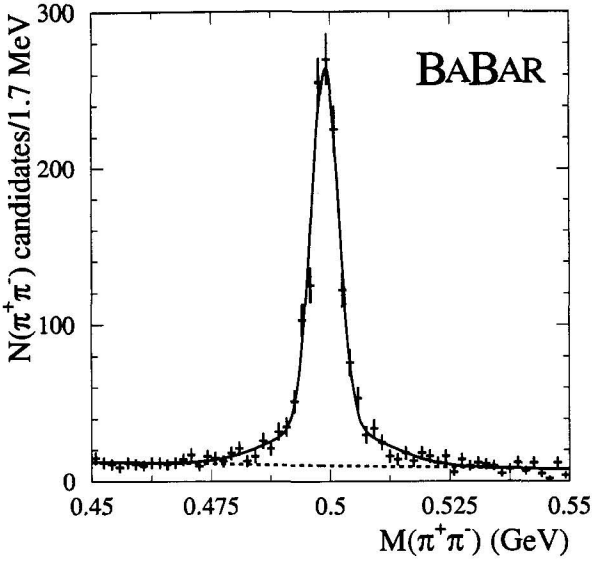


Figure 7. Oppositely charged pions pairs invariant mass ditribution

results:

$$m_{\Upsilon 4s}) = 10.5841 \pm 0.0007 GeV/c^2, \quad \Gamma_{\Upsilon(4s)} = 11.1 \pm 3.4 MeV, \tag{1}$$

where the fitted mass is measured on the PEP-II energy scale. These results compare well with the Particle Data Book (PDG) values[8].

*D** Reconstruction

A particularly important decay, also useful for detector studies, is the decay of D^* into $D^0\pi$, with the D^0 decaying into $K\pi$, which has an overall branching fraction product of 2.7%. These are clean decays, which can be selected just using kinematics and, hence, can provide control samples of pure kaons and pions for particle identification studies. Selecting D^* in cc events, we can achieve better resolution constraining the D^0 to originate from the beam spot (measured run by run) and refitting the slow pion using the new interaction point determination. This technique improves the resolution on the $D^* - D^0$ mass difference from 354 keV (narrow Gaussian component, with 27% of the signal peak) to 280 keV (with 47% of the signal peak).

K^0_s and J/ψ Reconstruction

Using a tight selection we obtain a quite pure sample of Ks candidates (see Fig. 6). They are identified as pairs of opposite sign charged tracks from a common vertex and with mass consistent with the K^0s mass. Furthermore we require that the K^0s candidates point back to the interaction point and a minimum transverse momentum in the decay (to suppress contributions from combinatoric and Λ decays). We reconstruct J/ ψ candidates in their decays modes into $e+e-$ and $\mu+\mu-$, which have a 12% combined branching ratio. Electrons are identified using the pattern of energy deposited in the calorimeter and by requiring the ratio, E/p, of the energy measured in the calorimeter to the measured track momentum to be close to one. This channel presents a significant

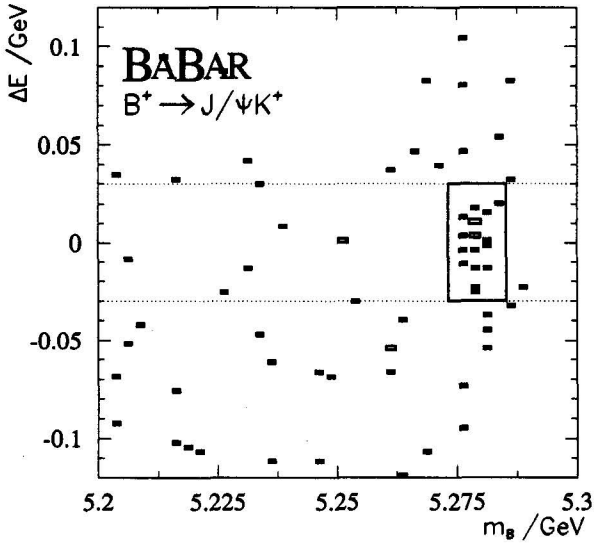


Figure 8. ΔE vs m_B for the exclusive decay B+ → J/ψK+.

tail in the invariant mass distribution due to bremmstrahlung. Muons are identified using their minimum-ionizing signature in the calorimeter.

Semileptonic B Decays

The exclusive channel B → D^*ev, D* → D⁰π, D⁰ → Kπ has been studied. This semileptonic mode has the B^0 largest branching ratio (4.6%) and the overall product of branching ratios for this decay chain is 0.12%. We require that electrons have a momentum of least 1 GeV/c in the center-of-mass frame to reduce backgrounds from charm semileptonic decays. Furthermore we ask for kinematic consistency with the missing v and the known B meson momentum in the Υ(4S) rest frame. The D^* and the electron are required to have opposite charge. Finally we cut around the expected value of the D^*–D^0 mass difference to select ~120 events (for 400 fb–1 of data), which constitute ~6 σ statistical significance.

The Channels: $B+ \rightarrow J/yK+$ and $B^0 \rightarrow J/\psi K^0_S$

A particularly interesting channel is the decay $B+ \rightarrow J/\psi K+$, since it constitute the charged equivalent of the "golden" mode $B^0 \rightarrow J/\psi K^0_S$ and gives a cross check of the sin 2β analysis. The kaon candidate is selected using the information from the DIRC, when available. J/ψ particles decaying into $\mu+\mu-$ and $e+e-$ are selected. Vertexing kaons and J/ψ, we reconstruct the B. We apply a constrained fit, using the PDG values for the masses of the kaon and of the J/ψ, fixing the B vertex to be the same as the J/ψ vertex. We can then calculate ΔE and m_B and cut on the distribution of these quantities, as shown in Fig. 8, to select 19 events from ~640 pb^{-1}, with an expected background of less than 2 events.

Finally, for the "golden" mode B⁰ → J/ψK0s, we use a technique similar to the one used for the charged case, selecting a total of 8 events (see Fig. 9).

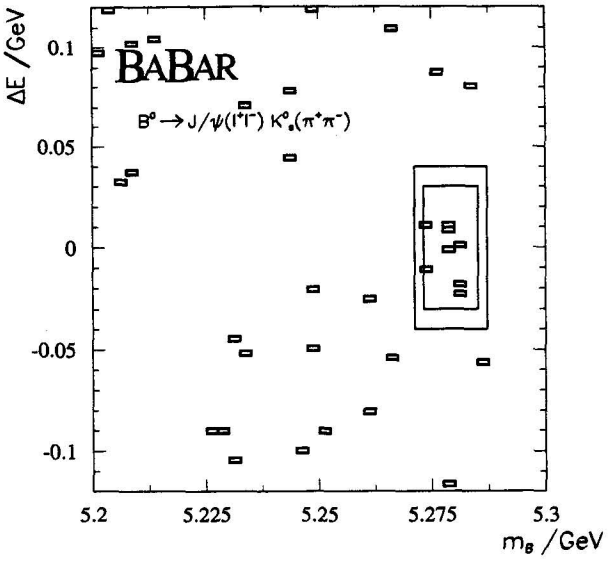


Figure 9. ΔE vs m_B for the exclusive decay $B^0 \to J/\psi K^0_S$.

CONCLUSIONS

PEPII is working well and routinely delivered luminosity in excess of 10^{33} $cm^{-2}s^{-1}$. BABAR has accumulated 1.7 fb^{-1} of data. The BABAR detector is complete and rapidly approaching the design performances. The goal is to accumulate 10 fb–1 of data by the end of the run (Summer 2000) and present the first physics results by then. In particular a first measurement of sin 2β will be attempted from 10 fb–1 of data.

Acknowledgments

I would like to thank the organizers of the Orbis Scientiae conference and in particular Prof. Behram Kursunoglu for inviting me to talk about the present and future of the BABAR experiment. I'd like to thank the BABAR collaboration and the staff of the SLAC accelerator department for their outstanding efforts. This work was supported in part by the U.S. National Science Foundation.

REFERENCES

1. Representing the BABAR Collaboration.
2. L. Wolfenstein, *Phys. Rev. Lett.* **13,** 562 (1964). A.D. Sakharov, JETP Lett. **5,** 24 (1967). M. Kobayashi and K. Maskawa, Prog. Theor. Phys. **49,** 652 (1973).
3. J. H. Christenson et al., *Phys. Rev. Lett.* **13,** 138 (1964).
4. D. Boutigny et al., (BABAR Collaboration), ed. by P. F. Harrison and H. R. Quinn, SLAC-R-504 (1998).
5. P. Oddone, Proceedings of the UCLA workshop on Linear Collider B Factory Conceptual Design, ed. by D.Stork, World Scientific (1987).
6. An Asymmetric B Factory Based on PEP: Conceptual Design Report, ed. by M.Zisman, SLAC-372 (1991) and SLAC-418 (1993).
7. D. Boutigny et al., (BABAR Collaboration), SLAC-R-95-457 (1995).
8. Particle Data Group, C. Caso *et al.,* Review of Particle Properties, The European Phsyical Journal C**3**, (1998).

This page intentionally left blank.

INDEX

ADS supergravity, 46
Anthropic, 26
Anti-De Sitter space, 43
Antihydrogen, 174
Antisymmetric field, 5
Axial current, 136, 148

B-decays, 224
B-factory, 218
B-meson, 217
BABAR, 217
Backlund transformation, 129
Baryon mass, 204
Baryonic monopole showers, 39
Bethe-Heitler pair production, 36
Big Bang, 73
Black Hole, 59
Bremmstrahlung, 36
Bosons, 90
Broken supersymmetry, 203
Brookhaven, 111,217

Cabibbo model, 134
Cartan subalgebras, 57
Cartan-Weyl basis, 58
CDF experiment, 101
CEBAF, 143
CERN, 111, 174, 176,210
CFT, 14,22
Charged Higgs boson, 104
Cherenkov imaging detector, 220
Chern-Simons theory, 53,54
CKM, 187
CKW matrix, 102
Clock comparison experiments, 164
COMPASS, 214
Conformality, 13, 16
Cosmic rays, 33
Cosmological constant, 13
Cosmological density fluctuations, 26
Cosmology, 3
Coupling of sources, 56
Covariant world sheet fields, 44
CP violation, 111, 115, 174,217
CPT, 154, 161, 174
CVC, 139

D-brane theory, 9
Density fluctuations, 29
DESY, 210
Diquark, 203
Dirac mass matrix, 182
DØ experiment, 101
Duality, 125

Einstein theory of gravity, 6
Electric dipole moment, 115
Entropy, 59, 83
Eternal inflation, 27
Event horizon, 67
Exotic hadrons, 206
Expanding universe, 66

Fermilab, 198
Form factors, 135
Flavor changing decays, 102
Flavor symmetry, 183
Froggatt-Nielsen mechanism, 183

G-2 experiments, 175
Galactic halo, 199
Galactic magnetic fields, 33
Gamma ray bursts, 3
Gauge coupling unification, 18
Gaussian fluctuations, 30
Generators, 128
Gluons, 211
Gluon structure functions, 214
Grand unification, 13
Gravitons, 90
GUT theories, 13
GZK cutoff, 33

Hadrons, 206
Helicity, 105
HERMES, 211
Higgs boson, 92, 102, 189
Hydrogen, 173
Hypefine levels, 177
Hyperons, 133

Inflation, 25

Kac-Moody algebras, 53,57
Kaluza-Klein, 116
Kaons, 162,217
KARMEN, 182
KEK, 217
Kerr metric, 65
Kursunoglu theory, 84

Lambda decays, 135,224
Lambda hyperon, 133
Lepton masses, 14
Liouville quantum mechanics, 123
Lorentz symmetry violation, 158, 166, 173
Lorentz transforms, 161
LSND, 181

Magnetic monopoles, 33,89,94
Magnets, 154
Majorana mass matrix, 182
Meson masses, 204
Monopole condensation, 6
Monopole Cherenkov signatures, 38
Monopoles, 6,33,34, 37,90
Monopole structure, 35
MSW, 181
Muon, 111

Neutral meson oscillation, 162
Neutral Sigma hyperon, 133
Neutrino masses, 183
Neutrino mixing, 184
Neutrino oscillation, 181
Neutrinos, 83,90
Neutron, 167
Non-abelian manifolds, 19

Orbitals, 209

PCAC, 149
PEP II.2 18
Planck length, 10
Proton, 168
Pseudoscalar bosons, 153

QCD, 14.102
QED, 36,174
Quantum fluctuations, 27
Quark, 203
Quark masses, 14

Regge trajectory, 203
Relativistic monopoles, 36

See-saw mechanism, 182, 186
Semi-inclusive scattering, 212
Silicon vertex tracker, 218
SIMP search, 197
Sine-Gordon theory, 121, 128
Sinh-Gordon theory, 121, 128
SLAC, 210,217
Soliton, 129
Speed of light, 4
Standard model, 81, 101, 102, 107, 112, 161,
Strangeness changing current, 133
Strings, 43,82
Symmetric tensor, 4
Supergravity, 47,49
Supergravity fields, 50
Superspin, 63
Supervirasoro generators, 44
SU(3), 133, 183,213
SUSY, 113

Tevatron, 101, 117,201
Thermalization surface, 28
Thermodynamics, 63
TJNAF. 133
Tomography, 38
Top quark, 101
Torsion balance, 155

Unification. 7
Unified theories of gravitation, 9

Variable speed of light, 3,4,9
Vector current, 136
Vertex operators, 43,45,50
VEV,21
Virasoro algebras, 53, 130

W-boson, 114
WZW theory, 53

Yukawa coupling, 102
Yukawa interactions, 16, 190

Zeeman hyperfine levels, 174